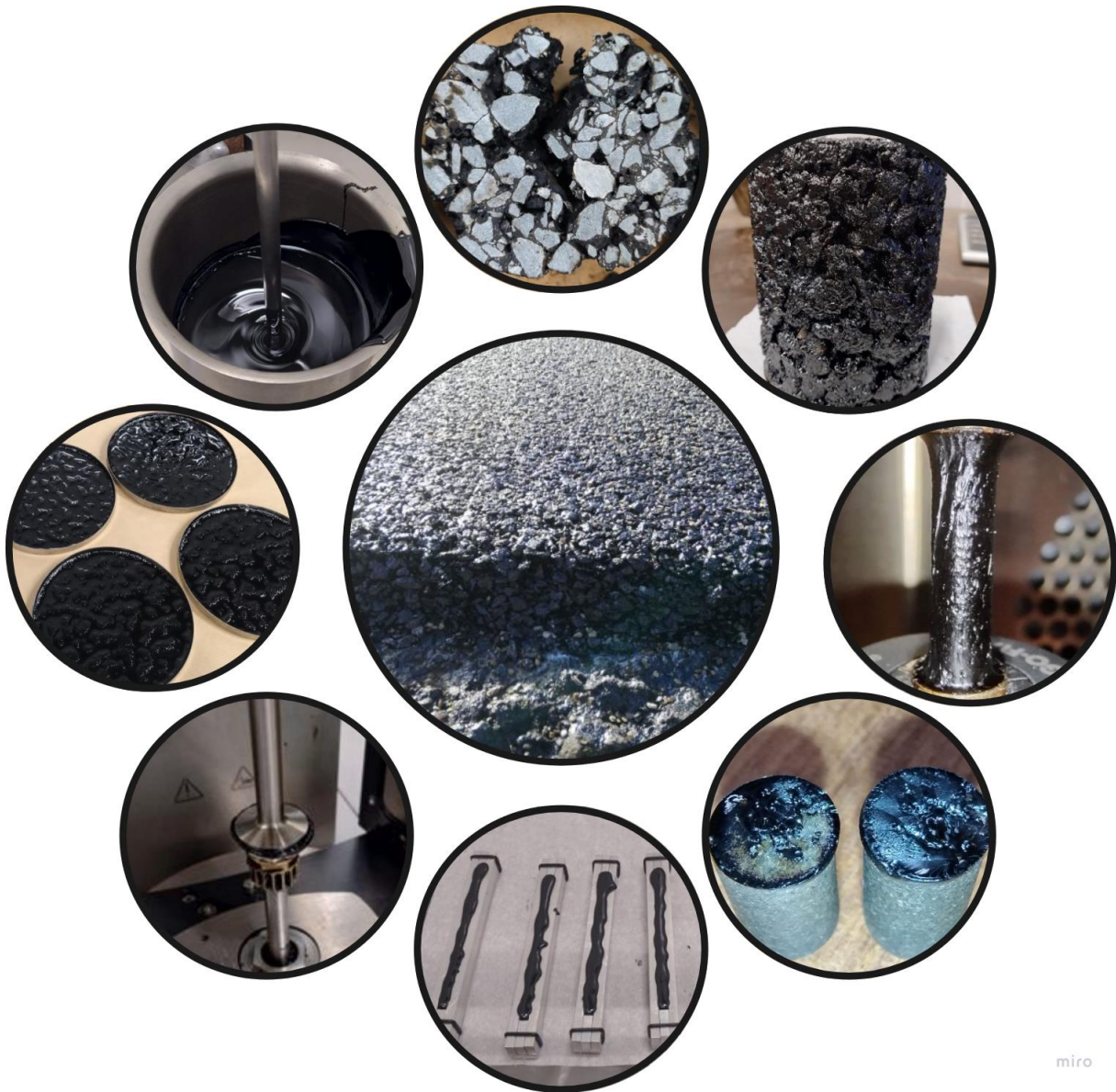


Evaluation of the implications on performance for Re-refined Engine Oil Bottoms (REOB) modified bitumen



miro

MSc thesis
Lucas Mortier

Figure 0.1: Logo of the Technische Universiteit Delft

Figure 0.2: Logo of TNO

Figure 0.3: Cover image with an overview of several different levels of the use and analysis of REOB modified bitumen: blending of bitumen with REOB, laboratory ageing, DSR frequency sweep, BBR test, DMA adhesion/cohesion, mastic tensile test, asphalt mixture compaction and IDT fracture

Evaluation of the implications on performance for Re-refined Engine Oil Bottoms (REOB) modified bitumen

by
Lucas Mortier

To obtain the degree of
Master of Science
in Structural Engineering
At the Delft University of Technology
to be defended publicly on Friday May 17, 2024, at 16:00

Student number:	4889789	
Chair:	dr. Xueyan Liu	TU Delft
Daily supervisors:	dr. Shisong Ren	TU Delft
	dr. Sayeda Nahar	TNO
Committee members:	prof.dr.ir. Sandra Erkens	TU Delft
	prof.dr.ir. Erik Schlangen	TU Delft
	dr. Milliyon Woldekidan	Boskalis

Preface

This thesis is the result of my work at both the Delft University of Technology and my internship at TNO. It has been made to evaluate the effects of REOB on bitumen and help both industry and universities with increasing understanding and awareness of this material. I have loved to work on this subject for all the months working on it and plan to continue doing research oriented work on bitumen/asphalt in the future as well; by pursuing a PhD at TU Wien.

I would like to thank my family and friends for their support during the whole of my studies. My parents, sister and brother have always backed me up and pushed me to strive higher and without their undying confidence in me I would have never pursued studying in the first place. When visiting them I have always felt back at home. Next to that, I truly believe I have made life-long friends and would like to thank: Anais for her sharp mind and skills to have saved me so many times, Martin for his exceptional skill to always understand everything and saving me from many mistakes and Bryan for his support and his skill to be able to get my mind off of stupid things in life.

During my master thesis I have met a lot of new faces and have been able to already build a small network of people that work in the research field where I will be working for the rest of my life. Sayeda thank you for all your feedback and your bright mind to help me stay positive and motivated throughout the internship, without you this work wouldn't have been so elaborate as it is. I want to thank all my other colleagues at TNO as well, for their support and for taking me in; I really feel like a roadie! Likewise I would like to thank everyone from the Pavement Engineering team at TU Delft as well; you have all intrigued me with this field of study and made me realise how interesting research truly is.

Lucas Mortier
Delft, May 2024

Summary

Re-refined Engine Oil Bottoms (REOB) are a waste product from the re-refining process of waste engine oil. There is a large incentive in the world to produce recycled engine oil and the production of REOB in this process is increasing. On the other hand refineries are going through transitions due to economic and regulatory reasons (i.e. IMO 2020) which has an impact on bitumen production process and its properties (Nahar et al., 2020). As a result, harder grades bitumen are readily available compared to the softer grades. Moreover, suppliers that are non-refiners are also part of the bitumen supply chain which has led to more variation in bitumen composition and properties. REOB, among other options of blending components, has posed a solution for this problem; making it possible to reach softer grade bitumen by blending the two. The pavement industry is however facing premature failures of pavements, less workable mixtures, earlier deterioration etc. and the question arises whether the diverse sources of blending components like REOB modification of the bitumen could be the cause of them. There exists no unique identification number (for example the CAS number used in the USA) for REOB as a material in Europe, which makes it untraceable and hence there are no restrictions on the use of REOB in Europe. No guidelines for the use of REOB in bitumen for asphalt mixtures exist, while one is not obliged to notify contractors on the presence of the REOB in bitumen; thus identification and quantification of REOB in bitumen and a clear evaluation of the bitumen properties and performance is wished for.

In the scope of research, a broad set of unmodified bitumen is evaluated next to two series of REOB modified bitumen. The two blends made in this thesis are made from two different hard grade bitumen; bit-P with PEN 15 and bit-K with PEN 20/30. These bitumen act as the base bitumen to be blended with 5; 10 and 15% REOB (of a single source), to compare what truly is the underlying effect of the base bitumen and not the REOB. This way compatibility can be shown of a bitumen to receive REOB modification and in future research a broader set of different REOB sources should be evaluated as well.

By using an extensive amount of chemical and thermal analysis tools like: Attenuated Total Reflectance Fourier-Transform Infrared Spectroscopy (ATR-FTIR), X-Ray Fluorescence (XRF), elemental analysis (CHNO+S), iatrosan chromatography (SARA fractioning), Gel Permeation Chromatography (GPC) and Differential Scanning Calorimetry (DSC) the characteristic properties of bitumen modified with REOB are mapped and identification and quantification of REOB in the bitumen are made possible. REOB can be mainly identified in bitumen by the presence of lubricant additives still residing in it, where trace metals can be measured with XRF and ICP-AES but alternatively the functional groups of PIB, Si-O-Si and P-O-C can be found with FTIR. Specifically the PIB peak can be used to effectively identify and quantify the presence of REOB, although exact quantification remains a challenge with limited datasets. An indication of high or low quantity of lubricant additives is possible however. Oxidation rates of REOB modified bitumen are increased in the case of the formation of carbonyls but seemingly not for the sulfoxides. The chemical composition of REOB modified bitumen is altered heavily by an influx of saturates, a decrease of aromatics and an addition of asphaltenes of seemingly different nature than found in bitumen. While general molecular weights of these modified bitumen seem to shift to higher orders, the asphaltenes fraction has shown to be of generally lower molecular weights, while saturates and aromatics seem to be actually of higher molecular weights, therefore creating a shift in the composition of the REOB modified bitumen. These changes in chemical composition therefore suggest REOB has a (negative) impact on the microstructural system of the bitumen.

This is followed up by performing rheological experiments to map viscoelastic properties of the bitumen, using the Dynamic Shear Rheometer (DSR) and Bending Beam Rheometer (BBR). Where blending with REOB shows to exponentially increase the PEN grade but the softening point and other viscoelastic properties seem to all change linearly with changing dosage. The viscoelastic behaviour of the base bitumen is heavily reflected in the REOB modified bitumen, mainly the time-temperature relation the bitumen owns seems to be altered. Higher dosages of REOB have shown larger

decline in viscous property and increase in stiffness with ageing and especially the low temperature behaviour seems to be compromised heavily for REOB modified bitumen both initially and after ageing.

Mechanical performance of the bitumen and asphalt mixtures modified with REOB is evaluated by carrying out Dynamic Mechanical Analyser (DMA) tests on both cohesive/adhesive behaviour of stone-bitumen film and mastic column tests. It has shown that comparing REOB modified bitumen, which had similar complex shear modulus behaviour, were much more susceptible to brittle fracture and stress build up than unmodified reference bitumen. Comparing fillers with and without hydrated lime has shown that the sensitivity of the change in properties in the presence of active filler is less for REOB modified bitumen. which could be related to the adhesion between the binder and filler, where possibly acidity of the binder and porosity of the filler could have played a role. Response of the mastics show higher stiffness and strength values than initially expected from shear modulus values from the modified bitumen.

Lastly, REOB modified asphalt mixtures are tested with Indirect Tensile (IDT) tests at dry and wet conditions and Cantabro Abrasion tests are performed to evaluate impact resistance of the mixtures to simulate ravelling susceptibility. Both these tests have shown that in asphalt mixtures, of exactly similar PEN grades, the REOB modified bitumen leads to a stiffer and stronger mixture compared to bitumen rheology, although being more susceptible to moisture and freeze-thaw conditioning. Again the PEN grade of REOB modified bitumen seems not to be a reliable indicator of resulting stiffness of the mixture.

Using the described approach, this study was able to present a methodology on how to analyse REOB modified bitumen to identify and quantify the presence of REOB and how to evaluate properties and performance of REOB modified bitumen and asphalt mixtures.

Content

Preface	iv
Summary	v
Chapter 1. Introduction	12
1.1. Context.....	12
1.2. Research objectives.....	12
1.3. Report structure.....	13
Chapter 2. Literature review	14
2.1. General application of REOB and nomenclature.....	14
2.2. Overview of literature on REOB modified bitumen.....	17
2.3. State-of-the-art research on REOB modified bitumen.....	20
Chapter 3. Research approach and material source	28
3.1. Research structure.....	28
3.2. Different bitumen sources analysed in thesis.....	29
3.3. Reference bitumen and REOB-blends.....	31
Chapter 4. Chemical characterization of bitumen, REOB and REOB modified bitumen	33
4.1. Introduction to chemical characterization.....	33
4.2. Identification, quantification and evaluation of REOB in bitumen (XRF & ATR-FTIR)....	34
4.2.1. Trace elements/metals found by XRF and/or ICP.....	34
4.2.2. Analysis and modification of ATR-FTIR spectra.....	38
4.2.3. Evaluation of ATR-FTIR spectrograms of bitumen and REOB.....	40
4.2.4. Effect of REOB in modified bitumen on ATR-FTIR spectrograms.....	49
4.2.5. Analysis of PIB peak using the derivative of the Transmittance spectra.....	56
4.2.6. Observations on trace elements and chemical functional groups.....	60
4.3. Elemental analysis (C,N,H,O & S).....	61
4.3.1. Principle of the EA technique and measurements.....	61
4.3.2. Apparent elemental composition of unmodified and REOB modified bitumen.....	63
4.3.3. Observations on elemental analysis of CHNO+S.....	68
4.4. Polarity based soluble fractions (SARA).....	69
4.4.1. Method description, retrieval of chromatograms and fraction calculations.....	69
4.4.2. SARA fractions of unmodified, aged and REOB modified bitumen.....	75
4.4.3. Colloidal instability index and other indices to describe changes in bitumen composition.....	79
4.4.4. Observations on SARA fractions.....	82
4.5. Molecular weight distributions (GPC).....	83
4.5.1. Molecular weight distributions of unmodified bitumen, REOB blends and REOB.....	83
4.5.2. Molecular averages; M_n ; M_w ; M_z ; M_{z+1} ; PDI.....	89

4.5.3.	Fractions of low, medium and high molecular weight	95
4.5.4.	Observations on molecular weight distributions	98
4.6.	Heat flow behaviour and glass transition (DSC)	99
4.6.1.	Principle of differential scanning calorimetry and used procedure	99
4.6.2.	Phase transitions of unmodified and REOB modified bitumen.....	100
4.6.3.	Measured phase transition temperatures; half ΔC_p and derivative methods.....	105
4.6.4.	Observations on phase transitions	108
Chapter 5.	Rheological characterization of non- and REOB modified bitumen	109
5.1.	Introduction to rheological characterization.....	109
5.2.	Viscous and elastic behaviour at various temperatures (DSR).....	110
5.2.1.	Sample preparation and tests with the Dynamic Shear rheometer	110
5.2.2.	Black space diagrams	111
5.2.3.	Master curves of $ G^* $ and δ	117
5.2.4.	Cole-Cole & complex viscosity diagrams	122
5.2.5.	Parameters retrieved from DSR tests.....	129
5.2.6.	Observations on general viscoelastic rheological behaviour	138
5.3.	Low temperature stiffness and relaxation properties (BBR)	139
5.3.1.	Test preparation, method and calculation procedure with the BBR.....	139
5.3.2.	S- and m-values, critical temperatures $T_c(S)$, $T_c(m)$ and ΔT_c values.....	141
5.3.3.	Observations on low temperature rheological behaviour	144
Chapter 6.	Rheological and chemical property correlations of unmodified and REOB modified bitumen.....	145
6.1.	Intrinsic chemical and rheological properties of bitumen and REOB blends	145
6.2.	Ageing susceptibility due to chemical composition and correlation with rheological change (FTIR-SARA-GPC-DSR)	151
6.3.	Ageing related to molecular weight distributions and molecular structures (GPC-SARA-DSC-DSR).....	158
6.4.	Low-temperature susceptibility and behaviour (SARA-GPC-DSC-BBR-DSR)	164
6.5.	Conclusions on intrinsic properties, ageing susceptibility, colloidal structure related to molecular weights and low temperature susceptibility.....	170
Chapter 7.	Mechanical characterization of REOB modified bitumen, mastic and asphalt mixtures	171
7.1.	DMA adhesive & cohesive analysis.....	171
7.1.1.	Adhesive/cohesive stone-bitumen-stone column DMA tensile pull test.....	171
7.1.2.	Cohesive mastic column DMA test tensile pull test.....	181
7.1.3.	Observations on adhesive and cohesive performance	186
7.2.	Asphalt mixture workability and performance.....	187
7.2.1.	Resistance to densification and the cohesion of asphalt mixtures with REOB; mixture preparation and gyrator compacting.....	187

7.2.2.	Dry & wet cracking resistance of asphalt mixtures; indirect tensile strength ratio test (ITSRT)	192
7.2.3.	Impact resistance of asphalt mixtures (Cantabro abrasion test)	197
7.2.4.	Observations on mixture performance	200
Chapter 8.	Discussion, conclusion and recommendations on REOB modified bitumen	201
8.1.	Discussion of chemical, rheological and mechanical results	201
8.2.	Conclusions on REOB modified bitumen	202
8.3.	Recommendations on REOB modified bitumen	204
References		206
Appendix		212
A.	Flow diagram for identification of REOB in bitumen	213
B.	Flow diagram for evaluation of REOB modified bitumen	214
C.	Identification of REOB in bitumen from “GOA” and “Leerruimte” data	215
D.	Comparison of frequency sweep (DSR) data to field performance of bitumen	217
E.	X-ray CT scanning of small REOB modified bitumen films on aggregates	220

Glossary

Term	Definition & Explanation
AFM	Atomic Force Microscopy
AI	Ageing Index; an index calculated from a parameter from fresh and aged states
ATR-FTIR	Attenuated Total Reflectance Fourier-Transform Infrared Spectroscopy
BBR	Bending Beam Rheometer
CAM model	Christensen-Anderson-Marateanu model
CAS number	Chemical Abstracts Service number used in America
CII	Colloidal Instability Index
CTOD	Crack Tip Opening Displacements; measured with DENT test of bitumen
DENT	Double Edge Notched Tension test
DMA	Dynamic Mechanical Analyser
DSC	Differential Scanning Calorimeter
DSR	Dynamic Shear Rheometer
ΔT_c	Critical difference between the critical temperatures; indicating the ageing susceptibility of a binder
EA	Elemental Analyser; used to determine element concentrations of carbon, nitrogen, hydrogen, sulphur and oxygen in a bitumen
EO	Engine Oil
EOR	Engine Oil Residue
FHWA	Federal Highway Administration; road authority in the US
GC-MS	Gas Chromatography - Mass Spectrometry
gel-type	Bitumen which acts like a gel and has relatively higher viscosity
GPC	Gel Permeation Chromatography
G-R	Glover-Rowe parameter
ICP-AES	Inductively Coupled Plasma Atomic Emission Spectrometry test
IDT	Indirect Tensile test
IMO 2020	International Maritime Organisation 2020 regulations
ITS	Indirect Tensile Strength
ITSR	Indirect Tensile Strength Ratio; comparing dry and wet conditioning strengths
LAS	Linear Amplitude Sweep test; a fatigue test on bitumen with the DSR
LTOA	Long Term Oven Ageing
LWF, MWF and HWF	Low, Medium and High Weight Fraction of a molecular weight distribution for bitumen; boundaries set at 500 and 4500 Daltons
LWT	Load Wheel Tracking test
MDSC	Modulated Differential Scanning Calorimeter
NMR	Nuclear Magnetic Resonance test
PAV	Pressurized Ageing Vessel (ageing protocol)
PCA	Principal Component Analysis; a statistical tool to see relationships between multiple parameters and to indicate clustering of data
PDA	Precipitation de-asphalting technique; used in refineries with for example propane to remove asphaltenes from a bitumen
PDI	Polydispersity index; often used for polymers to show the spread in size

PEN	The measured penetration grade of a bitumen
PG	Performance grade; bitumen standard used in the US
PIB	Poly-Iso-Butylene; a functional group heavily present in REOB and identifiable in bitumen
PLS	Partial Least Squares; mathematical regression tool
PMB	Polymer Modified Bitumen
RAP	Reclaimed Asphalt Pavement
RAS	Reclaimed asphalt shingles (roofing material)
REOB	Re-refined engine oil bottoms
RHVDB	Re-refined Heavy Vacuum Distillation Bottoms
RHVDO	Re-refined Heavy Vacuum Distillation Oil
RTFOT	Rolling Thin Film Oven Test (ageing protocol)
RVTB	Re-refined Vacuum Tower Bottoms
SARA fractions	Saturates, Aromatics, Resins and Asphaltenes fractions of oil or bituminous materials
SBS	Styrene-Butadiene-Styrene; polymer used commonly in bitumen intended for asphalt pavements
SCB	Semi-Circular Bending test
sol-type	Bitumen which acts like a solvent and has relatively lower viscosity
STOA	Short Term Oven Ageing
T_c(m)	Critical temperature where the relaxation of a binder is such that the slope of the stress strain diagram is 0.3 [-] after 60 [s] of BBR testing.
T_c(S)	Critical temperature where the stiffness of a binder is 300 [MPa] after 60 [s] of BBR testing
TFOT	Thin Film Oven Test (ageing protocol)
T_g	Glass transition temperature
TSRST	Thermal Stress Restrained Specimen Test
TTSP	Time-Temperature Superposition Principle
VTAB	Vacuum Tower Asphalt Binder
VTAE	Vacuum Tower Asphalt Extender
VTB	Vacuum Tower Bottom
WEO	Waste Engine Oil
WEOR	Waste Engine Oil Residue
WODB	Waste Oil Distillation Bottoms
XRF	X-Ray Fluorescence
ZOAB	Zeer Open AsphaltBeton; open graded asphalt mixture used in the Netherlands

Chapter 1. Introduction

1.1. Context

Challenges within the bitumen market are continuously present, with typical problems including availability, consistency of bitumen due to refinery transitions, workability, and durability of bitumen as a component of asphalt binder. Inconsistencies in bitumen supplies arise when different grades of bitumen are produced by blending secondary streams of various origins, which are not clearly specified and remain unknown. One such blending component is Re-refined Engine Oil Bottoms (REOB), which has lower viscosity compared to bitumen and when combined produces a softer-grade bitumen. Research findings have shown both positive and negative outcomes for the performance of bitumen containing REOB. These outcomes can be attributed to the variability of properties due to different feedstocks and dosages (AsphaltInstitute, 2016; Karki et al., 2019). REOB-modified bitumen has been reported to be more susceptible to aging, while low-temperature characteristics have shown increased susceptibility to cracking (Mogawer et al., 2017; Rubab et al., 2011; Xin-jun et al., 2016).

In Europe, REOB does not have a unique identifier like a CAS number and is instead sold as bitumen, whereas in the US, it has its own CAS number, therefore making it traceable in bitumen. This poses a challenge for many asphalt contractors who may not be aware of any trace of REOB in the bitumen they purchase. In recent years, reports have surfaced regarding poorly workable mixtures during asphalt production and premature damage development in road surfaces in the Netherlands (Besamusca et al., 2021). The potential changes in the consistency of the bitumen, especially of softer grades, necessitate awareness from the Dutch asphalt industry and knowledge of the performance of such binders.

Next to the unknown and varying effects that REOB can have in bitumen modification, one should be aware of the chemical composition of this compound itself. Waste engine oil (WEO) has a higher fraction of low-molecular weight component which can be volatile during asphalt processing temperature, compared to REOB in bitumen modification. Thus indicating a higher risk of fumes during construction of WEO modified asphalt pavements (Eleyedath & Swamy, 2020). The REOB residue results from re-refining this WEO, which can be done with various techniques. The already varying consistency that waste engine oil can have, because of the use of additives for improving viscosity, anti-wear capabilities, temperature sensitivity etc. in the lubricant, the resulting residue from re-refining will have always a different consistency for each source of WEO.

Using this reasoning, it becomes clear that some problems occurring in asphalt mixtures that have been unexplainable so far, could be very well related to chemical changes that have never been monitored before. Many of these problems have been supposedly correlated to the presence of REOB in the bitumen used for the pavement. Although no clear correlation was made as to what dosage was used and what the definite impact was on the bitumen performance. This therefore asks for a thorough analysis of (REOB modified) bitumen to identify the presence of REOB and to evaluate the performance of such binders; basically evaluating the quality of bitumen.

1.2. Research objectives

In Europe, there exists no unique identification number similar to CAS number in the USA for REOB and hence its use in bitumen is not regulated. A problem has therefore arisen as REOB is **not traceable** in supplied bitumen and there currently is **no guideline/procedure** available for the use of this residue for bitumen modification.

The goal of this thesis is therefore to address the following questions:

1. Is there an effective way to **identify** and **quantify** REOB when added to bitumen?

2. How does REOB modification, at **different dosages** and **ageing** levels, alter bitumen characteristics; *chemically*, *rheologically* and *mechanically*?
3. How does REOB modified bitumen perform as **compared to original/unmodified bitumen**?
4. What **correlations** exist between *rheological* and *chemical* characteristics of (non-) REOB modified bitumen?

To bundle these research questions into a single hypothesis that will be tackled in this report, it is formulated as:

- With **chemical analysis** one will be able to **identify REOB** in a bitumen and see its effects on the **chemical composition**; such chemical changes will reflect on changes in **rheological behaviour** of the bitumen but also on **mechanical performance**, concluding what chemical/rheological properties of a **base bitumen** are important to successfully receive REOB modification.

The goal of this research is to identify REOB qualitatively and possibly quantitatively in bitumen using a combination of chemical, thermal, and rheological characterization tools, with a specific focus on low-temperature properties. To apply a multi-scale approach on the evaluation of REOB modified bitumen behaviour and performance, other tests are performed as well. To show time-temperature relation of the material and its behaviour at varying temperatures rheological tests are carried out on the bitumen. This is expanded by assessing the adhesive/cohesive failure behaviour of the bitumen and mastic, addressing possible issues of REOB modification at microscale. Lastly, full-scale asphalt mixture tests including the indirect tensile test (IDT) and the Cantabro abrasion test are performed to give an indication of risk to cracking/ravelling and the susceptibility to moisture/freeze-thaw damage.

1.3. Report structure

The thesis proposes a methodology to identify REOB in bitumen and assess REOB-bitumen blend properties at varying REOB content. Its aim is to provide guidelines for the use of REOB in bitumen, offer a qualitative evaluation of performance, and characterize the properties of such blends. Additionally, an attempt will be made to create a methodology to present a quantification of total REOB content, while also mapping the chemical and rheological changes to performance characteristics. Adhesive/cohesive performance of the blends and asphalt mixture mechanical testing of the REOB blend are conducted to assess properties of the binder on application level.

All these tasks are handled in this thesis within separate Chapters. Chapter 2 presents the literature review of previous work performed on the subject of REOB showing the state-of-the-art around the use of REOB in the pavement industry. Chapter 4 will delve into the chemical characteristics of unmodified and REOB modified bitumen. This Chapter specifically includes the identification method of REOB inside bitumen, in paragraph 4.2. This is followed by Chapter 5, which comprises the evaluation of rheological characteristics of unmodified and REOB modified bitumen. Chapter 6 goes into detail on the correlations between rheological and chemical characteristics of REOB blended bitumen. Next, Chapter 7 presents the mechanical response and performance of REOB modified bitumen, mastic and REOB modified asphalt mixtures, including susceptibility towards moisture and freeze-thaw damage. A discussion of all results, followed by conclusions and recommendations are presented in the last Chapter 8.

N.B. If for any reason abbreviations are used to describe tests or tools but were not explained as to what they mean, one can use the Glossary on pages 10 and 11.

Chapter 2. Literature review

The literature review on REOB serves a dual purpose in this thesis. Firstly, it provides a chronological overview of the research conducted on REOB, offering insight into the evolution of knowledge in this field over time. Secondly, it serves as a guide for the reader, outlining the current state-of-the-art regarding the use, characterization and assessment of performance of REOB in the pavement industry. From this Chapter, the reader gains an understanding of the experimental tools employed in this thesis and the broader context in relation to the application of REOB. This review provides an overview of characterization tools and method of analysis while outlining the significance and relevance of the research conducted in this study.

2.1. General application of REOB and nomenclature

As the use of REOB has shown to be very inconsistent in both regulations and in the industry (Baumgardner et al., 2023), therefore the following question arises at first: *Why would one use REOB to modify bitumen or a binder to begin with?* There have been a number of situations where REOB, or a variant of this oil, have shown to be a possible solution to the occurring problems. Some of those are:

1. Usable as an extender for:
 - Hard grade bitumen
 - Oxidised/air blown bitumen
 - Polymer modified bitumen
 - To improve low temperature PG properties
(important in USA/Canada, especially cold climatic regions)
2. Usable as a rejuvenator for:
 - Reclaimed Asphalt Pavement (RAP) / Aged bitumen
 - Reclaimed Asphalt Shingles (RAS)
3. Motivation behind using REOB:
 - REOB is a residue from refining WEO where the re-usable lubrication oils are already removed. Finding a usable purpose for this otherwise waste source will be beneficial.
 - REOB is often cheaper than alternatives

Re-refined engine oil bottoms (REOB) can be known by other acronyms but are also related to similar residuum of oils. Some of these names and abbreviations are mentioned in Table 2.1.

Table 2.1: Various Names Associated with REOB/VTAE adapted from (AsphaltInstitute, 2016)

Acronym	Name
	Asphalt flux
	Asphalt blowdown
EOR	Engine Oil Residue
RHVDB	Re-refined Heavy Vacuum Distillation Bottoms
RHVDO	Re-refined Heavy Vacuum Distillation Oil
REOB	Re-Refined Engine Oil Bottoms
RVTB	Re-refined Vacuum Tower Bottoms
VTB	Vacuum Tower Bottom
VTAB	Vacuum Tower Asphalt Binder
VTAE	Vacuum Tower Asphalt Extender
WEOR	Waste Engine Oil Residue
WODB	Waste Oil Distillation Bottoms

It is therefore important to know the difference between these different oils, as well as what general processes actually can be applied to refining WEO. Such an overview, about how WEO can be re-refined to result in REOB as a residue, has been created before comprising of main processes such as the four mentioned below (Sarkar et al., 2023):

1. Acid-clay and its modification
2. Vacuum distillation and its upgradation
3. Hydro-treating
4. Extraction-flocculation with integrated adsorption process

These basic processes are also bundled and used together to re-refine the WEO. In the case of REOB, this will only be created with the process of Vacuum Distillation within such a refinery.

Important to note, is that the use of REOB is relatively new for the pavement industry although the counterpart of it, WEO, has been in use since before the 1980s (Baumgardner et al., 2023; Herrington, 1992). The following flowchart should clarify the difference between these two compounds better:

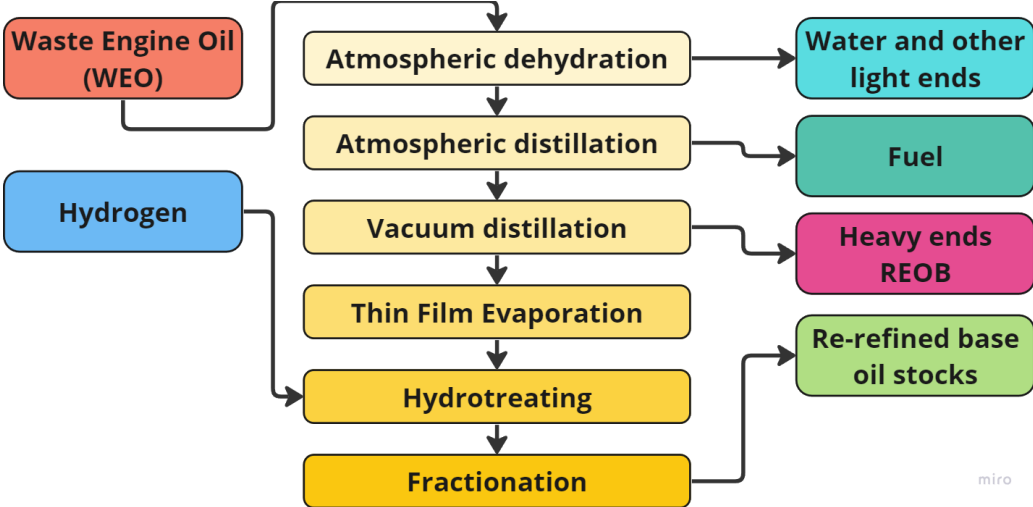


Figure 2.1: Flow chart of the vacuum distillation and hydrotreating process for re-refining of WEO adapted from (Baumgardner et al., 2023; Ratiu et al., 2022)

The use of WEO in the pavement industry was initially the solution for the previously mentioned problems, but as Figure 2.1 shows, the refining of these oils makes it possible to obtain re-refined base oil stocks. With environmental impacts rising and an increased motivation to recycle and improve processes, the chance that WEO will be used in the pavement industry as compared to REOB will thus only decrease more and more over time.

Before moving on and going into detail what research has been done on REOB, it is important to note that Engine Oil (EO) varies in properties due to additives used depending on its application in different engine types. WEO may come from various sources and mostly a mixture of different WEOs. Therefore processing each batch of WEO results in varying compositions of REOB. A combination of additives is commonly added to engine oil initially to obtain optimum lubrication within a broader range of operational temperatures and to ensure its prolonged use. Some trace metals, not linked to additives, are formed over time due wear during the use-phase. However the following list of characteristic components in engine oil is therefore presented based on literature (Minami, 2017; O'Brien, 1983; Speight & Exall, 2014; Wong & Tung, 2016).

Table 2.2: Trace metals present in REOB, which techniques to measure them and the origin of the metals

Trace metal or element	Element name	Origin	Main/most common purpose
Calcium	(Ca)	Lubricant additives, alternatives and from usage Calcium-sulfonate, calcium phenate, Calcium alkyl salicylate or calcium carbonate	Antioxidants, acid scavengers and anti-wear additives
Nickel	(Ni)	Nickel dibutylthiocarbamate, nickel borate, nickel sulphide or nickel nanoparticles:	Anti-wear additives
Phosphorous*	(P)	Phosphate esters, thiophosphate esters, metal-based phosphate esters and phosphorous containing ionic liquids	Anti-wear additives (but in the US one can also expect PPA in bitumen)
Copper	(Cu)	Copper nanoparticles, copper sulphide, copper carboxylate and copper naphthenate	Anti-wear additives, detergents and elimination of fungi or bacteria
Molybdenum	(Mo)	Molybdenum disulfide, molybdenum dialkyldithiocarbamate, molybdenum boride and molybdenum nanoparticles	Anti-wear additives
Zinc	(Zn)	Zinc dialkyldithiophosphate, zinc oxide, zinc alkyldithiophosphate and zinc carboxylate	Anti-wear additives and acid scavengers
Potassium	(K)	Not normally used for lubricants but: Potassium persulfate and potassium carbonate	Anti-oxidants and acid scavengers
Silicium	(Si)	Silicone (oil)	Commonly used in dashpots, wet-type transformers, diffusion pumps, and in oil-filled heaters but also antifoaming agents
Iron	(Fe)	Metal surface of engines	Wear particles
Vanadium	(V)	Present in the steel of engines	Wear particles
Magnesium	(Mg)	Magnesium sulfonate, magnesium phenate, magnesium alkyl salicylate and magnesium carbonate	Anti-wear additives and acid scavengers

*** Phosphorous can only be measured with the XRF when an inert gas like Helium is used to coat the sample**

The table above shows some of the trace metals to be found in bitumen, possible to link to the origin of REOB. Such trace metals can be linked to additives that were added to the engine oil initially and have ended up in the REOB, whereas vanadium, iron and nickel can already be present in the bitumen merely due to crude oil source. However copper, zinc, vanadium and iron can also be wear metals from the engines in which the lubricants were used.

As the composition of REOB can be varied due to its source, this very aspect should be considered while going through the literature on REOB and its performance as a component of asphalt binder. Only when papers show how the REOB differs chemically, one is able to effectively compare results between researches. One should be aware that REOB is definitely something different than both WEO and bitumen, thus one should keep in mind that its effects on bitumen modification would be vastly different.

2.2. Overview of literature on REOB modified bitumen

To show what the focus of research regarding the use of REOB in the pavement industry has been for the past years, a small diagram has been created and is shown in Figure 2.2. It covers the span of years between 1980s and the present, showing the different focus areas that researchers have worked on regarding the use of REOB.

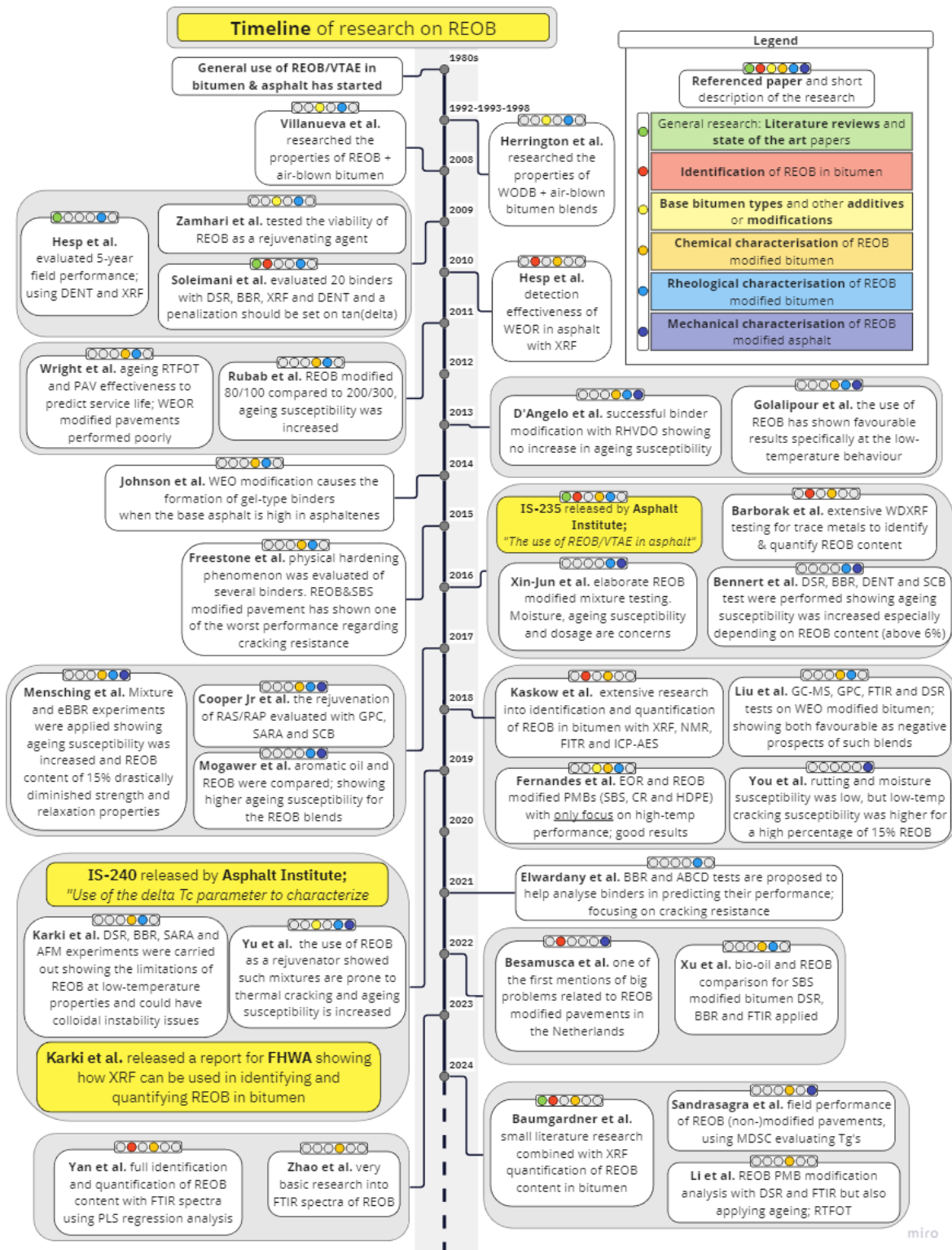


Figure 2.2: A timeline of research on WEOR/REOB/VTAE fluxing with bitumen

Using the legend in Figure 2.2 one can follow different aspects of REOB that have been studied already and which combination of topics are addressed in each research paper. Important to note is that not a single research has handled a REOB modified bitumen on all 6 different aspects, which therefore this thesis tries to achieve.

In the 1980s the use of REOB/VTAE to flux with bitumen in the industry has roughly started and the first three researches were performed by Herrington et al. a decade later (Herrington, 1992; Herrington et al., 1993; Herrington & Hamilton, 1998). They fluxed WODB with air-blown bitumen (hard grade and heavily oxidized) and got favourable results. Like Herrington et al., Villanueva et al. also researched blending air-blown bitumen with an oil, but in this case REOB, which gave again positive results regarding both low and high temperature limits (Villanueva et al., 2008).

Comparing this, to again a decade later, Hesp et al. started a field performance evaluation study on several different pavements throughout the region of Ontario (Hesp et al., 2009). The cold climate there had been quite demanding of several pavements and the pavements with REOB modified bitumen were some of the worst performing. This caused the need to use a detection method, to determine if in-service pavements had been modified with REOB. Here the use of XRF was selected as the an optimum tool to identify REOB. A PhD student, from the same research team, continued this work and presented an evaluation of several binders (with and without REOB modification) using experimental tools like BBR, DSR, XRF and specifically DENT (Soleimani, 2009). A proposal was made for minimum limit of $\tan(\delta)$ for fresh binders.

The following year evaluation studies were performed on ageing susceptibility of REOB modified binders. Wright et al. researched the effectiveness of the ageing protocols of RTFOT and PAV, which should represent in-service pavement performance. The conclusion was that these methods had insufficient accuracy and binders that were modified with WEOR deviated significantly (Wright et al., 2011). As these were showing excessive ageing levels as compared to similar counterparts. This was followed up by a binder study on a 80/100 pen bitumen fluxed with REOB, compared to a neat 200/300 pen bitumen. The main conclusion drawn from the results was that ageing susceptibility had increased significantly for the REOB modified bitumen.

In 2013 two separate studies were disseminated by D'Angelo et al. and Gosalipour et al., they both performed an extensive study on RHVDO and REOB modified bitumen on both binder and mixture levels. It was shown that the RHVDO modified binders had no significant increase in their ageing susceptibility (D'ANGELO et al., 2013) and the use of REOB as extender was quite favourable for performance at low-temperatures (Gosalipour, 2013).

The next two years some research papers were published, which went into sol/gel-type bitumen behaviour and physical hardening effects (Freeston et al., 2015; Johnson & Hesp, 2014). This showed how bitumen that initially had quite high asphaltene content, caused to become a gel-type bitumen after the fluxing with WEO. This explained the drastically poor performance of such binders at the low temperatures in the cold climate of Ontario, going against initial expectations. They became too stiff and inflexible, explaining the excessive cracking. Although it is also not suggested to use a base bitumen with very little asphaltene content, as then there is also no elastic micelle structure present in the bitumen anymore. In the same research the REOB+SBS combination has shown really poor cracking resistance for mixtures after an ageing period of 72h oven ageing, suggesting that a combination between both polymer and REOB modification is not optimal.

For all those years the discussion on if REOB modification of bitumen binders was beneficial or not ensued, and in 2016 the Asphalt Institute released a full-scale report on the use of REOB/VTAE (AsphaltInstitute, 2016). This comprised of both a literature study of papers and presentations on REOB and some variants, as well as several experiments carried out on a controlled group of different REOB, bitumen and blends of the two. In the same year a few other papers were released. An extensive analysis

was performed for the use of WDXRF to determine REOB presence and content in bitumen (Barborak et al., 2016). The two other papers focussed on REOB blends and mixtures, showing moisture and ageing susceptibility was increased as well as concerns of high dosages of REOB (Xin-jun et al., 2016), and the other paper going into detail on DSR, BBR, DENT and SCB tests which have shown that REOB modified bitumen with dosages above 6% showed unfavourable results (Bennert et al., 2016).

The year after, Mensching et al. performed both DSR and eBBR experiments, coming to the conclusion that REOB dosage at 15% would have clear detrimental effects on cracking resistance and general performance of the bitumen (Mensching et al., 2017). In a comparison between REOB and aromatic oil, it became clear that REOB had similar capabilities, although significantly increasing the ageing susceptibility of the binder, while the aromatic oil did not (Mogawer et al., 2017). And instead of using REOB to flux with a hard grade bitumen, its rejuvenation effect on RAS and RAP was evaluated, using mainly tests like SARA and GPC to look into changes in chemical composition which were complemented with SCB tests to show cracking susceptibility (Cooper Jr et al., 2017).

Next, an extensive study was carried out in using several chemical tools to identify and quantify REOB in bitumen, mainly using the already mentioned XRF but also FTIR, NMR and ICP-AES (Kaskow et al., 2018). A study on high-temperature behaviour for specifically PMBs, using SBS, CR and HDPE, when they are blended with EO or REOB, showing quite good results within the limited scope (Fernandes et al., 2018). Meanwhile a binder study was performed using DSR, FTIR, GC-MS and GPC showing both favourable as negative results for WEO blends (Liu et al., 2018). Lastly, mixture scale testing was performed on REOB modified asphalt mixtures which showed similar rutting and moisture susceptibility like unmodified bitumen, although the 15% dosage showed increased thermal cracking susceptibility (You et al., 2018).

In 2019 a number of three different reports were published; the Asphalt Institute released IS240, which focussed on the use of ΔT_c which is retrieved from BBR tests as a tool to predict performance issues of binders (AsphaltInstitute, 2019). The FHWA released two reports, one of them continuing the work of Cooper Jr et al. and showing the limitations of using REOB in combination with RAS/RAP (Daly et al., 2019). The other report focusing on how XRF can serve both the pavement as the roofing industry to determine REOB presence and dosage (Karki et al., 2019). Karki & Zhou also released a paper in which DSR, BBR, SARA and AFM experimental results were evaluated, giving an insight into the limitations of REOB blended bitumen at low-temperatures and colloidal instability concerns (Karki & Zhou, 2019). Next to that, thermal cracking and ageing susceptibility were big concerns when REOB was used as a rejuvenator for aged bitumen (M. Yu et al., 2019).

A single paper was released in 2020, implementing REOB in its research, which used BBR and ABCD tests to predict a binders performance, having a focus on cracking resistance (Elwardany et al., 2020). They were able to categorise modified (like REOB) binders in performance categories, when ΔT_c and dT_f are used in combination.

In 2021 a conference paper was submitted which, as one of the first, pinpointed waste engine oil as the cause of some of the workability problems of the mixtures (Besamusca et al., 2021). Mainly pavements using PMBs and WEO/REOB modified binders have shown to give poor performance, already during pavement construction. The same year an evaluation of bio-oil compared to REOB as extender for SBS modified bitumen (Xu et al., 2021). The bio-oil came out as a better option than the REOB, based on the fact that for REOB blends the ageing susceptibility was increased and fatigue life was lower. Low temperature behaviour was worse than neat bitumen for both blends and it was made clear that SBS deterioration was non-dependant on the oil added.

An application of PLS regression to ATR-FTIR spectra of bitumen that are modified with REOB, was used by Yan et al in 2022. Here a relatively accurate method was developed to predict REOB dosage using a full spectrum between 4000 and 600 [cm^{-1}] (Yan et al., 2022). The same year, a very limited

research was published, with the main value being that it analysed the FTIR spectrum of REOB and REOB modified bitumen (Zhao et al., 2022).

In the same year that this thesis is written, a few other researches have studied the REOB modification of bitumen as well. A small and concise literature review and the use of XRF to identify and quantify REOB in bitumen was published (Baumgardner et al., 2023). Several PMBs were studied, using DSR and FTIR to analyse the REOB modified binders, although regarding ageing only RTFOT was used (Li et al., 2023). Lastly, a study on binders which could be compared to in-field performance were analysed with the MDSC, which was able to show changes in T_g and how the REOB modified binders showed good compatibility at fresh stage at incompatibility at higher ageing levels (Sandrasagra et al., 2023).

2.3. State-of-the-art research on REOB modified bitumen

With the timeline of REOB usage evaluated, the different subjects regarding the use of REOB and the experimental tools used to evaluate it, are described in the following paragraphs; numbered in the following way:

- I. Impactful processes in refineries/distributors**
 - a. Deasphalting, Oxidation, Thermal cracking, Hydrotreating/desulphurisation
 - b. Fluxing; blending of bitumen with different grades and third-party blenders
- II. REOB modified binder properties**
 - a. Detection and quantification of REOB in bitumen (XRF/ICP & FTIR/NMR)
 - b. Rheological characterisation
 - i. Viscous and elastic behaviour both at low and high temperatures (DSR)
 - ii. Low temperature stiffness and relaxation evaluation (BBR)
 - c. Chemical characterisation
 - i. Functional groups ((ATR-)FTIR)
 - ii. Iatrosan chromatograms (SARA analysis)
 - iii. Molecular weight distributions (GPC)
 - iv. Glass transition and heat capacity evaluation ((M)DSC)
- III. Blending of REOB in combination with polymers**
- IV. REOB modified asphalt mixture properties**
 - a. Cracking and rutting susceptibility
 - b. Adhesion, cohesion properties and ravelling susceptibility

State of the art research performed on the above mentioned aspects are described in the following paragraphs. The goal is to bring all this background knowledge together in this Chapter, to create an overview of the impact of REOB in the bitumen on the industry and which tools have been and can be used to analyse REOB modified bitumen.

I. Impactful processes in refineries

a. Deasphalting, Oxidation, Thermal cracking, Hydrotreating/desulphurisation

Currently, the bitumen market and asphalt industry have to deal with variations in bitumen properties, that arise from the changes that happen in the refinery industry, the availability of crude sources and the diverse refining procedures and blending components applied by contractors at refineries and asphalt mixture plants.

An overview of bitumen manufacturing and characterisation methods, is provided by the Shell bitumen handbook (Read & Whiteoak, 2003). Several of current practices used in refineries, like: deasphalting, hydrotreating and desulphurisation are now commonly used techniques of which their impact on bitumen performance has not yet been clear.

In the Netherlands, there have been problems occurring regarding premature ravelling/cracking and poor workability of the asphalt mixtures (Besamusca et al., 2021). Research has been performed to map

different changes in refineries happening specifically in the Netherlands to figure out what the impact could be on performance (Nahar et al., 2020). These have both shown that many changes are happening in recent years and their impact on performance remains ambiguous.

For example, recently applied IMO 2020 regulation makes sure that less sulphur is allowed in bunker fuels; namely to a maximum of 0.50%. This regulation directly caused the refineries to apply techniques to remove the sulphur from those fuels, which can affect the composition of bitumen. The sulphur content of many bitumen has therefore steadily increased and its effect on performance has shown negative effects (Mousavi et al., 2022).

Fluxing; blending of bitumen with different grades and third-party blenders

Next to these changes in the way that bitumen is processed and produced, sometimes modifications are directly applied to bitumen. One of these is for example the technique of fluxing bitumen. Fluxing is effectively lowering the viscosity of bitumen with a solvent or another oil medium. Common practice is the use of kerosene, although the use of fluxing has been reduced over the years (Read & Whiteoak, 2003).

The benefits of fluxing, is the ability to turn a harder grade bitumen to a softer grade, by adding a solvent or softer component to it. An even better application is to use a solvent/soft binder that is already a waste product. This scope introduces the possibility of using Re-refined Engine Oil Bottoms (REOB), also known as vacuum tower asphalt extender (VTAE). An extensive research, both literature review and an addition of experimental research, was performed by the Asphalt Institute (AsphaltInstitute, 2016). The FHWA performed such a literature review and experimental research as well, showing the possibility to use XRF to identify presence of the compound in bitumen (Karki et al., 2019). Both have shown implications of the use of REOB and show what is a big problem with this fluxing ingredient/modification; the identification of it in bitumen. They state that using XRF is a viable option for identification, although it has its limitations.

Next to identifying or even quantifying the REOB dosage in bitumen, the performance of this modifier has also had varying results. It is able to mix well with bitumen, but has sometimes shown increased ageing and moisture susceptibility. Due to the many and sometimes contradicting research results on the performance of REOB modified bitumen, it is still unclear for the market what the best practice for its use would be.

REOB modification is currently not acknowledged when used in Europe, and does not hold its own CAS number and therefore is seen as “just bitumen”. In the USA the use of this product is better known, as is shown by the DOTs their regulations in the USA (Baumgardner et al., 2023). Limitations vary between: no use allowed; only <5%; between 5-8%; maximum 20% and lastly no limitations. This shows that there is no maximum dosage agreed upon, even within the bitumen market of the USA that has already applied REOB (or other variants of WEO) for the past 40 years.

II. REOB modified binder properties

a. Detection and quantification of REOB in bitumen (XRF/ICP & FTIR/NMR)

To tackle the problem of knowing if REOB is added to the bitumen or not, identification and quantification tools have to be applied. In several researches the use of XRF was chosen as the way to proceed (Baumgardner et al., 2023; Hesp & Shurvell, 2010; Karki et al., 2019; Kaskow et al., 2018). This method makes use of a handheld x-ray scanner, which is able to measure the presence of trace metals in binders. An alternative to XRF would be ICP, which is able to measure the concentration of specific elements directly. The most important metals to be measured are: Zinc (Zn), Calcium (Ca), Copper (Cu), Molybdenum (Mo), Vanadium (V) and Potassium (K). REOB contains these metals, although bitumen generally does not, or at very low levels only. Measuring the intensity and thus finding the ppm count of these metals, an effective estimation can be done of the REOB dosage in the bitumen.

The papers have shown though, that there are some limitations to the use of this method. One of the main things is REOB by itself. This material can vary quite a lot between the producers or moment of production and the amount of trace metals in them will therefore vary as well. Not knowing what kind of REOB was used in a modified bitumen, makes this quantification more difficult and inaccurate.

Additionally some recent study has reported the use of ATR-FTIR spectroscopy to characterise REOB (Kaskow et al., 2018; Yan et al., 2022). With this tool, retrieved spectra show distinctive changes in their profile due to the addition of REOB. Adding REOB namely introduces, or contributes to the intensity of them, carbonyl peaks, the presence of a small PIB peak and lastly a shift in the slope of the Si-O-Si region. Measuring the peak areas and slope was applied as a quick check for quantity of the REOB, but the paper mainly describes on how to apply a regression method/analysis for the REOB estimation. This regression method is, like with XRF, also quite dependent on knowing the profile of both neat bitumen and REOB to be accurate.

Seeing that FTIR spectroscopy is applied more throughout chemical laboratories that handle bitumen, this is possibly a much more preferred tool to identify and quantify REOB in bitumen than XRF would be. Both methods are quite quick to perform, although FTIR spectra of bitumen are commonly used to study the formation of specific functional groups with ageing and to identify the presence of polymer additives like SBS and XRF has not yet another use in bitumen research laboratories.

b. Rheological characterisation

i. Viscous and elastic behaviour both at low and high temperatures (DSR)

One of the ways to describe a materials' behaviour, is by performing rheological experimental tests. Dynamic shear rheometer (DSR) is one of such experimental tools, which is able to test the materials stiffness and viscous response at different temperatures and loading(rates). Tests should be performed at various temperature intervals, after which the obtained curves can be shifted towards a single master curve that represents a specific reference temperature. This procedure is based on the time-temperature superposition principle.

Different methods to obtain these master curves can be applied, as they vary from visual to mathematical, horizontal but also vertical shifting of the data. One of the most used models is the Christensen-Anderson-Marateanu model (CAM-model). Many researchers have discussed over the years, as to what is the best model and approach for obtaining the master curve (Anderson et al., 1994; Chen et al., 2022; Christensen et al., 2017; Marateanu & Anderson, 1996). But instead of fully applying such an alteration, one can shift the data horizontally and obtain a shifted but not excessively altered master curve.

Although master curves show a broad overview of a materials behaviour at otherwise impossible frequencies/temperatures to test at, black space diagrams are quite effective in showing stiffness-viscosity behaviour of the material as well. It also visualises a full curve without needing to shift any data. Ageing, rutting and cracking limits are easily visualised in diagrams like this (Airey, 2002; Airey et al., 2021; King et al., 2012).

Although the behaviour of single binder plotted in previously described diagrams will help comparing rheological behaviours of binders, distinctive values are comparable to other parameters found in rheology, chemistry or mechanical tests. The use of rheological indices is therefore also a valuable procedure to describe a binder its characteristics (Morian et al., 2015).

The previously described DSR test mainly was about performing frequency sweep tests. Although this gives a small insight in what certain limits are to a binders stiffness and its viscous response, it does not say anything about performance of the binder. Such a test is for example a linear amplitude sweep (LAS) test. This means a sample is put under increasing shear stress according to a linear increase in strains. Ultimately the material fails, showing a specific behaviour until failure. Binder modification can clearly redetermine the fatigue properties of a material, as has been researched before (Wang et al., 2015).

Not much can be said yet about the frequency sweep results of REOB modified binders, as they currently show to follow a similar trend as neat bitumen. Although with ageing they tend to achieve a more stiff and less viscous response; i.e. a lowering of the curve in a black space diagram, higher and flatter curve for a $|G^*|$ master curve etc.

ii. Low temperature stiffness and relaxation evaluation (BBR)

Instead of evaluating a broad range of different temperatures, one could also lay more focus on the rheological behaviour of a binder within the low-temperature region. This is possible to achieve with the use of the bending beam rheometer (BBR). An elaborate review of the use of this machine, has been performed by the Asphalt institute. Showing what use the ΔT_c has throughout the differences of bitumen and applied additives (AsphaltInstitute, 2019).

This experiment is able to describe the stiffness and relaxation capabilities of a binder at different temperatures below 0 [$^{\circ}C$]. It retrieves an S-value, m-value, $T_c(S)$, $T_c(m)$ and lastly the $\Delta T_c (= T_c(S) - T_c(m))$. These parameters have shown to be well correlated to parameters obtained from DSR tests (Lesueur et al., 2021; Rowe, 2016), for example the R-value.

By obtaining the ΔT_c , one can say something about the ageing level of a binder, which is thus well correlated to the R-value (Lesueur et al., 2021). Here it was made possible and proven the correlation between ΔT_c and the R-value. Looking at the binder modified with REOB, this had one of the lowest ΔT_c values (one of the most negative). Here it was also stated with much urgency, that ΔT_c is only strong related to a pure rheological origin and thus does not in any way describe cracking susceptibility, as rheology is defined as “defined as the science of deformation and flow of matter” does not consider cracking issues.

c. **Chemical characterisation**

i. Functional groups ((ATR-)FTIR)

To chemically characterise bitumen, several tools can be used. One such tool is for example ATR-FTIR, which is a variant of originally an FTIR. With it, one is able to identify and also quantitatively measure the presence of certain chemical functional groups in bitumen.

The spectrum of bitumen is quite consistent, although in the fingerprint area (at the lower wavenumbers) some specific changes can be measured. Regarding ageing of a binder, one can clearly see changes at peaks signifying carbonyl and at peaks signifying sulfoxide (Yut & Zofka, 2011). But next to ageing the presence and degradation of polymers such as SBS can be seen as well in the spectra obtained. With spectra easily obtained from ATR-FTIR tests, having high reproducibility of results is beneficial to further expand the use of the technique. Especially one wants to quantify changes, such as carbonyl and sulfoxide contents, and the common way to do this is with indices. It was found that using an ATR spectrum, baseline correction, normalising the distribution and to take areas integrated from the curve to the baseline, was the best way to obtain these indices (Hofko et al., 2017). Alternatively to using indices, one also has the possibility to apply multivariate analysis such as PCA, PLS and LDA. This is able to differentiate spectra on ageing level or even their heritage (Ma et al., 2023).

The previously mentioned PLS, an abbreviation for partial least squares analysis, can be used to determine the quantity of REOB present in a bitumen. This is quite an effective tool, although its accuracy partly depends on knowing the separate spectra of the used REOB and neat bitumen, which is often not possible for the industry (Yan et al., 2022).

Lastly, one should be aware of several procedures to alter obtained spectra with ATR-FTIR. Normalisation and baseline correction, like Hofko et al. applied as previously mentioned, are only partly of what is possible. Shortly after the development of the ATR technique, a correction was proposed for ATR-FTIR spectra, to correct the deviations that occur in the fingerprint area. The corrected spectra

have a much better correlation, at these lower wavenumbers, with spectra that are obtained from “standard” FTIR measurements (not depending on reflectance) (Nunn & Nishikida, 2003).

ii. Iatroscan chromatograms (SARA analysis)

The use of SARA, which stands for Saturates-Aromatics-Resins-Asphaltenes and follows from iatroscan measurements after separation of these fractions with n-heptane, has been quite common over the years in bitumen research. The division of these fractions can often explain rheological behaviours or changes, i.e. the asphaltene fraction has strong correlation with several rheological properties. “*Thereby, an increasing gel character of bitumen causes first an increasing stiffness captured by the complex shear modulus $|G^*|$, second an increasing viscosity captured by the softening point and the complex viscosity $|\eta^*|$, third an increasing elastic deformation behaviour captured by the phase angle δ and fourth a decreasing temperature sensitivity captured by the penetration index I_p .*” as found by Weigel et al. (Weigel & Stephan, 2018). Next to that, the molecular weights of the maltenes fraction seemed to be strongly related to low temperature behaviour, found with BBR measurements.

Regarding REOB blended with bitumen, other results have also been found. For example with the colloidal instability index, CII, which is calculated by:

$$CII = \frac{\text{Asphaltenes} + \text{Saturates}}{\text{Aromatics} + \text{Resins}} \quad (2.1)$$

Has shown that with increasing the dosage, this value goes up significantly. In theory the higher this index is, the higher the incompatibility of the binder (a low dispersive capacity of asphaltenes in maltenes), and similarly higher ageing (Karki & Zhou, 2019).

iii. Molecular weight distributions (GPC)

Next to using SARA or FTIR, the use of GPC has become quite common as well, mainly in polymer science/industry however. The main use of this technique lies in the fact that it can show the effect of ageing of a bitumen clearly or show the presence certain additives like polymers easily.

One of the first papers published on the use of GPC for bitumen evaluation, stated observations like viscosity properties of bitumen were mainly related to larger-size molecules and penetration values were mainly related to medium-sized molecules (Kim & Burati Jr, 1993).

Next to using GPC, the deconvolution technique that was developed is also possible to be applied to the weight distributions found with GPC. Especially with the weight distributions of bitumen, the maltenes have a skewed side but with deconvolution it is possible to separate such curves into separate fractions (Torres-Lapasió et al., 1997). This deconvolution was also used to split weight distributions into different fractions like asphaltenes, maltenes, polymers or trivial fractions (Daly et al., 2019). Next to that, it is possible to see that a bitumen was air blown or contained RAS clearly.

Similar results were found by Ma et al., using GPC one could quantitatively analyse the “emerging new asphalt binders developed in recent years such as high-viscosity asphalts and bioasphalts”. It was proposed that one should use normalised distributions, use specific thresholds for modified binders, use deconvolution to characterize changes in the profile (Ma et al., 2021).

Lastly, specifically regarding REOB blended bitumen was evaluated as well. It was found that REOB mainly consisted of medium-sized molecules, with a relative high quantity as compared to large-sized molecules. The blending of REOB with bitumen was deemed as diluting the bitumen, mainly reducing the stiffening effect that the asphaltenes have in the bitumen (Cooper Jr et al., 2017).

iv. Heat capacity evaluation ((M)DSC)

An extensive analysis of the use of MDSC was performed by Kriz et al., resulting in more knowledge on how the derivative of the reversible C_p can show incompatibility of an amorphous binder, the effect

of evaporation, weight loss and oxidation with ageing. Interesting was that it was not found that with ageing phase separation would take place on its own. The isothermal conditioning of the samples became very important, as significantly different results were obtained for the T_g values of aged bitumen (Kriz et al., 2008).

But the conditioning of samples and ageing effects are not the only thing the DSC can show. A good correlation can be found between AFM results and the heat flow found with DSC, one can see how bee-like structures (signifying wax in the bitumen) can form and dissolve with different temperatures, correlating with the endo or exothermic peaks measured with DSC. This means that changes in phases of a bitumen, can be both seen by AFM and DSC (Soenen et al., 2014).

To continue, one can evaluate the DSC thermal curve also by using derivatives of the obtained heat flow, to estimate T_g based on the peak that occurs in that curve (i.e. the maximum in slope and not halfway between onset and offset of the glass transition). This was used to estimate T_g , but next to that the Fox equation was used to describe the change in T_g when blending bitumen with a polymer (Apostolidis et al., 2021):

$$\frac{1}{T_g(PMB)} = \frac{w_{SBS}}{T_g(SBS)} + \frac{w_{bit}}{T_g(bit)} \quad (2.2)$$

As was proposed in the previous research, fractionating bitumen in different chemical compounds could be able to clarify certain behaviours of the bitumen as a total (Chailleux et al., 2021). It was then proven that the T_g 's of bitumen fractionated in four groups (similar as to iatrosan SARA analysis), show that the blending law applies to the maltene fractions to determine the glass transition of the unfractionated bitumen. Nevertheless, the asphaltenes were also important but mainly for crystallisation, linked especially to rheological characteristics, as they contribute to structuring within maltenes. Splitting the maltenes into three different fractions: F1, F2 and F3 one has a similar representation of the SARA fractioning, but the ability to test each of them separately. It was then shown how the F1 fraction would contribute to the viscous behaviour of the total bitumen, whereas the F2 and F3 would interact more with the crystallisable fraction, changes in ratios between these would explain how a bitumen can gain in viscosity with ageing.

To conclude, the effect of REOB on bitumen was evaluated with MDSC as well. Several bitumen were used, next to results from field samples and stored bitumen, to evaluate and compare the ageing susceptibility. The single pavement with REOB modified bitumen was arguably one of the worst performing and using artificial ageing on the original REOB modified bitumen, the DSC result could show already incompatibility issues after 20h PAV (Sandrasagra et al., 2023), as a clear doublet peak was present, thus stating that there were multiple phases present in the binder.

III. Blending of REOB in combination with polymers

As mentioned before, several pavements have shown workability issues or premature failing at early stages of life, many of which were PMB pavements modified also with REOB (Besamusca et al., 2021; Hesp et al., 2009). With that in mind, the combination of REOB blended bitumen and polymer modification, could make an incompatible blend, which worsens when mixed with aggregates. Regarding this problem, the blending of engine oil (EO) and/or REOB has been evaluated with several possible polymer additives, showing good rheological and chemical results, although all tests were heavily focussed on high temperature levels (Fernandes et al., 2018).

With the addition of REOB to bitumen, it has been found that it significantly deteriorates the performance of the bitumen, especially in the case that it was polymer modified with SB (Paliukaite et al., 2016). Using the DENT test, the CTOD value was able to show how strain tolerances were significantly reduced for REOB blended and SB modified bitumen. Only at very small quantities the

effects of the REOB would be detrimental, which would make a small change in grade possible or keep it roughly the same.

Alternatively, REOB can also be used as a compatibilizer for the SBS in bitumen. This is contradicting to what was stated before, as it was deemed unfavourable to mix the two. Although using only 1% of REOB, when using 5% of SBS, the results become actually favourable. A better uniformity and smaller particle sizes were possible for the SBS and REOB modified binder, compared to simple SBS modified bitumen (Li et al., 2023).

IV. REOB modified asphalt mixture properties

a. Cracking and rutting susceptibility

As binder chemical consistency and binder rheology alone can never fully describe the expected behaviour in the field, one needs to evaluate the full mixture as well. Several researchers have focussed on the possible performance issues that occur for REOB modified mixtures.

Performing long term oven ageing (LTOA) and short term (STOA) on REOB modified mixtures and following these up by rutting and cracking tests will give an overview of the limitations of REOB. This has been done by using the Hamburg Wheel tracking device, to measure rutting levels, performing Illinois Semi-Circular Bending tests and lastly low temperature cracking by using Disc Shaped Compact Tension tests (Mogawer et al., 2017). It was found that REOB modified bitumen had higher stripping susceptibility, binder ageing was increased for the REOB modified binders, REOB had way more variability in results as compared to aromatic oil and it was proposed to use an ageing protocol that ages the whole mixture (and not separate components).

Alternatively, to test cracking susceptibility, one can also use the indirect tensile test (IDT), including the moisture susceptibility tests. This was done on different dosages of REOB, and also different ageing levels STOA & LTOA, to see what effect this has on the performance (Xin-jun et al., 2016). The high REOB dosage of 15% had shown detrimental effects on the performance, especially with ageing, the lower dosages of 2.5% and 6% were varying a lot and seemed thus to be unaffected. Fatigue life clearly decreased with increased REOB dosage and the BBR measurements that were carried out as well, gave the conclusion that REOB modified mixtures had increased thermal cracking susceptibility. Rutting performance, cracking and moisture susceptibility and lastly low temperature thermal cracking resistance were all executed tests on REOB modified mixtures in separate research (You et al., 2018). Rutting resistance was not affected significantly by the REOB according to the Hamburg loaded-wheel test (LWT), as well as moisture susceptibility and stripping were not noticeably affected by the modification. A negative impact of the REOB was noticed with the semi-circular bend (SCB) test, which increased with increased dosage. The thermal stress restrained specimen test (TSRST) has shown too that an increase in thermal cracking susceptibility occurred with higher REOB dosage, however this only occurred at a dosage above 10%.

b. Adhesion/cohesion properties and ravelling susceptibility

Porous asphalt mixtures are very different to the commonly used SMA dense mixtures used in the world and in the previously described researches. One of the main problems with mixtures like these, is the failure phenomenon of ravelling. Because of the high void ratio and relatively low bitumen content, stones are more easy to come loose over time with mixtures like this. No effective tests have been developed yet to effectively describe the ravelling failure mechanism fully. There have been however several tests developed that focus directly on specific aspects of a binder or mixture, which have their own correlation to ravelling. Specifically adhesion and cohesion are important aspects that describe ravelling susceptibility partly, and these properties therefore will lead to an insight in the ravelling resistance of a mixture.

Adhesive tests, for example testing a thin bitumen film between 15-25 [μm] on tensile strength will show the adherence of the bitumen on the stone surface (Mo et al., 2009). The layer has to be so very thin, otherwise not the adhesion, but the bitumen cohesion will be measured. A typical temperature range for these tests is between -10 and 20 [$^{\circ}\text{C}$], although testing at -10 [$^{\circ}\text{C}$] makes the bitumen become too brittle to have accurate measurements and is therefore not recommended. There is always a transition between when adhesive or cohesive is more predominantly present, it was found that with low temperatures or significantly aged binders the adhesive failure will occur (Mo et al., 2011). Temperatures of either 0 [$^{\circ}\text{C}$] or 10 [$^{\circ}\text{C}$] show to give repeatable results and give a reachable temperature, but still causing an adhesive failure, for the test carried out.

Alternatively to focussing only on adhesion, cohesive failure is important too. Not only the cohesive failure of bitumen alone, but especially the effect of filler (making mastic) or even fine aggregates (making mortar), will show how well a binder will adhere and remain its cohesive strength when pulled apart (Wang et al., 2021). It was found that cohesive failure of a porous asphalt mixture below 30 [$^{\circ}\text{C}$] will exhibit a similar cohesive failure of mortar. At temperatures higher than 40 [$^{\circ}\text{C}$], it exhibits a similar cohesive failure of mastic.

The effects of using different fillers can also have an impact on the mastic/mortar cohesive properties. Typically used fillers in the Netherlands are Wigro, Wigro 55k and Wigro 60k. Standard Wigro is only based on limestone/calcium carbonate (CaCO_3), while the other two fillers have a percentage of hydrated lime ($\text{Ca}(\text{OH})_2$) in them, making it possible to react with water and other particles. It was found that the performance of these mastics and mortars were heavily dependent on the binders themselves, although in general the fillers (and especially the ones with hydrated lime) increased the stiffness of the mastic/mortar significantly (Woldekidan & Gaarkeuken, 2013).

To conclude: no tests like these have been performed yet on REOB modified bitumen, although the origin of this oil is being a lubricant and therefore one should not per se expect good adhesion. The lubricant additives present in REOB, or the stability of the oil in the bitumen, could have an effect on the adhesive and/or cohesive properties of mastic and should therefore be evaluated.

Alternatively, the use of the Los Angeles Cantabro Abrasion test has been applied for ravelling susceptibility in the past. With steel balls in a drum, the impact of these balls on the samples will lead to steady ravelling of the samples. By modifying the base consistency of a mixture, one can vaguely draw some conclusions on the susceptibility to ravelling. For example, the effect of asbuton (a natural asphalt rock material in Indonesia) on the ravelling susceptibility has been evaluated (Mabui et al., 2020). With increasing the modification content of the asbuton to “standard” mixture, it was found that the weight loss in the test decreased significantly. Alternatively to letting the full sample deteriorate in the machine, one can also wrap the samples partly to only allow one surface to receive the steel ball impacts and thus ravel. It was found that a low temperatures (-10 [$^{\circ}\text{C}$]) brought better ravelling resistance, rejuvenated bitumen had the least stone loss, followed by polymer modified bitumen and lastly the emulsified bitumen performed the worst (Xu et al., 2018).

Chapter 3. Research approach and material source

3.1. Research structure

To answer the research questions and thus the hypothesis stated, six different tasks will be carried out. These will each have their own results and can be compared to each other to give a full overview of different aspects of the problems described.

- Task 1:** Rheological and chemical characterization of bitumen and REOB (separately)
- Task 2:** Chemical characterization of REOB blends
- Task 3:** Rheological characterization of REOB blends
- Task 4:** Assessment of adhesive & cohesive properties of REOB blends
- Task 5:** Durability assessment of REOB blended asphalt mixtures

With this in mind, each task will be increasing the scale at which the problem of REOB modification is looked at. One can therefore connect every used test to the sub-nano, nano, micro, meso and macro scales as shown in Figure 3.1 below:

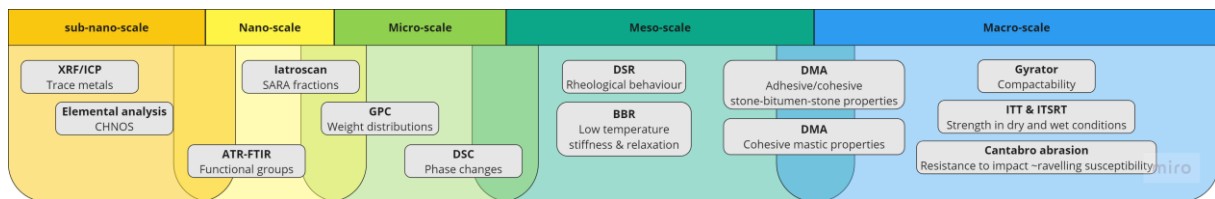


Figure 3.1: Overview of multiscale study with characterization methods

To give a short overview of all the used experiments and tests, the following flow diagram, Figure 3.2, describes which experimental tools are used in what tasks and the workflow that is followed.

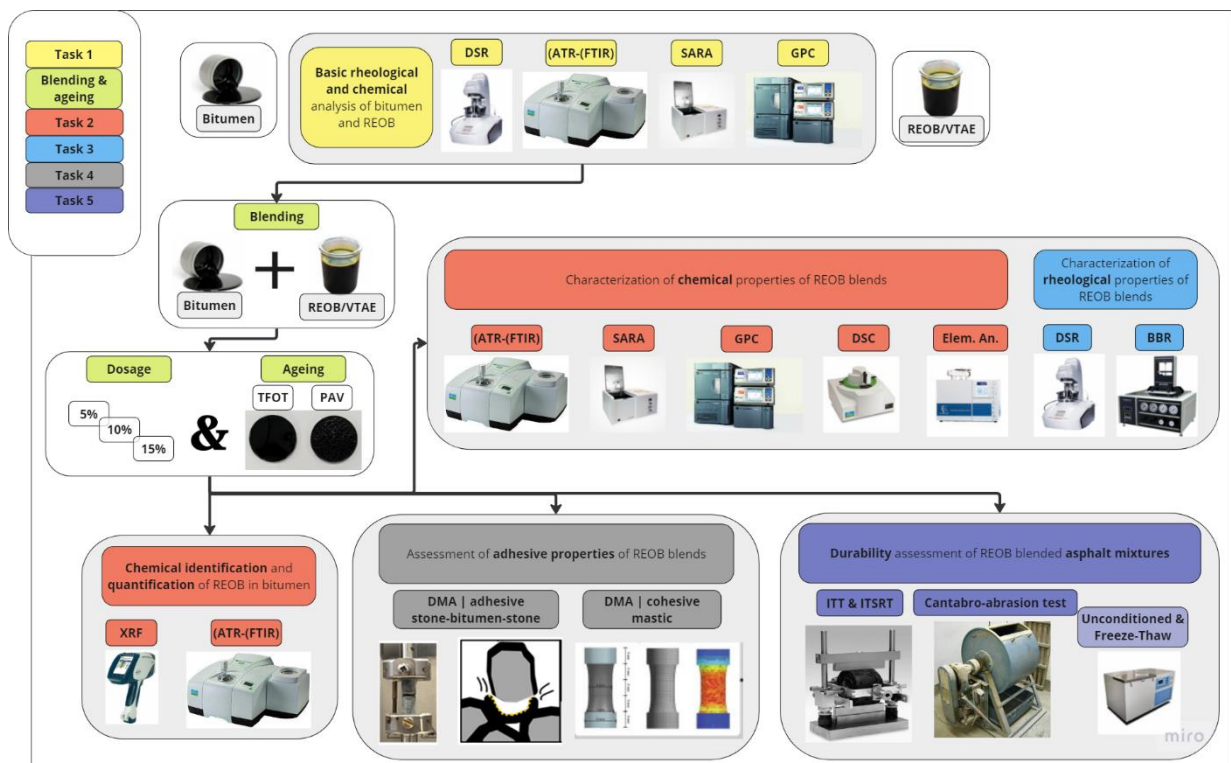


Figure 3.2: Workflow of tasks 1-6 for REOB (un-)modified bitumen

3.2. Different bitumen sources analysed in thesis

In the current thesis many abbreviations will be used to reference the different binders that are analysed. The following tables gives an overview of all of them used for each analysis; being of chemical, rheological and mechanical of nature:

Table 3.1: Unmodified and REOB modified bitumen for several chemical experiments at fresh and aged stages

Sample code	Grade (PEN)	Supplier	Chemical								
			Elem. An.		FTIR		SARA		GPC		
			Fresh	Aged	Fresh	Aged	Fresh	Aged	Fresh	Aged	
Unmodified bitumen											
bit-K	(20/30)	Sup1	X	X	X	X	X	X	X	X	X
bit-J	(70/100)	Sup1	X	X	X	X	X	X	X	X	X
bit-V1	(160/220)	Sup1	X		X		X		X		
bit-P	(15)	Sup2	X	X	X	X	X	X	X	X	X
bit-O	(85)	Sup2	X	X	X	X	X	X	X	X	X
bit-Q	(190)	Sup2	X		X		X		X		
bit-L	(70/100)	Sup3	X		X	X	X		X	X	
bit-G	(40/60)	Sup4	X		X	X	X		X	X	
bit-I	(160/220)	Sup4	X		X				X		
bit-M	(70/100)	Sup5	X		X		X		X		
bit-N	(40/60)	Sup5			X				X		
bit-6604	(40/60)	Sup6	X		X		X	X	X		
REOB											
REOB-X	-	Sup8	X	X	X	X	X	X	X	X	X
REOB-Y	-	Sup8	X		X		X		X		
REOB-Z	-	Sup9	X		X		X		X		
Bitumen + REOB blends (from suppliers)											
bit-6604+0%	(40/60)	Sup6	X		X		X	X	X		
bit-6602+~4%	(70/100)	Sup6	X		X		X		X		
bit-A+0%	(35/50)	Sup2	X		X		X		X		
bit-B +~8%	(70/100)	Sup7			X		X		X		
Bitumen + REOB-X blends (self-made)											
bit-K+5%	(20/30)				X	X					
bit-K+10%	(40/60)		X	X	X	X	X	X	X	X	X
bit-K+15%	(90/110)				X	X					
bit-P+5%	(20/30)				X	X					
bit-P+10%	(30/50)		X	X	X	X	X	X	X	X	X
bit-P+15%	(40/60)				X	X					

Table 3.2: Unmodified and REOB modified bitumen tested with DSR and BBR at fresh and aged stages

Sample code	Grade (PEN)	Supplier	Rheological tests			
			DSR		BBR	
			Fresh	Aged	Fresh	Aged
Unmodified bitumen						
bit-K	(20/30)	Sup1	X		X	
bit-J	(70/100)	Sup1	X	X	X	X
bit-V1	(160/220)	Sup1				
bit-P	(15)	Sup2	X		X	
bit-O	(85)	Sup2	X	X	X	X
bit-Q	(190)	Sup2				
bit-L	(70/100)	Sup3	X	X	X	
bit-G	(40/60)	Sup4	X	X	X	
bit-I	(160/220)	Sup4	X			
bit-M	(70/100)	Sup5	X			
bit-N	(40/60)	Sup5				
Bitumen + REOB blends (from suppliers)						
bit-6604+0%	(40/60)	Sup6				
bit-6602+~4%	(70/100)	Sup6				
bit-A+0%	(35/50)	Sup2	X			
bit-B +~8%	(70/100)	Sup7	X			
Bitumen + REOB blends (self-made)						
bit-K+5%	(20/30)		X	X	X	X
bit-K+10%	(40/60)		X	X	X	X
bit-K+15%	(90/110)		X	X	X	X
bit-P+5%	(20/30)		X	X	X	X
bit-P+10%	(30/50)		X	X	X	X
bit-P+15%	(40/60)		X	X	X	X

Table 3.3: Unmodified and REOB modified bitumen tested with DMA, IDT and Cantabro test

Sample code	Grade (PEN)	Supplier	Mechanical tests			
			DMA-bitumen film adhesion/cohesion	DMA-mastic cohesion	IDT Dry & wet	Cantabro Abrasion test
bit-J	(70/100)	Sup1	X	X	X	X
bit-K+10%	(40/60)	Self-made	X	X		
bit-O	(70/100)	Sup2	X	X		
bit-P+10%	(40/60)	Self-made	X	X		
bit-K+15%	(70/100)	Self-made			X	X

These three tables show the experiments performed on the different bitumen for each chemical, rheological and mechanical level. When a percentage is used next to the name, REOB has been blended with the bitumen to create the REOB modified bitumen.

3.3. Reference bitumen and REOB-blends

To evaluate the effect of REOB on bitumen, its use as a fluxing material will be evaluated on two different bitumen, i.e. bitumen from two different suppliers. Both binders are of a stiff nature, as their noted penetration grade is (20/30) in the case of bit-K and (15) in the case of bit-P. For these two blend series, three different dosages of REOB will be applied: 5%; 10% and 15 wt%, with the goal to approach a (70/100) grade bitumen as used commonly in the Netherlands.

To be able to compare the performance of these bitumen at different dosages of REOB, two (70/100) grade bitumen, bit-J and bit-O, will be used as a reference. These are each also delivered by the same supplier, to have a similar background as the base bitumen of the modified binders.

The bitumen is blended with the REOB by first heating up the base bitumen at 163 [°C] for ~2 hours and the REOB at 130 [°C] for 30 minutes. They are weighed and the exact amount to reach the three different dosages is added while using a low shear device rotating at roughly 200-300 [rpm], being still heated at 135 [°C] blending roughly for 20-25 minutes. This is shown too in Figure 3.3.



Figure 3.3: Blending of bitumen and REOB with a low-shear device (200-300 rpm) and keeping the blend warm at 135 [°C]

As shown in Chapter 2, bitumen ageing has undesirable effects on performance and REOB modification of bitumen has been deemed to increase ageing susceptibility, binders in this research will also be aged. This is done by first ageing the binders in the oven for 5 hours at 163 [°C], to represent short-term ageing. The so-called thin-film oven testing (TFOT). This is then followed up by ageing the binders in a pressure ageing vessel (PAV) for 20 hours at roughly 20 [bar] / 300 [psi] and 103 [°C].



Figure 3.4: (left) REOB-bitumen blends, the reference bitumen & ageing procedure and (right) TFOT+20hPAV aged bit-K+10% and bit-P+10% blends

To be able to characterise the prepared binders correctly, the standardized tests of determining the PEN grade and softening point are performed. The PEN test depends on letting a needle drop for 5 seconds, with a specific weight of 20 [g], into the bitumen and measuring the depth the needle penetrates into the binder. This will give an indication of how stiff a binder is, as a stiff binder will allow only low penetration and a soft binder lets the needle penetrate deeper.



Figure 3.5: (left) PEN and R&B test samples, (middle) PEN test apparatus and (right) the Ring&Ball test

Next to that, one can perform a ring and ball (R&B) test as well. This is a test where two rings, the inside filled with bitumen, are placed in clamps with small steel balls lying on top of them. The clamps with the rings and balls are submerged in water and this is all heated up from an initial temperature of 5 [°C]. The balls will slowly sink through the bitumen once this gets warm and soft enough. When the balls have sunk a preset distance of a few centimetres, one has to denote the temperature at that specific moment. This is seen as the softening point, which is also related to a stiff or soft binder like the PEN grade. Higher softening points are often contributed to stiffer binders and lower to softer binders.

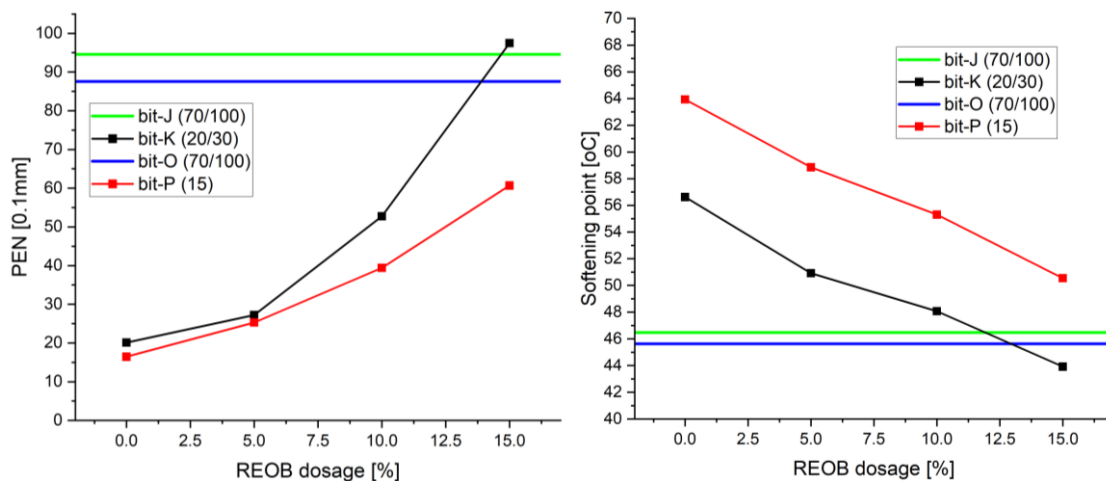


Figure 3.6: (left) Penetration grade of the REOB modified bitumen and reference bitumen and (right) Softening point of the REOB modified bitumen and reference bitumen

It is clear that the PEN grade increases exponentially with increasing REOB dosage, depending on the base bitumen. The softening point however shows that there is a linear correlation to the softening point depending on the REOB. The slope of the softening point to the REOB dosage is the same for both blend series, therefore one can perfectly design and predict the softening point at different dosages.

Bit-K is more sensitive to change in PEN grade value with increasing REOB dosage as compared to bit-P. Next to that the softening point is significantly lower for bit-K than for bit-P, causing the overall values of the softening points for the blends to lay lower as well. This therefore suggests that quite different behaviours will be found in the following analysis on chemical and rheological properties of these two binder series.

Chapter 4. Chemical characterization of bitumen, REOB and REOB modified bitumen

4.1. Introduction to chemical characterization

Now that the basic background of the several experimental tools has been evaluated in Chapter 2, the first step towards understanding the effect of REOB on bitumen, is to analyse the changes in chemical composition of the bitumen, REOB and of the REOB modified bitumen.

In Table 3.1 in Chapter 2.2 the used chemical tools and on which specific bitumen they are used are mentioned. The unmodified bitumen has been retrieved from several suppliers and has different PEN grades. Important is to note that there will be expected similarities in the bitumen that came from the same supplier, as the source of the crude and the production process of the bitumen similar.

Namely bitumen bit-J, K and V1 are all from the same supplier. The same holds true for bit-O, P and Q. These are the main bitumen series that are evaluated in this thesis, as these were the only available sufficiently hard PEN grade bitumen, (20/30) and (15), that could be blended with REOB. Bitumen bit-G and bit-I came from the same supplier as well, and bit-M and bit-N from another supplier. Important is to note that the REOB that is evaluated, is partly from a refinery in Italy (REOB-X & Y) and the other from one in the USA (REOB-Z). These three REOB will therefore show some basic differences that one should expect from different suppliers, although many more REOB should be evaluated to give a broader picture of the variance in material properties and consistency.

Bit-A PEN 35/50 is effectively blended with, an unknown, REOB at 8wt% to make bit-B PEN 70/100. Alternatively the bit-6602 comes from the same supplier as bit-B6604, although the bit-B6604 does not act as a base for bit-6602. Bit-6602 contains REOB at around 4 wt%,. The bit-B is bitumen prepared at another lab and bit-6602 obtained from a commercial supplier.

These bitumen will act as a guideline for the self-made bitumen blends in this thesis and should show similar differences to unmodified bitumen. Lastly, the different REOB-X blends for both bitumen series bit-P and bit-K are analysed as well. ATR-FTIR is performed on all different dosages and aged states, but to cut in the amount of tests only the 10% blends are analysed for other chemical tests. The 10% blends were chosen (and not the other dosages) as the rheological performance in the obtained DSR frequency sweeps of the initial blend bit-K+10% perfectly overlapped with the viscoelastic response of bit-J, and the bit-P+10% came sufficiently close to the behaviour of bit-O (which is made visible in Chapter 5.2.3).

The goal of doing these chemical experiments, is to show what exactly the REOB effectively changes in bitumen when it tries to make it softer, showing the characteristic elemental changes and molecular shifts which bitumen undergoes when modified with REOB.

4.2. Identification, quantification and evaluation of REOB in bitumen (XRF & ATR-FTIR)

4.2.1. Trace elements/metals found by XRF and/or ICP

The use of the X-ray Fluorescence (XRF) or an alternative technique called Inductively coupled plasma atomic emission spectroscopy (ICP-AES) comprises, within bitumen research, mainly to determine the presence of specific elements that are normally not present in bitumen. This technique is able to measure characteristic trace elements, such as Calcium (Ca), Copper (Cu), Zinc (Zn), Molybdenum (Mo), Phosphorous (P) or Potassium (K) in relation to presence of REOB (Hesp & Shurvell, 2010; Karki et al., 2019). which are trace elements that should be present only at low levels or not at all in unmodified neat bitumen. Good to note is the XRF and ICP can also measure trace elements like Iron (Fe), Nickel (Ni) and Vanadium (V); which unmodified bitumen from certain sources can also contain and are at the same time present in REOB as wear particles from the service life of the engine oil.

The XRF can have different applications, being a handheld device or full bench-top apparatus. A portable device makes it possible to perform on-site measurements, whereas a bench-top system can be used for the evaluations in a lab. The device counts particles per second at different energy levels of x-rays. The peaks measured at specific energy levels can be attributed to specific elements. For example zinc (Zn) at 8.64 keV and molybdenum (Mo) 17.48 keV.

With the use of engine oils (EO), waste engine oils (WEO) or re-refined engine oil bottoms (REOB), one can effectively lower the viscosity of a binder, but this will lead to the measurable presence of the previously mentioned trace metals. These trace metals are present in these engine oils, as come from the use of the oil in motors (wear of metal surfaces) or from the use of additives in the lubricants (thickeners, anti-wear etc.)

The use of such engine oil based modifiers in bitumen, has been evaluated before by several researchers (AsphaltInstitute, 2016; Baumgardner et al., 2023; Hesp et al., 2009; Hesp & Shurvell, 2010; Kaskow et al., 2018). They showed that the technique was quite accurate at identifying the presence of engine oil, although quantification could depend on different factors such as REOB consistency, bitumen consistency and high sulphur content affecting the zinc determination.

The XRF is deemed to be an effective tool to identify the presence of REOB in bitumen, although it's general use in asphalt and bitumen research labs is not common. The main focus in this thesis will therefore lie on using FTIR to identify and quantify REOB in bitumen. Nevertheless, it was deemed useful to analyse a small set of samples of both bitumen and REOB, to make these better comparable with other research that only uses XRF for identification and quantification.



Figure 4.1: Handheld XRF scanner as benchtop



Figure 4.2: (left) REOB samples for XRF scanning; (right) cooled bitumen samples wrapped in plastic foil

N.B. the used XRF handheld devices has in no way been calibrated to scan bituminous materials for the trace metals. A procedure is followed from plastic materials and thus some deviations are possible from the true present trace metal amounts.

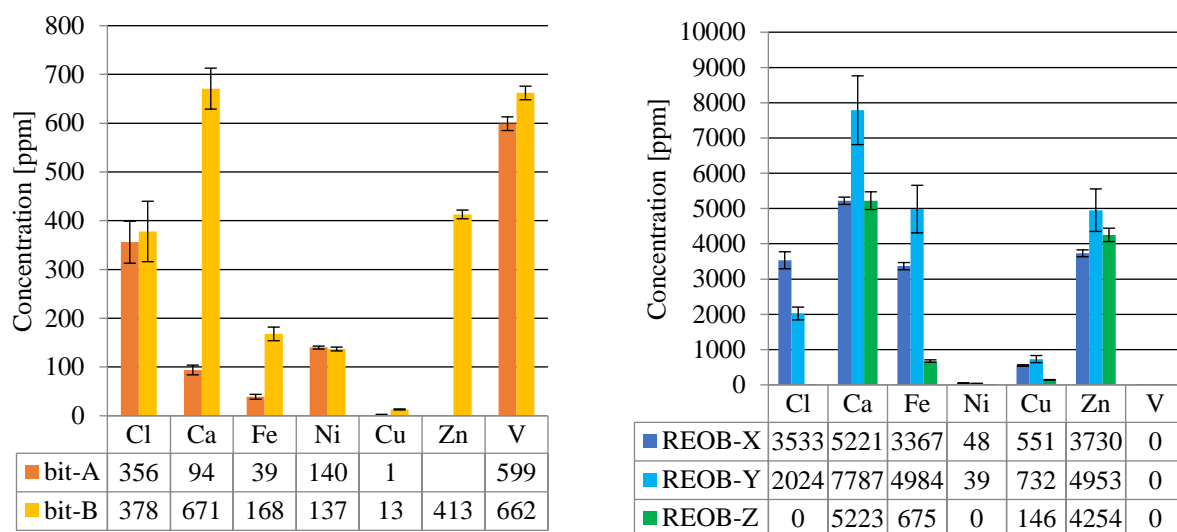


Figure 4.3: Trace elements found with XRF for (left) unmodified and REOB modified bitumen and (right) for three different REOB

Bitumen bit-A is an unmodified binder and bit-B is the same base bitumen but in this case 8wt% of REOB is added. Three different REOB variants are also analysed, namely REOB-X, REOB-Y and REOB-Z.

A small set of binders have also been analysed with ICP, therefore giving a similar indication of the presence of specific trace metals in the bitumen. The difference between modified and unmodified binders is all the more pronounced. As Calcium (Ca), Nickel (Ni), Phosphorous (P), Molybdenum (Mo), Zinc (Zn), Kalium (K), Silicium (Si) and Iron (Fe) are suddenly present or have increased in concentration, as visible in the plot below:

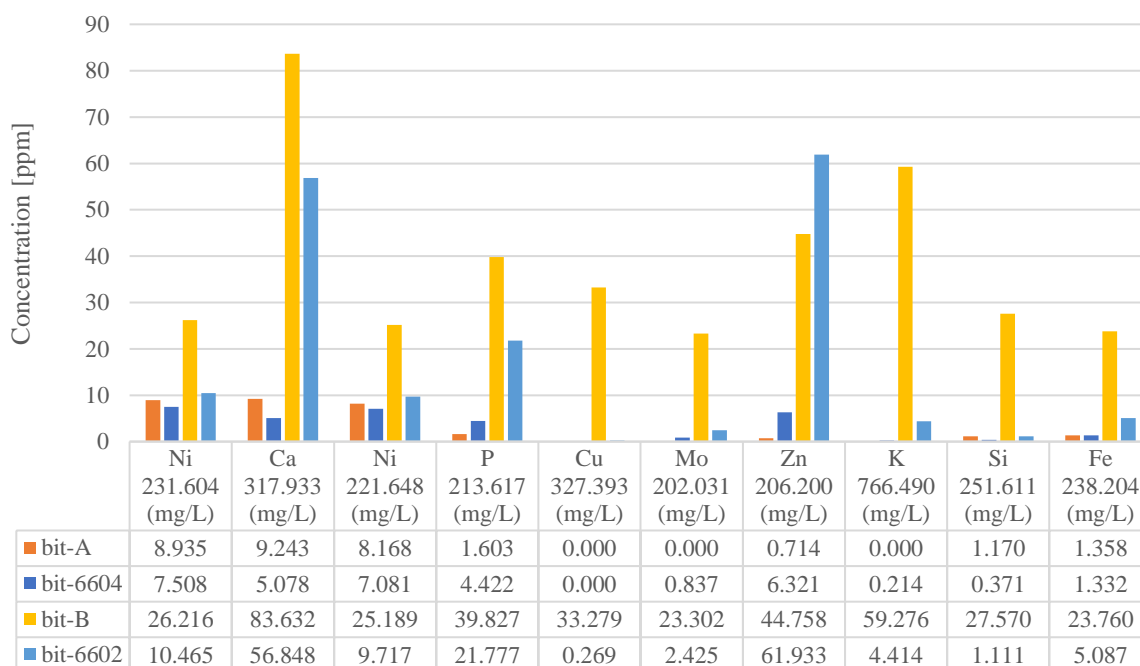


Figure 4.4: Trace elements found with ICP-AES for unmodified and REOB modified bitumen

From the XRF measurements one can see that the unmodified bitumen (bit-A) has low levels of calcium, copper and zinc, as compared to the REOB modified bitumen (bit-B). These changes are quite significant, which makes identification of the presence of REOB in the binder easy. Looking at quantification, one can first compare the bitumen with the sole REOB consistencies. Here below the averages of those three compounds are calculated. This is followed by an estimation of the dosage of REOB in bit-B, using the averages of the three evaluated REOB sources, although one can see that a lot of variance is possible.

$$avg_{calcium} (Ca) = \frac{5221+7787+5223}{3} = 6077 [ppm] \rightarrow content_{(Ca)} = \frac{671-94}{6077} * 100 = 9.50\%$$

$$avg_{copper} (Cu) = \frac{551+732+145,5}{3} = 476 [ppm] \rightarrow content_{(Cu)} = \frac{13-1}{476} * 100 = 2.52\%$$

$$avg_{zinc} (Zn) = \frac{3730+4952+4253}{3} = 4312 [ppm] \rightarrow content_{(Zn)} = \frac{413-0}{4312} * 100 = 9.58\%$$

(4.1)

Knowing that the added content of REOB was around 8%, one can see that it is quite difficult to estimate accurately from XRF measurements alone what the true dosage of REOB is. Not knowing the average ppm count of trace metals in the base REOB, but also of the base bitumen, makes quantification difficult. Calibration of the XRF is therefore certainly necessary and only a large library of measurements on different REOB and on several blends is needed to make estimation this way effective. But with WEO sources constantly and easily changing, this will always reflect on the REOB consistency and it will always remain hard to quantify with XRF.

This makes it hard to use the XRF in practice. Normally when one wants to know if REOB is present and at what dosage, one does not know what the chemical composition was initially of both the base bitumen as well as the REOB. Though, there have been developments in making the method more accurate. This has been done by for example introducing WD-XRF, instead of the previously described ED-XRF (Karki et al., 2019; Wielinski et al., 2015). But also phosphorous and magnesium have been found to be indicators of REOB/VTAE as well.

Using the ICP-AES instead of the XRF, will bring an increased accuracy with it. One can see that much higher calcium (Ca) is measured for example. The measurement of phosphorous (P) is only possible to measure in XRF when the samples are in an inert environment like Helium. But Molybdenum (Mo) and Silicium (Si) can be measured as well, giving a clear indication of the concentration of these particles in the bitumen. The problem with the ICP-AES is, however, that the machine is not commonly available in bitumen research labs and also quite an expensive tool to buy and use. Then again the problem that remains present for the ICP-AES like for the XRF, is that the REOB dosage is hard to quantify in the bitumen as the REOB differs quite a lot between different sources and bitumen itself can also contain some trace metals.

Many of the mentioned trace metals cannot be found in bitumen itself. Although, depending on the “geological” crude oil source, one could indeed find some of these metals to already be present in unmodified bitumen. It is therefore important to differentiate between which are truly indicative of lubricant additives or wear particles in a bitumen, and haven’t been present in the crude oil source to begin with. In Figure 4.5 one can observe the deviations between bitumen that come from different crude oil sources, important to note is the maximum intensity measured. Only around 9 [ppm] is observably a maximum, whereas for the REOB modified bitumen the calcium, phosphorous, copper, zinc, molybdenum and kalium are measured above 20 [ppm] easily. The trace metals that can be found in some crude oils, and therefore in the resulting bitumen that is produced, are mainly Fe (Iron), Ni (Nickel) and V (Vanadium) (Nahar et al., 2016). It was concluded that the presence of these trace metals could also be linked to higher presence of sulphur, increase in ageing susceptibility and they were mainly present in the asphaltene fraction of the binders.



Figure 4.5: Trace elements found with ICP-AES for unmodified bitumen

To make clear what typical trace elements can be found in REOB, and therefore in REOB modified bitumen, the Table 2.2 in Chapter 2.1 lists them with their respective possible origins mentioned as well in previous research (Minami, 2017; O'Brien, 1983; Speight & Exall, 2014; Wong & Tung, 2016). With these origins obtained, one can perform clear identification of a bitumen, or REOB itself, and see which components are heavily present in it still (after re-refining).

Nevertheless, the XRF or ICP being often inaccurate tools for REOB quantification but also the fact that research labs mostly do not own such devices, makes them a less usable tools for standard labs. An alternative to using the XRF or ICP for quantification, one could use an (ATR-)FTIR to measure chemical changes to the composition functional groups on molecules in bitumen. Adding REOB to bitumen one can see the appearance of specific functional groups in its spectrogram profile. The FTIR, being a more commonly used tool in bitumen research, could be a viable alternative to XRF and possibly be more accurate in quantification or relation to changes in rheological and mechanical properties (Kaskow et al., 2018; Yan et al., 2022).

4.2.2. Analysis and modification of ATR-FTIR spectra

The use of Infrared spectrometry (IR), or to be specific Fourier-Transform Infrared spectrometry (FTIR), has been quite common tool over last years in bitumen research. In more recent years the use of Attenuated total reflectance FTIR (ATR-FTIR) has been more frequent, as it has higher accuracy to show the small differences between different (aged) bitumen better.

The principle of the use of IR spectrometry for bitumen, is to use the infrared beam to measure energy changes at certain wavelengths, when the emitted beam is absorbed. Specific functional groups that are present in and at the molecules that bitumen is composed of, can absorb the infrared beam at very specific wavelengths. A few examples are a C=O functional group, which vibrates at 1700 [cm⁻¹], or the S=O that vibrates at 1030 [cm⁻¹]. More functional groups can of course be found, but specifically these two are the most prevalent peaks to measure regarding bitumen ageing. This effectively shows the relative total oxidation that a binder undergoes.



Figure 4.6: ATR-FTIR spectroscope “Frontier” from PerkinElmer

To be able to quantify the peaks of several functional groups, one should take note that spectra can deviate because of various reasons. One of them is for example varying pressure on the sample when performing the IR scan using ATR-FTIR. A pressure should only be applied when the binder is very stiff, having an initial PEN grade of (20/30) for example or when a binder has aged. This is only to ensure that the bitumen surface has a good contact to the ATR crystal. Applying a pressure on a soft binder can induce a local flow which influence the measurement in a negative way, as spectra tend to show bigger absorbance levels than expected as well as increasing variance between measurements.

The most variance between measurements will occur in the so-called “fingerprint area” of a spectrogram. This is the range of wavenumbers lower than 2000 [cm⁻¹], at least for bitumen. Several techniques exist to retrieve quantitative results from the spectra. For one, indices can be retrieved that are calculated by dividing the area under a peak with a tangential baseline underneath (Van den Bergh, 2011; H. Wang et al., 2020). But as one can see from measurements with ATR-FTIR, the spectra tend to curve upwards in the fingerprint area. To counteract this problem, but also to optimise the calculation of indices from spectra, different methods were analysed (Hofko et al., 2017). From the different methods that were evaluated, it became clear that to retrieve the best approached indices of C=O and S=O, one should baseline correct the spectra, normalise the data using the peak value at 2923 [cm⁻¹] and to calculate the index areas by integrating under the peaks. Recently, a paper used Partial-Least-Squares (PLS) regression to evaluate the spectra of REOB modified binders (Yan et al., 2022). Here the spectra were also baseline corrected, but ATR-correction was applied initially. This correction takes into account the reflectance deviation that the technique imposes, which deviates from results that one measures with standard FTIR measurements (Nunn & Nishikida, 2003).

Table 4.1: Applied method of analysis of ATR-FTIR spectra of several researchers

Authors/Researchers	(Van den Bergh, 2011; H. Wang et al., 2020)	(Hofko et al., 2017)	(Yan et al., 2022)
ATR-FTIR analysis procedure	1. Baseline correction 2. Take tangential areas under peaks 3. Calculate index of area compared to total	1. Baseline correction 2. Normalisation at 2930 [cm ⁻¹] peak 3. Integration of areas below peaks 4. Calculate index of area compared to total	1. Advanced ATR correction 2. Baseline correction 3. Take tangential area under peaks 4. Calculate index of area compared to total
Alternative method applied			PLS-regression

The suggested and used analysis of the retrieved ATR-FTIR spectra is the following:

- I. One series of indices are retrieved using the method that Van den Bergh and Wang et al. have used.
- II. The second series of indices are retrieved using a combination of both Hofko et al and Yan et al that is believed to be more accurate out of the several options, ordered in the following way:
 1. Advanced ATR correction of the spectrum
 2. An automatic baseline correction of the spectrum
 3. Normalisation to 1.0 at the peak at 2923 [cm⁻¹]
 4. Integration by areas under each of the interested peaks

Figure 4.7 shows these four different steps clearly in how it alters the spectra. One can see that the fingerprint area has now shifted vertically and is stretched out significantly to make changes in its spectrum more pronounced specifically for bituminous materials.

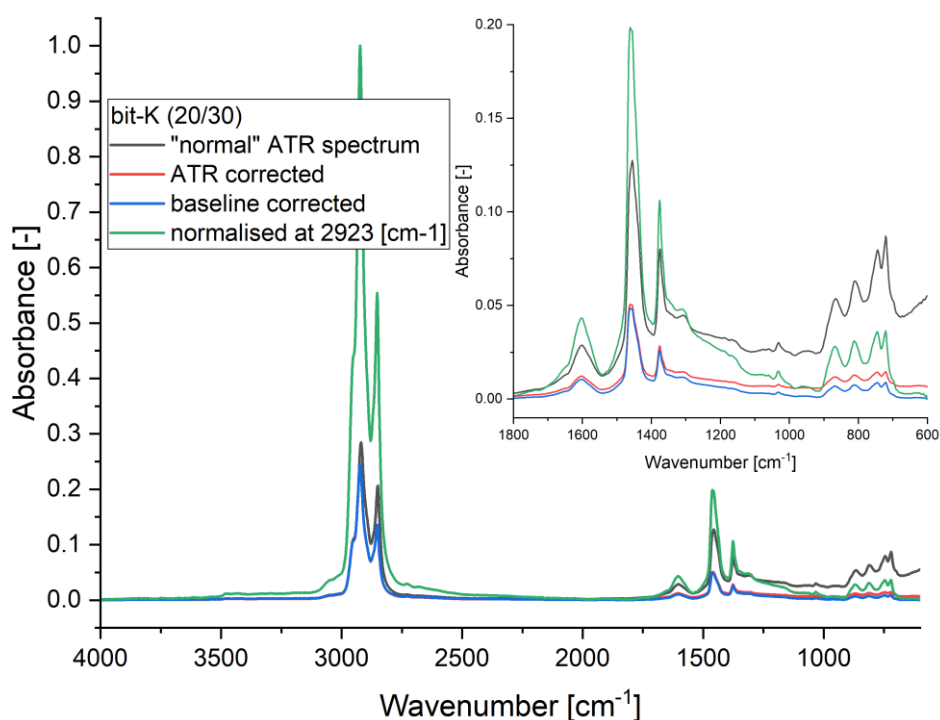


Figure 4.7: ATR-FTIR spectra of bit-K modified at the proposed different steps of analysis

Spectra shown in this Chapter are all from the second method of modification, due to an abundance of plots otherwise, it is chosen that the calculation of the indices only will be shown also of these modified spectra. The goal is that the benefit of using Advanced ATR correction, which handles inaccuracies resulting from the refraction of the IR beam better, will show what changes ageing does to unmodified and REOB modified bitumen, show the consistency of REOB itself and lastly show how one can identify and quantify REOB in bitumen.

4.2.3. Evaluation of ATR-FTIR spectrograms of bitumen and REOB

The modified spectra are here analysed around their most interesting functional groups. Firstly there are qualitatively evaluated, followed by quantitative evaluation of the spectrograms. Both indices of unmodified spectra and of ATR-modified spectra will be analysed, to show the benefit of modification of the spectra.

The total area of indices, follows from the sum of areas of each separate index. This is shown in the following formula:

$$\sum A = A_{(2953;2862)} + A_{(1700)} + A_{(1600)} + A_{(1460)} + A_{(1376)} + A_{(1030)} + A_{(864)} + A_{(814)} + A_{(743)} + A_{(724)} \quad (4.2)$$

To be more specific, the following indices will be evaluated, each having their own specific wavenumbers that are attributed to specific functional groups:

Aromaticity:	-C=C-	$ARO = \frac{A_{(1600)}}{\sum A}$	1670-1535 [cm ⁻¹]
Aliphatic:	-C-H antisymmetric bending	$ALI = \frac{A_{(1460)} + A_{(1376)}}{\sum A}$	1525-1395 [cm ⁻¹]
Branched aliphatic:	-C-H symmetric bending	$BAL = \frac{A_{(1376)}}{A_{(1376)} + A_{(1460)}}$	1390-1350 [cm ⁻¹]
Long chains:	-C-H stretching	$LCI = \frac{A_{(724)}}{A_{(1376)} + A_{(1460)}}$	734-710 [cm ⁻¹]
Ageing; Carbonyl:	-C=O	$ICO = \frac{A_{(1700)}}{\sum A}$	1743-1660 [cm ⁻¹]
Ageing; Sulfoxide:	-S=O	$ISO = \frac{A_{(1030)}}{\sum A}$	1047-995 [cm ⁻¹]
Combined ageing:		$CAI = ICO + ISO$	

These indices are calculated from the obtained areas for each specific peak, but they are calculated differently between the unmodified and modified spectra. The unmodified spectra will have areas calculated by using a tangential line, valley-to-valley method. The modified spectra will have index areas calculated by using integration towards the baseline, in this case the horizontal x-axis.

Firstly the spectra are qualitatively analysed, followed by first the indices for the unmodified and secondly the modified spectra. Spectra are collected and analysed first for unmodified bitumen which followed three bitumen, each aged for TFOT, 20hPAV, 40hPAV and 80hPAV. Then the functional groups are analysed, which is followed up by the analysis of REOB itself and then lastly the REOB modified bitumen of the blends.

I. FTIR spectrograms of unmodified bitumen

As one can see in Figure 4.8, that generally all the functional groups their presence and intensity do not depend clearly on the PEN grades of the bitumen, see for this Table 3.1. Although one can roughly say that on average the spectrum is higher (more absorbance) for bitumen with higher PEN grades/softer binders and less for the stiffer binders.

One can see typical differences in the carbonyl, sulfoxide, aromaticity and aliphaticity functional groups between all the binders. Especially the carbonyl ($\text{C}=\text{O}$) at $1700\text{ [cm}^{-1}\text{]}$ peak is already present in binders bit-O, bitQ, bit-P and bit-J. Specifically binder bit-V1 shows a peak at $1743\text{ [cm}^{-1}\text{]}$ (another vibration of $\text{C}=\text{O}$), only occurring for bit-N too but not for any other unmodified bitumen.

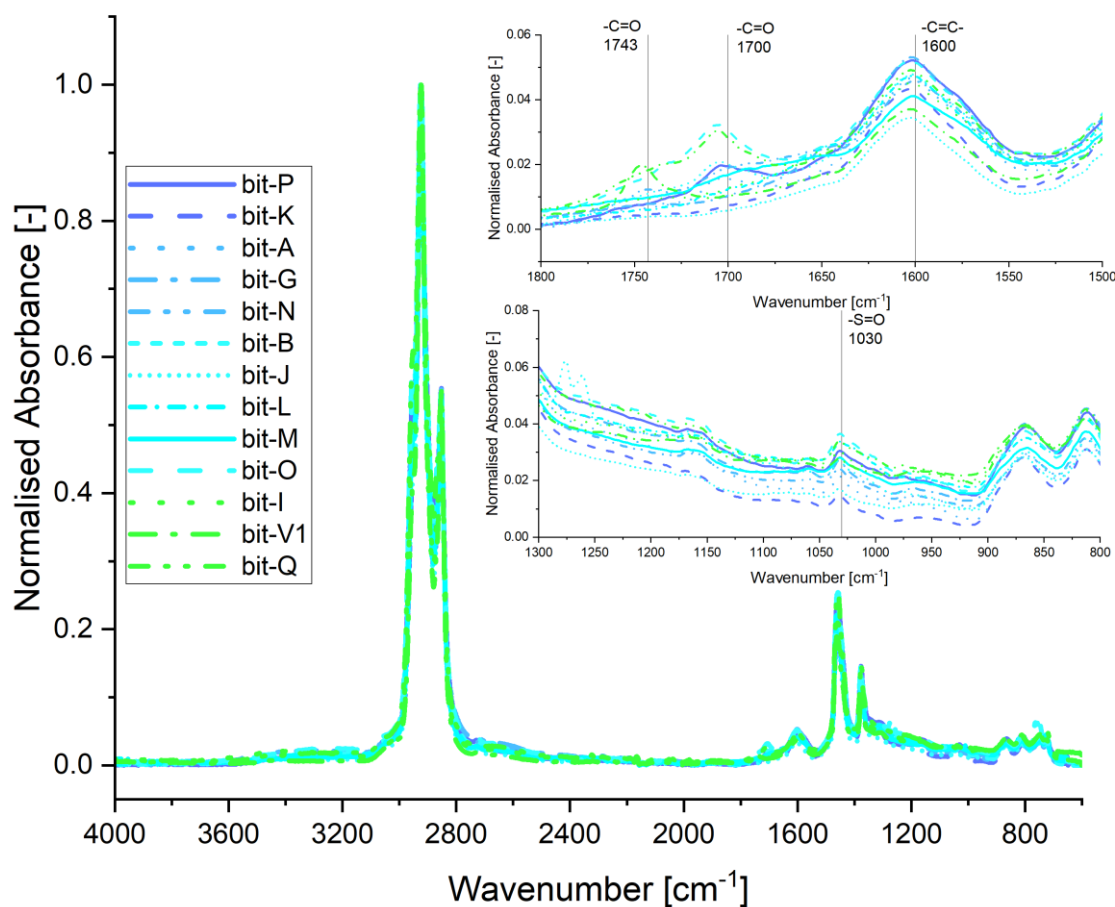


Figure 4.8: Modified and corrected ATR-FTIR spectra of unmodified bitumen

The aromaticity ($-\text{C}=\text{C}-$) is measured to be significantly different between all bitumen, with bit-I, bit-V1 and bit-M to have exceptionally low amounts and bit-P, bit-O and bitQ exceptionally high. This seems to therefore be linkable to the supplier and origin of the binders, as these are all from the same source of supplier(although of different grades).

The unaged binders do not show a very significant presence of sulfoxide ($\text{S}=\text{O}$) yet at $1030\text{ [cm}^{-1}\text{]}$. Only bit-O and bit-V1 seem to have already a small sulfoxide peak, as compared to the others.

Next are the three series, bit-L, bit-J and bit-G, which are aged for TFOT, 20hPAV, 40hPAV and 80hPAV shown in Figure 4.9, Figure 4.10 and Figure 4.11. It becomes clear that ageing mainly has an impact on functional groups at $1700\text{ [cm}^{-1}\text{]}$, $1600\text{ [cm}^{-1}\text{]}$, the range between $1300 - 900\text{ [cm}^{-1}\text{]}$, the peak at $1030\text{ [cm}^{-1}\text{]}$, $814\text{ [cm}^{-1}\text{]}$, $743\text{ [cm}^{-1}\text{]}$ and lastly $724\text{ [cm}^{-1}\text{]}$.

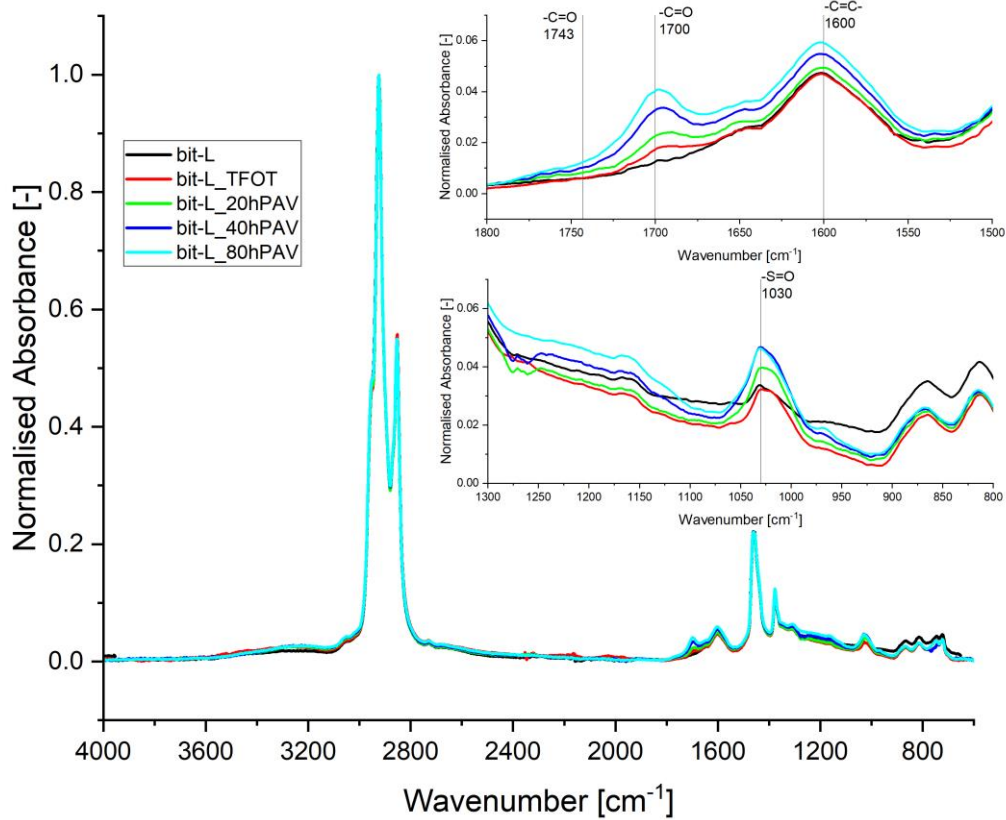


Figure 4.9: Modified and corrected ATR-FTIR spectra of aged bit-L (70/100)

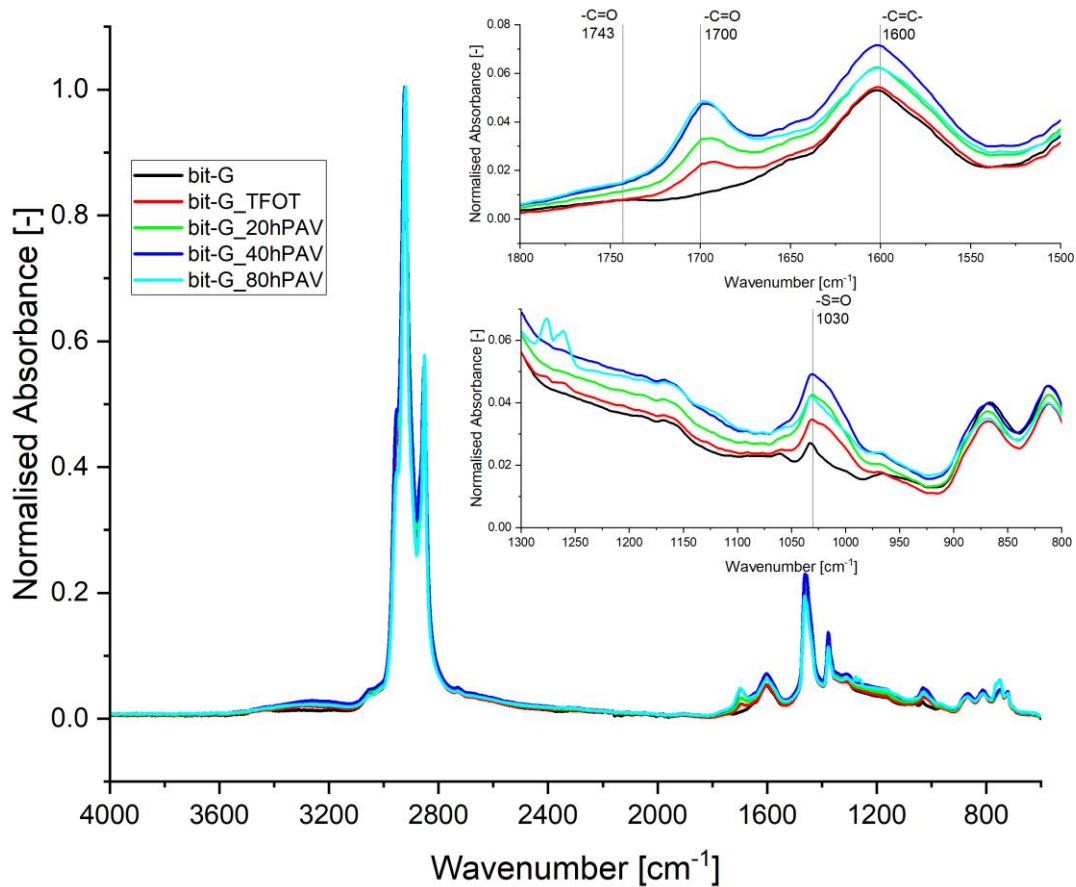


Figure 4.10: Modified and corrected ATR-FTIR spectra of aged bit-G (40/60)

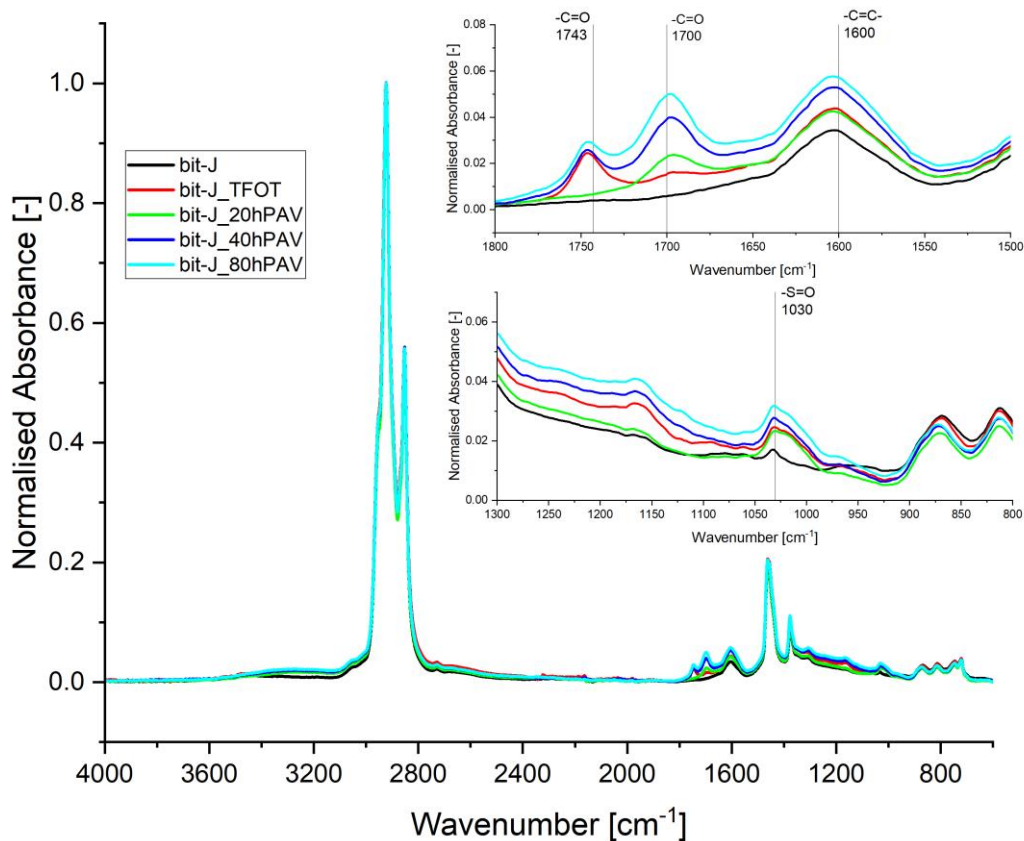


Figure 4.11: Modified and corrected ATR-FTIR spectra of aged bit-J (70/100)

All aged series show an incremental increase in carbonyl as well as sulfoxide peaks with ageing from fresh to 80hPAV. bit-J shows higher rate of changes in carbonyl with increasing ageing, but relatively smaller changes in sulfoxide. Bit-G shows intermediate changes for both carbonyl and sulfoxide. bit-L shows the biggest changes in the general spectrum when comparing Figure 4.9 to Figure 4.10 and Figure 4.11, although when comparing indices in Figure 4.12, bit-L has one of the smallest changes with ageing.

One can also observe that the height of the spectrum between 1300 and 900 $[\text{cm}^{-1}]$ lays significantly higher each time with ageing. These qualitative observations can be compared to the quantitative indices shown in Figure 4.12. The lowest wavenumber peaks, indicating aliphaticity, shows a small decrease. Next to that all bitumen seem to have a significant increase of their aromaticity ($-\text{C}=\text{C}-$) with ageing, which suggests stronger intermolecular interactions due to π - π stacking and van der Waals forces. This can result in a more rigid and less flexible molecular structure, contributing to the stiffness and brittleness of the binder. This can be explained by the changes in SARA fractions which bitumen undergoes with ageing. With ageing typically a shift between an increase in resins and a decrease in aromatics will take place and asphaltenes will rise in weight fraction as well. The fact that asphaltenes and resins relatively have higher aromaticity and lower aliphaticity, and aromatics (as SARA fraction) vice versa, explains this phenomenon therefore very well (Ren et al., 2023).

The aromaticity rises a lot with ageing for bit-L and even more so for bit-J. The aliphaticity however, shows to be stable for bit-L and increases slowly in the case of bit-J. The branched aliphatic structures are in fact increasing in the case of bit-J and remaining stable for bit-L. In stark contrast bit-G shows to have actually a slow decrease in branched aliphatic structures while a slow increase in aliphaticity. This shows how bit-L shows a more stable aliphaticity and branched aliphatic structures, while bit-J and bit-G a complete opposites.

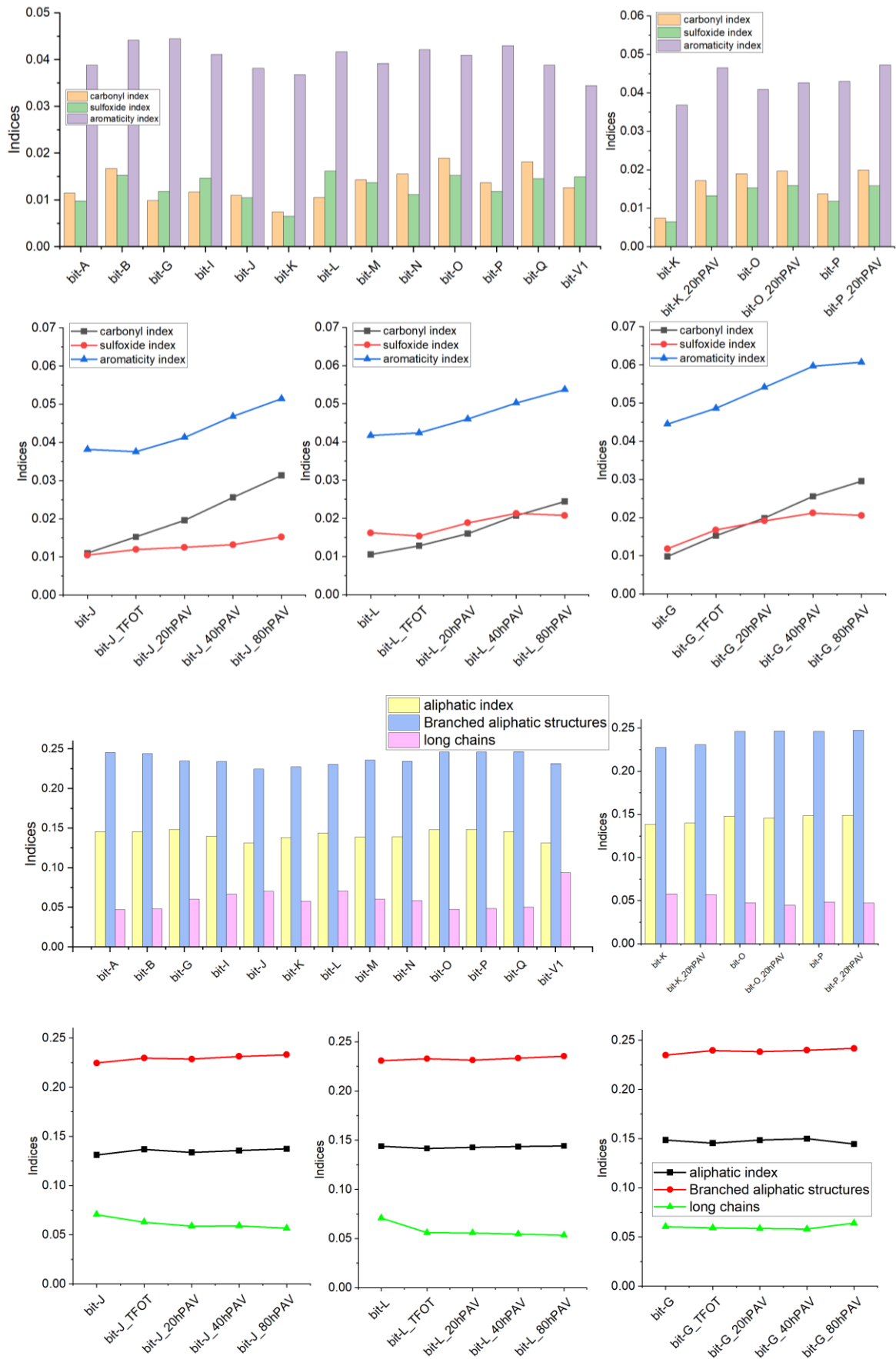


Figure 4.12: Indices for modified spectra | unaged and aged unmodified bitumen

The carbonyl index differs between the fresh binders, but with ageing a clear linear rise is visible for all three aged bitumen series. This is the strongest for bit-J, then bit-G and lastly bit-L. The sulfoxide index behaves similarly as the carbonyl, although with ageing it has a lower slope. For bit-J it almost doesn't change with ageing, bit-L and bit-G have also a relatively higher starting point and it seems that the index starts to drop at 80hPAV for these two binders.

Comparing bit-K and bit-P with ageing, one sees that they both have a similar slope for forming both carbonyl and sulfoxide. However bit-O, does not do this. It remains actually stable. This is very interesting, as this shows that bit-O is very resistant to oxidative ageing, at least for the ageing step of 20hPAV that is analysed.

The aromaticity index increases very similar between all different binders but interestingly it is very low for bit-V1. Which should be a very soft binder and therefore one would expect maybe more aromatics and resins to be present, which is not the case according to this measurement.

The binders of bit-K, J and V1 show to have relatively much long chains present, low branched aliphatic chains and a bit lower aliphatic compounds present, when compared directly to the bit-P, O and Q series. The bit-P, O and Q actually have some of the highest presence of aliphatic compounds and branched aliphatic chains present.

With the addition of REOB to bit-A, creating bit-B, one cannot see much difference between the indices, except for the carbonyl and sulfoxides. Here it is visible that both indices increased significantly after its addition, although they do not rise to a level that one could distinguish it from the other bitumen.

II. FTIR spectrograms and indices of REOB

In Figure 4.13, three different REOB and one 20hPAV aged REOB are analysed. Overall a lot of the peaks that were present for bitumen, seem to be present for the REOB as well. The typical peaks at 2923 [cm⁻¹], 2862 [cm⁻¹], 1700 [cm⁻¹], 1600 [cm⁻¹], 1460 [cm⁻¹], 1367 [cm⁻¹] and 723 [cm⁻¹] are again very well present for the REOB.

Alternatively, several different peaks seem to be now very pronouncedly present in the REOB. Mainly the ones at 1745 [cm⁻¹], 1229 [cm⁻¹], 1157 [cm⁻¹], 1103 [cm⁻¹], 1043 [cm⁻¹], 1011 [cm⁻¹], 966 [cm⁻¹] and 700 [cm⁻¹] are distinctively different peaks that were not present or not this pronouncedly present as in bitumen.

The first different peak at 1745 [cm⁻¹], is a typical different vibration of carbonyl (C=O), than the normally measured vibration at 1700 [cm⁻¹] found in bitumen. Only bit-V1 and bit-J seemed to have some molecules in them that had this variation of the carbonyl group. What is clear though, is the difference between the three REOB in this respect. REOB-X has a very high 1745 [cm⁻¹] peak, REOB-Y lower and REOB-Z almost no peak there at all. Accounting both peaks as carbonyl groups, one can observe that REOB is oxidized relatively a lot, as compared to what is seen in fresh bitumen.

One can see that the aromaticity differs much between all REOB. As an engine oil, or REOB as its derived form, is actually not expected to have asphaltenes. With the low peak at 1600 [cm⁻¹] this would therefore suggest that REOB is expected to have low amounts of resins and aromatics. This is a logical observation as the REOB is expected to be distilled and refined in such a way that these fractions mainly are tried to be retrieved from it to be able to make the recycled lubrication oil from the waste engine oil (WEO).

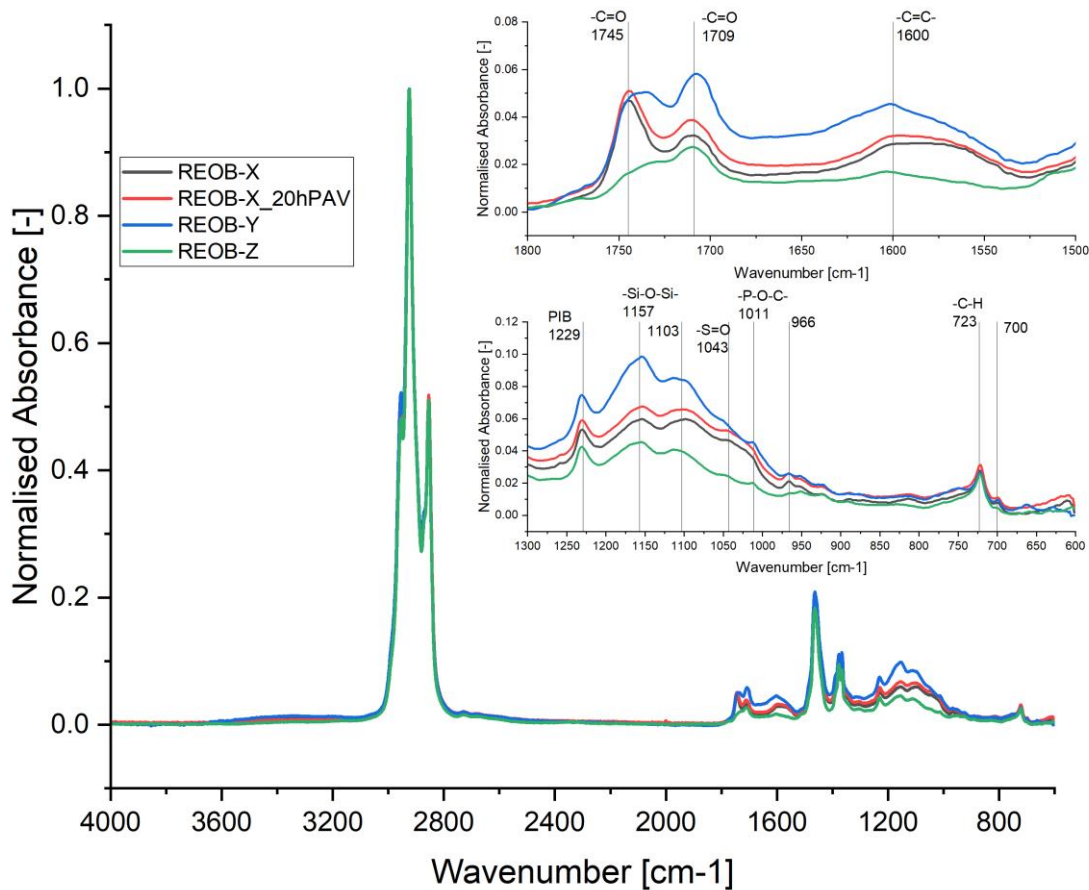


Figure 4.13: Modified ATR-FTIR spectra of unaged (and one) aged REOB

From the aromaticity peak one can suggest that REOB-Y is expected to have the highest amount of aromatics & resins and REOB-Z the lowest. The peak at 1229 [cm⁻¹] shows the presence of polyisobutylene (PIB) (Kaskow et al., 2018; Yan et al., 2022), which is an additive commonly used to modify lubrication oils. It acts as a thickener to the oil, to increase its viscosity and therefore changing the range in which the lubricant can be the used in practice. This peak at 1229 [cm⁻¹] effectively shows the -CH₃-CH₃ functional group, which is not commonly found in bitumen. The three REOB differ again very clearly, with again REOB-Y having a higher amount of the PIB present and REOB-Z the lowest.

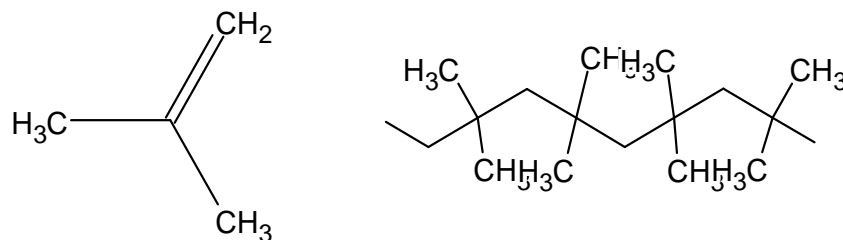


Figure 4.14: Isobutylene monomer (left) and a short polymer chain of polyisobutylene (right)

The peaks of 1157 and 1103 [cm⁻¹] are some of the highest present in the REOB. These typically represent the presence of -Si-O-Si- which is also an additive for lubricants (Yan et al., 2022). This additive is a silicium based polymer, in other words: silicone oil. The effect of silicone oil on bitumen has not been researched much, although its addition to crumb rubber modified asphalt seems to be positive (Lushinga et al., 2019) and some interesting insights are already found as the oil can be used to de-asphalt heavy crude oil (Yadykova et al., 2023). Like with all the other peaks so far, also here one

can see that REOB-Y has the highest presence of this functional group, followed by REOB-X and the least is present for REOB-Z.

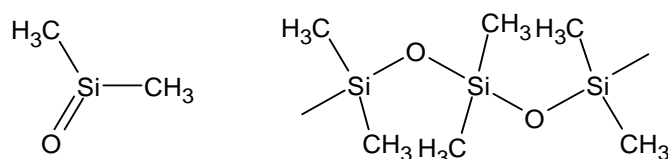


Figure 4.15: Silicon oil monomer and a short polymer chain of typical silicon oil

Sulphur is also present in the REOB, which is shown by the small peak at 1043 [cm⁻¹], which is a different vibration of the sulfoxide (S=O) functional group. One can see that it is only present in a very small amount for the REOB-Z and a similar intensity between REOB-X and REOB-Y. The sulfoxide does not necessarily represent an additive of the lubrication oil though.

The peaks at 1011 and 966 [cm⁻¹] do however. These wavenumbers are typically found for the -P-O-C- functional group, which is a phosphorous bond often connected to a Zinc metal, creating a small particle with these phosphorous and carbon chains attached to it. A typical additive that is often added to lubricants, is zinc-dithiophosphate (ZDP) / zinc-dialkyldithiophosphate (ZDDP). These are anti-wear additives, that effectively prevent metal-to-metal contact and wear inside engines, further improving thus the lubricating effect of the oil. Clearly these particles are, although in small amounts, present in the REOB. How these particles work in lubricants, is that they react with metal surfaces to form a protective layer called a tribofilm. Next to that they are able, in general, to reduce friction between non-metallic surfaces as well (Kontou et al., 2021). One can see that these peaks are actually not that big in the REOB, suggesting only low amounts are present in the lubricants in the first place or the re-refining process is able to retrieve most of the particles. REOB-X seems to have the highest presence, closely followed by the other two REOB.

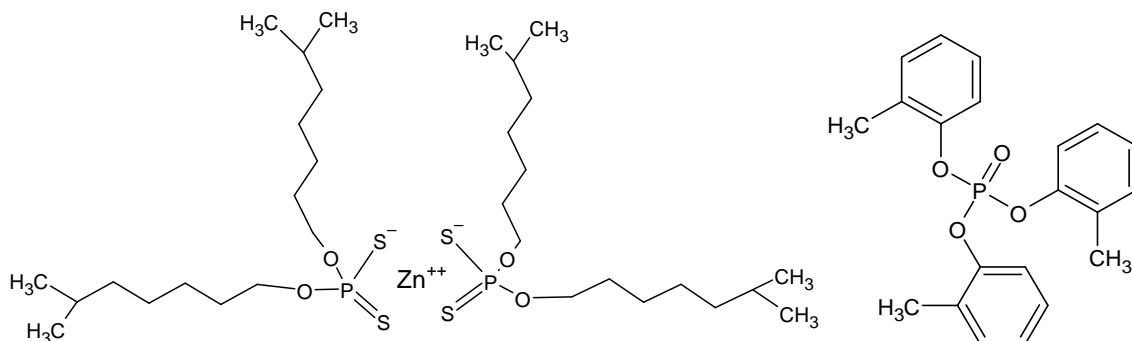


Figure 4.16: (left) zinc-dialkyldithiophosphate (ZDDP) molecule and (right) a tricresylphosphate (TCP) molecule

Comparing this to the XRF measurements, estimating the Zinc trace metals, this seems to deviate. This could be explained by the fact that zinc is not always the base of the dialkyldithiophosphate (DDP) and for example Tungsten can be used as well. This would explain a deviation between the two results. An alternative explanation could also be that tricresylphosphate (TCP) is measured instead, not having a metal in it at all, which acts as an anti-wear and extreme pressure additive for lubricants.

The last few peaks, at 723 and 700 [cm⁻¹], represent respectively an -CH and -CH bending functional groups. These are not that uncommon for bitumen to be present of course and the different REOB do not seem to differ much in intensity for these specific functional groups.

To clarify on what distinctive peaks can be found in REOB, and what they correlate to, they are summed up in the table below:

Table 4.2: Functional groups specifically present in REOB and their expected origin

Peak [cm ⁻¹]	Functional group	Representing	Origin
1745 & 1700	-C=O	Carbonyl	Oxidized hydrocarbon molecules
1600	-C=C-	Aromaticity	Presence of resins or aromatics
1229	-CH ₃ -CH ₃	Polyisobutylene (PIB)	Viscosity modifier for lubrication oils
1157 & 1103	-Si-O-Si-	Silicon oil	A lubrication oil and present in waste engine oil (WEO)
1030	-S=O	Sulfoxide	Oxidized sulphur containing hydrocarbon molecules
1011 & 966	-P-O-C-	ZDP, ZDDP, TDTP or TCP	Anti-wear additives for lubrication oils

To show that the PIB, Si-O-Si and P-O-C do vary in a similar way between the three REOB (and even the aged variant), indices are calculated for these functional groups:

$$\sum A = A_{(2953;2862)} + A_{(1700)} + A_{(1600)} + A_{(1460)} + A_{(1376)} + A_{(1030)} + A_{(864)} + A_{(814)} + A_{(743)} + A_{(724)} + A_{(1229)} + A_{(1157)} + A_{(1103)} + A_{(966)} \quad (4.3)$$

Above the calculated total area under the functional groups is mentioned, where one can see four distinctive peaks added to the list.

Polyisobutylene	PIB	$PIB = \frac{A_{(1229)}}{\sum A}$	1240-1210 [cm ⁻¹]
Silicone oil	Si-O-Si	$SOS = \frac{A_{(1157)} + A_{(1103)}}{\sum A}$	1210-1130 [cm ⁻¹]
Ani-wear	-P-O-C-	$POC = \frac{A_{(966)}}{\sum A}$	980-935 [cm ⁻¹]

With these added indices, one can effectively calculate an index for the present (main) lubricant additives in REOB. The deviations between the three REOB, and one aged version, are plotted below:

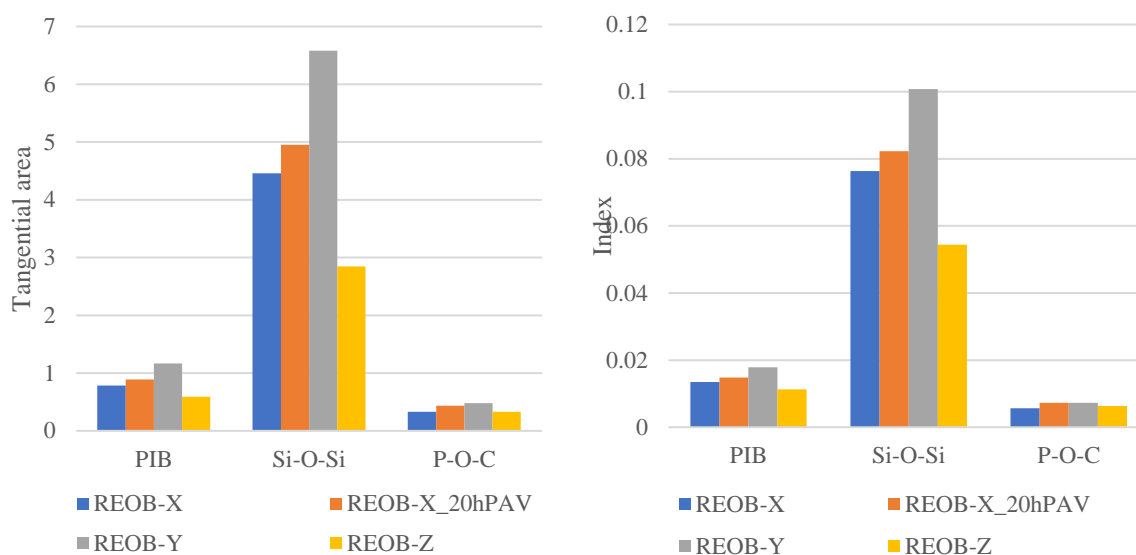


Figure 4.17: (left) tangential areas of functional groups and (right) index values of the main lubricant additives present in REOB

One can see that both as tangential area and an index value for REOB the relative PIB is very consistent between the different REOB. Meaning that one can clearly see that when the PIB is more highly present, then immediately other functional groups like the Si-O-Si and P-O-C are more present as well: seen in REOB-Y. Whereas when it is lowest present, it will be low for all again, seen in REOB-Z. This therefore means that additives will relatively remain at the same consistency (high PIB -> high Si-O-Si for example), but their general amount can definitely differ. This is important to remember, as many identification tools, be it XRF, ICP, NMR or FTIR all depend on finding these distinctive trace metals and functional groups, that only come from the specific lubricant additives that are still present in REOB.

4.2.4. Effect of REOB in modified bitumen on ATR-FTIR spectrograms

With the bitumen and the REOB itself analysed first, now the blends of both bitumen and REOB-X can be analysed as well. The goal is to see how well one can identify the presence of REOB in the blends, but also to select which functional groups can be used specifically for quantification.

In Figure 4.18 and Figure 4.19 one can see the base bitumen spectra that were used for the REOB modification. Ageing of the unmodified binders is shown as well, to be able to show the clear difference between unmodified and REOB modified binders, with respect to the formation (or deformation) of functional groups. These figures are immediately followed up by the spectra of the REOB blends at the different dosages 5%; 10% and 15%. The REOB-X is again showed here as well, to show where the differences in functional groups are expected because of REOB addition.

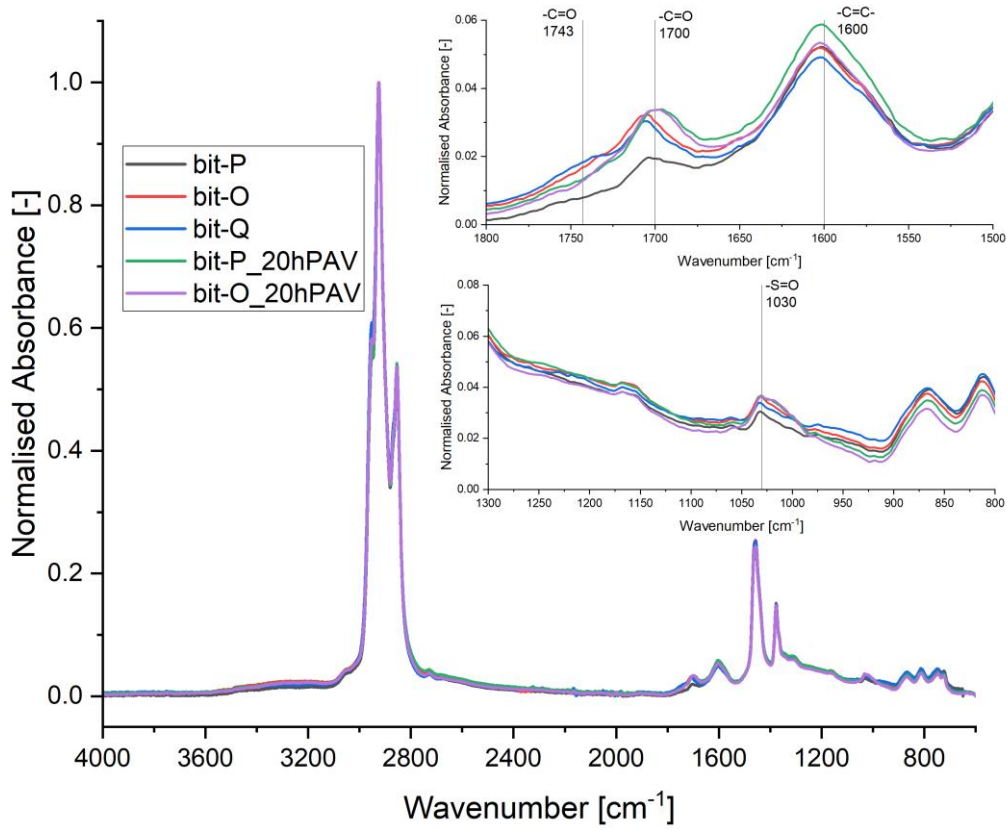


Figure 4.18: ATR-FTIR spectra of bitumen P, O and Q including aged versions

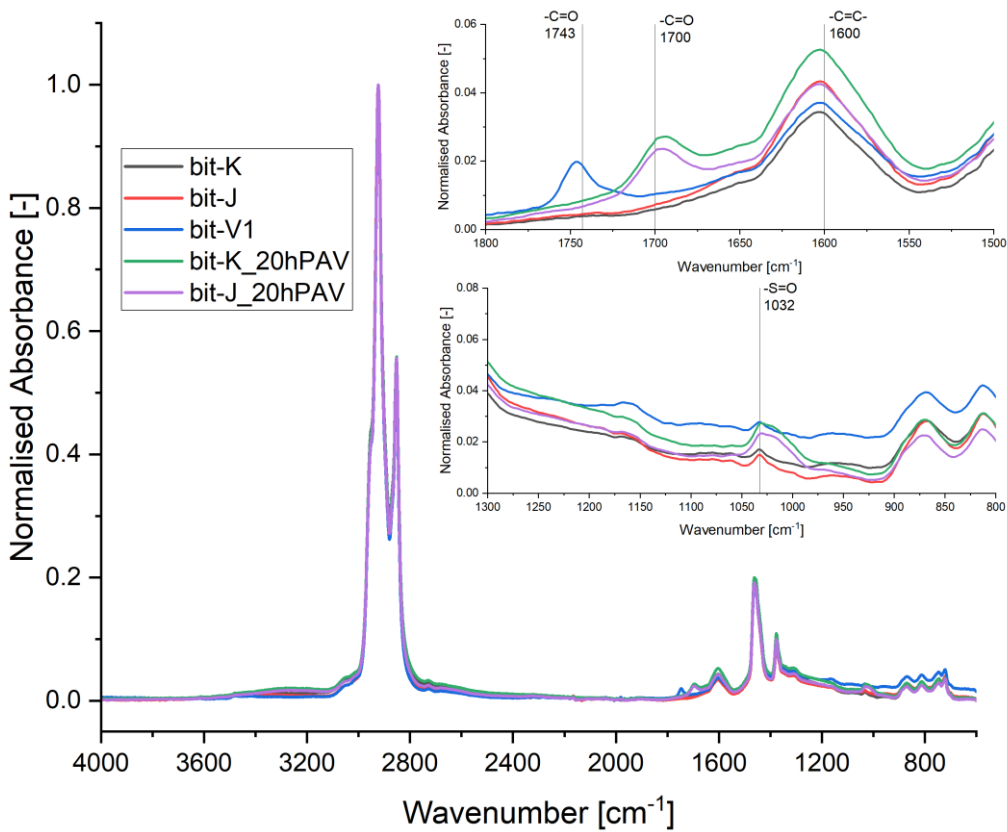


Figure 4.19: ATR-FTIR spectra of bitumen K, J and V1 including aged versions

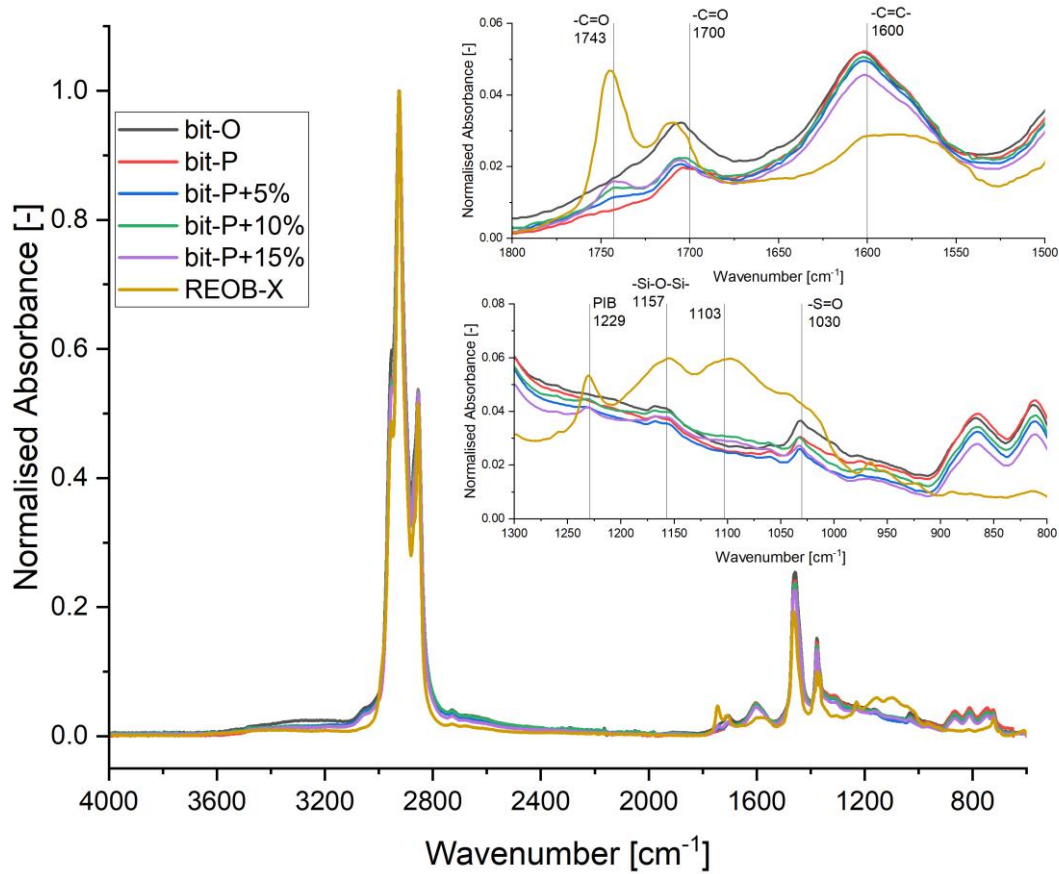


Figure 4.20: ATR-FTIR spectra of bitumen P, O, the 5; 10 and 15% blends and lastly the REOB-X

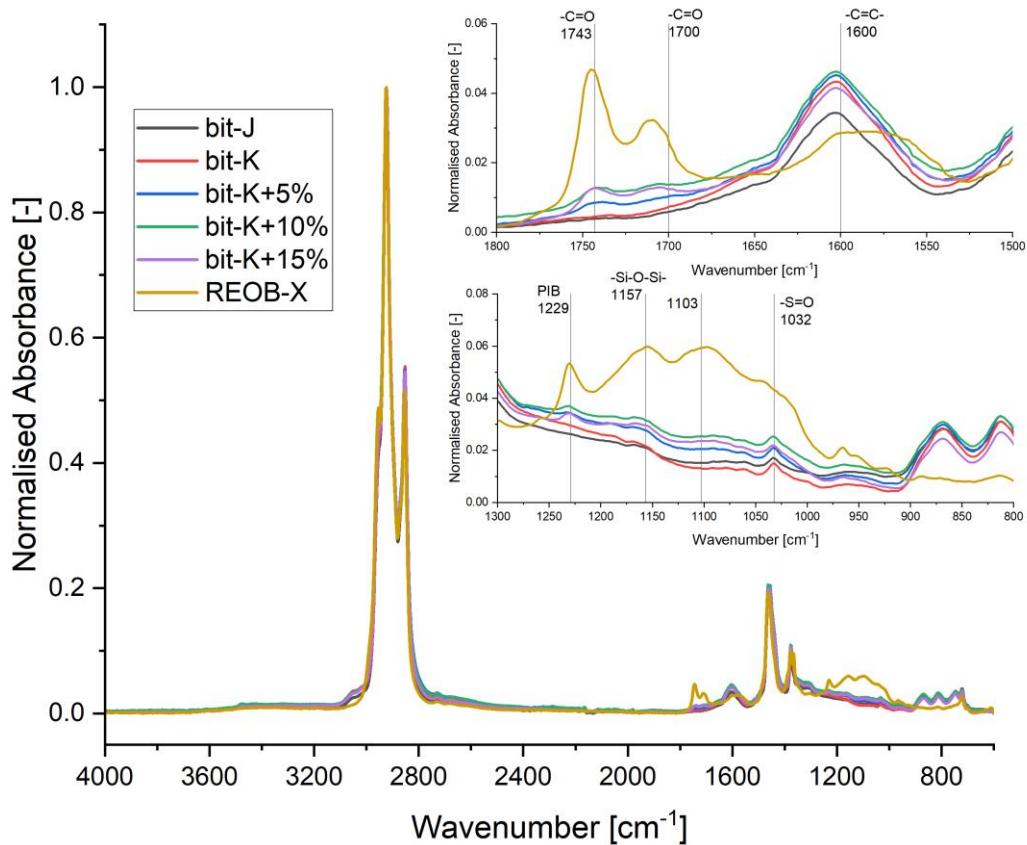


Figure 4.21: ATR-FTIR spectra of bitumen K, J, the 5; 10 and 15% blends and lastly the REOB-X

Regarding the unmodified bitumen series, one can see the following differences in base bitumen and when they are 20hPAV aged. Carbonyl (C=O) groups seem to be similar between bit-O, bit-O_20hPAV, bit-Q and bit-P_20hPAV and only bit-P unaged has a significantly lower value. However no carbonyl was measured for the bit-K, bit-J and bit-V1 fresh binders. Next to that the formation of carbonyl was significantly higher for bit-K_20hPAV than bit-J_20hPAV. The peak at 1738 [cm⁻¹] indicates the presence of C-OH groups, which are interestingly only measured in the case of bit-V1. The aromaticity at 1600 [cm⁻¹] indicates no changes with ageing for bit-O and a small increase for bit-P. Similarly there is no visible increase for bit-J but there is for bit-K. Clearly the sulfoxide (S=O) group at 1030 [cm⁻¹] only increases with ageing, as seen for bit-O, P, K and J_20hPAV.

However the bitumen blends show some distinctive different peak intensities of its functional groups. Mainly the peaks at 1750, 1710, 1229, 1150, 1100 and 962 [cm⁻¹] clearly increase in presence in the spectrograms of the blends, when the dosage is increased of the REOB. The carbonyl peak at 1710 [cm⁻¹] is considerably higher for bit-O, although this bitumen does not have a peak at 1750 [cm⁻¹]. Both REOB-X and REOB-Y can cause this peak at 1750 [cm⁻¹] to appear, but adding REOB-Z would not create this peak, showing therefore that quantification of the REOB based on this peak alone (although significant in height), would not accurately predict REOB dosage. Compared between the two blend series; one can see that the peak of 1700 was not present for bit-K and bit-J yet, but with increasing dosage it became more intense. Compared to bit-O and bit-P, there the carbonyl peak was already present so the change with dosage was not as apparent. The aromatic peak at 1600 [cm⁻¹] remains relatively stable with changing the dosage, although slightly undergoes as decrease with REOB dosage. It is interesting to see how bit-J has less aromatics than the bit-K (stiffer) bitumen, whereas bit-O has significantly more than bit-P.

Lastly, the PIB peak increases similarly between both series. The functional groups of the base bitumen do not seem to have an effect on the peak. This is contrary to the complete area between 1250 and 950 [cm⁻¹], which differs a lot between both binder series when REOB is increased in dosage. Comparing between bit-P and bit-K blend series, one can see that the overall functional groups change only slightly for bit-P whereas they change quite a lot for bit-K blends. This mainly has to do with the measurement procedure. Bit-P is slightly stiffer than bit-K, meaning that the ATR crystal is covered similarly between tests with less variance than a softer binder.

On the next page one can find Figure 4.22 and Figure 4.23, which show the changes in functional groups for the aged bitumen and blends. With the aged blends and REOB, one can see a significant increase for the carbonyl peak at 1700 [nm]. It is also clear, for both blend series, that this carbonyl peak has increased differently for each REOB dosage. One can see that 0% dosage has the lowest increase in carbonyl peak, then the 5%, then the 10% and lastly the highest increase is present for the 15% dosage. This proves, regarding the carbonyl functional groups, that the oxidative ageing for these groups has increased because of the REOB and therefore one can say the blend in total has aged more. Comparing this to the sulfoxide peak at 1030 [cm⁻¹], this is not the case. The REOB does change the height of the curve between 1250 and 950 [cm⁻¹], but it does not seem to have an effect on the formation of sulfoxide with ageing.

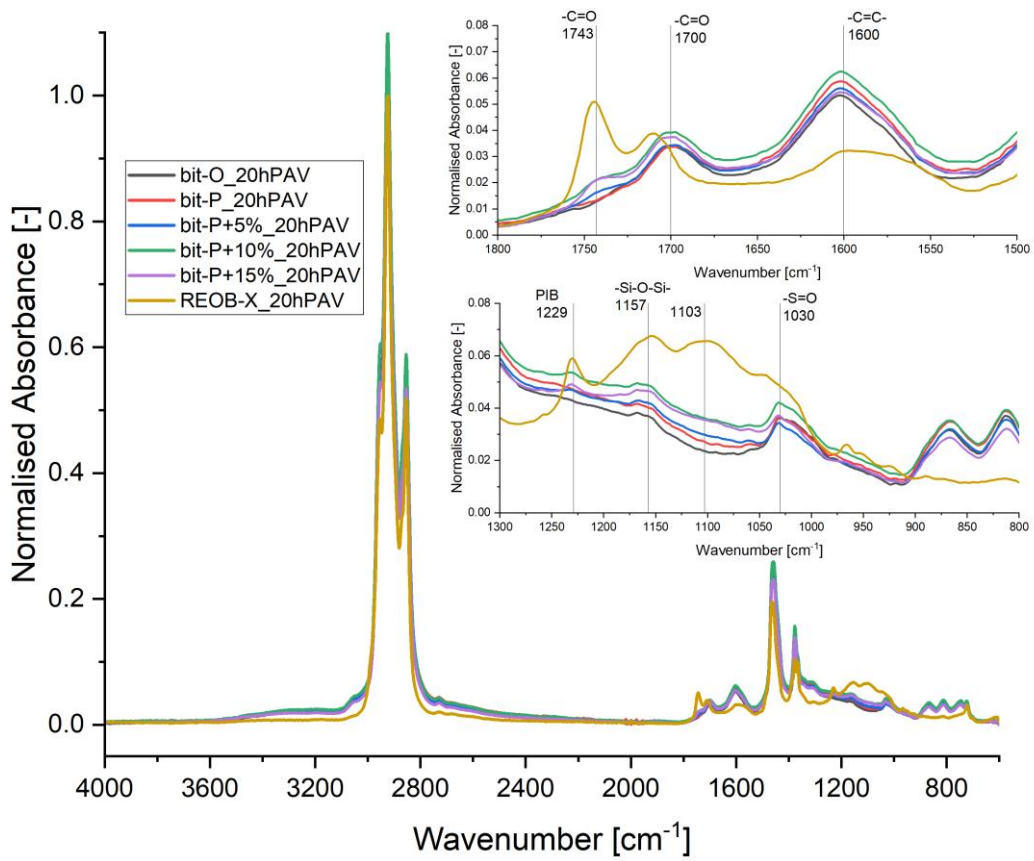


Figure 4.22: ATR-FTIR spectra of aged bitumen P, O, the 5; 10 and 15% blends and lastly the REOB-X

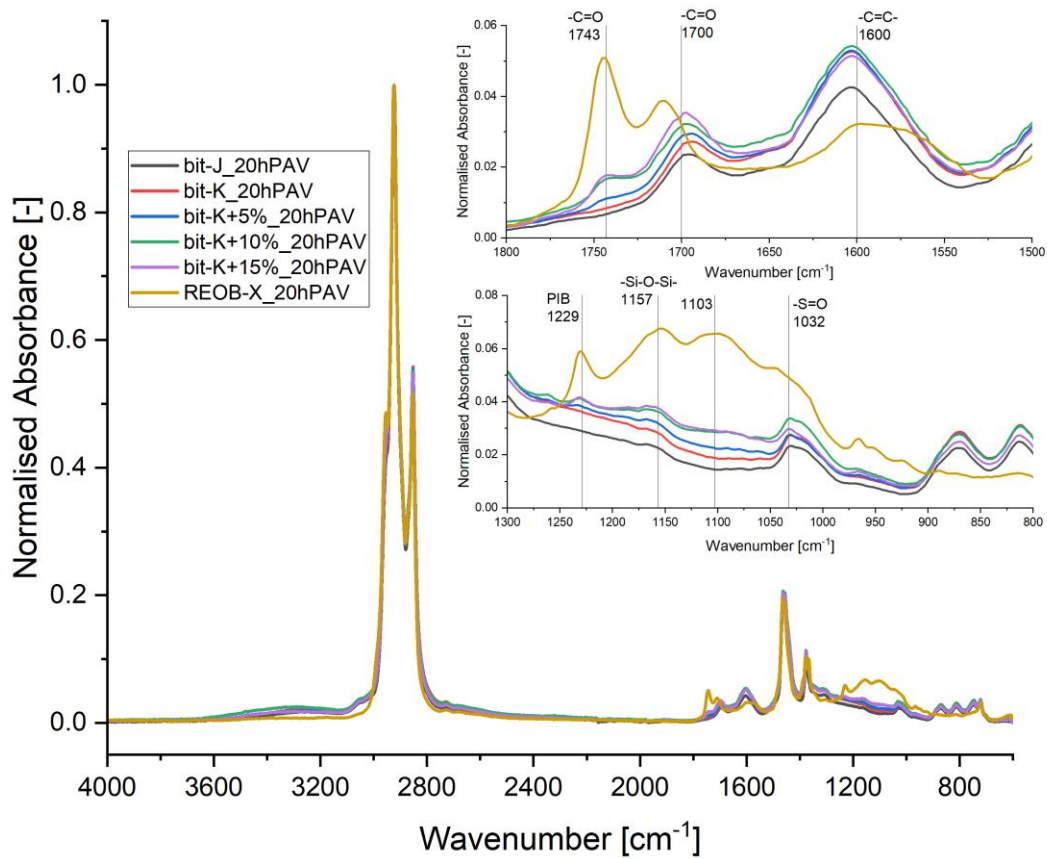


Figure 4.23: ATR-FTIR spectra of aged bitumen K, J, the 5; 10 and 15% blends and lastly the REOB-X

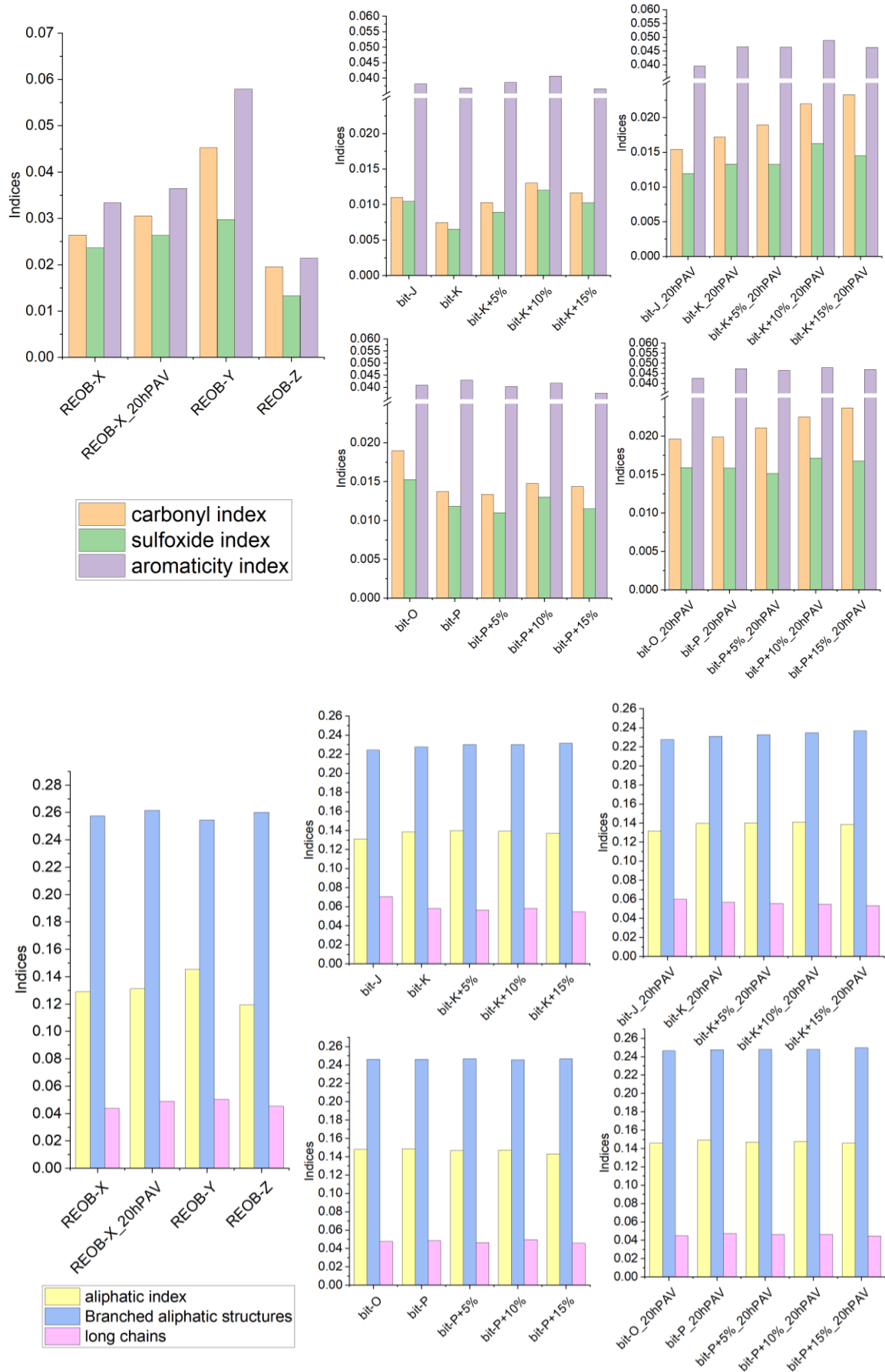


Figure 4.24: Indices for modified spectra | REOB modified bitumen

In Figure 4.24 one can find regarding the carbonyl index that by simply increasing REOB dosage, one does increase the initial values. But especially with ageing, just a single ageing step of 20hPAV, one can see that more carbonyls have formed for the 15% than for the 5% according to a linear relation. The slope of carbonyl index over dosage at an unaged stage is lower than that of the slope at an aged stage. This effectively shows that REOB is detrimental to the ageing susceptibility, specifically when increasing the dosage.

It also shows, between using bit-K or bit-P, that a different behaviour can be observed in their compatibility with the REOB. Although initially the carbonyl and sulfoxide were certainly lower for bit-K blends than for bit-P, after ageing this is not true anymore. Bit-K blends show an increased slope in the carbonyl index, which indicates they had higher oxidation rates than the bit-P blends, suggesting a higher susceptibility to ageing.

The reference bitumen, bit-J and bit-O, differ interestingly from the REOB blends. bit-J seems to increase in carbonyl and sulfoxide like bit-K+5% does, although starting lower. But bit-O has initially very high indices and they do not change that much when 20hPAV aged. Therefore it is expected that bit-O will show less ageing susceptible behaviour than bit-J and all the blends should have the worst ageing behaviour compared to both bit-J and bit-O.

With ageing, one can see a small decline in both aliphatic and branched aliphatic structures, although clearly the REOB dosage seems to not have an impact on this decline, like was observed for the carbonyl and sulfoxide.

4.2.5. Analysis of PIB peak using the derivative of the Transmittance spectra

Quantification of REOB has been a tough challenge for many researchers (Hesp & Shurvell, 2010; Karki et al., 2019; Kaskow et al., 2018; Yan et al., 2022). Using both XRF and FTIR has shown that REOB differs a lot between different suppliers, having different origins of use and composition.

As trace metals, measured with XRF, have shown to vary a lot between different REOB sources and its use being less common, the worth of FTIR is deemed higher. There is less difference in components in REOB and they vary approximately similarly see Figure 4.17 (a high peak in PIB will also show a high peak in Si-O-Si and vice versa). But because the changes to the bitumen spectrum are very small, almost invisible, one needs to find an accurate way to zoom in on these specific differences. Simply by calculating the area under the small peak of PIB is practically impossible to do and will result in very inaccurate measuring and calculations. Another way to predict this better is therefore needed.

One of the ways to do this, is by looking at the rate of change of the spectra, in other words the derivative of the spectrum. The derivative is taken from the transmittance spectra, and shown in Figure 4.25. Here one can see how the peak between 1250 and 1230 shows to increase with higher dosage of REOB. It is also clear to see that the bit-P+5% and bit-K+5% exactly overlap, and similarly also for the other two dosages. When no REOB is added the PIB peak does not appear. This means a quantitative value can be connected to the different dosages of REOB.

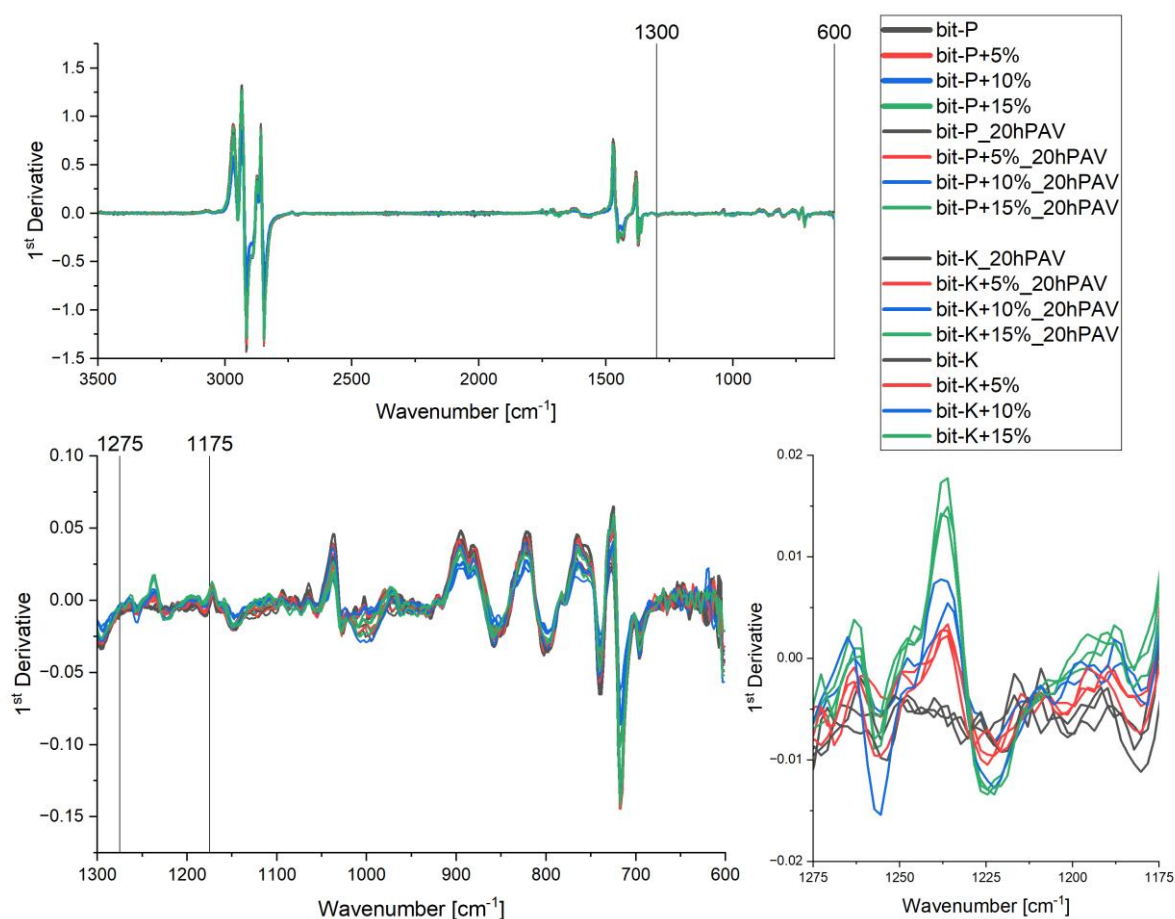


Figure 4.25: Derivative plots of transmittance spectra of unaged and aged bit-P and bit-K blends, each figure zooming in further on the peak distinctive for the presence of PIB

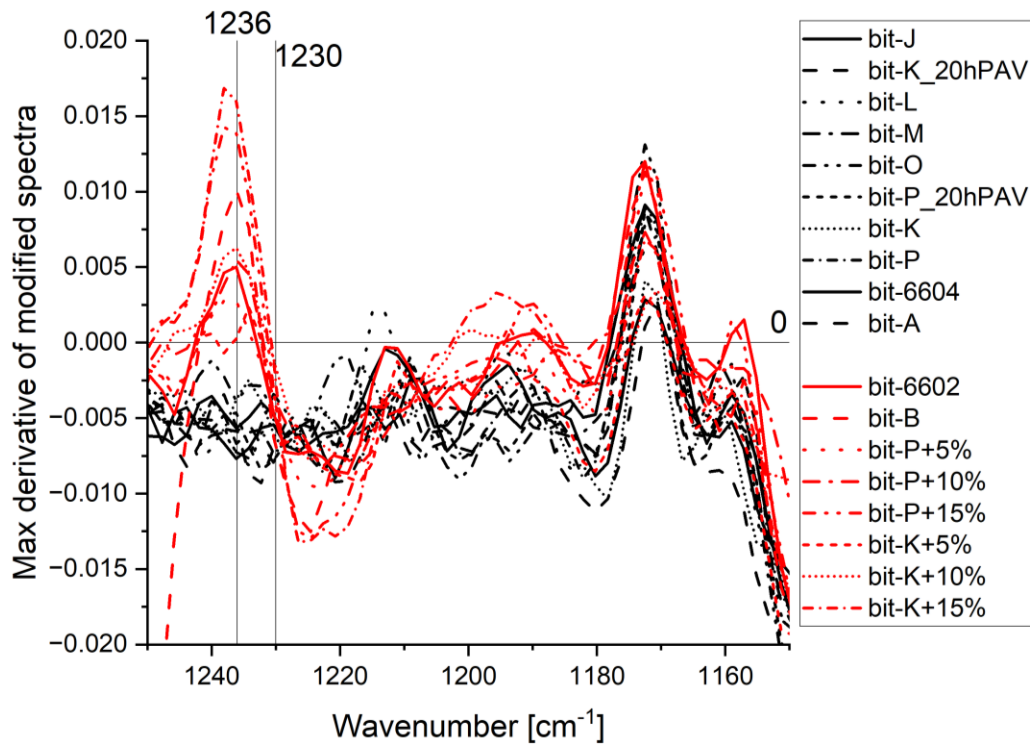


Figure 4.26: Maximum derivative values for unmodified and REOB modified bitumen

To further prove that the maximum derivative of the modified spectra is indeed an effective measurement of PIB presence, one can plot all modified and unmodified spectra next to each other. This is done in Figure 4.26. One can clearly identify if a PIB containing REOB has modified the bitumen. Making sure the measurements done on one bitumen is actually an accurate measurement, that there will not be too much variance in measured absorbance in this area, would be best reached by performing multiple FTIR scans of the bitumen (4x at least).

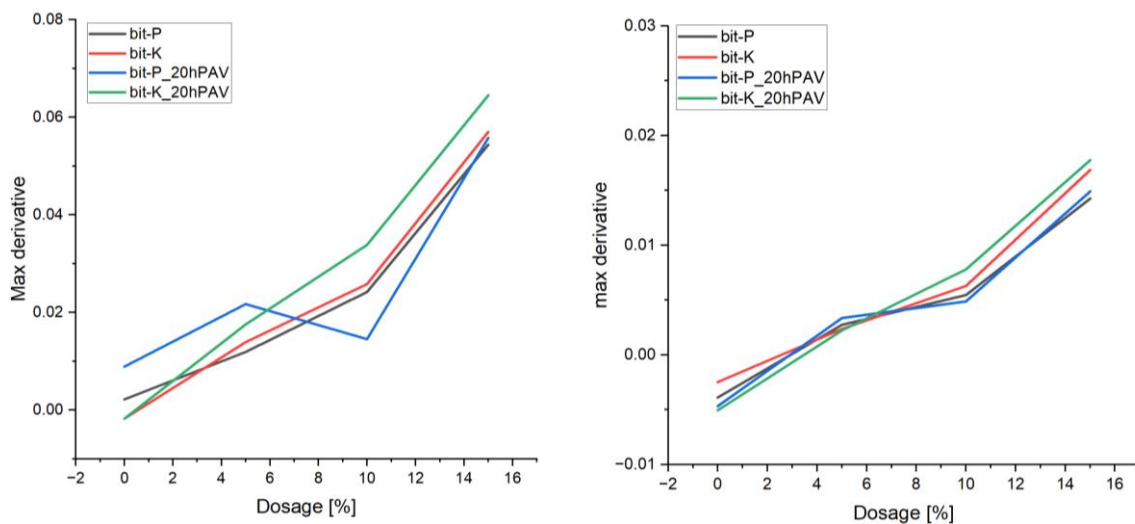


Figure 4.27: (left) measured maximum derivative for unmodified spectra and (right) for modified spectra

In the above figure one can see how important it is to use ATR modification in the fingerprint area, as it will reduce variance in the resulting measurements. The slope will be decreased significantly, but the difference between measurements will relatively be reduced.

If the relationships are assumed to be linear, the following formula can be used:

$$y_{\max \text{ derivative}} = 0.001158553 * \text{dosage}(\%) - 0.00306$$

$$\rightarrow \text{dosage}(\%) = \frac{y_{\max \text{ derivative}} + 0.00306}{0.001158553}$$

(4.4)

One can see that the datapoints do not follow a precise linear path, but some bumps in the measurements can be noticed. This is deemed to be related to the exact dosage that was actually used, for example the REOB blend of 10% was aimed to be of this quantity but could in fact be more close to 9%. Similarly the 5% blend could actually be more close to 6%, there is no exact way to know precisely how much has actually been added, but as the deviations seem to be small (between 1% difference) this is not deemed to be bothersome.

To compare this to the REOB modified bitumen that was provided by refineries themselves, one obtains the following maximum derivative behaviour shown in Figure 4.29. Although REOB-X was not used for blending but two completely unknown REOB, one can still measure a significant presence of PIB. Quantifying this does show though that REOB differs a lot between each other, as is shown in the right part of the figure where the bit-B and bit-6602 seem to differ a lot from the prediction line of using REOB-X. The fitted line used for REOB-X shows an overestimation of the actual known dosage for both bit-B and bit-6602 bitumen. Bit-B is expected to have to contain 11.5% REOB, while it was known to be 8% and in the case of bit6602 it is expected to be around 7% instead of the actual 4%. This does not say that using the maximum derivative around the PIB peak is not accurate, but merely means that the used REOB for those other binders has been containing a higher concentration of PIB, resulting in a higher measured PIB peak than the dosage used actually suggests.

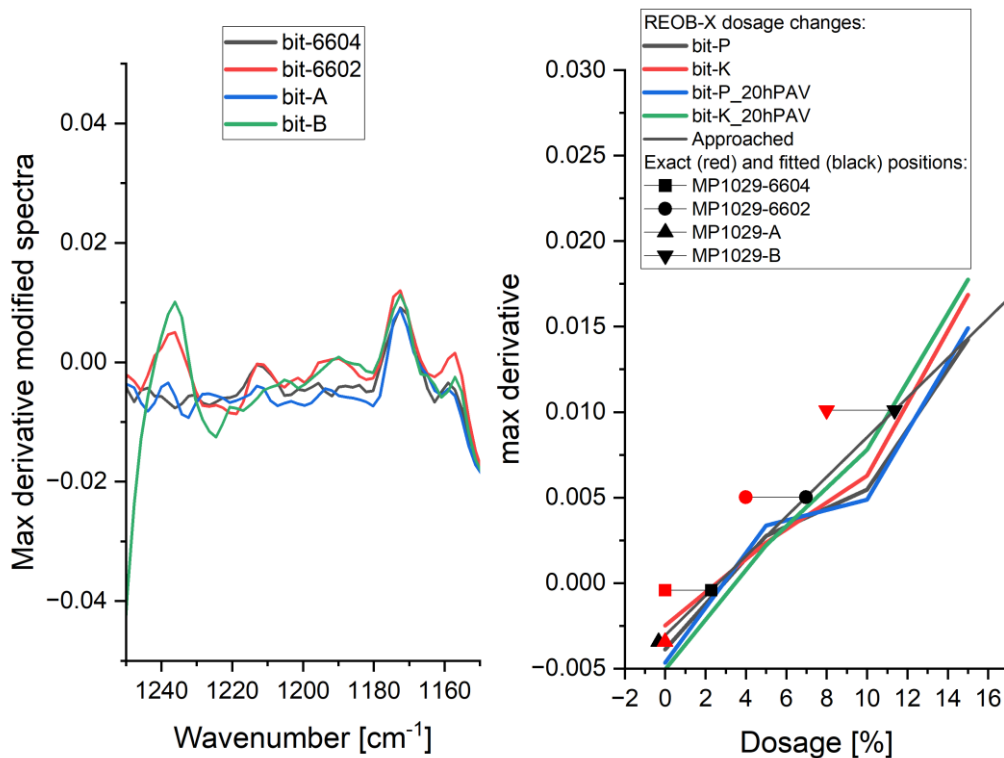


Figure 4.28: Maximum derivative values for unmodified and unknown REOB modified bitumen samples bit-B and bit-6602

Compared to the use of XRF this means however that one can measure REOB presence and content, regardless of knowing what the composition was of the base bitumen. The main difference that

contributes to the maximum derivative peak in the REOB modified bitumen, is the added PIB from the added REOB. This means the use of the PIB maximum derivative peak is a much more reliable tool than the XRF and above all a much more easy and quick to use analysis.

However, basing a REOB dosage in bitumen completely on the presence of PIB would be inaccurate. The current maximum derivative values are only fitted well to the addition of REOB-X specifically. Other REOB have different PIB intensities and therefore will lead to different maximum derivatives to be measured in blends. A better representation of REOB addition, would be to signify an index value of lubricant additives present in the bitumen, because of their presence in REOB, and relate changes in performance to this value and not the REOB dosage. This means that the PIB would be used to quantify the presence of PIB, Si-O-Si, P-O-C, i.e. all additives for lubricants. As was seen before in Figure 4.13, the REOB mainly differ in that the functional groups representing lubricant additives will change in intensity, but do so roughly in the same way. This means that when high PIB is present, high Si-O-Si can be expected, as well as high P-O-C etc.

Knowing an index of the present lubricant additives in REOB, is deemed more valuable than knowing the weight percentage of REOB in the blend. It is in fact expected that not the consistency of REOB, being a mixture of mainly saturates and resins (seen in Paragraph 4.4), but the fact that so much (and complex) lubricant additives are present in REOB are what has had negative impact on the researched REOB modified mixtures. Problems regarding bad mixture workability, compactability, premature ravelling and/or cracking and the increased ageing susceptibility are assumed not to be problems caused by the mere hydrocarbon composition of the oil, but specifically these lubricant additives that still reside in the REOB.

4.2.6. Observations on trace elements and chemical functional groups

With the analysis of several bituminous samples with the XRF and a large group of bitumen analysed with the ATR-FTIR, one can say something definitive about the trace elements/metals and functional groups present in both unmodified and REOB modified bitumen.

- (1) Trace elements like Calcium (Ca), Nickel (Ni), Phosphorous (P), Molybdenum (Mo), Zinc (Zn), Kalium (K), Silicium (Si) and Iron (Fe) become more pronouncedly present in REOB modified bitumen (Hesp & Shurvell, 2010; Karki et al., 2019; Kaskow et al., 2018). Although one needs to keep in mind that Fe (Iron), Ni (Nickel) and V (Vanadium) can already be present (Nahar et al., 2016). The main heritage of these trace metals can be traced back to their origin as lubricant additives in the engine oil. Think of anti-wear particles, detergents, viscosity modifiers etc (Minami, 2017; O'Brien, 1983; Speight & Exall, 2014; Wong & Tung, 2016).
- (2) REOB modification of bitumen leads to specific functional groups to appear in the FTIR spectrograms. Specifically the PIB, Si-O-Si or P-O-C peaks reference to the presence of lubricant additives in a bitumen (Kaskow et al., 2018; Yan et al., 2022).
As the PIB peak itself is not large in modified bitumen, although its position and sharpness are unnatural for a bitumen spectrum, one should use the derivative of the spectrogram to pinpoint the presence of this compound. The maximum derivative that can be measured at $1236 \text{ [cm}^{-1}]$ can be directly related to the REOB dosage. Merely identifying the presence of REOB in a bitumen is very simple this way, although quantification remains hard as the PIB content between different REOB can vary. This however still provides a better approach than basing the identification or quantification on the presence of trace metals, as some trace metals can already be present in a bitumen and there is even more variance in trace metal quantity between REOB sources (Karki et al., 2019; Kaskow et al., 2018).
- (3) ATR-FTIR is effective in showing the increases in carbonyl and sulfoxide indices for unmodified and REOB modified bitumen. This clearly brings to light how REOB modified bitumen has an initial increase in both functional groups, and that mainly the formation of carbonyl is heavily accelerated with dosage of REOB; a behaviour partly already observed for REOB modified bitumen (Rubab et al., 2011).
- (4) Bit-J, bit-L and bit-V1 specifically show to have a very strangely high index for long chains (-C-H stretching). After TFOT ageing this drops drastically for both bit-J and bit-L and could therefore possibly have a significant effect on viscosity and rheological performance of specifically these bitumen.

4.3. Elemental analysis (C,N,H,O & S)

4.3.1. Principle of the EA technique and measurements

Bitumen consists mainly of hydrocarbon molecules, where the hydrogen sometimes has been swapped by nitrogen, oxygen and sulphur. To effectively measure the weight percentage of the presence of these main atoms, one can use a CHN analyzer. Here the concentrations are effectively measured, by performing a combustion analysis and measuring the products that come from it: CO₂, H₂O and N_xO_y. Those gases are separated in chromatographic columns and then detected on a thermally conductive detector (TCD) (Frąckowiak et al., 2022).

As Oxygen and Sulphur are not measured with this technique, but very well present in bitumen, they have to be analysed separately. A pyrolysis process is performed to do the CHNS+O analysis, using inert gases (He; Ar) and after the pyrolysis has finished, a catalytic bed of copper (Cu) or WO₃ is used to obtain the N₂, N_xO_y, CO₂, HO, SO₂ and SO₃. Accurate measurement of sulphur is thus made possible too. Alternatively, to estimate the oxygen amount, the CO peak should be the basis of the pyrolysis (Frąckowiak et al., 2022).

From this, one can conclude that the measurement of oxygen is the hardest to measure and one should carefully analyse the found concentrations before drawing any conclusions.

In a first series of CHNS+O measurements, 14 different bitumen were analysed with the technique, see Table 4.3. The technique was effective in analysing the bitumen, stating clearly that specifically bitumen series bit-J, bit-K and bit-V1 had extremely low sulphur contents and bit-6604 and bit-6602 had relatively the highest amounts. It is also interesting to notice the extremely lower hydrogen content for bit-A and the very high carbon content of both bit-J and bit-K.

Table 4.3: First set of CHNS+O measurements

	C, Carbon	N, Nitrogen	H, hydrogen	O, oxygen	S, sulphur	Total
[u]	12.011	14.007	1.008	15.999	32.060	
	[wt%]	[wt%]	[wt%]	[wt%]	[wt%]	[wt%]
bit-A	84.741	0.679	9.963	2.311	2.900	100.594
bit-G	84.721	0.836	10.523	2.166	3.200	101.446
bit-I-1	84.869	0.706	10.678	2.089	3.100	101.442
bit-J-1	86.694	0.668	10.644	2.025	1.300	101.332
bit-K-1	86.520	0.799	10.546	1.968	1.100	100.933
bit-V1	85.054	0.694	10.902	1.289	1.165	99.104
bit-L	83.907	0.781	10.555	2.641	3.500	101.384
bit-M	84.455	0.537	10.819	2.348	3.100	101.260
bit-N	84.763	0.521	10.857	2.434	3.500	102.075
bit-O	84.860	0.672	10.703	2.581	2.700	101.516
bit-P	84.771	0.717	10.673	2.835	3.000	101.996
bit-Q	85.040	0.617	10.768	2.441	2.800	101.665
bit-6604	84.451	0.615	10.599	2.268	4.400	102.332
bit-6602	83.880	0.723	10.869	2.425	3.900	101.798

Only bit-6602 contained REOB and from this one cannot clearly discern heavy changes in the elemental composition of the binder. A separate series on other blends and REOB itself is also performed, shown in Table 4.4.

Table 4.4: Second set of CHNS+O measurements

	C, Carbon	N, Nitrogen	H, hydrogen	O, oxygen	S, sulphur	Total
	[u]					
	12.011	14.007	1.008	15.999	32.060	
	[wt%]	[wt%]	[wt%]	[wt%]	[wt%]	[wt%]
bit-J	86.694	0.668	10.644	2.025	1.300	101.332
bit-J_20hPAV	86.296	0.708	10.946	1.400	1.247	100.597
bit-K	86.520	0.799	10.546	1.968	1.100	100.933
bit-K_20hPAV	86.081	0.830	10.474	1.507	1.407	100.298
bit-K+10wt%	85.670	0.866	10.628	1.244	1.342	99.749
bit-K+10wt% 20hPAV	85.402	0.836	10.560	1.829	1.349	99.976
bit-V1	85.054	0.694	10.902	1.289	1.165	99.104
bit-O	84.860	0.672	10.703	2.581	2.700	101.516
bit-O 20hPAV	84.710	0.708	10.677	1.504	3.004	100.603
bit-P	84.771	0.717	10.673	2.835	3.000	101.996
bit-P 20hPAV	84.392	0.764	10.451	1.532	3.233	100.373
bit-P+10wt%	84.241	0.807	10.517	1.467	3.102	100.135
bit-P+10wt% 20hPAV	84.173	0.805	10.383	1.800	2.961	100.122
bit-Q	85.040	0.617	10.768	2.441	2.800	101.665
REOB-X	78.759	0.485	11.756	3.839	1.183	96.021
REOB-Y	77.818	0.589	11.526	9.866	1.286	101.085
REOB-Z	82.948	0.369	13.293	3.951	0.694	101.256

Now a series of tests have been performed on both aged bitumen and REOB modified bitumen. Here one can clearly see that oxygen amounts have dropped with ageing, which is impossible. This shows the error in the first (but also second) series of measurements, in estimating the oxygen content.

Usually the oxygen content is estimated by linking it to the remaining part out of 100%, after subtracting C, H, N and S. This would possibly give a better estimation than the supposedly measured oxygen based on the pyrolysis, although the measuring of sulphur is also not as accurate as CHN. The elemental ratios will therefore also be based on recalculated values of oxygen and sulphur, otherwise the data is shifted too much and mainly ageing will not be represented well enough (as oxygen content would otherwise drop).

4.3.2. Apparent elemental composition of unmodified and REOB modified bitumen

To recalculate the Oxygen and Sulphur contents, to reduce the error in the measurement, the average of the measurement and the expected content is calculated. So oxygen and sulphur contents are recalculated in the following way:

$$\begin{aligned} \text{Oxygen } (O)_{mean} &= \frac{O_m + O_c}{2} = \frac{O_m + (100 - C_m - H_m - N_m - S_m)}{2} \\ \text{Sulphur } (S)_{mean} &= \frac{S_m + S_c}{2} = \frac{S_m + (100 - C_m - H_m - N_m - O_m)}{2} \end{aligned}$$

(4.5)

Where the subscript “m”, stands for the measured weight fraction [%] and “c” for the calculated fraction. The following calculated results are then obtained:

Table 4.5: Calculated and mean weight percentages of Oxygen (O) and Sulphur (S)

	O, oxygen			S, sulphur		
	O_m	O_c	O_{mean}	S_m	S_c	S_{mean}
	[wt%]			[wt%]		
bit-A	2.311	1.717	2.014	2.900	2.306	2.603
bit-G	2.166	0.720	1.443	3.200	1.754	2.477
bit-I-1	2.089	0.647	1.368	3.100	1.658	2.379
bit-J-1	2.025	0.694	1.359	1.300	-0.032	0.634
bit-K-1	1.968	1.035	1.501	1.100	0.167	0.633
bit-V1	1.289	2.185	1.737	1.165	2.062	1.613
bit-L	2.641	1.257	1.949	3.500	2.116	2.808
bit-M	2.348	1.088	1.718	3.100	1.840	2.470
bit-N	2.434	0.359	1.397	3.500	1.425	2.463
bit-O	2.581	1.066	1.823	2.700	1.184	1.942
bit-P	2.835	0.839	1.837	3.000	1.004	2.002
bit-Q	2.441	0.775	1.608	2.800	1.135	1.967
bit-6604	2.268	-0.065	1.101	4.400	2.068	3.234
bit-6602	2.425	0.628	1.526	3.900	2.102	3.001

Still the oxygen amount is somewhat too high for the initial condition and too low for the aged variant, but correcting the values further will make it impossible to say if modification has impacted the results too much or not.

To calculate the elemental ratios, representing the relative amount of H-C, N-C, S-C and O-C connections, one needs to use the elemental molecular weights and calculate the fractions in the following way:

$$C (12.011); N (14.007); H (1.008); O (15.999) \& S (32.060)$$

$$\frac{H}{C} = \frac{(H_m/1.008)}{(C_m/12.011)} = \frac{H_m}{C_m} \cdot \frac{12.011}{1.008}$$

(4.6)

This is done in a similar way for N/C, O/C and S/C.

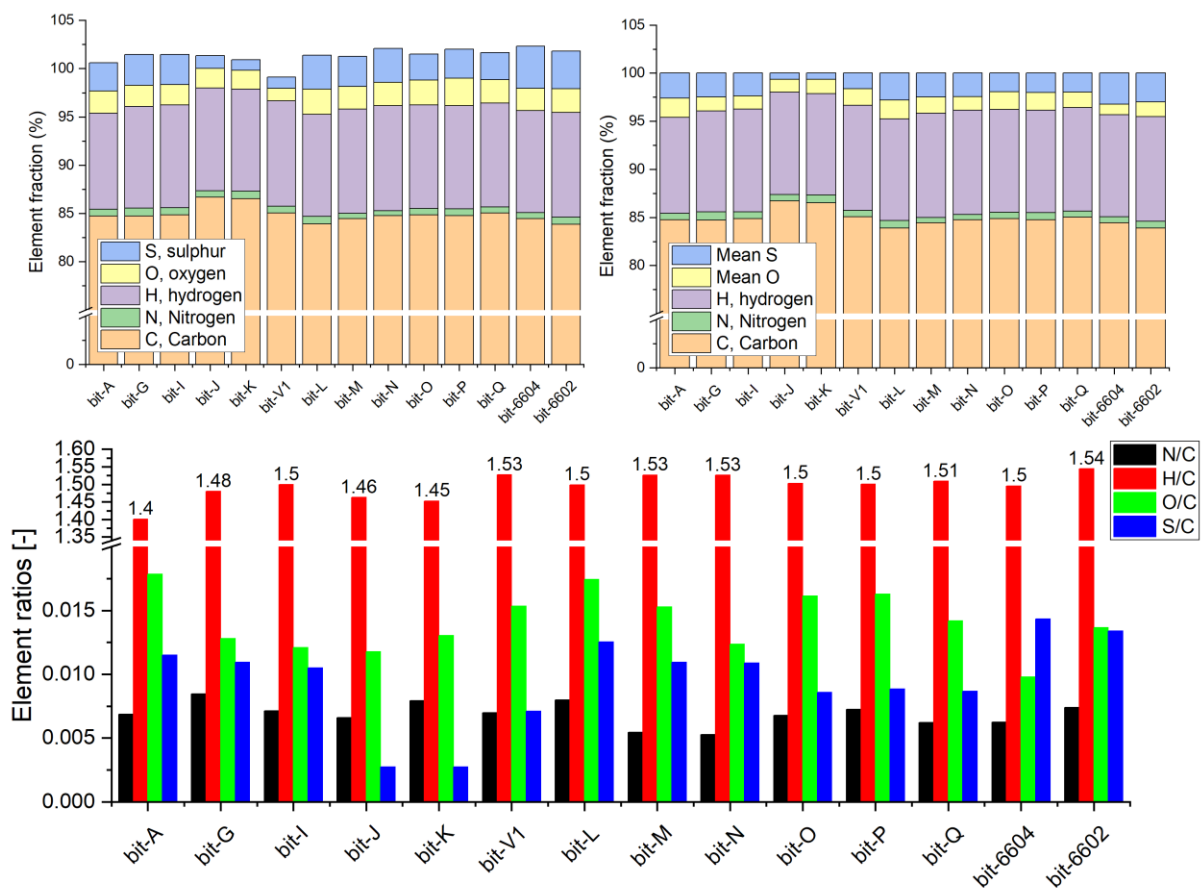


Figure 4.29: left) Unaltered and altered Element fractions [wt%] of unaged bitumen and (right) the element ratios [-]

It is clear again that bit-K, bit-J and bit-V1 have the lowest sulphur contents of all bitumen. Recalling the observations in the functional groups from FTIR spectra, this can be correlated to how the sulfoxide (S=O) has increased with ageing for bit-J. Having a low sulphur content in bitumen will prevent oxidation on this element and therefore lead to lower sulfoxide (S=O) contents. Nevertheless, it is also possible that less oxidation on sulphur means that more oxidation will take place on available carbons, creating carbonyls (C=O). It was not possible to discern this effect with this dataset alone though.

Bit-A clearly shows it has a very low H/C ratio, meaning it will have relatively long carbon chains, whereas bit-6602 has an extremely high H/C ratio compared to other bitumen. Bit-A is a 40/60 bitumen, which thus shows that longer or more complex (asphaltenes) carbon molecules can be related to creating a higher stiffness of that bitumen (longer or complex molecules will increase the higher molecular weight fraction and making the blend of molecules harder to change in microstructure with changing temperature).

Bit-K and bit-J show to both also have very low H/C and bit-V1 doesn't, although they come from the same supplier. The reason for the low values of bit-K and bit-J could be that a large portion of these binders are bitumen produced from the PDA unit. The fact that bit-V1 is not so low, could be explained by the fact that it is blended with a larger portion of other straight-run bitumen. Bitumen produced from the PDA unit is known to have filtered out a larger portion of asphaltenes and therefore reduced in longer chains, thus the resulting lower H/C for bit-K, bit-J and bit-V1 could be explained by this.

The reason that bit-6602 has such a high ratio, can be related to the fact that it has been fluxed with REOB. REOB consists mainly of shorter molecules, as it is a residue from refining the waste engine oil, a compound consisting of mainly smaller molecules. This could be a good indicator for suspicion of the presence of REOB, or other engine oil derivatives, in bitumen. Very soft bitumen, like bit-V1 and bit-Q,

which are of (160/220) grade, are normally used to flux with hard grade bitumen to soften it. Looking at the H/C ratio of those, one can see that this is sufficiently lower than the blend that bit-6602 represents. The N/C ratio shows to be very stable and not deviate much between bitumen. This suggests that nitrogen is not a leading entity in the rheological differences between the bitumen.

Although the oxygen content is deemed to be estimated with low accuracy, some distinctive big differences are still visible. Mainly bit-A shows to have a very high ratio and bit-B6604 interestingly low. Between the bitumen of the same suppliers, one can see a steady higher content for bit-V1 as compared to bit-J and bit-K, whereas bitQ lies interestingly lower than bit-O and bit-P in oxygen content.

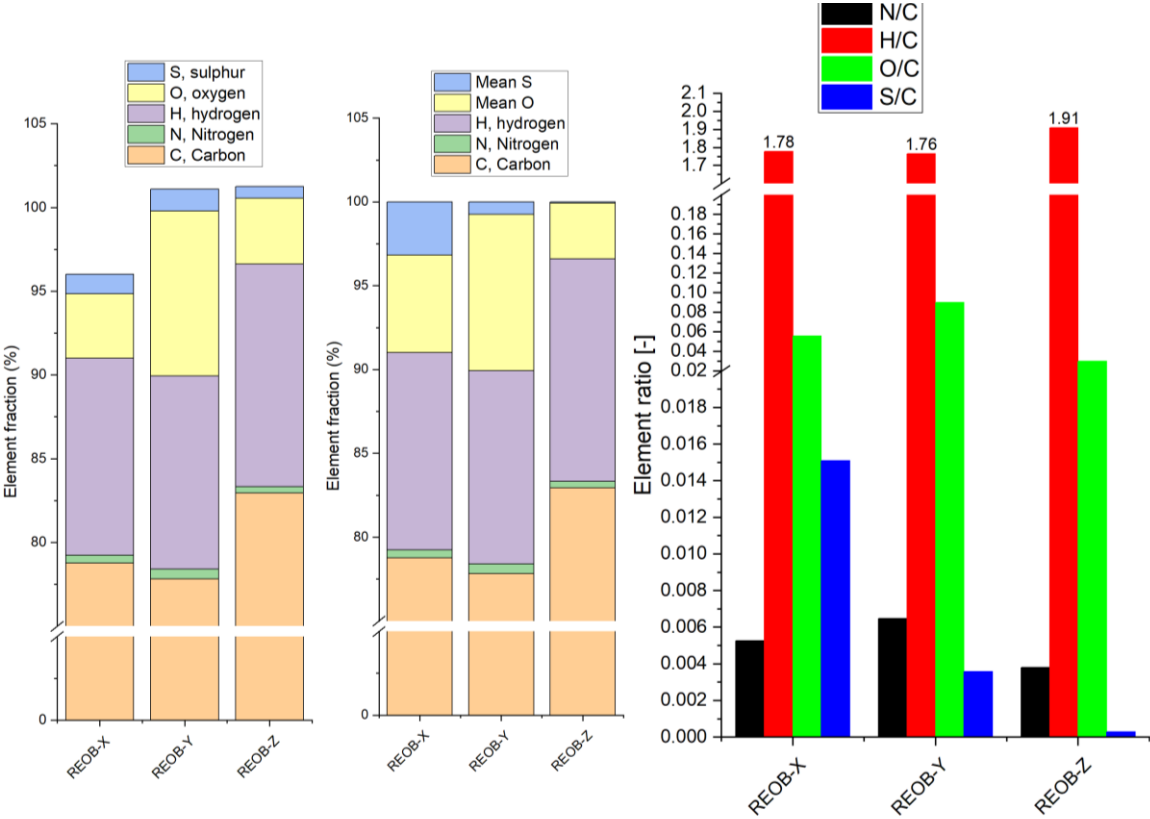


Figure 4.30: (left) Unaltered and altered Element fractions [wt%] of REOB and (right) the element ratios [-]

Next to bitumen, knowing the elemental composition of the REOB itself is important as well. This shows what kind of expected impact it will have on modified bitumen. In the figure above one can immediately see that the REOB has an extremely high H/C ratio, showing that the material consists mainly of smaller or shorter chains of hydrocarbon molecules. Its direct impact on fluxing with bitumen will therefore be to increase this ratio drastically.

The oxygen content of REOB is also of a significantly higher order, meaning the material has already been heavily oxidized. The fact that so much oxygen is found, can be related to the fact REOB results from waste engine oil. When engine oil is used in motors, it will have a service life in which oxidization can take place easily. When the waste engine oil is distilled, the goal is to mainly get the lighter fraction out of it for recycled lubricants will be retrieved and the residue stream is REOB. This makes it logical that such high oxygen content is found in the REOB, as the larger and heavier particles tend to have been oxidised more.

Interestingly the N/C ratio has not changed much as compared to bitumen, this shows that regardless of bitumen or REOB, there is a clear average of nitrogen content to be found with little variance.

The S/C ratio differs heavily between the different REOB. One can therefore expect a totally different effect of the REOB on the ageing susceptibility. If the notation of linking the oxidation of sulphur to how the binder ages and behaves differently is correct, then the REOB is expected to have a significant effect on it.

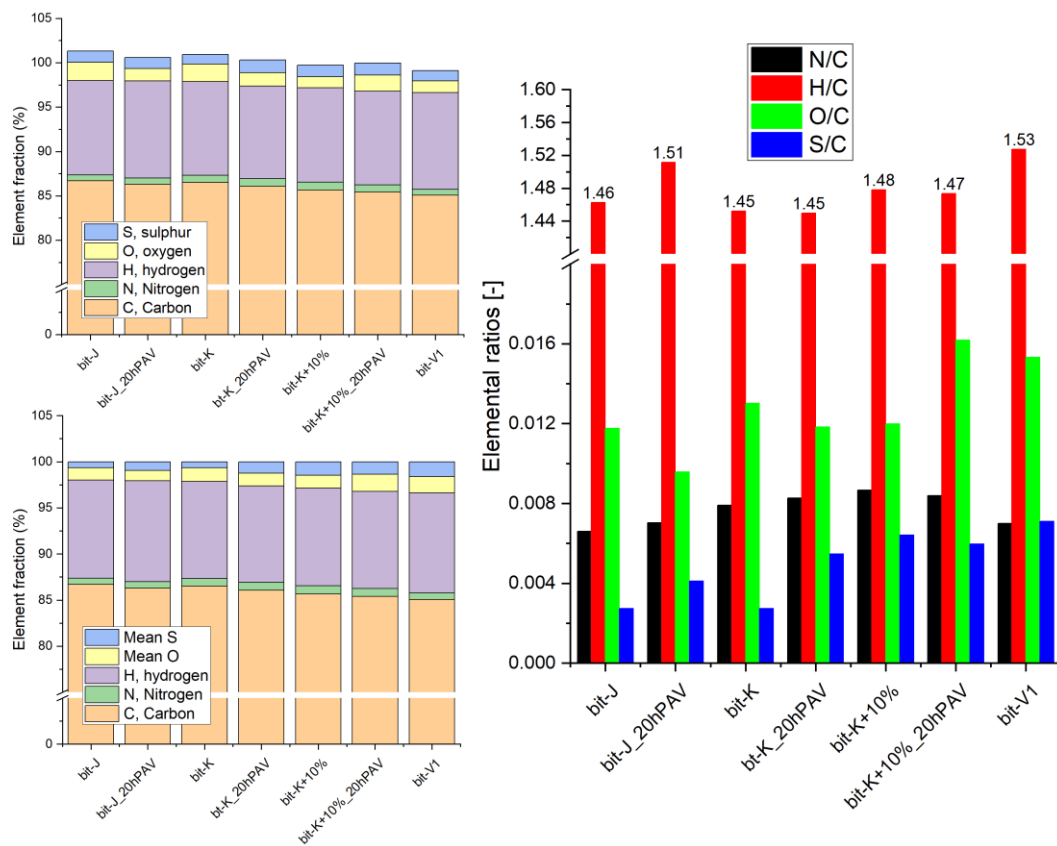


Figure 4.31: (Left) Unaltered and altered Element fractions [wt%] of aged and REOB modified bit-K bitumen and (right) the element ratios [-]

Ageing of bit-J or bit-K results in a small reduction in oxygen content, which is still a weird phenomenon and it is unclear if this results from sampling (not homogeneously mixed samples) or measurement inaccuracies. What is clear though, is the fact that the REOB blend has a very significant increase in O/C. Instead of a small decrease, one can observe the ratio to be 1.5x times higher with 20hPAV ageing. This can therefore be clearly related to the already observed faster oxidation that was already found with FTIR spectra.

The ageing of bit-J does do something interesting however. It increases the H/C. This means that highly complex or long chain hydrocarbon molecules present initially in bit-J, seem to break/fall apart with 20hPAV ageing. Comparing this to bit-K and the bit-K+10% this does not happen. Next to that one can see indeed that REOB modification increases the H/C as compared to the initial value for bit-K. Ageing of the blend shows however that it decreases again (although marginally small).

The sulphur content shows to do interesting things as well. bit-J does not show a change with ageing, but bit-K shows a significant increase. The fact that bit-K initially had quite a low sulphur content, has also changed when the REOB was added, though with ageing the bit-K+10% does not show an increase in sulphur. This therefore suggests that the bit-K base measurement has a bad measurement of sulphur and oxygen, or the machine was not able to estimate the sulphur accurate enough.

As expected, the addition of REOB and afterwards the ageing of the blend, does not change anything about the nitrogen content. It remains stable.

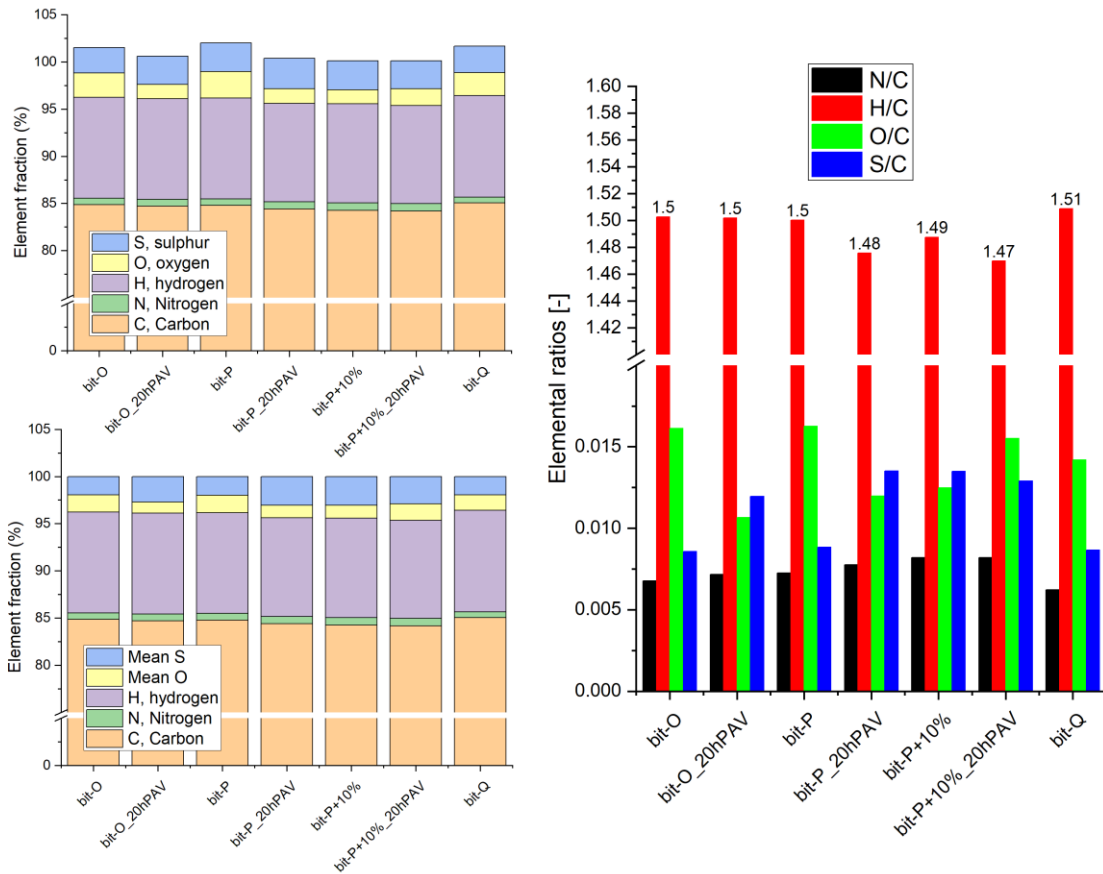


Figure 4.32: left) Unaltered and altered Element fractions [wt%] of aged and REOB modified bit-P bitumen and (right) the element ratios [-]

Ageing of bit-O and bit-P show here more significantly, as compared to bit-J and bit-K, how they have a big decrease in oxygen and a gain in sulphur content. The bit-P+10% blend shows to have increased the sulphur content and decreased oxygen, although ageing of the blend shows to have increased the oxygen content significantly and decreased the sulphur a little.

One can again see that blending with REOB causes the H/C to significantly rise, although ageing of the blend drastically drops this again. This shows how the smaller and less complex hydrocarbon molecules, in the REOB, that are used to make the bitumen softer already lose this ability with ageing 20hPAV. The H/C also is significantly high for bit-Q, showing that a REOB blend cannot merely be discerned from this ratio (as this binder is a 160/220 grade unmodified bitumen). Nevertheless, the steady decrease of H/C with ageing of blends seems to be very different from unmodified bitumen and therefore a good indicator for engine oil derivatives that are fluxed with bitumen. The nitrogen content is again very stable, even more than compared to the other binders.

4.3.3. Observations on elemental analysis of CHNO+S

By performing elemental analysis on different bitumen, the basic content of the most common atoms present in bitumen can be calculated. From the analysis the following conclusions can be drawn:

- (1) Bit-J, bit-K and bit-V1 were bitumen that had very low S/C ratio around 0.003, whereas bit-L, bit6604 and bit6602 had very high S/C ratios around 0.014. Next to that bit-P, bit-O and bit-A were bitumen with high O/C ratios around 0.016 [-], whereas most other bitumen had significantly lower ratios around 0.012. The N/C ratios were some of the most stable throughout all bitumen, with not much variance being around 0.007 [-].

This seems to align well with elemental weight fractions measured in other research (Boysen & Schabron, 2015; Yang et al., 2017).

- (2) This can be easily compared to the REOB, which has an H/C around 1.75 [-], N/C around 0.005 [-], O/C around 0.08 [-] and a lot of variance in S/C between 0.0001 and 0.01 [-]. REOB modification is therefore expected to have the most influence on the blend viscosity, because of its very high H/C ratio. Next to that, the oxygen content should rise significantly too, which suggests that oxidation acceleration noticed with FTIR to have its increase because of the increased presence of, possibly free, oxygen to react with. Ageing susceptibility has been clearly higher for the REOB modified bitumen, as with only 20hPAV ageing the oxygen content has increased significantly, whereas this content was actually measured lower for the unmodified bitumen. The increased presence of trace metals and possibly an increase in acidity of the blends could be a good reason for the increased oxidation rate. Some trace metals and acidity are actually known to promote oxidation rates (Nahar et al., 2016; Yang et al., 2017).

4.4. Polarity based soluble fractions (SARA)

4.4.1. Method description, retrieval of chromatograms and fraction calculations

The principle of using the iatroskan for bitumen research, is to give an insight of certain molecular structures that are or are not pronouncedly present in a bitumen. In the case of bitumen, specifically four fractions of these molecular structures are split and deemed to describe differences in composition. An iatroskan can be used to perform this task, the machine is shown in the figure below:



Figure 4.33: Iatroskan for performing the SARA analysis using different solutions to dissolve the bitumen

An iatroskan is able to burn mass of a sample in a solvent using a hydrogen powered flame and then measure the mass that has settled & burned at a specific position on a quartz rod. A metal frame with quartz rods is used to place the bitumen samples in solvents and after the different solving steps it is placed in the machine. The first solvent to use is n-heptane for 30 minutes, followed by a solvent with heptane-toluene for 10 minutes and lastly a dichloromethane-methanol solvent for 3 minutes.

This will lead to fractionation of the different groups of SARA; Saturates, Aromatics, Resins and Asphaltenes. Knowing how the bitumen consists of these four groups, gives an indication about the colloidal structure of the binder. For example the Gaestel index, also called the colloidal instability index, gives an insight in how good the ratio is between the insoluble particles distributed in the particles that mix well together; i.e. the saturates and asphaltenes will be surrounded by resins and aromatics (Lesueur, 2009). Too much saturates and asphaltenes will cause the binder to increase in viscosity and lose the ability to move its particles around. Vice versa too much resins and aromatics will lead to a binder that is too soft and will not be elastic, as no strong structure will exist between molecules.



Figure 4.34: (left) metal frame with quartz rods, in which the bituminous samples can be injected and (right) the metal frame placed in a heptane-toluene (20/80) solution

Next to that the asphaltenes content has been related to the penetration index and the ratio between aromatics and asphaltenes to the softening point of a binder (Weigel & Stephan, 2018). The consistency of REOB modified bitumen has been evaluated before, although the consistency of REOB itself was not evaluated (Karki & Zhou, 2019). The main conclusion was that REOB modification drastically increases the saturates fraction and lowers the aromatics fraction. The goal of the iatroskan tests evaluated in this thesis, is to see if there are deviations of this result and if one can assume REOB does indeed consist of similar SARA fractions, like with bitumen. Next to that the storage stability of the REOB is tested as well, to see if the consistency of the REOB alters much overtime (including heating and ageing of the REOB as well).

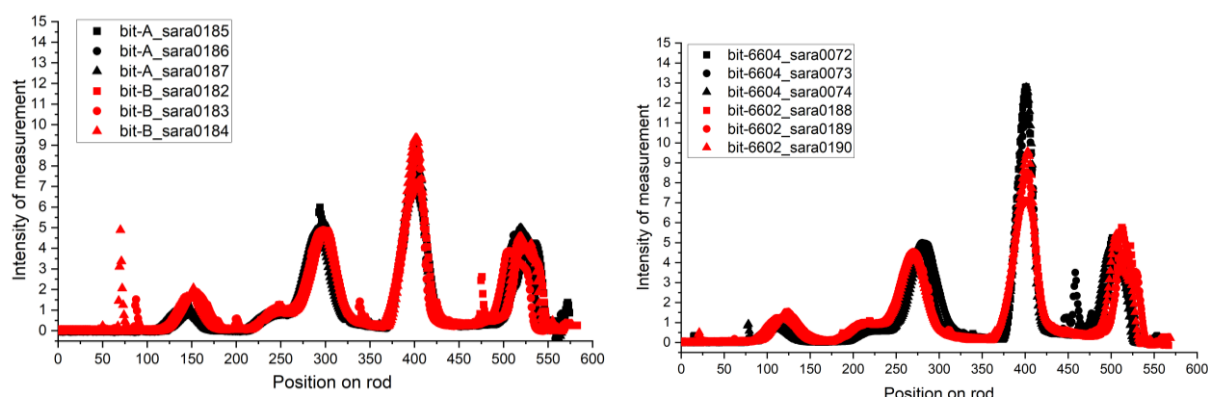


Figure 4.35: Iatroskan chromatograms of bit-A & B and bit-6604 & 6602

The figure above shows iatroskan chromatograms, with different peaks of intensities of material measured that are spread over the quartz rods as described before. One can observe four distinctively different peaks, starting with saturates, aromatics, resins and lastly asphaltenes. The data has been shifted horizontally, so the centre of the resins fraction (which is one of the most sharp peaks in the bitumen) is fixed at position 400. This way one can see if small changes occur within each SARA fraction.

In the figure, one can observe the bitumen with (and without) REOB modification. The height of the peaks, and more so the covered area of these peaks, are what describe the total weight fraction represented by the SARA fraction. Some horizontal shifts can be observed in the peaks, the saturate fraction clearly shifts more to the right of the rod, stating that it had become more difficult to precipitate. One can relate such changes in position of precipitation, to the changes in polarity of the molecules of that group. In this case one can easily observe that for bit-A the addition of REOB, thus making bit-B, caused the saturates content to significantly increase. The aromatics seem to have remained stable/lowered slightly, the same goes for the asphaltenes. The resins have increased as well.

Comparing this to bit-6604 and bit-6602, please note that bit-6604 is not a base bitumen for the REOB modified bit-6602, one can see still similar effects. The saturates have increased significantly and aromatics decreased slightly. The resins show this time to have lowered significantly and the asphaltenes to be increased, but this will mainly have to do with the fact that the bit-6604 is not the base bitumen for bit-6602.

Ageing of such bitumen however, would also show distinctive changes in both the SARA fractions as well as their positions on the quartz rod. This is visualised for binders bit-K and bit-P below:

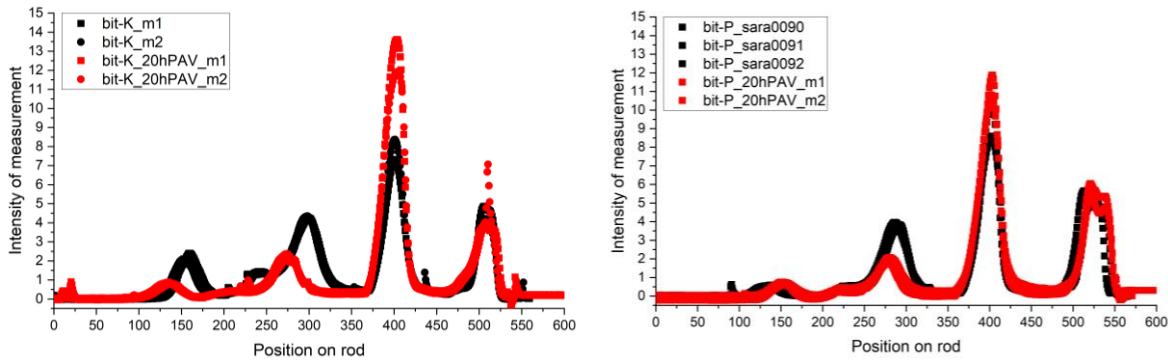


Figure 4.36: Iatroskan chromatograms of bit-K and P at fresh and 20hPAV ageing states

One can clearly observe that with ageing the resins fraction rises significantly and aromatics fraction decreases. For bit-K one can observe a decrease in saturates fraction, compared to bit-P where it merely shifts towards higher on the rod -> indicating more difficult precipitation of those saturates in this state.

To show what the differences in the composition of REOB are, assuming similar molecular structures will be present in this oil, these are split in SARA fractions too. The figure below shows their respective differences, but also their differences with bitumen.

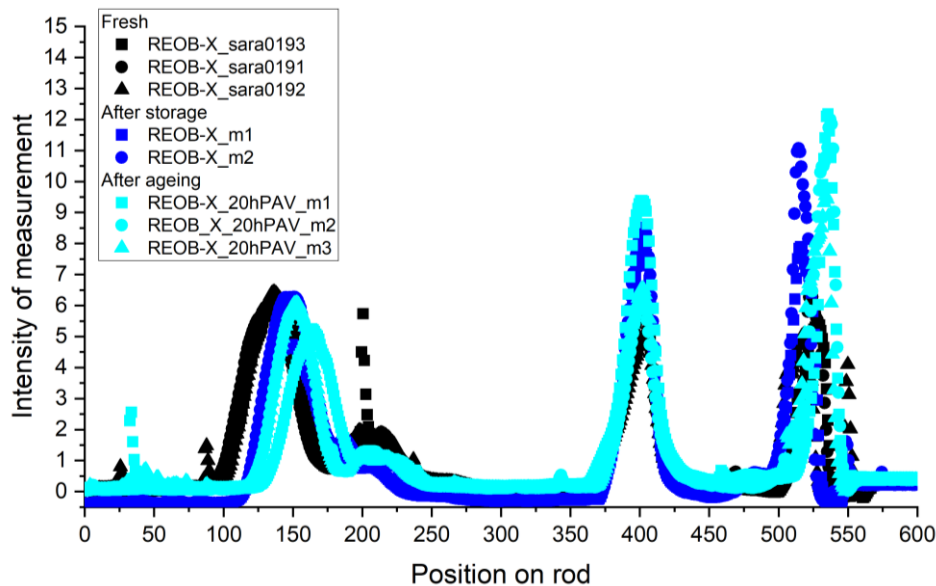


Figure 4.37: Iatroskan chromatograms of REOB-X, at fresh, storage aged and 20hPAV aged

One can immediately observe from the chromatograms of REOB-X, that there are only three distinctively high peaks present in the REOB. Close to the right-side of the saturates fraction (the far left peak), one can though still observe a small hill of measured mass. It is deemed that this represents the aromatic fraction that is separated in the second solvent and is seen as a distinctively different composition than the aromatics fraction present in bitumen. Therefore it will be measured at lower mass and also precipitate faster and thus closer to the peak of the saturates.

It is easy to observe that the saturates fraction is very significantly present in the REOB. Normally base bitumen does not have such a large quantity of saturates, therefore the addition of REOB will likely be noticeable with the increase in this fraction. It is not surprising that the aromatics fraction is so low for the REOB, as this fraction specifically is distilled out of the waste engine oil during re-refining.

Resins are of similar quantity present, possibly a bit lower. Especially the presence of asphaltenes is interesting though. For an engine oil, or a re-refined oil like REOB, one does not expect asphaltenes to be present (at least not at a similar quantity as for bitumen). This molecular group mainly represents very hard and complex particles present in the bitumen, and therefore are mostly quite large molecules that are normally distilled out in the very first refining process of fossil oil. The service life that the engine oil is used for, is not at all long enough to allow the formation of asphaltenes in such quantities as normally found in bitumen. Next to that, the peak that represents the asphaltenes is much sharper and not at all a dual peak as observed with bitumen.

One should conclude therefore, that this represents partly a different molecule group, that still is separated in a similar way as the asphaltenes found in bitumen. These asphaltenes are present at relatively high quantity and their effect on the composition of bitumen is therefore very important to take into account. The other option is that the asphaltenes that in fact are formed, are effectively distilled out in refining the waste engine oil, that the quantity is therefore this high for the REOB end product.

The Figure 4.37 shows in fact four different chromatograms. This is to show how the REOB changes in consistency during storage. The difference between the fresh and the first storage aged sample is 1,5 years being stored in a fridge at 5 [°C]. The next REOB sample had been put two times in the oven at 130 [°C] for half an hour, to make it warm for blending. The last sample has undergone 5h TFOT and 20hPAV ageing and therefore shows the most ageing. Ageing for the REOB shows to decrease the saturates slightly, decrease the (already small amount of) aromatics slightly, increase the resins slightly and lastly increase the (supposedly) asphaltenes fraction significantly.

N.B. one needs to be aware that REOB undergoes significant changes during storage and oven heating and therefore is expected to have a different effect on bitumen at these different lifecycle changes.

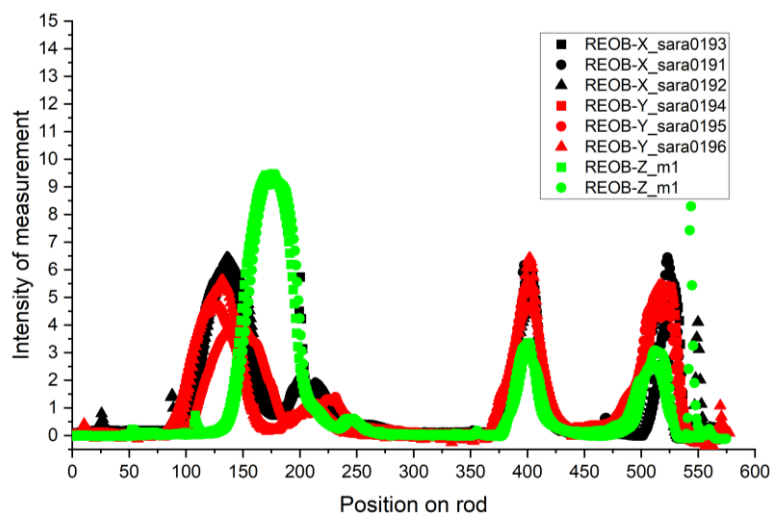


Figure 4.38: Iatroskan chromatograms of REOB-X, REOB-Y and REOB-Z

To show the difference between all REOB, REOB-Y and REOB-Z are plotted in Figure 4.38. Here one can see that the basic differences in REOB can be quite large. X and Y do not differ too much. Mainly REOB-X shows to have a bit bigger fraction of aromatics and Y a larger portion of resins and (supposedly) asphaltenes. Whereas REOB-Z shows to have a very significant saturates portion and a very small fraction of aromatics. REOB modification of bitumen with this specific REOB-Z, will therefore be easily noticeable in the very significant increase in saturates.

The addition of specifically REOB-X to bitumen, is evaluated as well. Both blends of bit-K+10% REOB and bit-P+10% REOB are visualised in the following plots:

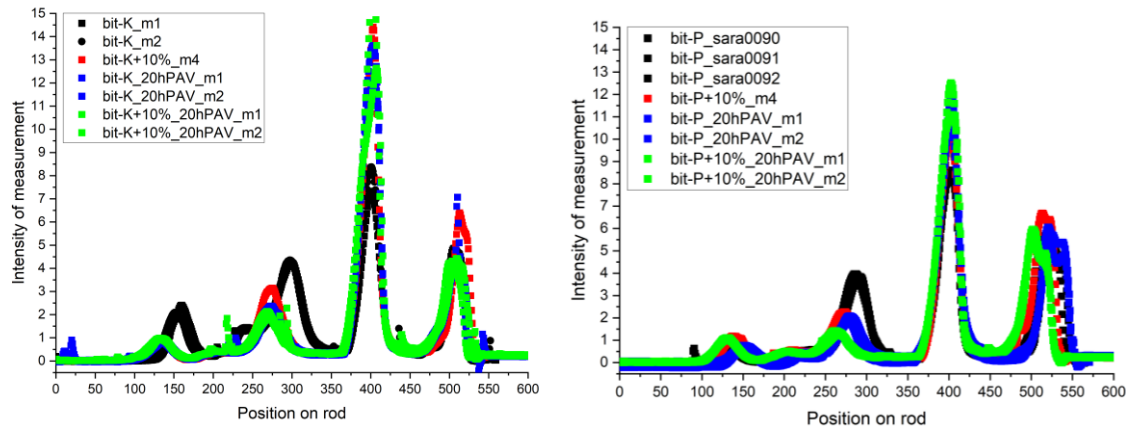


Figure 4.39: Iatroskan chromatograms of the blends bit-K+10% and bit-P+10%, their base bitumen bit-K and bit-P and lastly their 20hPAV versions

REOB modification causes a drastic decrease in aromatic fraction. Saturates seem to have increased not as much as was expected. Both resins and asphaltenes show to have increased significantly, for both bit-K+10% and bit-P+10%. The REOB modified bitumen, the bit-K+10% and bit-P+10% blends, show to have a small peak in between the saturates and the aromatics peaks. This could be clearly connected to the right side portion of the supposedly aromatics fraction present in REOB, as shown in Figure 4.38. Mainly bit-K+10% shows this peak clearly, whereas bit-P+10% shows an increase in the small plateau present there.

To be able to not only qualitatively analyse the chromatograms, they are also analysed by applying a deconvolution method, part of the OriginPro program. Here small Gaussian curves are fitted to the data, to make the calculations of their respective areas easy and to also be able to neglect any peaks that result from deviating data/contamination of the samples.

Gaussian curves are created according to the following formula:

$$y = y_0 + \frac{A}{w\sqrt{\frac{\pi}{2}}} * e^{-2*\left(\frac{x-x_c}{w}\right)^2}$$

(4.7)

Where one should see A as the distribution area, w as its width, x as the horizontal position on the curve and x_c as the horizontal position of the curve its centre.

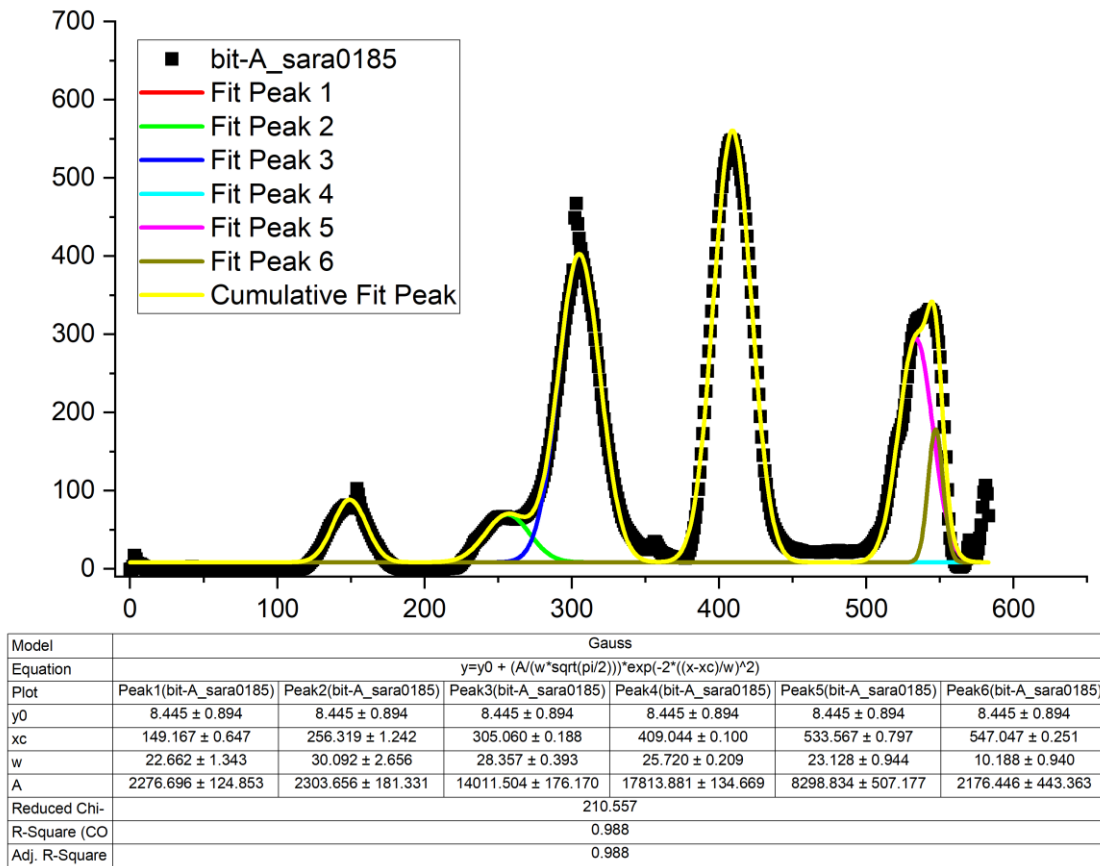


Figure 4.40: Deconvolution of the iatroscan chromatogram of bit-A; including a table showing the parameters for these Gaussian curves

The use of six Gaussian curves is enough to get a good fit to most of the obtained chromatograms. The first curve denoting the saturates, the second and third the aromatics, the fourth the resins and lastly the fifth and sixth curve denote the asphaltenes.

Summing the areas of these Gaussian curves, one can obtain the respective weight fractions of each SARA fraction of a bitumen/REOB. In the case of bitumen bit-A this leads to:

$$Saturates\ wt\% = \frac{2276.7 * 100}{2276.7 + 2303.65 + 14011.5 + 171813.9 + 8298.8 + 2176.4} = 4.856\ [%] \quad (4.8)$$

And the same for the other fractions:

Aromatics 34.801 [%], resins 37.998 [%] and asphaltenes 22.344 [%]

4.4.2. SARA fractions of unmodified, aged and REOB modified bitumen

This is then done for all chromatograms that are obtained for the evaluated bitumen and the received fractions are plotted in the coming graphs.

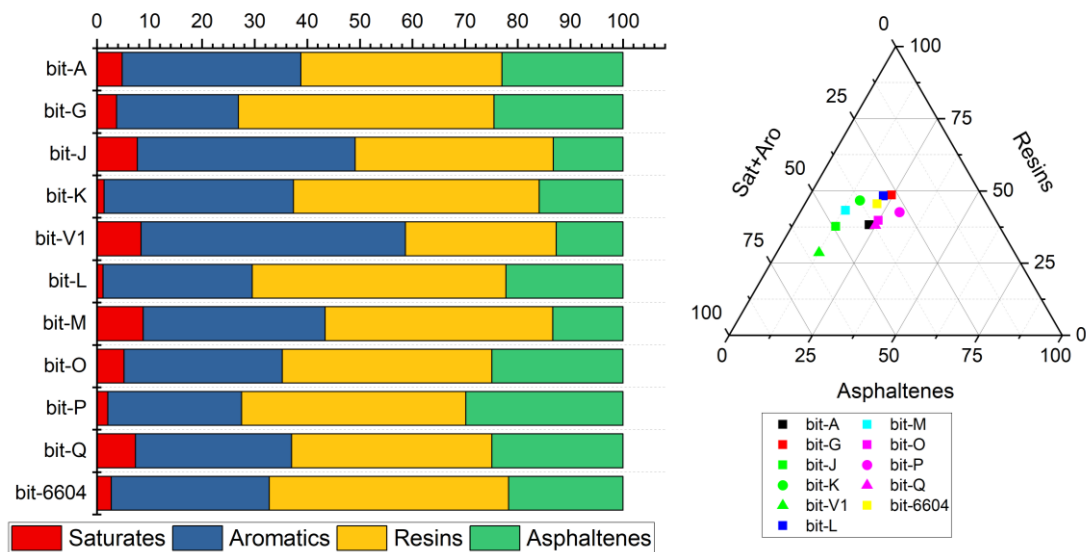


Figure 4.41: Overview of SARA weight fractions of all unmodified bitumen

From Figure 4.41 one can quickly observe the following limitations of unaged, unmodified, bitumen that they have certain expectable ranges for their SARA fractions, which are:

Saturates	0 – 10 %
Aromatics	20 – 55 %
Resins	25 – 50 %
Asphaltenes	10 – 30 %

Some extreme values are for example the very low saturate content of both bit-K, bit-L, bit-P and bit-6604. In the case of bit-K and bit-P, this could explain why these bitumen are more stiff, as saturates are often described to represent small sized, low molecular weight molecules, which are typically contributing to a softer behaviour for bitumen.

One can also observe how bit-K, bit-J and bit-V1 (all from the same supplier) have all very low asphaltene contents at around 14%, also with low variance between their values. Especially bit-V1 has quite high levels of aromatics and seems to receive its soft nature from this high fraction of low molecular weights (it is a 160/220 grade). The fact that these bitumen have such a low asphaltene content can be related to the fact that they are bitumen produced using a solvent deasphalting technique, which in principle will filter out the asphaltenes (and partly the saturates). The resulting bitumen has been mixed with other, straight-run, bitumen to form the bit-K, bit-J and bit-V1 binders. This, and the fact that the binder is of a paraffinic nature, will therefore have a huge influence on the composition of these asphaltenes and therefore the behaviour of the binder too.

Bit-P, bit-O and bit-Q however show to have low deviation in their resins fraction, fixing it at around 40%. BitP differs from the others mainly in having an increased content of asphaltenes. These binders are made from an straight-run process, from a Venezuelan crude source being mainly a naphthenic oil.

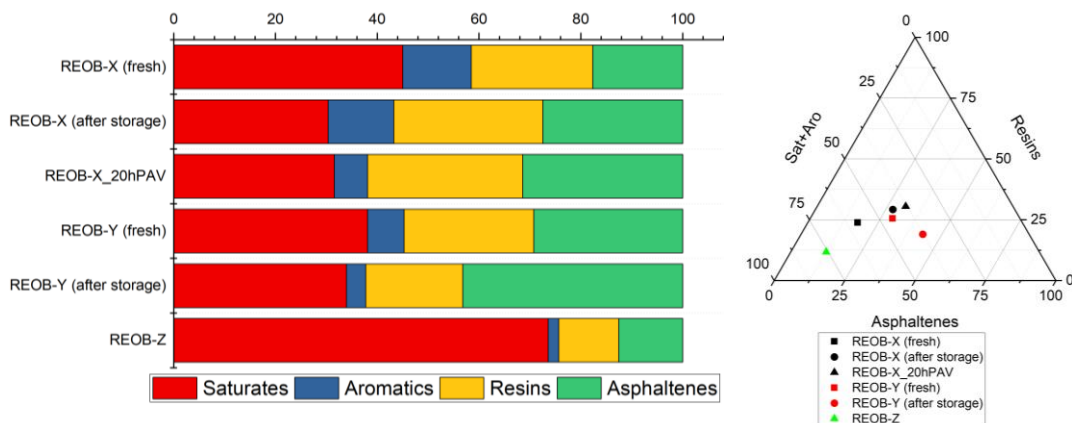


Figure 4.42: Overview of SARA fractions of REOB at different lifetime stages

The SARA fractions of three different REOB, as well as their changes in composition during storage and with ageing, are shown in Figure 4.42. Here one can easily observe the general differences, as they basically come to the point that the saturates fraction is significantly high for REOB itself, and in the case of REOB-Z extremely high. One can also observe that aromatics are almost non-existent in the REOBs and with during storage and direct ageing of the REOB itself one can observe a drastic decrease in this fraction. The main ranges of the four fractions, in the case of REOB, are:

Saturates	25 – 75 %
Aromatics	0 – 15 %
Resins	10 – 30 %
Asphaltenes	15 – 45 %

Comparing between the three REOB, only the consistency of REOB-X comes the closest to bitumen itself. Blending of this REOB is expected to influence bitumen characteristics the least and not increase instability of the blend drastically. Nevertheless, all REOB will cause the aromatic fraction to drastically decrease, impacting the ageing susceptibility of a binder.

This will affect the ageing susceptibility, as normally lower molecular weights, like aromatics, in the bitumen are what make a binder softer. However for a REOB modified binders will have an increased resins fraction. This means a larger portion of resins is present, which will allow oxidation to occur at this fraction more (because there are more molecules present), resulting in a drastic change in molecular weights within the resins fraction. A standard bitumen will allow the, bigger portion, aromatics to oxidise and then transition towards resins. It basically results in a step in the ageing to be skipped, as ageing will now be resins based, instead of a distribution over the oxidation over both aromatics and resins.

In Figure 4.43 one can observe the typical changes in bitumen its SARA fractions are shown with ageing. Both bit-J and bit-6604 have undergone extended periods of ageing and show to have a stable presence of saturates, significantly decrease in aromatics, drastically increase in resins and increase in asphaltenes.

Bit-K and bit-P both show to have a slight increase in their saturates fraction with ageing. Next to that they, but also bit-O, show to lose half of their aromatics fraction after only 20hPAV ageing. Changes of the fractions with ageing can therefore be summarised to the following range:

		Absolute	Relative	
Saturates	stable/decrease	0 – 1 %	10 %	with 20hPAV ageing
Aromatics	decrease	10 – 20 %	40 – 50 %	with 20hPAV ageing
Resins	increase	10 – 15 %	40 – 50 %	with 20hPAV ageing
Asphaltenes	increase	2 – 8 %	20 – 40 %	with 20hPAV ageing

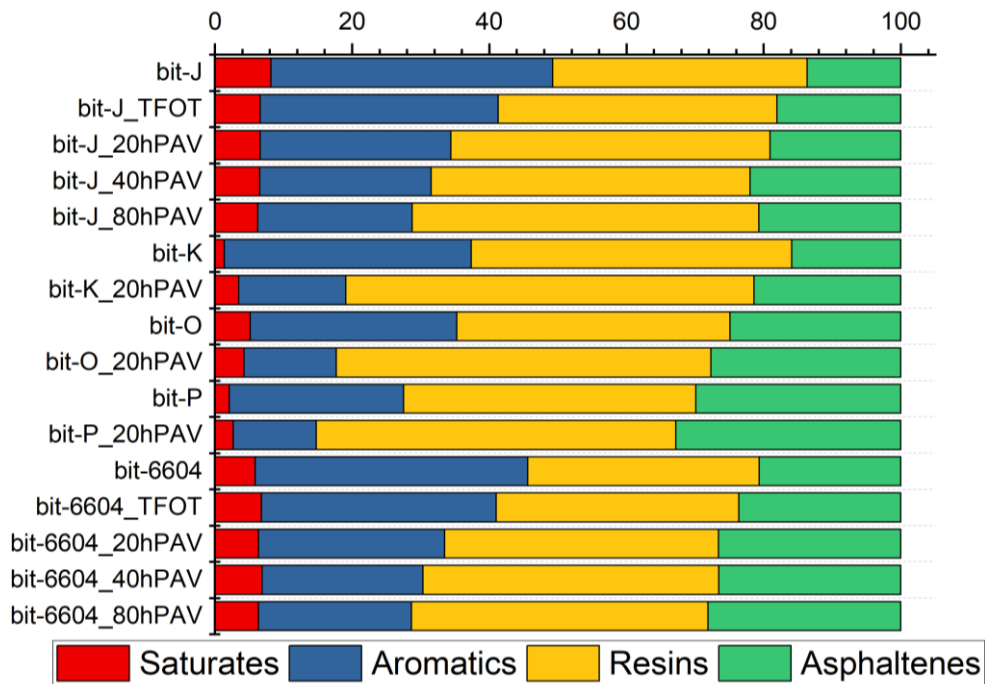


Figure 4.43: Stacked column plot of SARA fractions of aged bitumen

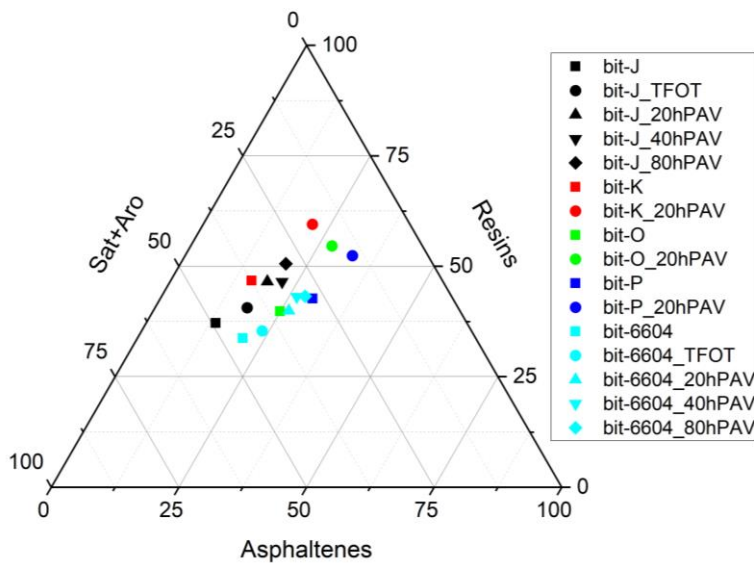


Figure 4.44: SARA fractions of aged unmodified bitumen; plotted on a ternary graph

In Figure 4.44 the changes in composition of the aged bitumen are visualised differently. One can easily observe that ageing makes the datapoints move towards higher asphaltenes, significantly higher resins and decreases the saturates + aromatics fraction. Although bitumen have a different starting position, it is clear that the route the datapoints take with ageing is similar between the binders.

To be able to show that the stated changes of REOB itself and the ageing of bitumen itself indeed occur for REOB modified binders too, these are evaluated below as well. In Figure 4.45 one can observe the changes in SARA fractions of these binders:

As was expected, the addition of REOB causes the saturates fraction to increase significantly. One does have to note though that both bit-K and bit-P already had a smaller fraction present and therefore are now closer towards the average of other 70/100 grade bitumen.

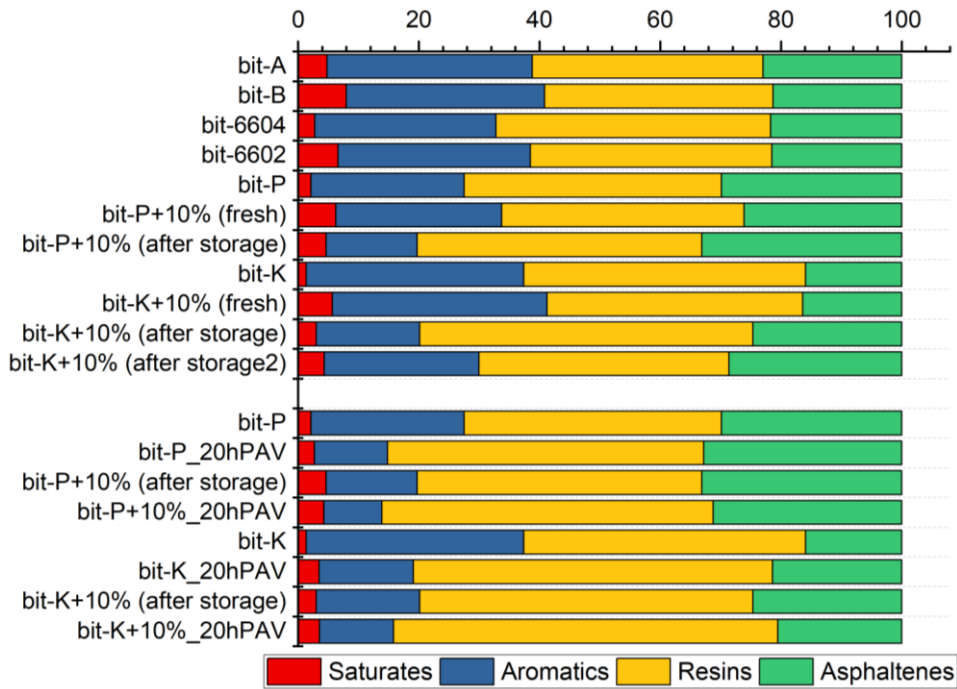


Figure 4.45: Stacked column plot of SARA fractions of REOB modified bitumen

One cannot really observe a drastic decrease in the aromatics, one could even argue that it has increased initially. Interestingly, the resins fraction seems to have lowered slightly. Storage and some re-heating, for sample pouring for the BBR, of the REOB modified bitumen seem to have a drastic effect on the presence of aromatics and saturates though. These decrease significantly, which is more drastic than with standard bitumen. As can be seen for the bit-P and bit-P_20hPAV but also the bit-K and bit-K_20hPAV bitumen. A more visual figure is plotted below to show the changes in fractions:

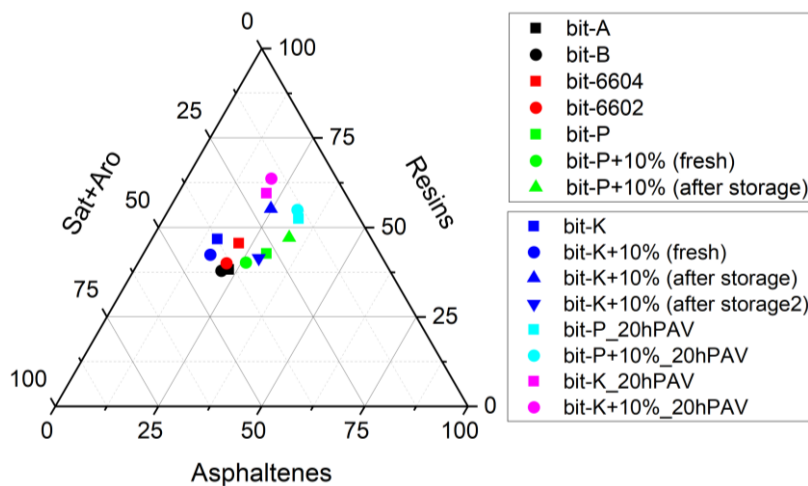


Figure 4.46: Overview of SARA fractions of blends and some aged versions

Comparing this to the changes already found in other research (Karki & Zhou, 2019), one can see that the changes in REOB blends in this work have differentiated the effect of storage and ageing better. One can see how REOB blends alter in their consistency accelerated as compared to unmodified bitumen. This is visible by comparing bit-K_20hPAV and bit-P_20hPAV to the bit-K+10%_20hPAV and bit-P+10%_20hPAV compositions. Where first the addition of the REOB led to an increase in Sat+Aro fraction, this was more excessively lost than the base binder itself would after 20hPAV.

4.4.3. Colloidal instability index and other indices to describe changes in bitumen composition

Instead of merely looking at the absolute SARA weight fractions, one can also retrieve ratios between these fractions. Especially the Gaestel index, or the Colloidal Instability Index (CII), can say something about a binder its consistency and what tendency it has to change and how well the fractions are distributed (Karki & Zhou, 2019; Lesueur, 2009; Mirwald et al., 2020; Porot, 2019).

The Gaestel index/CII is calculated in the following way (shown below). But some other ratios related to the penetration index and to the softening point (Kleizienė et al., 2019) and lastly two ratios showing the changes that specifically REOB blends undergo are given as well:

$$CII = \frac{Sat+Asp}{Aro+Res} \quad I_1 = \frac{Res}{Asp} \quad I_2 = \frac{Asp}{Sat+Aro+Res} \quad I_3 = \frac{Aro}{Asp} \quad I_4 = \frac{Sat}{Aro} \quad (4.9)$$

These each give their own insights into the direct ratios in SARA fractions and therefore will give a direct insight into expected behaviours. The CII should show if the ratio between the insoluble and the solvent parts of the bitumen are too high, meaning the bitumen approaches a gel-type phase risking too stiff and highly viscous behaviour, or alternatively too low, meaning the bitumen approaches a sol-type phase risking too soft and too brittle with no elastic strength behaviour (Lesueur, 2009). For unmodified bitumen the figure below shows all these indices:

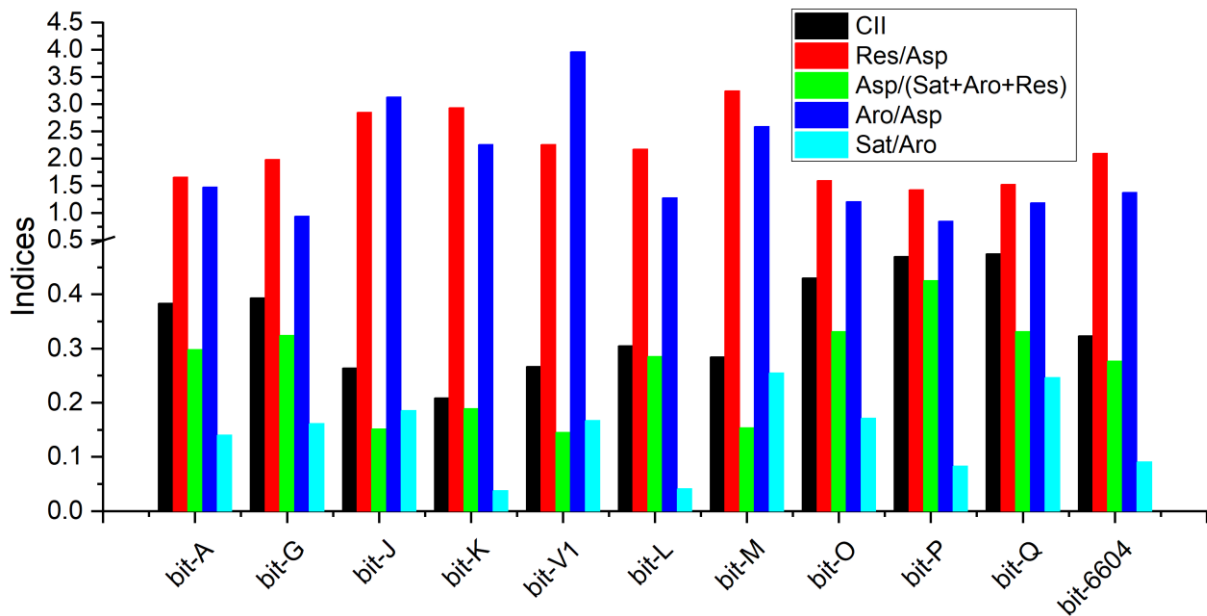


Figure 4.47: CII and other indices for unmodified bitumen

The colloidal instability index shows to be highest for the bit-P, O and Q series and lowest for the bit-K, J and V1 series. The higher ageing susceptibility of bit-P as compared to bit-K, which was found in FTIR indices, could be correlated to this phenomenon.

Specifically bit-V1 seems to have an irregularly high ratio of Aromatics to Asphaltenes. It is possible that the binder receives its lower stiffness from this, as it is a 160/220 grade and a high aromatics or low asphaltene fraction can contribute to how soft a binder is. Although bit-Q, which is also a 160/220 grade bitumen, clearly does not receive its softness from a difference in SARA fractions.

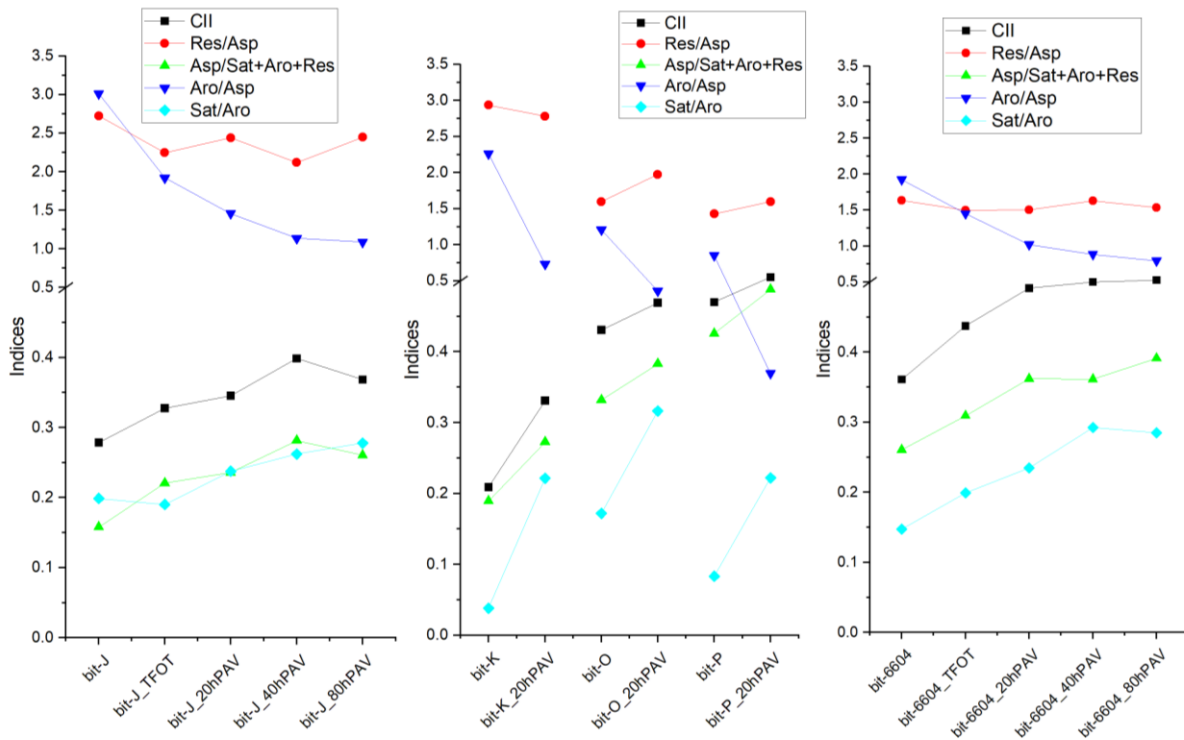


Figure 4.48: CII and other indices for aged bitumen

Ageing of bitumen shows to drastically decrease the aromatics fraction and increase the asphaltenes fraction. The CII steadily increases, as well as the Asp/Sat+Aro+Res and Sat/Aro ratios. The most interesting behaviours are the drastic increases in Sat/Aro and Aro/Asp ratios of bit-K and bit-P with ageing. This means, knowing the Saturates are quite stable with ageing, that the aromatics have such a drastic decrease that does not occur with the same magnitude with the ageing of bit-J and bit6604. It is important to note that this is not beneficial for a binder, as it means that it has high ageing susceptibility and will thus change easily towards a binder that becomes brittle and stiff.

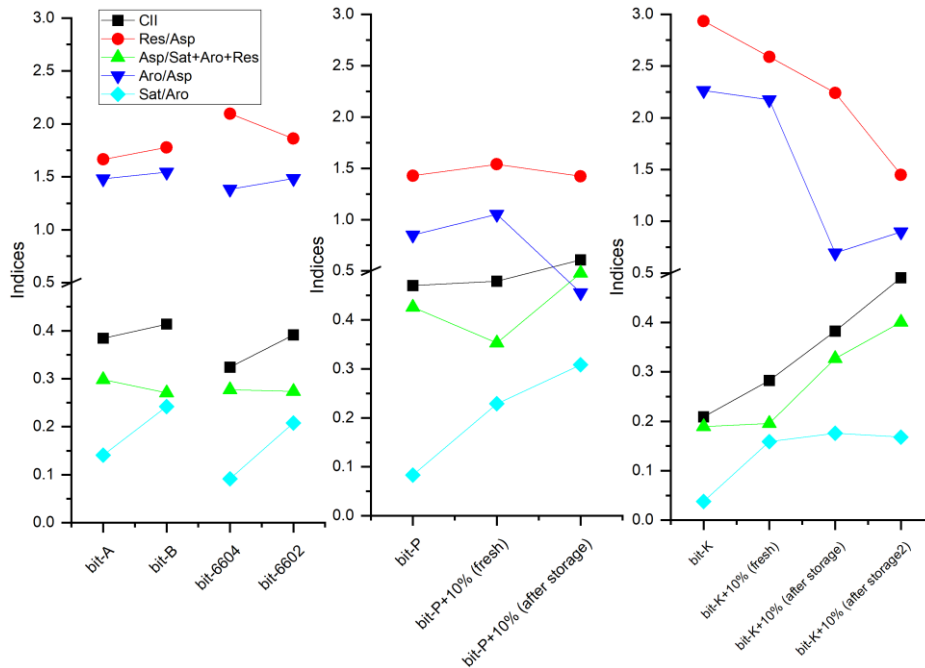


Figure 4.49: CII and other indices for REOB modified bitumen blends

Addition of REOB will lead to an initial increase in CII, Sat/Aro and Aro/Asp ratios. The ratio between Res/Asp can possibly differ between REOB though, as is seen between bit-A&B and bit-6604&6602. The CII seems to very drastically change for the bit-K+10% blend, much more than compared to the bit-P+10% and the blends bit-B and bit-6602.

One can observe that the Sat/Aro ratio is a good indicator of the presence of REOB in the case of bit-P, although bit-K does not show this as pronounced, or in other words bit-P blends seem to have an increased loss in aromatics as compared to bit-K blends. One has to keep in mind however that bit-K initially had already a lower amount of aromatics in the first place. Resins are much more present in bit-K than in bit-P and with the addition of the REOB this comes to a more stable equilibrium than for bit-P blends, as seen with the Res/Asp ratio.

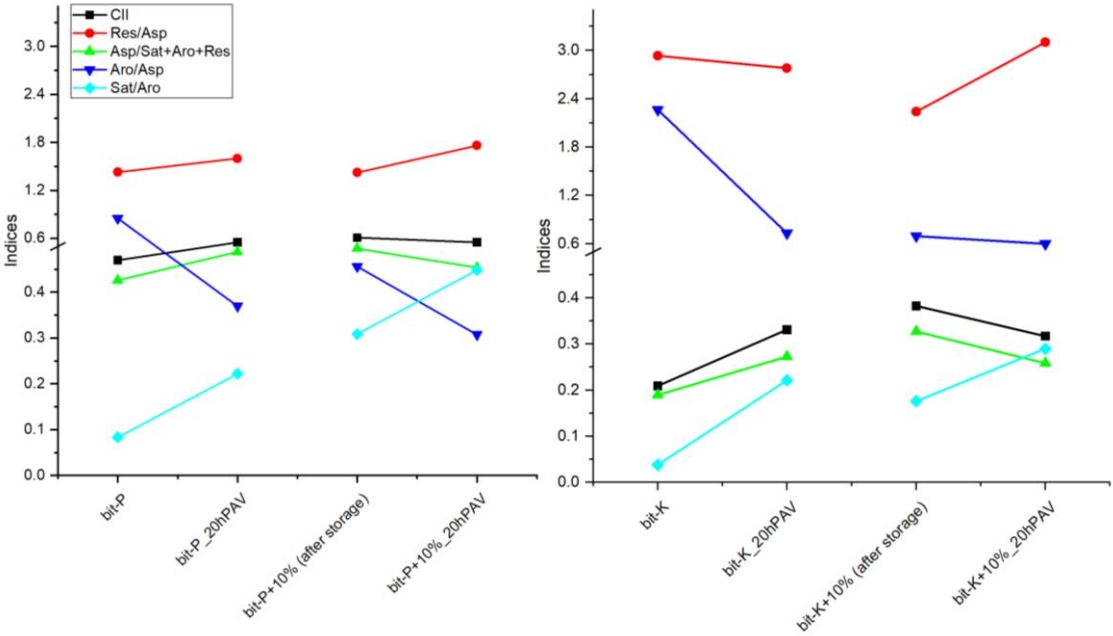


Figure 4.50: CII and other indices for REOB modified aged bitumen

Ageing of the REOB blends shows that there is a significant decrease in CII, which is counterintuitive. Upon ageing this index should rise and here one can thus notice the effect of the decrease in both saturates and asphaltenes fractions in the REOB modified bitumen. The resins fraction becomes so much more pronouncedly active as compared to the other fractions, that one should be afraid of the molecule structural balance. Initially but especially with ageing this imbalance seems to grow. Knowing that sol phase structures typically are of high resins & aromatics nature, these bitumen should be seen as such (Lesueur, 2009). This means low temperature behaviour could show significant susceptibility to brittle failure, as asphaltene structures have a harder time to take on forces and create an elastic stiff deformation, more so for bit-K blends than for bit-P as well.

4.4.4. Observations on SARA fractions

From the obtained chromatograms measured with the iatroskan, the weight fractions of SARA molecular arrangements have been found. The following conclusions can be drawn from the tests performed on unmodified, aged and REOB modified bitumen:

- (1) Basic bitumen differs heavily in their SARA fractions, but within expectable ranges like the following:

Saturates	0 – 10 %
Aromatics	20 – 55 %
Resins	25 – 50 %
Asphaltenes	10 – 30 %

- (2) Ageing of unmodified bitumen however shows expectable changes to those fractions in the following way (percentages are in absolute drop):

		Absolute	Relative	
Saturates	stable/decrease	0 – 1 %	10 %	with 20hPAV ageing
Aromatics	decrease	10 – 20 %	40 – 50 %	with 20hPAV ageing
Resins	increase	10 – 15 %	40 – 50 %	with 20hPAV ageing
Asphaltenes	increase	2 – 8 %	20 – 40 %	with 20hPAV ageing

Similar observations with ageing have been found in research before although being with different ageing methods (Mirwald et al., 2020; Werkovits et al., 2023).

- (3) REOB itself has shown to also consist of similar SARA fractions, although the saturates and aromatics seem to have an overlap in the chromatograms. A small peak on the right shoulder of the deemed saturates fraction is deemed as this aromatics fraction. The following rounded SARA fractions are to be expected of REOB itself:

Saturates	25 – 75 %
Aromatics	0 – 15 %
Resins	10 – 30 %
Asphaltenes	15 – 45 %

- (4) Addition of REOB will lead to a significant increase in saturates and resins. Also a significant decrease in aromatics should be noticed. Asphaltenes will increase or decrease mainly depending on the REOB that was used. This correlates partly well to what has been found before, where two different REOBs blended with two different base bitumen were analysed with SARA fractions (Karki & Zhou, 2019). Although it was observed then that the resins fraction was actually decreased after REOB addition, here the variance between REOB sources clearly can have different impacts.

- (5) Upon ageing REOB modified bitumen will have a significant loss in both saturates and aromatics fractions. This already occurs for the REOB itself during storage and could therefore indicate the poor ageing susceptibility of this oil to be used in bitumen modification. As saturates and aromatics normally represent lower molecular weights in a bitumen, one should thus be wary of using a REOB that loses these components easily, as it is has shown it will lose these fractions too after being blended with bitumen.

N.B. that it has been found before that saturates can be exudated in ethanol from REOB modified bitumen, whereas this does not happen for unmodified bitumen (Zhang et al., 2023).

4.5. Molecular weight distributions (GPC)

4.5.1. Molecular weight distributions of unmodified bitumen, REOB blends and REOB

The gel permeation chromatography (GPC) technique is a commonly used tool to evaluate polymers, but also (polymer modified) bitumen. Its principle is mainly based on using a solution to dissolve the polymer or bitumen into separate molecules and letting these flow through gel columns. These columns have different permeable holes through them, with some smaller and some larger. Large particles in the solvent will only be able to pass through the largest openings, whereas the smaller particles will pass easily through the smaller holes. This means that large particles will take a faster route out of the columns and will be measured first by the measurement device, and smaller particles later.



Figure 4.51: Waters Acquity GPC setup to measure intensities of molecules at specific elution volumes/retention times

This makes measurement of intensities of particles possible at different elution volumes (EV) or retention time (RT). These diagrams on their own do not say much about specific characteristics of the measured polymer or bitumen, but when one calibrates this data to a precisely known material, it is possible to relate the intensities and elution volume to molecular weights.

This calibration material for bitumen is commonly polystyrene, with manufactured lengths and therefore with a precisely known molecular weight distribution.

Table 4.6: GPC test conditions and used procedures

Mobile phase	THF (Tetrahydrofuran)
Solvent	THF
Sample preparation	Bitumen and REOB blends dissolved in THF, are shaken with 100 rpm for 30 minutes at room temperature.
Concentration of sample	30 mg bitumen / 25 ml
Injection volume	20 μ l
Pump flow speed	0.5 ml/min
Test temperature	35°C
Detector	PDA, 254 nm
GPC columns	Acquity APC XT type XT45 1,7 μ m, XT200 2,5 μ m en XT450 2,5 μ m
Calibration standards*	Polystyrene Mp: 66000, 42400, 25500, 15700, 8680, 6540, 4840, 3470, 2280, 1306, 474, 266

* the calibration of polystyrene will only be accurate between $\log(M)=4.42$ and 2.42 or $M=26303$ and 263 [Daltons]. This means that particles that are smaller (or bigger) than those limits will not be able to be calibrated accurately and thus not be shown in distributions.

The calibration of the polystyrene to the bitumen, to obtain molecular weight distributions, is shown in Figure 4.52. Here the transition from intensities over retention time to the molecular weight distribution is shown. One can see the shapes of bit-P and bit-O look alike, similarly also for bit-K and bit-J. The shapes therefore seem to correlate well to which supplier provided the binders.

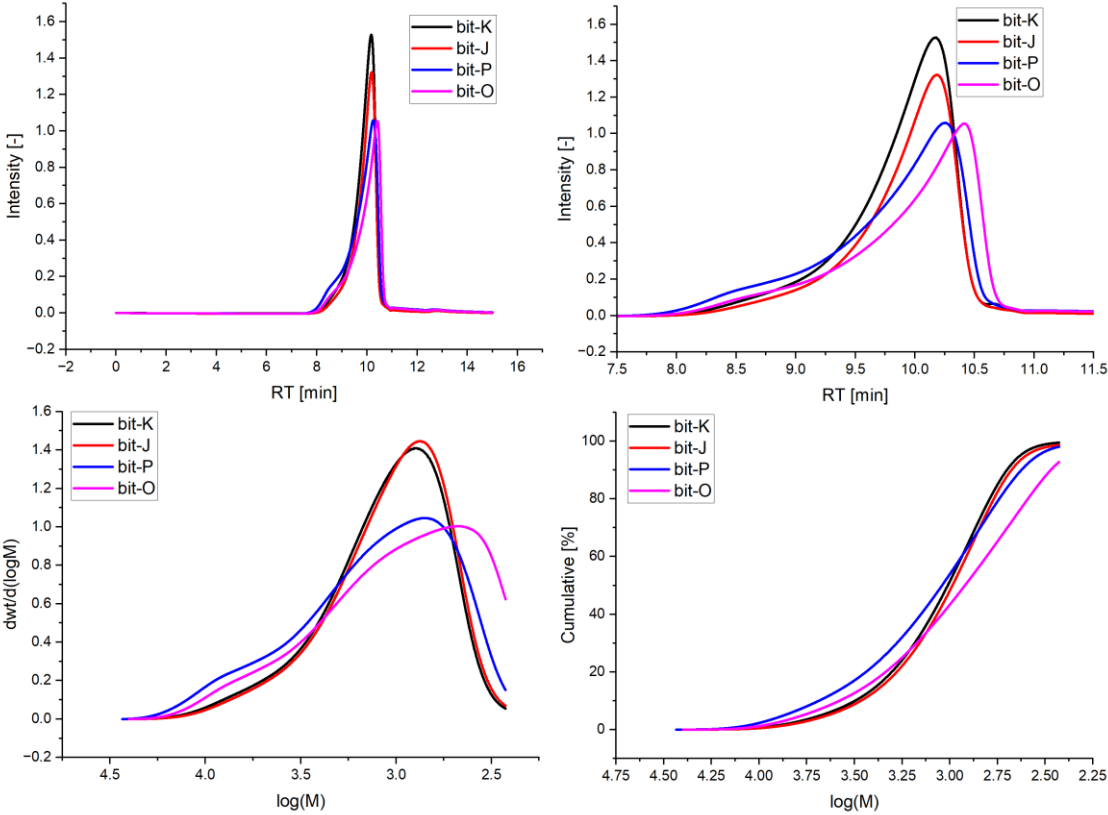


Figure 4.52: (top left) Intensity of molecules measured at certain retention time and (top right) zoomed in, (bottom left) the converted graphs to represent molecular weights and (bottom right) the cumulative of measurements over molecular weights.

The retention time plots are deemed to show data that is not well comparable to other measurements (as RT alone does not say anything), only the molecular weight distributions are plotted further on. To start off, the molecular weight distributions of fresh bitumen and the three main aged bitumen are shown in the plots below.

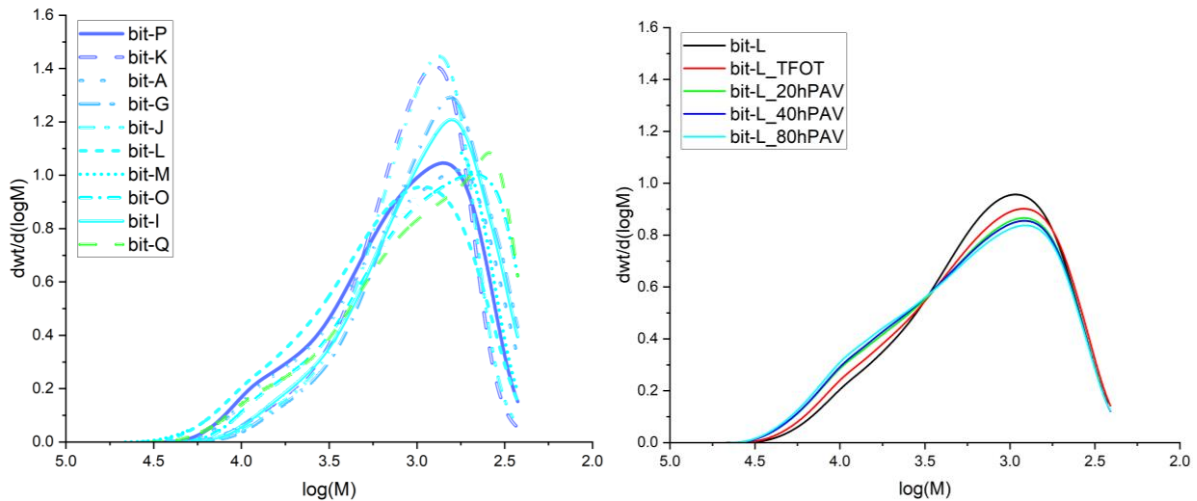


Figure 4.53: (left) molecular weight distributions of unaged bitumen and (right) of aged bit-L (70/100)

The differences between the fresh bitumen are very versatile, differing both in molecular weights in the high, medium and low fractions. Softer binders are generally expected to have a low fraction of high molecular weights (>4500 Daltons) and a high fraction of low molecular weights (<500 Daltons).

One can also observe a clear cut-off at the $\log(M)=2.42$; which occurs because of the range in which the calibration of polystyrene is still accurate. Lower than this value the curve cannot be approached accurately anymore and therefore it is not plotted.

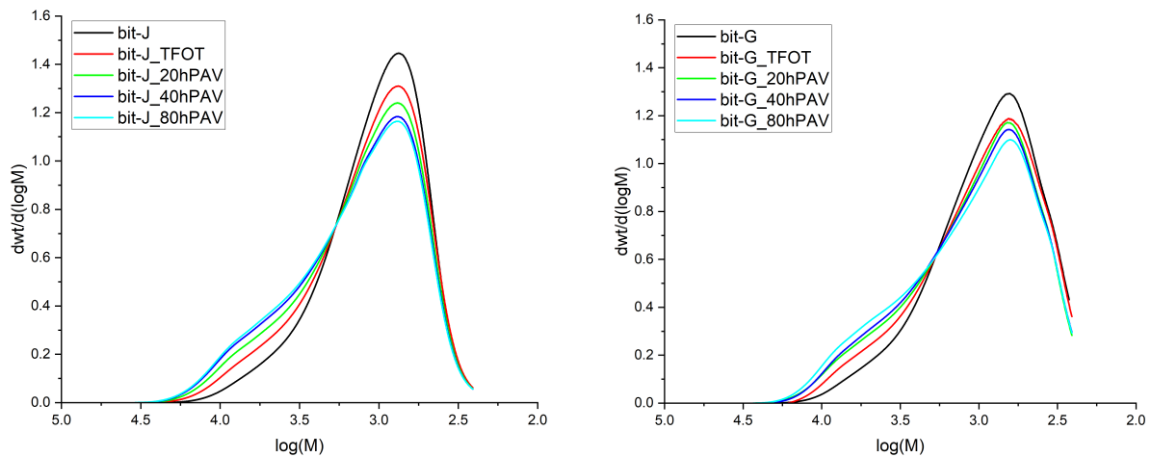


Figure 4.54: (left) molecular weight distributions of aged bit-J (70/100) and (right) of aged bit-G (40/60)

Doing a comparison between the three aged bitumen series, one can immediately state that they do not have a similar molecular weight distribution, although they do age similarly. Ageing happens in such a way that a clear drop occurs in the peak height and the tail of the curve (at the high molecular weight end) starts to rise. The smallest changes to the distribution, happen for bit-L. Its distribution is relatively broad, as compared to the steep and skewed distributions of bit-J and bit-G and one can say that the increments of change are not as big as for the others.

Specifically bit-J shows to have only a small amount of low molecular weights, below 500 Daltons, pointing to the fact this binder has relatively little saturates or little aromatics and resins of very low molecular weights. The bit-J does however, have a very high peak around $\log(M)=2.9$; meaning it has a relative high amount of resins and aromatics, although their molecular weight range will be small as the peak is so narrow.

Bit-G shows to have a lower peak, than bit-J does. This could therefore explain the fact that bit-G has a higher stiffness than bit-J, as higher molecular weights on average correlates well to stiffer binders. The increments of change in the peak height with ageing however are of smaller nature, whereas the tail of the curve seems to age very similar to bit-J. From these distributions however, one can easily discern aged bitumen from unaged bitumen. If one would not have all the curves next to each other however, this would be almost impossible.

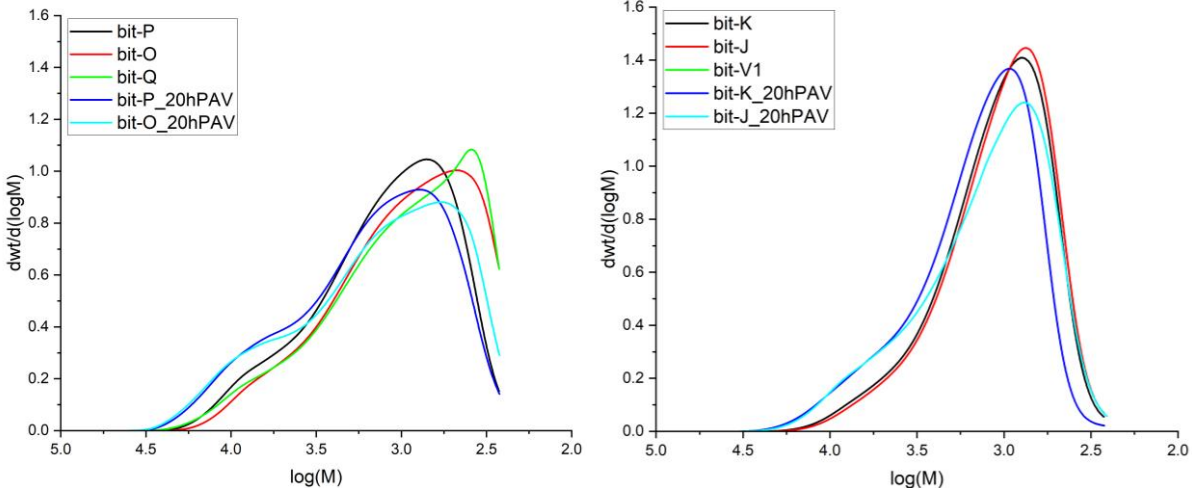


Figure 4.55: (left) molecular weight distributions of unaged and aged bit-P (15), O (70/100) and Q (160/220) and (right) of unaged and aged bit-K (20/30), J (70/100) and V1 (160/220)

One can see from Figure 4.55 that the bit-P, O and Q look very similar and bit-K, J and V1 as well. How they differ is for each in a similar way as well: the stiff binders bit-P and bit-K have a higher fraction of high molecular weights. BitO and J interestingly differ quite a lot, as bit-O has a very large portion of low molecular weights and bit-J actually does not and has an increase medium weight fraction instead.

Those two series of bitumen were used to blend with REOB, and the changes that happen to the distribution have been measured as well. In the case of using bit-P as the base bitumen, one can see that the peak height is increased a little but the peak is especially shifted towards the higher weight fraction. This shows that, bit-P+10% and bit-O differ quite a lot in their profiles.

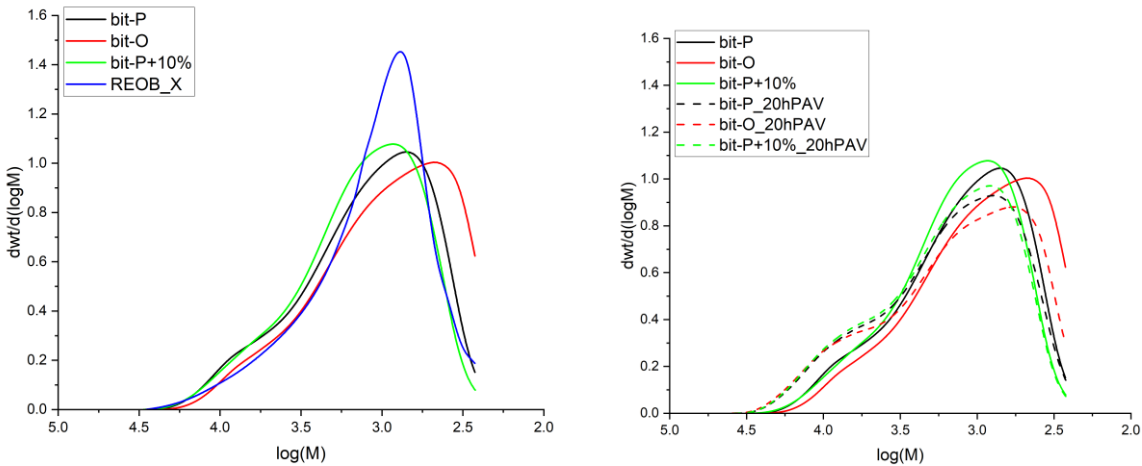


Figure 4.56: (left) Unaged bit-P, O, REOB-X and bit-P+10% and (right) the distribution changes with 20hPAV ageing

Ageing of the blend shows to do exactly what was expected, as it changed like the unmodified bitumen. The tail increases and the peak drops in height. What is interesting to observe, is the fact that now the aged bit-P+10% almost has a similar distribution as the 20hPAV aged bit-P. This would suggest that the changes caused by the REOB have already been nullified after 20hPAV and it would act as similar as an unmodified 20hPAV aged binder.

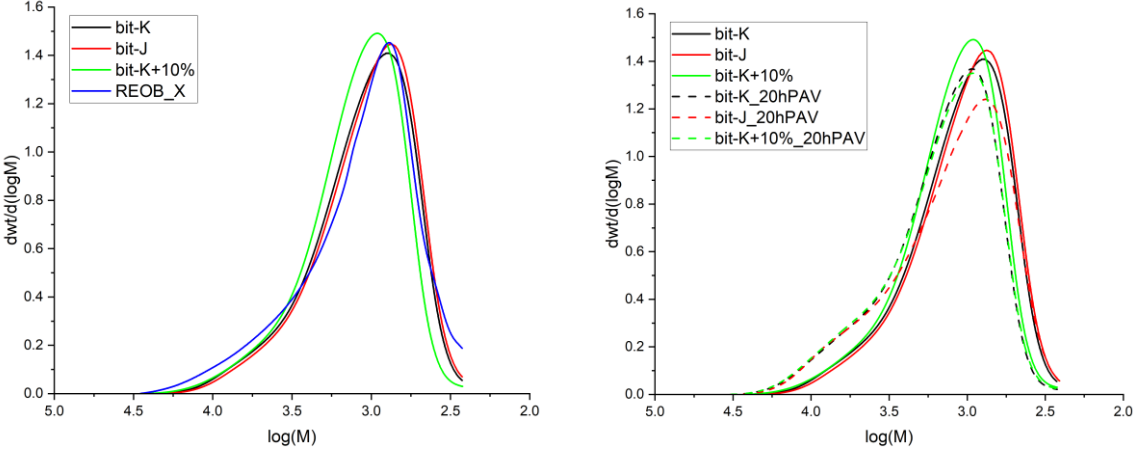


Figure 4.57: (left) Unaged bit-K, J, REOB-X and bit-K+10% and (right) the distribution changes with 20hPAV ageing

The bit-P+10% blend can also be compared to the bit-K+10% blend. One can observe similar changes in the distribution when the REOB is added initially: namely the peak is shifted towards higher molecular weights. Ageing does also do something very similar, one can see here better how the bit-K+10%_20hPAV overlaps perfectly the bit-K_20hPAV. Whereas it is found later, in Chapter 5, that bit-K+10% and bit-J had similar rheological behaviours as well as their 20hPAV counterparts.

- A clear indication of REOB modification in bitumen, will therefore mainly be visible in the fact that the peak of the molecular weight distribution will have shifted significantly to the higher molecular weights, and at the same time the binder will act soft and unaged regarding DSR measurements and PEN grades (as seen in Chapter 5).

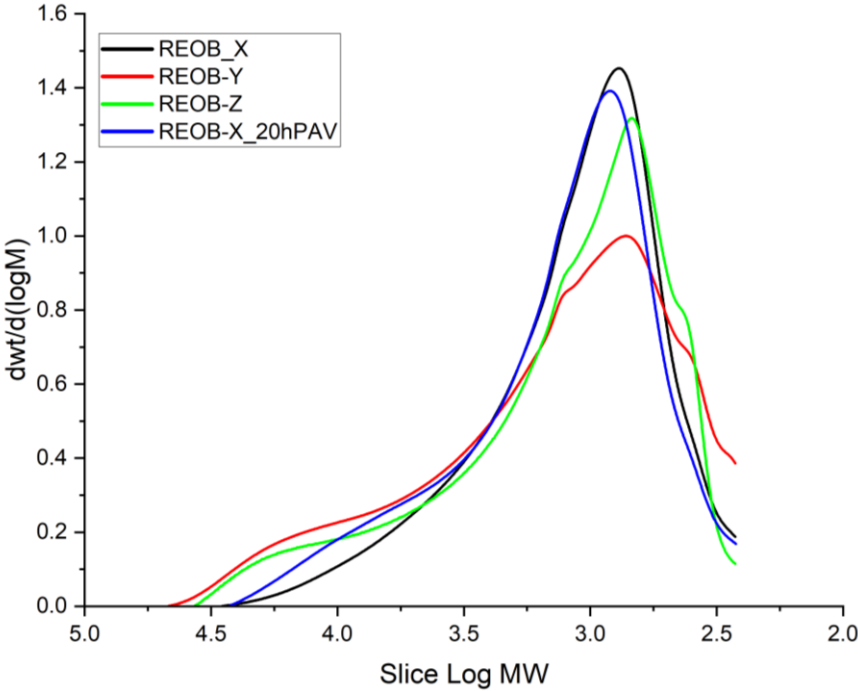


Figure 4.58: Molecular weight distributions of three REOB and one 20hPAV aged REOB

The molecular weight distributions of REOB have been plotted in Figure 4.58. Here one can see distinctive differences between all three REOB, where REOB-X shows a neat and clean curve without extra peaks, very well comparable with the weight distribution of bitumen like bit-J. Both REOB-Y and REOB-Z however show a pair of distinctive peaks at $\log(M)=0.84$; 2.60 and 2.45. These indicate that there are a high amount of specific molecules or groups present in these REOB, with low variance in molecular weights at these specific weights.

Ageing of REOB-X has shown to not only lower the peak, but also shift the curve towards higher molecular weights. One can clearly observe a loss in small sized/low molecular weight molecules (<500 Daltons) and a clear gain in high molecular weights (>4500 Daltons).

Comparing the three REOB, one can see that the addition of REOB-X will likely not change too much about the weight distributions of bitumen, when it is blended. However when REOB-Y or Z would have been added they would significantly increase the high molecular weight fraction, while at the same time also increase the low molecular weights. An addition of these two REOBs would differ a lot from REOB-X, as instead of a heightening of the peak (with a small shift towards higher molecular weights), one would in that case observe a broadening of the distribution, both heavily increasing high and low molecular weights.

- Addition of REOB-X will mainly heighten the peak and cause a shift towards higher molecular weights. This means though too that there is a smaller buffer of smaller molecular weights for ageing.
 - This would describe REOBs effect on increasing ageing susceptibility
- The addition of REOB-Y and Z would both increase the smaller molecular weights, although they also would significantly increase the high molecular weights. Next to that, these REOB do have other peaks in their distributions, suggesting they have a specific molecules (of same size/weight) present at a high amounts. This would suggest they could create separate phases and are more susceptible to causing phase separation in bitumen.
 - This would describe REOBs effect on initial ageing of bitumen and the phase separation concerns
- Both REOB variants however will increase the ratio between high and low molecular weights. An indicator of this, is the polydispersity index. This is deemed therefore as a good initial indicator of the presence of the oil and ageing of the blends is expected to increase the PDI more than the unmodified bitumen.

Indices, to describe the molecular weight distributions quantitatively and make them easy to compare with other quantitative results, are produced in the following paragraph.

4.5.2. Molecular averages; M_n ; M_w ; M_z ; M_{z+1} ; PDI

Instead of looking only qualitatively at the molecular weight distributions, one can also directly retrieve some specific characteristic values from them. Commonly used molecular weight averages (Hagos, 2008; Van Lent, 2014) were calculated with the following formulas:

$$M_n = \frac{\sum w(M)}{\sum w(M)/M} = \frac{\sum m}{\sum n} = \frac{\sum_i(n_i \cdot M_i)}{\sum_i(n_i)} = \frac{\sum_i(c_i)}{\sum_i(c_i/M_i)}$$

$$M_w = \frac{\sum w(M) * M}{\sum w(M)} = \frac{\sum_i(n_i \cdot M_i^2)}{\sum_i(n_i \cdot M_i)} = \frac{\sum_i(c_i \cdot M_i)}{\sum_i(c_i)}$$

$$M_z = \frac{\sum_i(n_i \cdot M_i^3)}{\sum_i(n_i \cdot M_i^2)} = \frac{\sum_i(c_i \cdot M_i^2)}{\sum_i(c_i \cdot M_i)}$$

$$M_{z+1} = \frac{\sum_i(n_i \cdot M_i^4)}{\sum_i(n_i \cdot M_i^3)} = \frac{\sum_i(c_i \cdot M_i^3)}{\sum_i(c_i \cdot M_i^2)}$$

(4.10)

Which all contribute with showing a different distribution phenomena, a high M_n will mean the basis of the peak lies at a high molecular weight. Next to that a high M_{z+1} would indicate there are very large and heavy molecules present in the binder.

One last, often used in polymer science to show deviations between lengths of polymers, one can calculate the polydispersity index:

$$PDI = \frac{M_w}{M_n}$$

(4.11)

This index will show that, when it is high, that there is a larger ratio of longer/heavier molecules present than the shorter ones and vice versa. This can give an indication tending towards higher molecular weights, when a high PDI and therefore a stiffer material. Ageing of a bitumen would mainly lead to M_w to increase and M_n to stay relatively stable, this therefore results in a steady increase of the PDI with ageing. But with ageing the tail is expected to increase as well, therefore M_z and M_{z+1} should significantly increase as well.

As was discussed before as well, was that the addition of REOB-X causes the peak to shift to the left. This means the M_w would rise because of this and suggests that the PDI would increase with REOB dosage. If REOB like Y and Z would have been used, one would have a harder time noticing the differences.

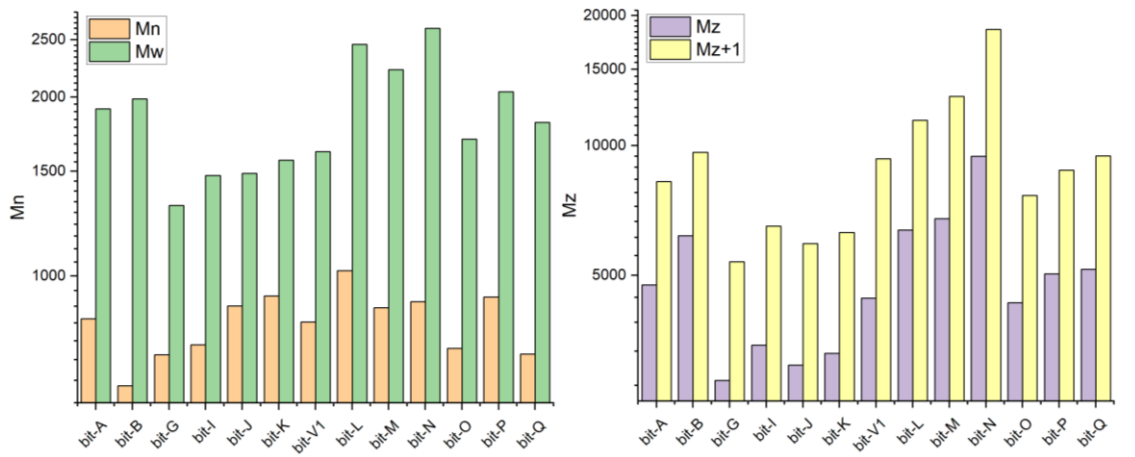


Figure 4.59: (left) the M_n and M_w averages for fresh bitumen and (right) the M_z and M_{z+1} averages

From the weight averages plotted in Figure 4.59, one can observe several bitumen have certain extreme values. Mainly bit-N shows to have very high values for M_z and M_{z+1} , suggesting that this binder is possibly a stiff binder (as it is a 40/60 grade) more so because of this high presence of high molecular weights. As on the contrary bit-K and bit-P both have very low values for M_z and M_{z+1} , this suggests that their relative height in M_n and M_w is what causes them to be stiffer.

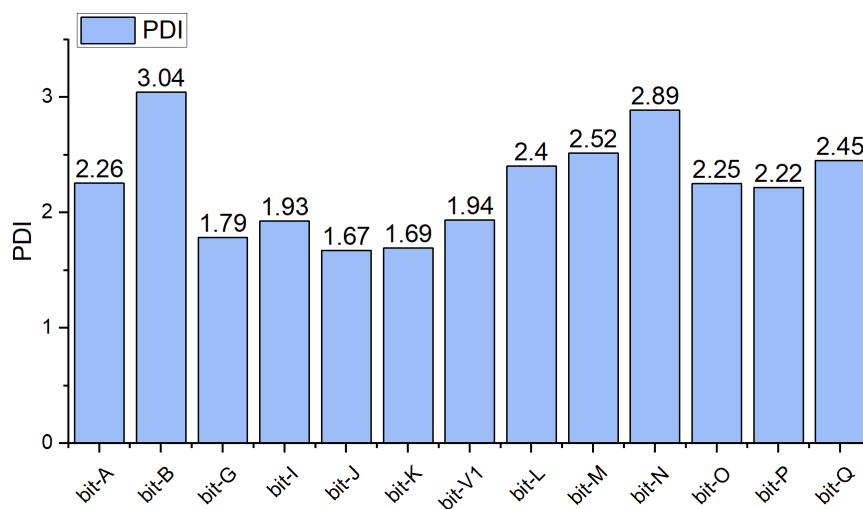


Figure 4.60: Column plots of the PDI for fresh bitumen

The PDI value shows both bit-B and bit-N to be extremely high as compared to the rest. bit-B is in fact a REOB blend, therefore pointing to the fact that this index rises with REOB addition. bit-N was already observed to have extreme M_z and M_{z+1} values, therefore it is not surprising that the M_w would be causing the PDI to rise this much as well.

It is interesting to see that the PDI shows very low values for bit-J, K and V1, which had shown in Figure 4.55 that they had one of the most narrow peak distributions of all the binders. This therefore indicates that these binders have a lot of room to increase in PDI, partly suggesting to have a high buffer for weight distribution change ageing.

Because the addition of REOB will cause the PDI to rise, it is expected that the REOB will be more compliant with bit-K than with bit-P. This will be visible in Figure 4.63, as here the indices of the blend molecular weights are plotted as well as their aged variants.

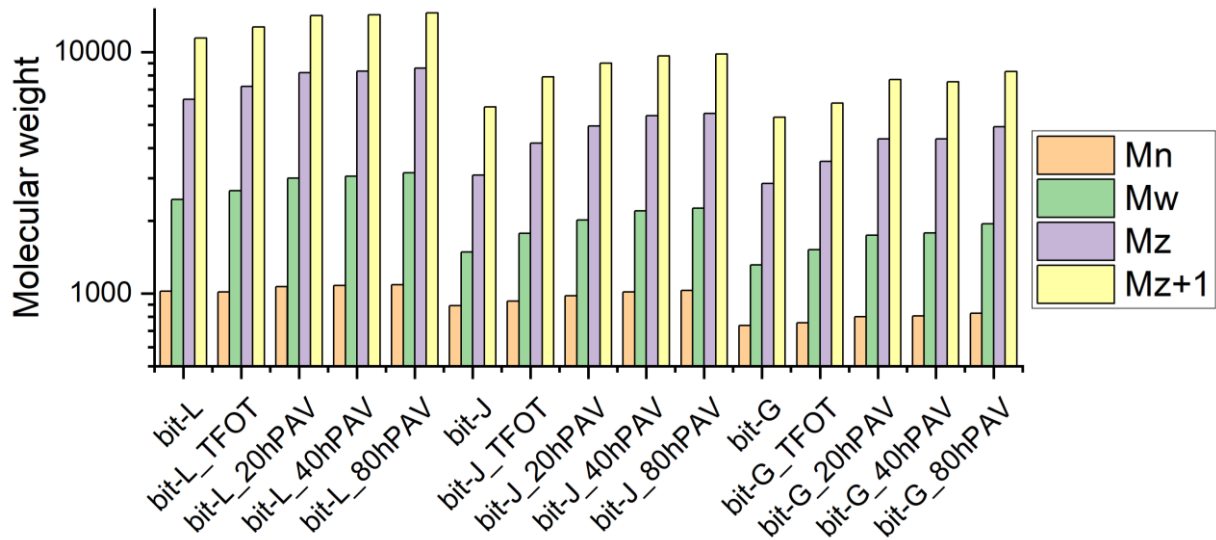


Figure 4.61: M_n & M_w , M_z and M_{z+1} parameters for aged bit-L, aged bit-J and aged bit-G

The initial molecular weight averages of the three bitumen, show to be very different. bit-G has some of the lowest M_n , M_w , M_z and M_{z+1} values of them all. On the contrary bit-L has some of the highest averages. This is also clearly visible in the calculated PDI too. One can see that all the three binders have a linear increase in molecular weight averages, and surprisingly they are all with a similar slope for the lower molecular weight averages. Bit-L seems to however have a lower tendency for change than the bit-J and bit-G, although being of a significantly higher order.

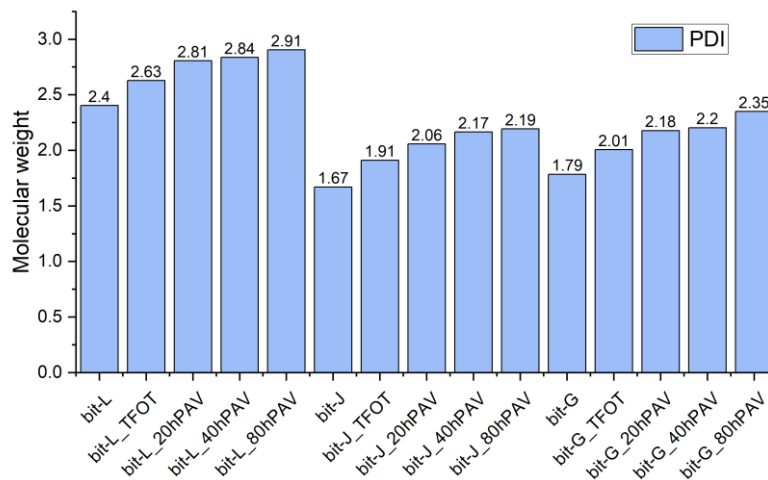


Figure 4.62: PDI parameter for aged bit-L, aged bit-J and aged bit-G

One can see that the PDI has a different starting point for all three bitumen, but ageing is so much the same that one can say that the PDI increases with ~0,5 with 80hPAV ageing.

This behaviour should now be compared to the REOB modified bitumen, to see what differences exist between them.

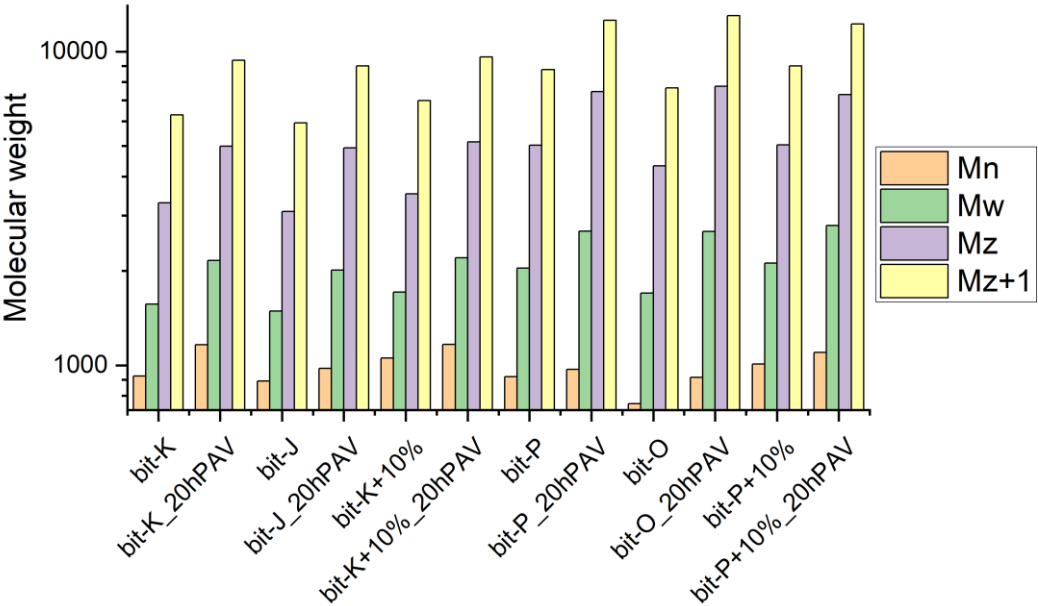


Figure 4.63: M_n & M_w , M_z and M_{z+1} parameters for bit-K blends, bit-P blends and different REOB

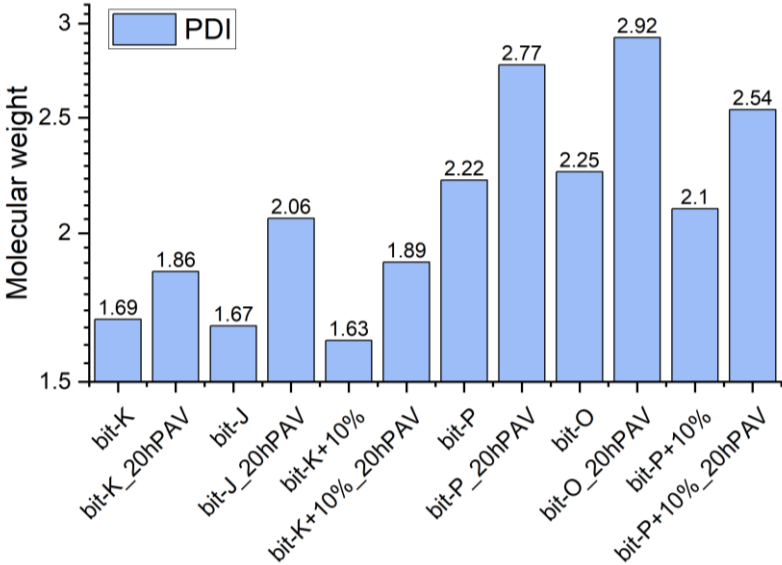


Figure 4.64: PDI parameter for bit-K blends, bit-P blends and different REOB

Unexpectedly, the PDI has decreased for both blends from their initial values after the addition of the REOB. What one should notice though, is the fact that the REOB blends have some of the highest M_n and M_w values. The difference between the two, shown by the PDI, apparently does not change, but their separate values are drastically increased.

This means that not the PDI, but the M_n and M_w values, are what is indicating REOB modification. Other REOB, than REOB-X, may have less impact on M_n and therefore cause the PDI to rise as well, but the main important change is the rise in M_n and M_w both. Merely basing REOB modification on shifts in M_n and M_w alone is not effective however, as a bitumen like bit-L already has higher M_n and M_w weight averages. The important deviation what REOB seems to do however is increase M_n and M_w ,

while actually keeping M_z and M_{z+1} stable or even lower these. This shows a deviation in the weight distribution of such modified bitumen, not necessarily being beneficial.

The differences between all indices are very close to each other however, and to truly see what is different, one should calculate the ageing indices of these averages. They are calculated in the following way:

$$AI = \frac{\log(M_{aged})}{\log(M_{fresh})} \tag{4.12}$$

So the initial ageing index starts at 1 and when a parameter increases, then the index will increase as well. This way the following plots can be generated:

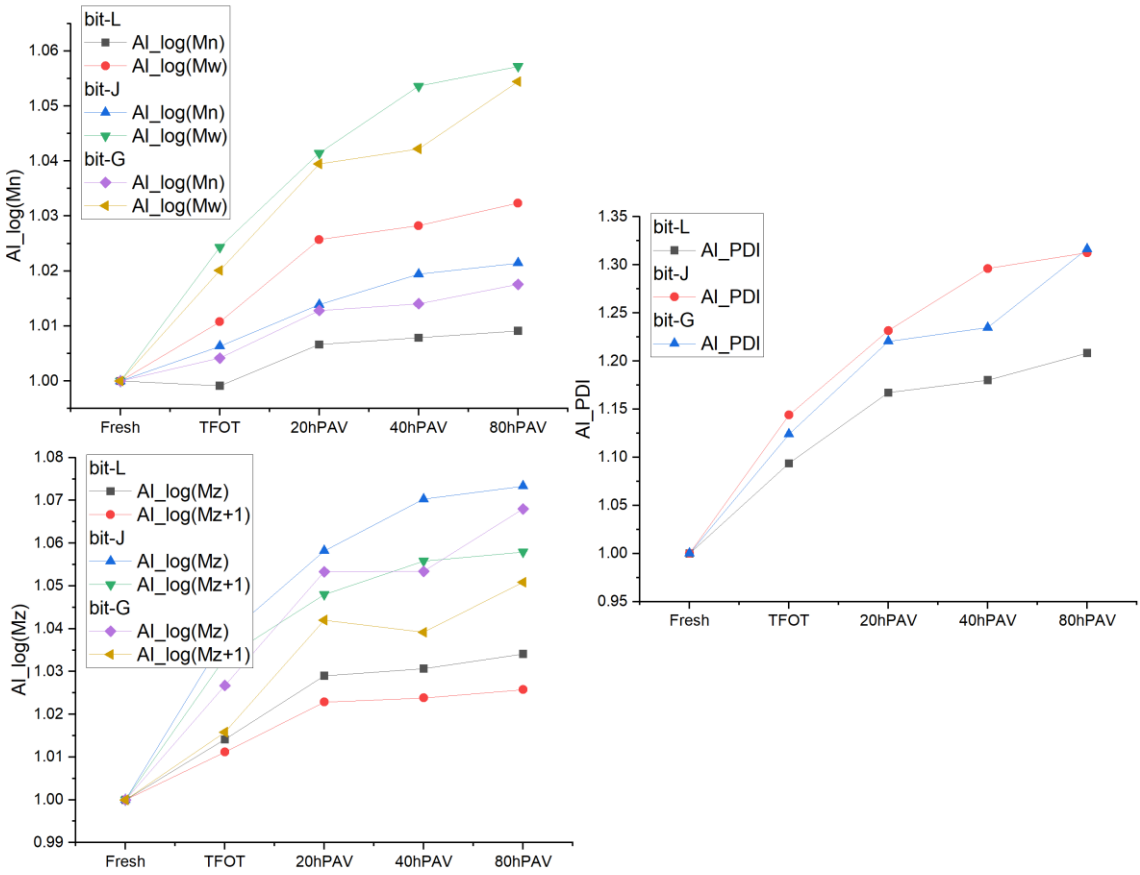


Figure 4.65: Change in ageing index with ageing for unmodified bitumen

One can easily see that the ageing indices do show the differences in ageing better than the parameters on their own. bit-L clearly has the lowest change in parameters with ageing, whereas both bit-J and bit-G have quite high calculated changes. bit-J shows to be the most susceptible to molecular weight changes with ageing, whereas bit-G lies very closely second.

Comparing the ageing susceptibility of the weight distributions of REOB modified bitumen is done below:

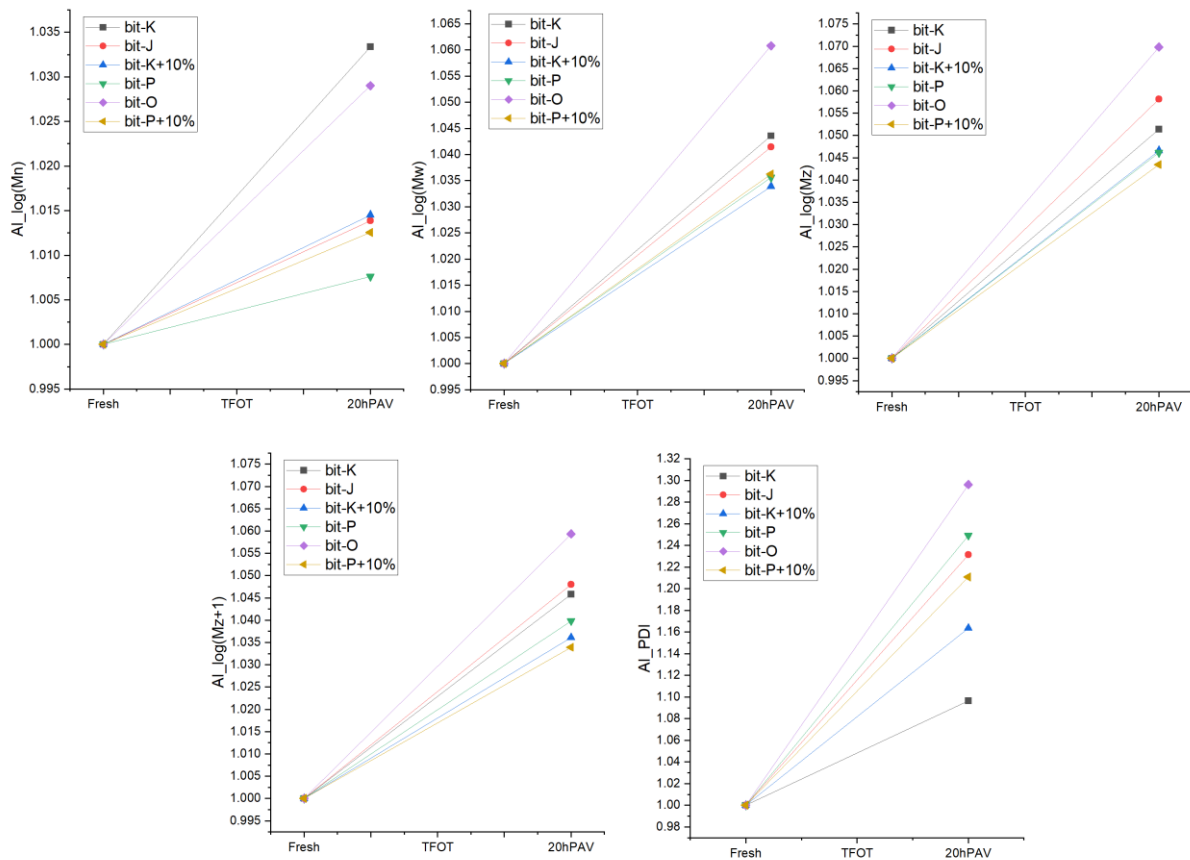


Figure 4.66: Change in ageing index with ageing for REOB modified bitumen

This seems to be well comparable with what was observed in the carbonyl index. bit-L had the lowest changes in carbonyl, whereas bit-J the highest and bit-G close second. The biggest part of weight changes in bitumen, will be mainly through oxidation and therefore the weight increase of molecules. Therefore it is logical to relate the weight changes in the molecular weight distribution to the measured increase in functional groups related to oxidation.

Because bit-J has so little sulphur present and therefore the formation of sulfoxide was very small, the impact on the weight changes should be accounted for. This will be compared to the weight changes measured with the GPC, see for this Chapter 6.2.

It is also interesting to see how the REOB modified bitumen actually does not show to have an increased change in weight averages, neither at the higher or the lower weight fractions. Actually the proportional change of bit-O is one of the highest as compared to the others. What one can notice however, is that the change is not equal for REOB modified bitumen. This means that for bit-O all ageing indices seem to change in proportionally an even way, however the REOB modified bitumen shows a much more drastic change with ageing at the M_w and M_z , whereas the other weight averages seem to alter much less drastic.

4.5.3. Fractions of low, medium and high molecular weight

The true reason however, why the M_n and M_w have both increased, is the fact that REOB-X does not have much low molecular weights; REOB-Y and REOB-Z do, but these have such distinctively different shapes, that these will change the overall distribution very differently altogether.

Evaluating these vast differences in effect of REOB-X on the bitumen will be needed. One can therefore split the cumulative molecular weight distribution into three different sections: lower, medium and high weight fractions (LWF, MWF and HWF). The boundaries for these are selected below 500 Daltons for low molecular weights and above 4500 Daltons for the high molecular weights.

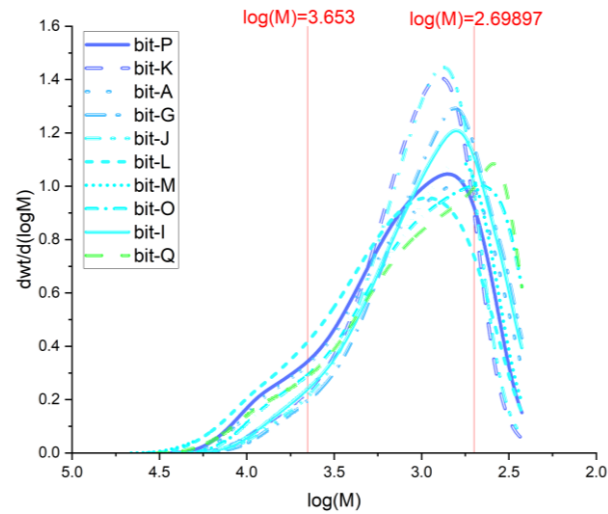


Figure 4.67: LWF boundary at 500 Daltons and HWF boundary at 4500 Daltons

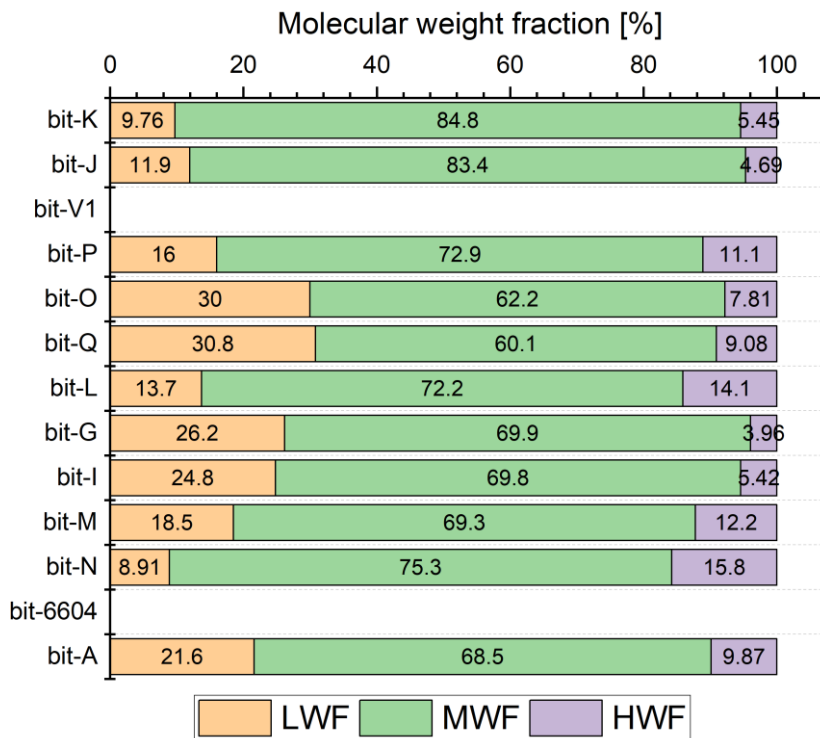


Figure 4.68: Low, medium and high weight fraction (using set boundaries at 500 and 4500 Daltons) of unmodified bitumen

From simply splitting the distribution in these three fractions, one can observe one very interesting thing: although bit-K and bit-P have been softened with the REOB, there is an observable decrease of low molecular weights. BitK+10% has extremely low quantity of low molecular weights and bit-P+10% is comparable to bit-K, bit-J and bit-N. Bit-K and bit-J have such a LWF and HWF, that this can directly be related to their origin: they are paraffinic crude oil based binders that have been partly produced by bitumen retrieved from a solvent deasphalting technique.

bit-G, bit-M and the bit-P, O and Q all show to have some of the highest amounts of LWF present. With regard of the bit-P, bit-O and bitQ binders, this could be explained by the fact that these are all straight-run produced bitumen and come from the a naphthenic Venezuelan crude oil.

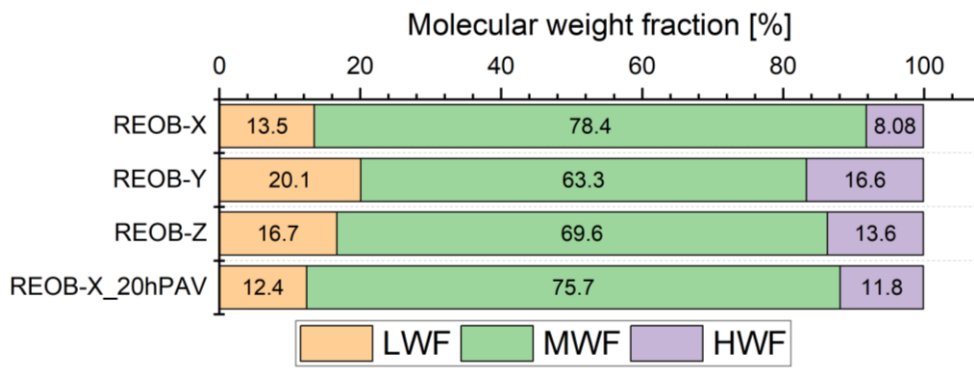


Figure 4.69: Low, medium and high weight fraction (using set boundaries at 500 and 4500 Daltons) of REOB

Here the basic principle of the effect of REOB becomes the most clear: **REOB softens the bitumen not in a similar way as bitumen can be soft on its own**. A straight run bitumen that is soft on its own will be generally soft because of a higher ratio of LWF as opposed to HWF and MWF.

- The effect of REOB however is to increase the MWF substantially to soften the bitumen enough to pass the limit of becoming soft enough for the PEN grade to pass (in the case of REOB-X).
- Or, in the case of REOB-Y and REOB-Z, to increase LWF but similarly increasing the HWF too and therefore again eliminating the benefit of these REOB.

The problem with heavily increasing the MWF, means that the curve centre (and thus all molecular weight averages) is shifted towards a higher molecular weight. This means basically that one is preparing the bitumen to become increasingly stiff in a shorter time, as there is less of a back-up of smaller molecules that can age as well.

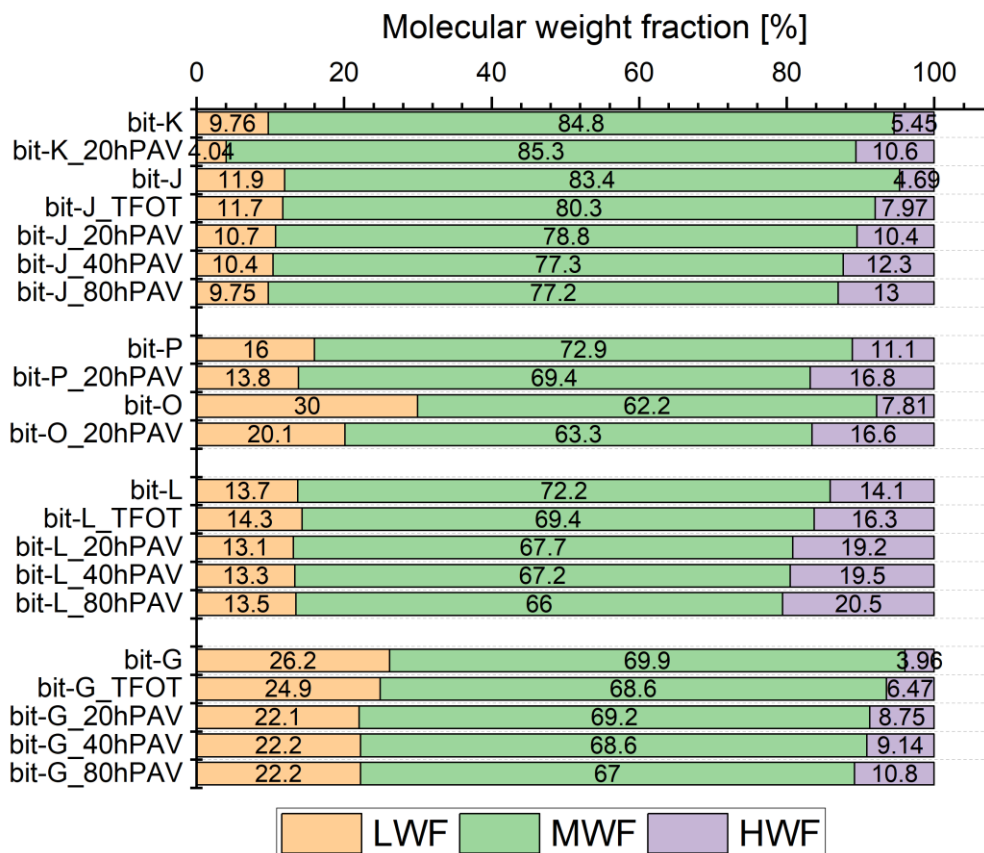


Figure 4.70: Low, medium and high weight fraction (using set boundaries at 500 and 4500 Daltons) of aged bitumen

Ageing the unmodified binders shows that both bit-L and bit-G have very stable LWF, but have a different fraction to start from. BitO has the highest initial LWF, but after 20hPAV most is lost. This suggests that bit-O has one of the biggest buffers to ageing out of all bitumen, but does not necessarily have a lower ageing susceptibility.

Comparing this to bit-J, which has one of the lowest LWF, one can see where the effect of the PPA unit comes from. This was already visible in the weight distribution shown before, as the curve was very narrow, but one can see again that this binder will have a low buffer towards ageing (but this does not say something about how quick it ages).

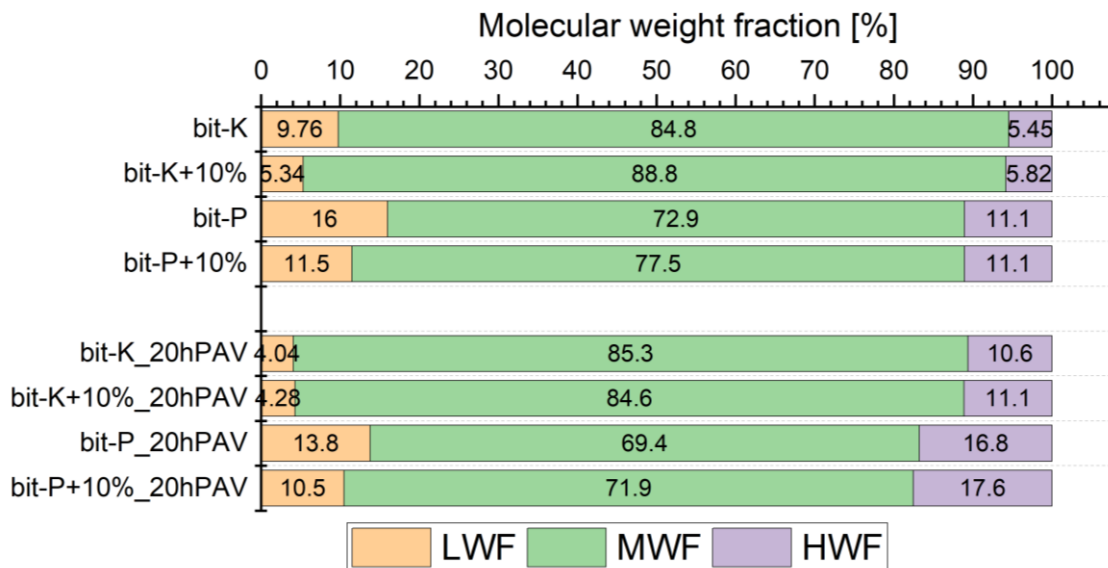


Figure 4.71: Low, medium and high weight fraction (using set boundaries at 500 and 4500 Daltons) of (aged) REOB modified bitumen

From the distributions it becomes very clear that bit-K+10% and bit-J are very similar and therefore are expected to act very similar, as well with ageing. The LWF however shows to be substantially lower, thus low temperature susceptibility is expected to be significant. Bit-O and bit-P+10% are not similar at all, bit-O has one of the highest LWF and lowest HWF and is expected to change the least with ageing as compared to all other binders. BitP+10% looks like it accepts the REOB better than the bit-K+10% does, as bit-P already had a substantial buffer of LWF.

- The recommendation for REOB modification would be to choose binders that have a substantial LWF, to be able to accept the changes in composition well and have a good buffer towards the ageing susceptibility that is increased because of the REOB.
- The ageing susceptibility of REOB modified bitumen, that saw an increase with the formation of carbonyl and sulfoxide in FTIR results, does not seem to be increased in a similar trend regarding overall changes in weight percentages. This suggests that the weight distributions are much more stable and comparable with ageing, between different REOB modified binders, than FTIR and SARA show to be.

4.5.4. Observations on molecular weight distributions

With the weight distributions of unmodified, aged and REOB modified bitumen analysed, the following conclusions can be drawn:

- (1) The apparent molecular weight distributions typically range within the boundaries of the used polystyrene with which the bitumen is compared; which are 26303 and 263 [Daltons]. Only bit-O, bit-P and bitQ seem to consist of smaller molecular sizes, that therefore cannot be plotted on the apparent molecular weight distribution graphs. Typical distributions mainly seem to consist of 1/3 in area for the left shoulder (roughly representing asphaltenes) and 2/3 in area for the high peak (representing the maltenes) (Lu et al., 2021).

General molecular weight distributions have shown that bit-L has generally very high molecular weights and bit-G, bit-O and bitQ very low. bit-J, bit-K and bit-V1 show to have a very steep and narrow distribution as compared to the broader distributions of the other bitumen.

- (2) Ageing occurs typically along the following lines:
 - a. A decrease in the biggest peak and an increase in the left (high molecular weight) shoulder
 - b. A horizontal shift of the general molecular weight distribution towards the higher molecular weights

Molecular weight averages, ageing indices and general weight distributions have shown that out of all bitumen the smallest horizontal shifting can be observed for bit-L and bit-O with ageing. bit-G and bit-J have much higher shifts towards higher molecular weights, but proportionally similar to each other.

- (3) Molecular weight fractions, splitting the distributions in three separate fractions of LWF, MWF and HWF (using suggested boundaries of 500 [Daltons] and 4500 [Daltons]) have shown clear differences in the consistency between bitumen.

Averages of the fractions range typically between:

LWF	5 – 30 %
MWF	60 – 90 %
HWF	5 – 20 %

This brings to light that the bit-O, bit-P and bitQ indeed have both very high LWF and HWF fractions. Whereas bit-K, bit-J and bit-V1 have actually some of the lowest. Ageing shows to have large effect on the LWF for the bit-O and bit-P bitumen, although in the case of bit-L, bit-G and bit-J one cannot notice drastic changes. However all bitumen will substantially increase in HWF with ageing. This all seems to be similar to observations done on ageing according to other research (Kim & Burati Jr, 1993; Lee et al., 2008; Tang et al., 2019).

- (4) REOB itself has shown to vary in weight distribution between different sources, where REOB-X has one of the cleanest curves (no separate peaks throughout the curve apart from the typical maltene peak), although the general curve lies more at the heavier molecular weight fraction as compared to typical bitumen. REOB-Y and REOB-Z both show to have larger LWF fractions, although their HWF is substantially bigger as well.
- (5) REOB-X modification has shown to initially change the M_n and M_w values heavily, indicating a large influence on the low molecular weight portion of the bitumen blend. This is further shown by the LWF fraction, where one can clearly see that this fraction has decreased with the addition of REOB, and after ageing both the base bitumen and the REOB modified bitumen will actually end up at a similar LWF.

The observed weight distributions of REOB and the modified bitumen are also similar to distributions measured in other research (Cooper Jr et al., 2017).

4.6. Heat flow behaviour and glass transition (DSC)

4.6.1. Principle of differential scanning calorimetry and used procedure

As described before in the literature review in Chapter 2, the DSC is expected to give insights into compatibility issues of binders; mainly showing different phases to be present or not. With the differential scanning calorimeter (DSC), one applies a certain heat scan on a small bitumen sample, and measures the difference in mass with an empty sample to obtain a difference in heat capacity. This means that a sample that is heated, and it has to change its phase structure, it will need an increase of energy into its system to make the different molecules move. This means an endothermic peak/drop should be visible in the heat flow diagram that is retrieved with a DSC.

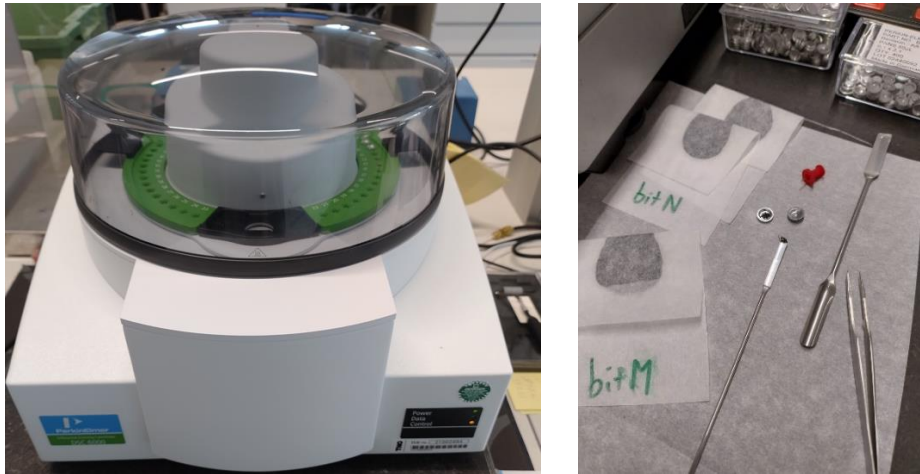


Figure 4.72: (left) Differential scanning calorimeter (DSC) including carousel system for automatic testing and (right) cutting of small bitumen samples in aluminium measurement pans

To be able to perform tests with the machine, one needs to be careful with sample preparation and setup the test program accordingly. Bitumen samples were all prepared in a similar way and poured on silicon paper, later cooled down and put in the fridge at 5 [°C]. These bitumen samples were then, when the DSC samples would be prepared, all taken out of the fridge and small pieces of bitumen (10 ± 5 [mg]) were cut and put into small aluminium containers. These aluminium containers consisted of an aluminium pan at the bottom; and a perforated aluminium pan at the top.

The samples were placed in the carousel, shown in Figure 4.72, and the machine would place the sample in the heating chamber when the test would be performed. A heating cycle of the following order was chosen:

- Start at 30 [°C] and bring to 80 [°C] with a rate of 10 [°C/min].
Once there, stabilize for 5 [min] (this is to apply some isothermal conditioning and thus lose some thermal history of the samples, higher temperatures/longer times is expected to evaporate light components; especially for REOB modified bitumen)
- Now steadily lower the temperature to -65 [°C] with a rate of -10 [°C/min], where the machine should stabilize for 20 [min]. The big problem with the cooling system of this DSC though, is that it cannot reach the -65 [°C] fast enough and therefore extra time should be applied to really reach the temperature.
N.B. the cooling rate of -10 [°C/min] that was initially decided, is therefore not reached, between -20 [°C] and -65 [°C] the rate comes more close to -5 [°C/min].
- A heating rate of 10 [°C/min] is applied to bring the sample from -65 [°C] to 140 [°C] to obtain the full curve in which noticeable changes are present in bituminous materials.

To show the change in temperatures over time, the heat flow program is presented in the following figure:

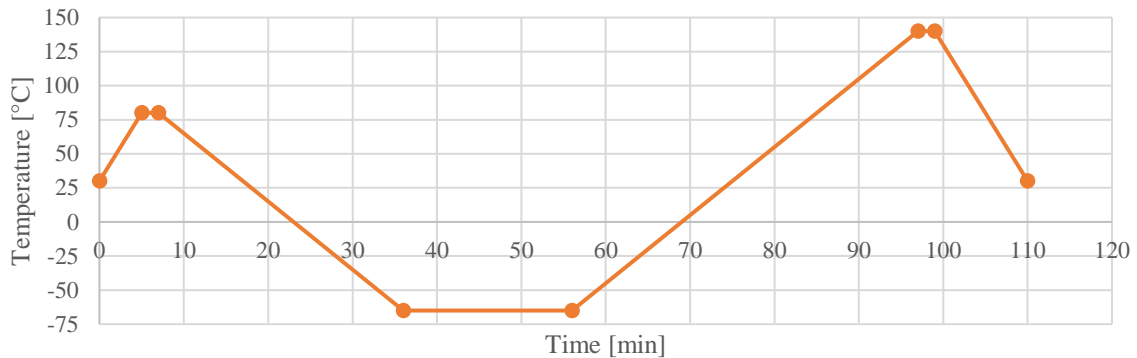


Figure 4.73: Heat flow program for the DSC tests of unmodified and REOB modified bitumen

Once the test has been performed, the DSC obtains a Heat flow diagram (with the endothermal energy down for example) in [W/g] over the changing temperature in [°C]. The energy levels of the heat flow, measured in [mW], have been normalised by dividing it by the used sample mass, to make curves better comparable to each other. This is done for the calculation of the ΔC_p value too. Above 85 [°C] no interesting changes occur for the bitumen and therefore a cut-off is introduced in the coming graphs.

4.6.2. Phase transitions of unmodified and REOB modified bitumen

In the figure below the first set of DSC heat flow diagrams is shown of the bit-K, bit-J and bit-V1 bitumen series:

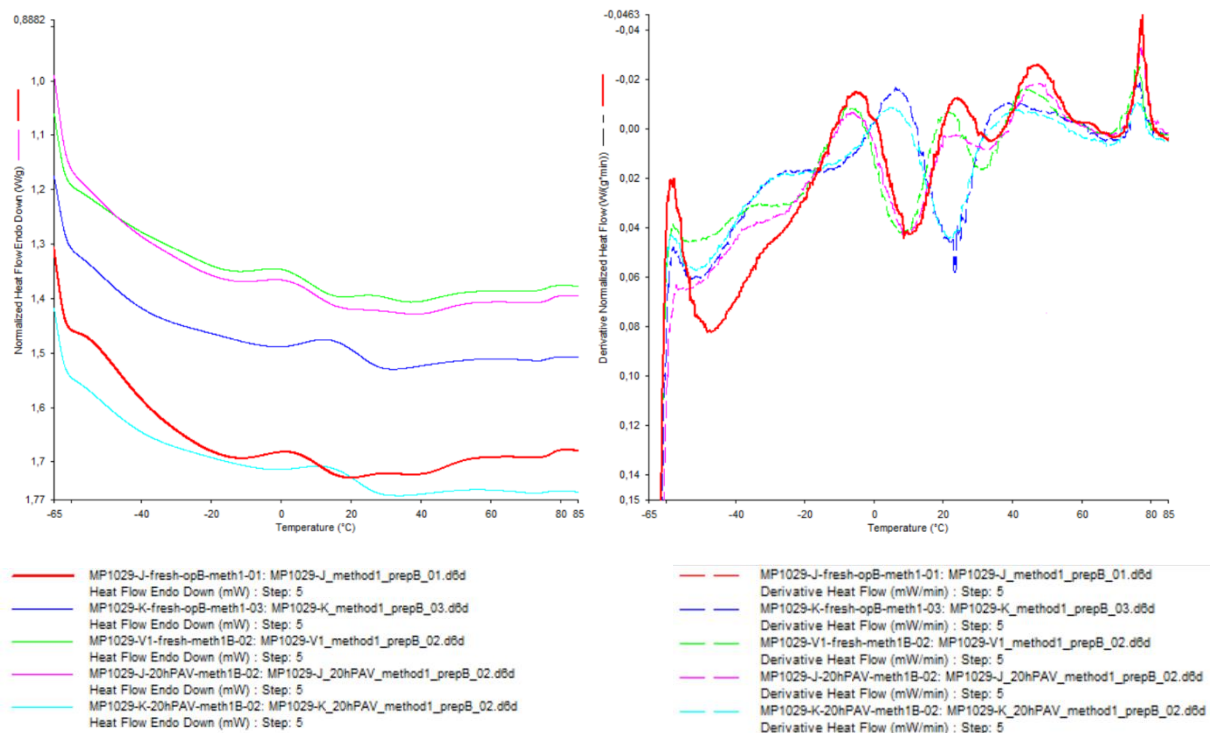


Figure 4.74: Heat flow diagrams of bit-K, bit-J, bit-V1 and their derivative curves

Throughout all three different bitumen grades, from the same supplier to say, one can notice distinctively similar (in shape and in number) phase shifts, although for some of them they occur at different temperatures.

From all three curves, one can observe in total three specific glass transitions (or endothermic phase changes), although bit-K has one small transition extra at around -15 [°C]. For bit-J and bit-V1 this extra transition lies more closely to -25 [°C].

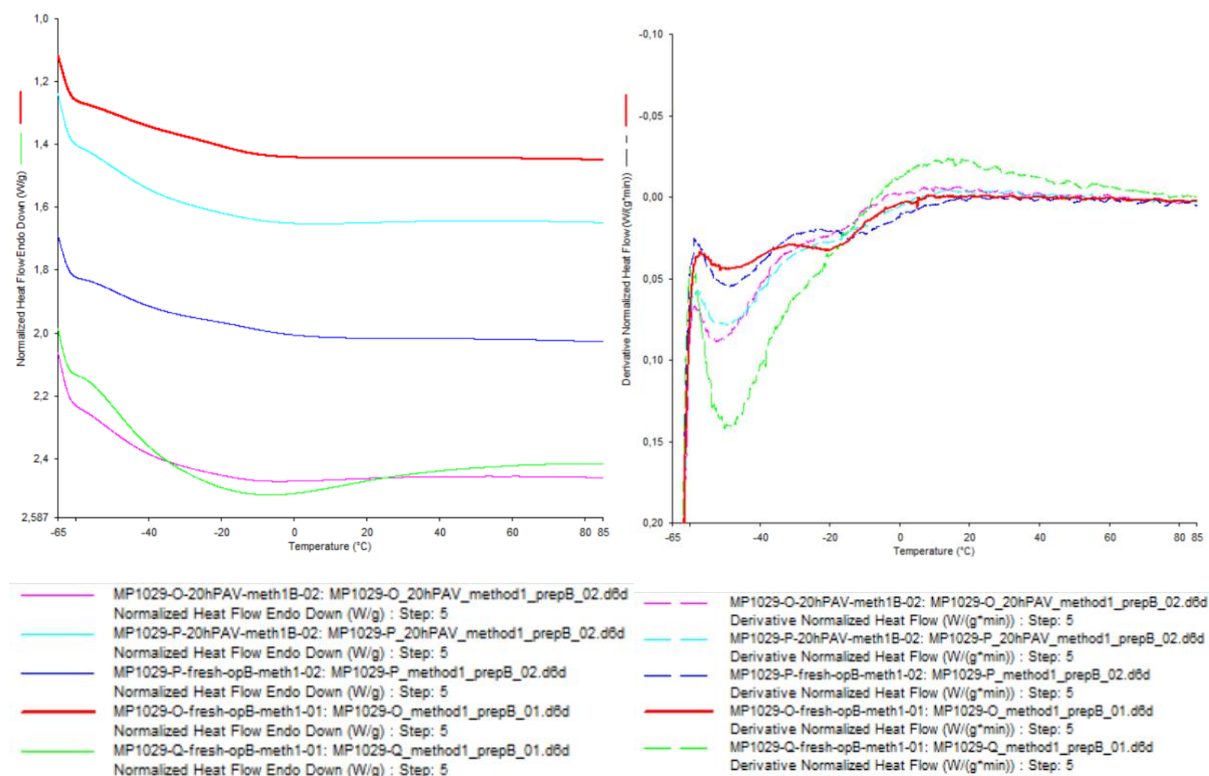


Figure 4.75: (Left) heat flow diagrams of bit-P, bit-O, bitQ and (right) their derivative curves

This can be compared to the bitumen series of bit-P, bit-O and bitQ too. Here one can observe from both the normal heat flow diagram as well as the derivative, that only one transition occurs for bitQ and two transitions for both bit-P and bit-O.

One can see that the for both bitumen series, bit-K and bit-P etc, that the lowest glass transition remains quite stable between the different bitumen grades, although the transitions happening at higher temperatures undergo larger shifts. It is interesting to notice that the bit-K series have so many transitions, where the bit-P series does not. One can also notice that when the bitumen grade is increasing, so bit-K (20/30) towards bit-V1 (160/220), that the phase transitions shift towards lower temperatures.

What this basically means is that the present molecules take their new phase positions and form a structure at lower temperatures. This makes a lot of sense, as bitumen with larger/heavier/complex molecules will need more energy to start vibrating and take their new position with the phase change. A bitumen with more of these larger/heavier/complex molecules are directly related to increase in stiffness of the structure and therefore an increase in viscosity.

Ageing of these bitumen has also been performed and therefore also evaluated in DSC heat flow scans. It was expected that mainly a broadening of the transitions should occur and a small shift towards a higher temperature for these glass transitions, based on previous research (Kriz et al., 2008).

Interestingly, one can observe that the lowest glass transition actually becomes lower with a decrease around -0.5 ± 0.25 [°C]; this means that it has become easier for the material to reach the stable state of the new phase. The thought is that this fraction actually relates to the very small molecular weight fraction, which is able to vibrate at very low temperatures, as opposed to larger/heavier molecules. This

could therefore very heavily correlate to the saturates/aromatics fractions (from SARA analysis) or specifically the molecules lower than 500 Daltons (from GPC analysis). With ageing one knows that there is a heavy decrease in low molecular weights. This is for, a very small, partly because of loss of volatiles (TFOT ageing) but also the oxidation of molecules, where the aromatics fraction is lost and they transition into resins/asphaltenes. However the other glass transitions do show an increase in temperature with the ageing. Ageing causes for a small increase which is around 1 ± 0.5 [°C]. Next to this horizontal shift, the broadening of the transition is observable as well. Where bit-J had its onset and offset for the second glass transition at 0 [°C] and 15 [°C], the 20hPAV aged version showed this to occur between 0 [°C] and 20 [°C].

To show the variance between different bitumen a bit more, bit-L, bit-M and bit-N are scanned as well. In Figure 4.76 one can observe the heat flow behaviour of bit-L, but also bit-M (70/100) & bit-N (40/60) which are from the same supplier but with different PEN grades.

Like with the bit-K, bit-J and bit-V1 series, one can observe that the PEN grade is directly related to how high the glass transition temperatures exist (at the higher temperature ends).

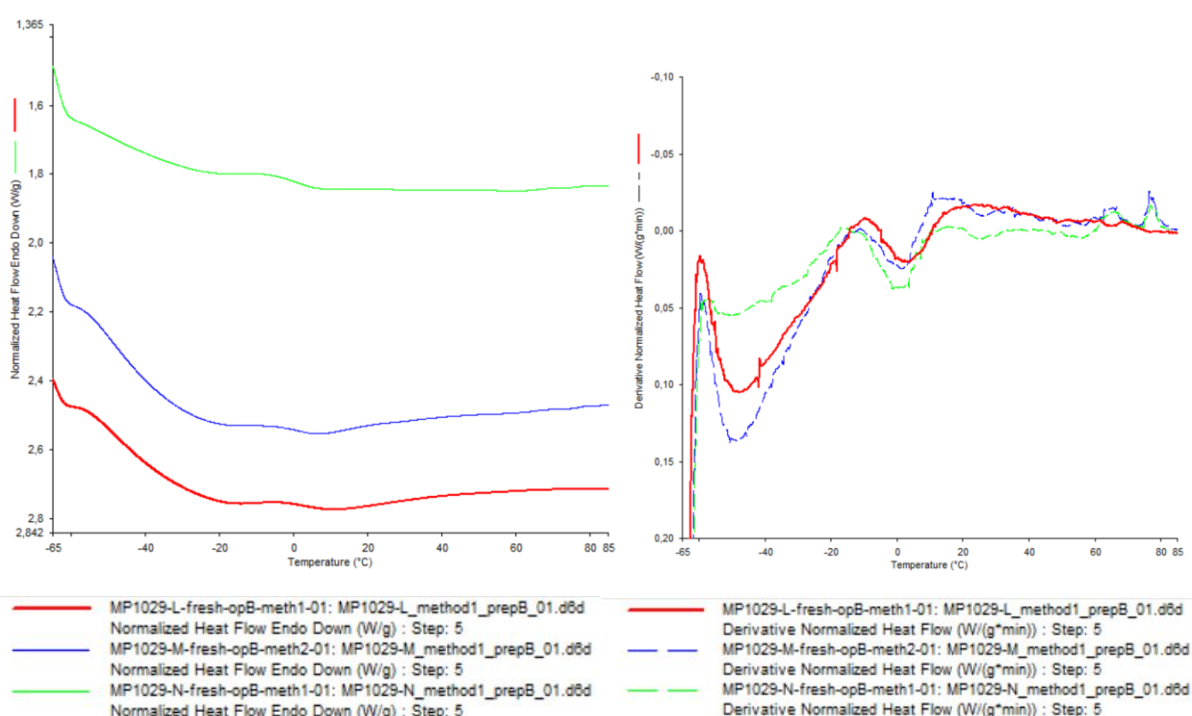


Figure 4.76: (Left) heat flow diagrams of bit-L, bit-M and bit-N and (right) their derivative curves

Very interestingly, the bit-M and bit-N differ in a totally other way than the bit-K and bit-J did. BitN does have a very significantly lower glass transition at the low temperatures around -47 [°C], whereas bit-M has one at -43 [°C]. What is extremely different though, is the fact that the second glass transition lies lower for bit-N (at 0.27 [°C]) than for bit-M (at 3.37 [°C]). This is a stark contrast with bit-K and bit-J, where the difference was bigger, but the lower grade also would have a lower transition temperature.

This shows that bit-N probably retrieves its stiffer nature, already because of the significant difference in the lower glass transition and the difference at the higher transition temperature does not matter as much apparently.

Both bit-L and bit-M seem to have a very high glass transition at the lower temperatures, namely -43 [°C]. This is very different from the previously observed bit-J and bit-O, which each had -50 [°C] and -46 [°C] temperatures. One can mainly point to the fact that bit-L and bit-M also have much bigger width over which the transition occurs, this will always increase the measured T_g and can be related to the fact

that there is much more molecular weight variance for this specific molecular fraction. Both bit-J and bit-O have much less variance in molecular weights for that specific phase to form and this will therefore happen quicker.

The other reason could be that the second glass transition, which is not present for bit-L and bit-M, is actually connected to the first glass transition. In the case of bit-L, bit-M and bit-O there is just a large variance in molecular weights, but not a split between phases that can form. For bit-J however, there does exist a split in molecules fractions, where there can occur two different phases both at around -50 [°C] and -15 [°C].

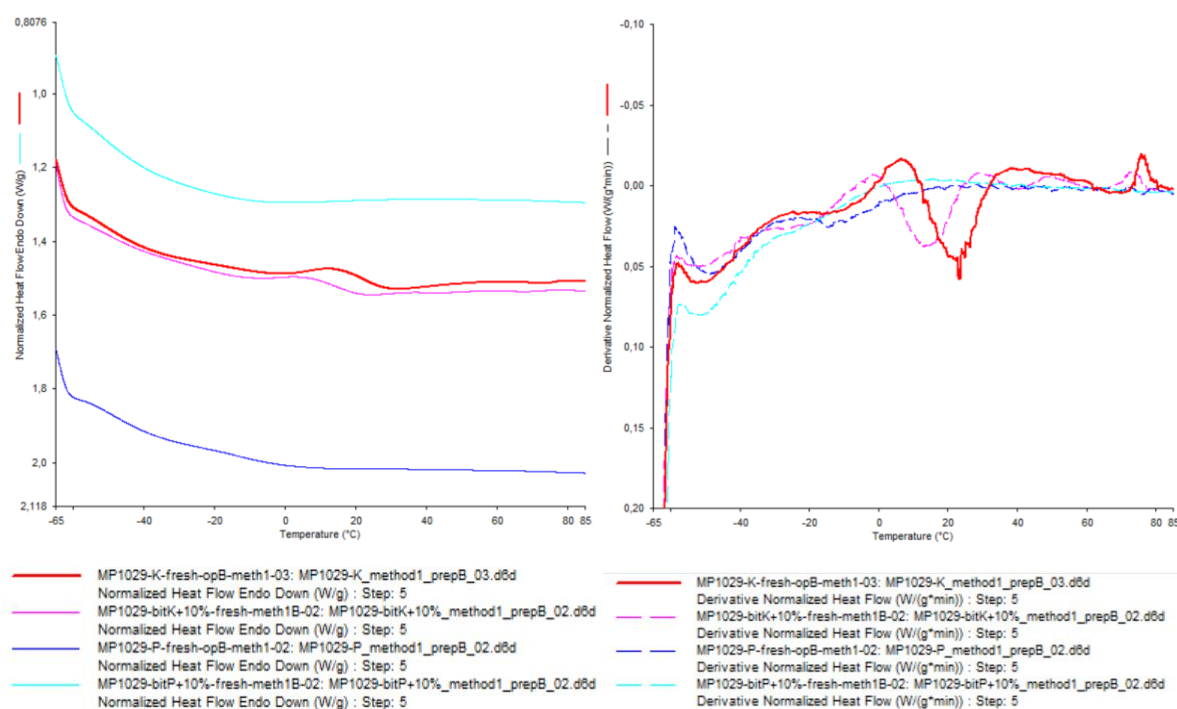


Figure 4.77: (Left) heat flow diagrams of bit-K, bit-P, their +10% REOB blend versions and (right) their derivative curves

With unmodified bitumen now qualitatively analysed, the REOB modified binders are evaluated as well. In Figure 4.77 one can see both the bit-K and bit-P unmodified base bitumen and their 10% blend counterparts.

Very significantly present one can observe the shift of T_{g3} for bit-K+10% blends because of the addition of the REOB. Adding the REOB causes a difference in the composition of the binder, tending for an earlier glass transition than one later. This makes sense when the REOB itself would not have a glass transition at this high of a temperature and therefore will always cause the glass transitions to decrease in values. There is a T_{g4} at 40 [°C] present for the bit-K+10% blend, which was not at all present for the bit-K base bitumen.

For the bit-P+10% however, one cannot observe either a T_{g3} or T_{g4} and no extra glass transitions have appeared. Looking closely to both T_{g1} and T_{g2} , one can observe that the T_{g2} has significantly shifted to lower temperatures, because of the addition of the REOB. Instead of around -15 [°C], one can observe it to be located more at -20 [°C].

The aged variants of the base bitumen and the blends have been scanned as well, and are presented in the following graph.

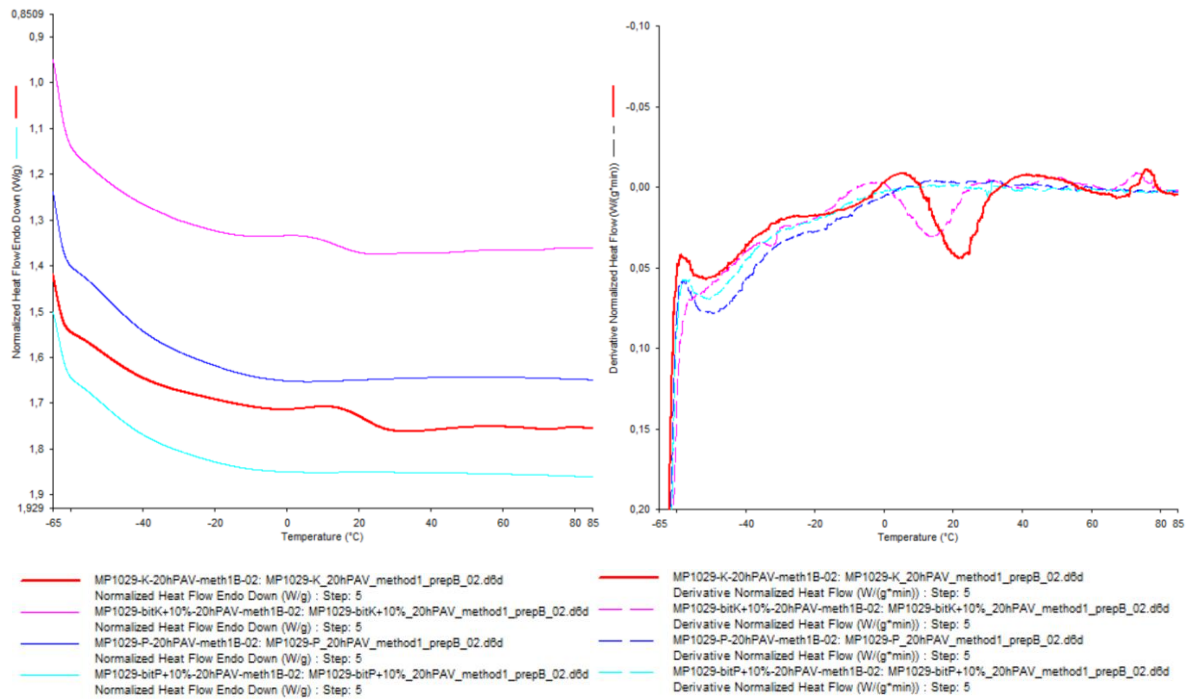


Figure 4.78: (Left) heat flow diagrams of 20hPAV aged bit-K, bit-P, their +10% REOB blend versions and (right) their derivative curves

Comparing the 20hPAV aged base bitumen, bit-K and bit-P, to the 10% REOB blends, bit-K+10% and bit-P+10%, one can see the same differences as with the unaged variants.

The T_{g1} does not seem to have shifted at all, being located at around -50 [°C] without much variance. For the bit-K+10%_20hPAV blend one can observe something interesting. There is a very small transition occurring at around -38 [°C]. This is regardless of T_{g1} and T_{g2} , and seems to only occur for this 20hPAV aged bit-K+10% blend. The T_{g4} at 40 [°C] seems to still occur for bit-K+10%_20hPAV and has not appeared for bit-K_20hPAV. The bit-P+10%_20hPAV blend does not show similarities to bit-K+10%_20hPAV. The changes that it does go through, as compared with the unmodified bit-P_20hPAV, are marginally small. The T_{g1} and T_{g2} seem to lie at a bit lower levels, going from -50 towards -51 [°C] and -20 to -21 [°C].

For all bitumen the T_{g2} has become less prominent, but it is also clear that this transition has shifted towards the lower temperatures more for the bit-K+10% than it did for the unmodified bitumen or for the bit-P+10% blend.

4.6.3. Measured phase transition temperatures; half ΔC_p and derivative methods

Next to a qualitative analysis of the heat flow behaviour of these bitumen, a quantitative approach to analyse the data is presented here. Below one can observe the heat flow behaviour of bit-J, where the derivative is also plotted. The heat flow shows three clear different transitions with heating of the sample at 10 [°C/min]. However the derivative of the curve shows different maximum drops in slope, one can observe where the heat flow itself had only one transition, the derivative shows that there are actually two. These averaged out give actually the same glass transition observed in the heat flow itself:

$$T_{g1} = -35.63 [^{\circ}C] = \frac{-49.34 - 22.98}{2} = -36.16 [^{\circ}C]$$

(4.13)

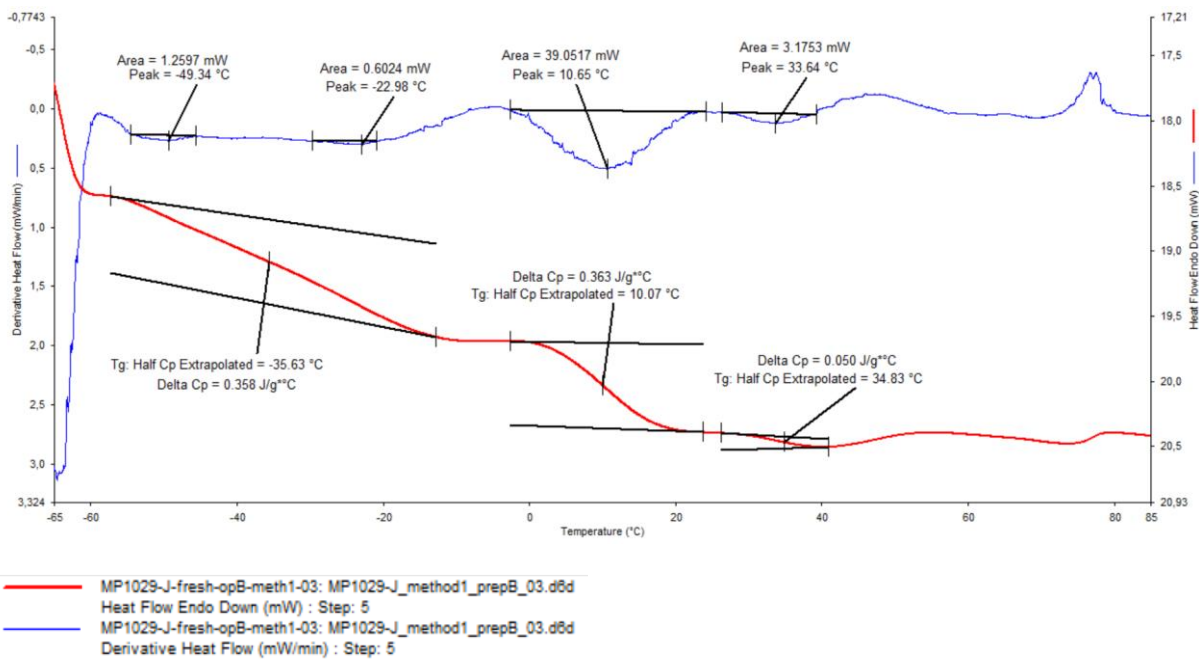


Figure 4.79: Heat flow diagram of bit-J and its derivative curves

The same procedure is applied to all other heat flow diagrams of the measured bitumen samples. The measured values using the half ΔC_p method averaged with the measured values with the maximum derivative method, which are noted in Table 4.7. Some bitumen show therefore to have more glass transitions than the others, but the average shows that there are either:

- One glass transition around -50 or -40 [°C]
- Two glass transitions around -50 and -25 [°C] which are sometimes combined into -40
- Three glass transitions around -50; -25 and +2 [°C]
- Four glass transitions around -50; -25; +10 and +35 [°C]

Between the binders one can observe clear deviations on where exactly their transitions lie. Ageing does not seem to influence the position of the glass transition at the lower temperatures, although the glass transitions that are above 0 [°C] do seem to shift towards lower temperatures with around a decrease of -1 [°C] for 20hPAV ageing. See for example the T_{g3} of bit-J:

$$T_{g3;bitJ} = 10.24 [^{\circ}C] \rightarrow T_{g3;bitJ_{20hPAV}} = 9.37 [^{\circ}C]$$

(4.14)

The shifts at the lower temperatures are marginally small, although this is not the case for the REOB blended bitumen. One can observe that the $(T_{g1}+T_{g2})/2$ does not shift for bit-J with ageing, however a very big decrease is present for the bit-K+10% blend:

$$\text{For bit-J:} \quad (T_{g1} + T_{g2})/2 = -39.08 \rightarrow -39.02 [^{\circ}\text{C}]$$

$$\text{For bit-K+10\%:} \quad (T_{g1} + T_{g2})/2 = -36.93 \rightarrow -42.24 [^{\circ}\text{C}]$$

(4.15)

This is an interesting behaviour and results from the fact that either T_{g1} or T_{g2} has decreased, or both. Looking at the measured values mainly T_{g2} has decreased significantly. This shows that specifically the phase that was previously changing at around -22 [°C], has now already changed at -33 [°C]. Very interestingly, this is totally not the case for the bit-P blends. There is no observable increase in the shift for the phase transitions, because of the REOB addition. For a binder this means that on general the phase structure can change drastically over ageing. This is not to the benefit of a material, as it means that it will change in rheological properties way more drastically than a standard binder does, it will change its stiffness and viscoelastic behaviour significantly with changes in temperature and behave like a different binder.

Table 4.7: Found glass transitions of all unmodified and REOB modified bitumen and some of their 20hPAV versions; positioning based on an average between the method using half ΔC_p value and the maximum derivative

Glass transition	T_{g1}	T_{g2}	T_{g3}	T_{g4}
Unit	[°C]	[°C]	[°C]	[°C]
bit-K	-50.18	-14.97	22.32	
bit-J	-46.95	-23.32	9.98	34.42
bit-V1	-49.99	-23.55	7.32	31.55
bit-K_20hPAV	-51.15	-14.14	22.95	
bit-J_20hPAV	-51.77	-25.02	9.00	32.34
bit-P	-48.36	-15.12		
bit-O	-49.52	-21.82		
bit-Q	-48.23			
bit-P_20hPAV	-48.76	-18.87		
bit-O_20hPAV	-50.42	-21.28		
bit-L	-48.44	-27.28	4.04	
bit-M	-47.75		0.97	24.02
bit-N	-47.82		-0.23	24.07
bit-K+10%	-50.98	-21.44	13.50	39.57
bit-K+10%_20hPAV	-51.16	-32.34	13.35	39.32
bit-P+10%	-50.65	-17.89		
bit-P+10%_20hPAV	-52.10	-18.67		

One can observe some differences between both tables, for example the fact that some T_g 's are not measured for the half ΔC_p method, but they have been for the maximum derivative method. This is because the maximum derivative method uses the full derivative curve and is therefore able to show very small changes in the slope of the curve. With the normal heat flow diagram the transitions are almost not visible and therefore harder to estimate, hence some shifts are present.

To visualise the data denoted in the tables, they will be combined and an average is taken from all measurements and both calculation methods, these are noted in the following column plots.

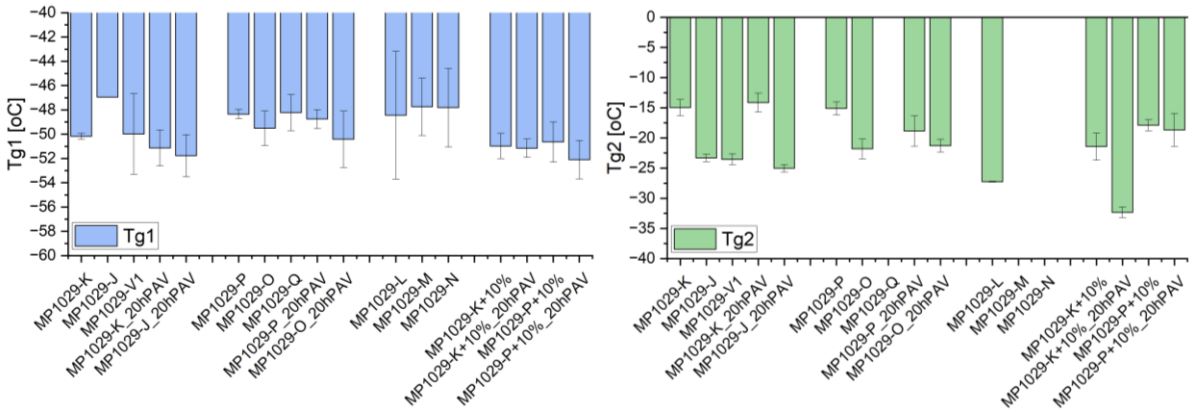


Figure 4.80: Column plots of T_{g1} and T_{g2} for all tested bitumen

One can now more easily observe the differences between the bitumen, where T_{g1} shows to be quite stable for all binders at around -50 [°C]. A lot of variance was measured in bit-L, bit-M and bit-N, which could be contributing to an average that lies closer to -48 [°C]. On average the T_{g1} lies between -50 and -52 [°C] for the bit-J, bit-K and bit-V1 series. However for the bit-P, bit-O and bitQ series this is more between -50 and -48 [°C].

A T_{g2} can also be found for some bitumen, specifically not for bitQ, bit-M and bit-N. Interesting to notice is that the T_{g2} of bit-K+10% and also the aged bit-K+10%_20hPAV lie extremely high as compared to the other bitumen, as well as compared to the other REOB modified bitumen bit-P+10%_20hPAV. This is only after the modification and then the ageing and thus suggests that the bit-K bitumen is an interesting base bitumen for this specific phase structures to appear.

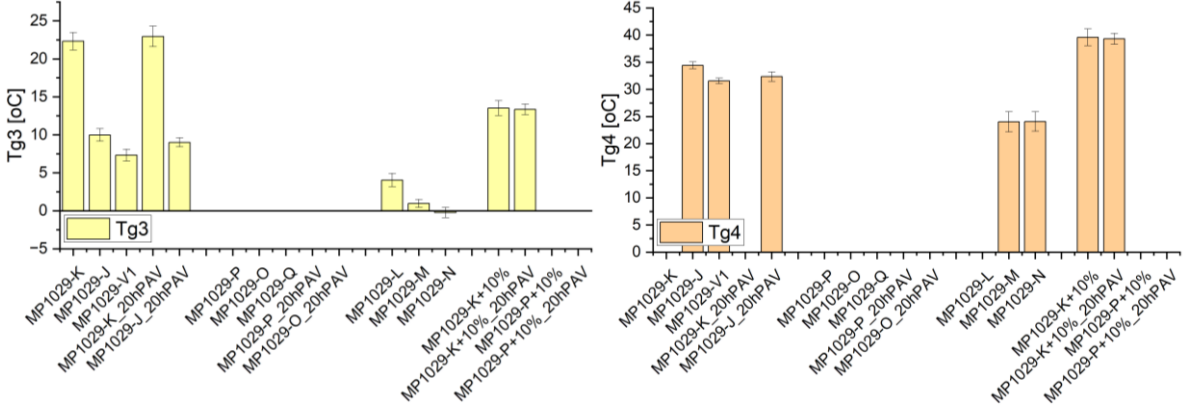


Figure 4.81: Column plots of the T_{g3} and T_{g4} for all tested bitumen

As noted before, the T_{g3} is not present in bit-P, bit-O and bitQ and does not become present after REOB addition of ageing. The REOB modification is able to lower the T_g significantly, as it changes from +22 [°C] to +12 [°C] for the bit-K when adding 10% REOB. Which is quite close to the bit-J, which has a T_{g3} at around +10 [°C]. The bit-L, bit-M and bit-N are significantly different, as they have their T_{g3} at around +5 [°C] to 0 [°C]. Ageing of the bitumen does not change the T_{g3} at all.

Lastly, the measured T_{g4} is not noticeable for bit-P, bit-O and bitQ, however it also is not present for bit-K and bit-L. It is interesting to see however, that when adding the REOB, one starts to notice the T_{g4}. Ageing does not seem to have an effect on the position of this temperature transition.

Phase transitions are not necessarily a bad thing for a bitumen. A bitumen undergoing a lot of transitions suggests however that with changing temperature the bitumen will change differently in rheological behaviour. This rheological behaviour changing because of the phase structures undergoing a transition, makes the performance of such a bitumen less predictable. And specifically this is not a good aspect for a binder.

This suggests that binders that do not undergo much transitions, are the better predictable and more reliable bitumen to use for asphalt mixtures or in general the REOB modification. BitP, bit-O and bitQ would in that sense present the best reliability for REOB modification as compared to the bit-K, bit-J and bit-V1 series. Especially the drastic change in T_{g2} for the initial bit-K+10% but also the bit-K+10%_20hPAV shows a significant change in binder properties (after REOB modification and later the ageing) in the low temperature region. This suggests that bit-K+10% will perform significantly worse at lower temperatures than bit-P+10%, as bit-P+10% will more slowly change in phase structure as compared to bit-K+10%.

4.6.4. Observations on phase transitions

With the DSC heating scans performed, although on a limited number of samples and with the cooler of the machine not reaching the -65 [°C] in time and therefore allowing the material to relax during cooling, still a comparative study between the tested bitumen could be performed. This has shown distinctive differences between all bitumen and the following conclusions can then be drawn from the tests:

- (1) Unmodified bitumen differs in the amount of phase transitions that occur between -65 [°C] and 80 [°C]. Where bitumen always has a T_{g1} at around -50 [°C] and a T_{g2} around -20 [°C]. With T_{g1} differing less between different bitumen, than T_{g2} . Only some bitumen have more phase transitions, which occur at different temperatures like T_{g3} at around either 0 [°C]; 10 [°C] or 20 [°C]. Only a select number of bitumen shows even a fourth glass transition T_{g4} at either 20 [°C]; 30 [°C] or 40 [°C]. Only bit-K, bit-J, bit-V1 and bit-M, bit-N have a T_{g3} and T_{g4} and lastly bit-L only a T_{g3} . Because of the small increase at around 60 or 80 [°C], suggesting a melting peak, one can say that these transitions actually represent the crystallisation of natural wax in the bitumen (Kriz et al., 2008; Soenen et al., 2014).
- (2) Ageing has not shown to have a significant effect on the transitions in general. Only small shifts can be found where there will be a shift for example in T_{g2} from -20 [°C] towards -22 [°C]. The shift, although not always that big, shows to always be negative (meaning the onset of the transition is earlier, although broadening of the transition has been observed as well).
- (3) REOB modification has almost no effect on the transitions, as in that there are no new glass/phase transitions appearing. However shifting of the existing transitions does take place where T_{g2} , T_{g3} and T_{g4} are noticeably shifted in the blend; being heavily shifted towards a lower temperature. This can be seen in T_{g2} of bit-K set at -15 [°C] which is shifted towards -21 [°C] for bit-K+10%. Similarly the T_{g2} of bit-P at -15 [°C] and shifts towards -19 [°C]. Comparing this to the reference bitumen bit-J and bit-O, one can find that their T_{g2} already was around -23 and -22 [°C].
- (4) Ageing of REOB modified bitumen has shown a drastic difference between the T_{g2} glass transition of both blends. Where bit-K+10% has shifted from -21 [°C] towards -32 [°C]. This shift is much more drastic than for bit-P+10%, which is shifting from -18 [°C] to -19 [°C].

Chapter 5. Rheological characterization of non- and REOB modified bitumen

5.1. Introduction to rheological characterization

Now that the chemical composition/consistency of unmodified and REOB modified bitumen has been evaluated, one needs to move up a scale and look at the characteristic rheological behaviour of bitumen as well. Mere chemical characteristics will not suffice for making statements about the expected behaviour of such a binder in a mixture and in service. And before making a complete mixture, one has to first research the binder itself on its rheological properties to predict already possible limitations of the bitumen itself. These will give knowledge on the materials ability to elastically deform, showing the stiffness and viscous characteristics.

In Table 3.2 one can see a full overview of which binders have been tested with the dynamic shear rheometer (DSR) and the bending beam rheometer (BBR). Both are devices effective in showing rheological behaviour of bitumen, where the DSR gives the properties of bitumen with relative temperature boundaries within -10 and 60 [°C]. Whereas the BBR can zoom in on the relaxation and stiffness of a binder at lower temperatures, between -40 [°C] and 10 [°C]. The reason to use the DSR is to obtain a view of the full rheological behaviour at different temperatures and frequencies, to see where limitations occur of the binders. The fluxing of the REOB with the binders will be very clear to show the softening effect, but ageing of the binders should also be clearly be visible in stiffening and making the binders brittle. The BBR however is believed to show very conclusively if a binder will be too brittle or be still flexible at low temperatures, and show this also with ageing. The retrieved ΔT_c parameter is deemed to give a clear statement about the rheological aged properties of a binder.

All reference binders: like bit-K; bit-J; bit-P and bit-O, have been tested with both devices. Although only the 70/100 grades have been aged with TFOT+20hPAV, as the harder grade bitumen was expected to be too stiff to measure with the devices when it would have been aged. Bit-L, M, G and I are tested with DSR and only bit-L and bit-G are tested with the BBR.

Specifically bit-L, bit-G and bit-J have been aged for different ageing steps as well, like the used bitumen in the GPC results, see Paragraph 4.5. These bitumen have each been aged for TFOT, 20hPAV, 40hPAV and lastly even 80hPAV. This gives clear insight in what differences occur for aged bitumen for very extended periods and therefore come close to long service life experiences of these bitumen.

Lastly all the REOB modified binders have been tested with both the DSR and the BBR, to give a full picture of the changes that bitumen undergo because of changes in dosage of the used REOB-X. This is similarly also done for the aged TFOT+20hPAV REOB modified bitumen. The goal is to see what the effect of a REOB dosage does on these two different bitumen, with their fully known chemical composition, as seen in 3.3.

5.2. Viscous and elastic behaviour at various temperatures (DSR)

5.2.1. Sample preparation and tests with the Dynamic Shear rheometer

The rheological behaviour of unmodified bitumen and two bitumen series with different dosages of REOB were characterized with a dynamic shear rheometer (DSR), shown in Figure 5.1. As bituminous binders are a viscoelastic material, one can quantify these specific response properties by applying sinusoidal shear loads at different frequencies and temperatures, using the parallel plates in the machine.



Figure 5.1: (left) Modular Compact Rheometer MCR 502, Anton Paar and (right) bitumen sample ready for the excess bitumen to be cut and then be tested

For samples that were tested at and below 30 [°C], a plate geometry with 8 [mm] diameter was used. For temperatures at and above [30°C], a 25 [mm] diameter plate geometry was used. With an air temperature controlled chamber, the temperature condition of the sample was controlled. The bottom plate, on which the sample is applied, will remain static during the test. The top parallel plate will be lowered on the binder and will apply the shear strains on the sample. Samples are prepared by using a thermal scoop and retrieving small amounts of bitumen from the storage cans. The heated bitumen is then poured on a silicon mould of the respective size (8 or 25 mm). These samples are cooled at room temperature, or when really soft shortly put in the fridge for easy removal.

Following the norm EN 14770-2022 (3), the binders undergo constant strain sinusoidal loads at different frequencies, namely in the range of 0.01-400 [rad/s]. These frequency sweep tests are performed at -10 to 60 [°C], with 10 [°C] intervals. Using the time-temperature superposition principle (TTSP), one is able to construct master curves from the separate frequency sweep measurements. Nevertheless, many master curve formulas exist, so a minimum of fitting should be applied with altering the data. The data will therefore be fitted to the CAM model curve, but only the frequencies will be horizontally shifted (no vertical shifting will be applied on the datapoints). See for this more in Chapter 5.2.3.

5.2.2. Black space diagrams

The DSR data that is retrieved with the frequency sweep tests that are performed on the several mentioned bitumen in Table 3.2, can be directly plotted into a so-called black space diagram.

A black space diagram effectively shows the stiffness and the phase angle of a samples, that undergoes a certain frequency at a specific temperature. This plot is therefore able to remove the dimension of both the frequency and temperature, simplifying the behaviour of a binder and allows to look at data without applying any shift or modification to the curves.

Next to general black space diagrams, one can also retrieve specific parameters from these curves. One should obtain both the complex shear modulus and the phase shift angle when the $T_{ref} = 15^{\circ}C$ and $\omega = 0.005 [rad/s]$ and when $\omega = 10 [rad/s]$ (Airey et al., 2021). Those values can be plotted on a $G^* - \delta$ plot/black space diagram. For the samples that were aged with TFOT and PAV a shift can be observed when cracking will be more apparent. The lower frequency is used for the cracking limits and the higher frequency is used for both the rutting and thermal cracking limits. These limits are set at the following values:

$$\text{Rutting: } \frac{G^*}{\sin(\delta)} = 2.2 [kPa] \rightarrow G^* = 2,200 \cdot \sin(\delta) \text{ in } [Pa] \quad (5.1)$$

$$\text{Cracking onset: } G^* \frac{\cos^2(\delta)}{\sin(\delta)} = 180 [kPa] \rightarrow G^* = 180,000 \cdot \frac{\sin(\delta)}{\cos^2(\delta)} \text{ in } [Pa] \quad (5.2)$$

$$\text{Block cracking: } G^* \frac{\cos^2(\delta)}{\sin(\delta)} = 450 [kPa] \rightarrow G^* = 450,000 \cdot \frac{\sin(\delta)}{\cos^2(\delta)} \text{ in } [Pa] \quad (5.3)$$

$$\text{Thermal cracking: } G^* \sin(\delta) = 5000 [kPa] \rightarrow G^* = \frac{5 \cdot 10^6}{\sin(\delta)} \text{ in } [Pa] \quad (5.4)$$

Next to defining these cracking limits, other papers have researched how the ageing behaviour can be set to certain limitations (Kriz et al., 2020). Here the use of the R-value, i.e. the rheological index, is plotted in the black space diagram. The $R = 1$ shows the supposed behaviour of a perfectly unaged bitumen. A curve that stays above the $R = 2$ value shows a sample that is not aged too much and behaves still in stiff yet also flexible way. Curves that are between $R = 2$ and $R = 3$ show how too much ageing has affected the bitumen. Curves that are even lower than the $R = 3$ limit, have aged too much. In the same paper as mentioned before, a proposal is made for a specific limit to the curve that is set at $\delta = 42^{\circ}$ and a horizontal limit of $G^* = 8967 [kPa]$ is used. These try to achieve a better approximation of ageing limits and tries to include the colloidal stability of bitumen into the limitations. As was proven in the paper, a strong relation between the phase shift angle and the colloidal stability index (which is a ratio between asphaltenes, saturates, aromatics and resins) exists. This relation is represented by the boundary of $\delta = 42^{\circ}$, meaning the phase shift angle should not be lower than that.

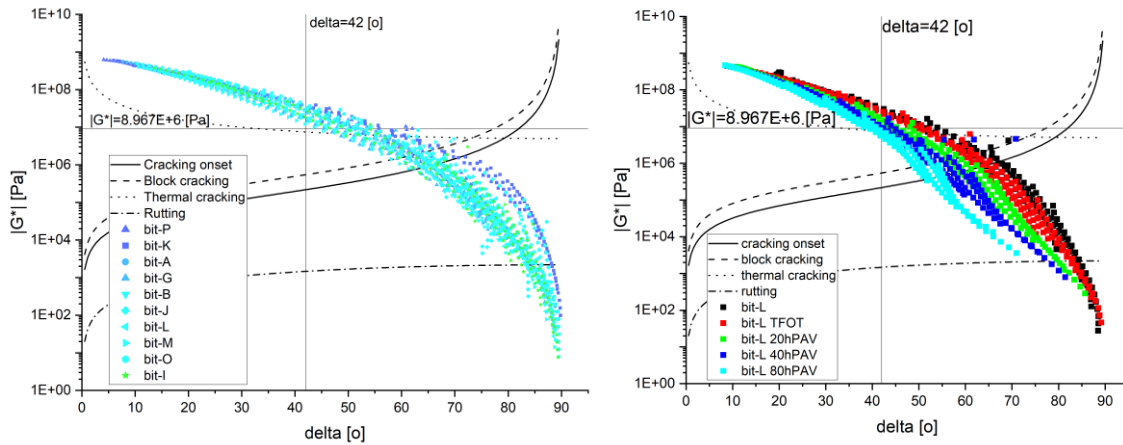


Figure 5.2: black space diagrams of (left) unaged bitumen and (right) different ageing levels of bit-L (70/100)

There is not clear distinction to be made between the different binder black space curves, regarding their PEN grades. They all overlap quite clearly around the same area, with only bit-K and bit-J as distinctively different. These have the highest curves and therefore clearly show to have the lowest R-value/ageing index. I.e. one can say the bit-K and bit-J have the best starting point ageing wise.

bit-L shows to have clear changes in its black space curve with ageing. One can say that the phase shift angle changes proportionally equal as to the complex shear modulus. Next to that one can observe that the black space curve takes on a relatively different shape. At the unaged state, it has quite a continuous curve, whereas with ageing and especially at the 80hPAV ageing one can see the curve consists out of two separate parts. The upper curve seems to range only from 0-45 [°] phase angle, where the lower curve ranges only from 45-90 [°] phase angle.

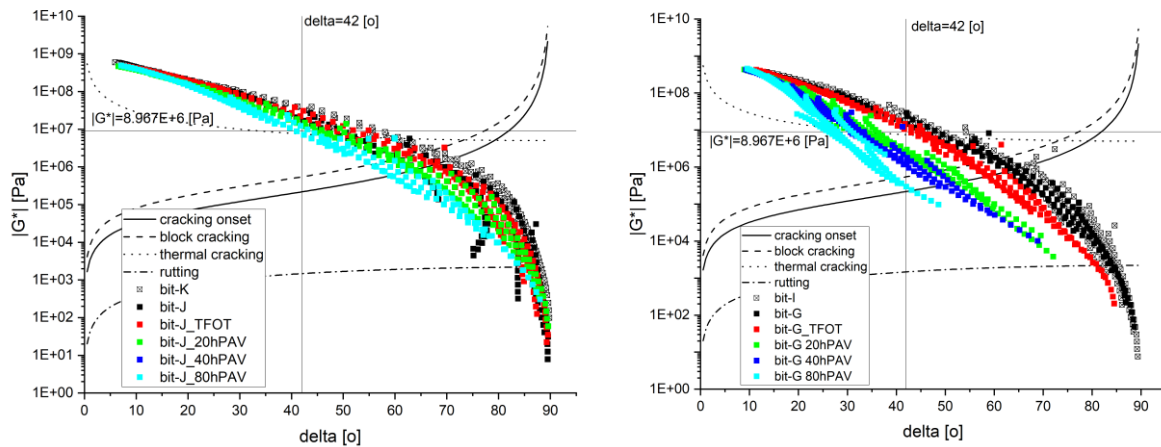


Figure 5.3: black space diagrams of (left) different ageing levels of bit-J (70/100) and (right) different ageing levels of bit-G (40/60)

Bit-J shows to age clearly differently. One can say that the stiffness is lost more proportionally than it loses its phase shift angle. This is why the curve is dropping vertically, as opposed to shift to the left (as with bit-L and bit-G). The unaged bit-J shows interestingly a very different behaviour, as opposed to its aged versions. One can see a so-called feathering-effect, which apparently is lost after ageing. The guess is that this bitumen has a small polymer like behaviour at different temperatures, showing specific phases in the material that take over its stiffness and viscous behaviour.

bit-G undergoes the most drastic changes, here one can see that it loses its phase shift angle values at very high degree and shifts significantly its curve to the left.

This therefore makes clear that bit-G has the highest ageing susceptibility, followed by bit-L and then bit-J. Nevertheless, the ageing between bit-J and the other bitumen is drastically different, as bit-J does not seem to lose that much viscous property as the other bitumen, it seems to mainly increase in stiffness.

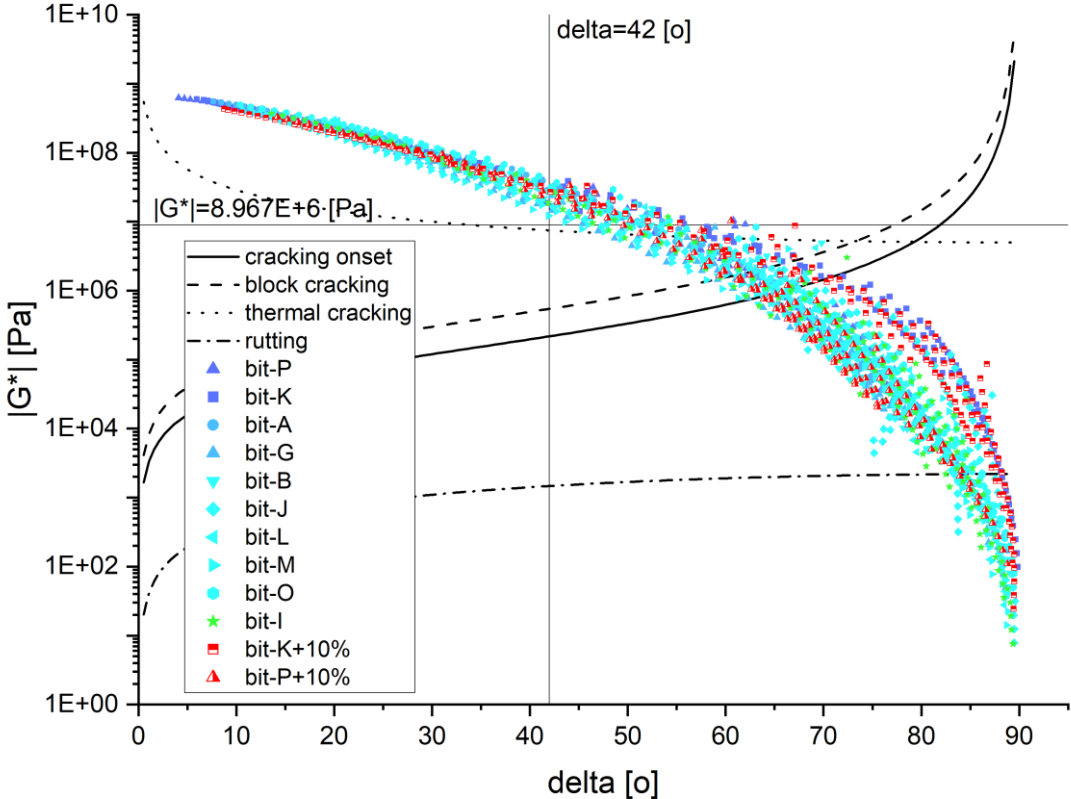


Figure 5.4: black space diagram of all unaged bitumen and both 10% REOB modified bitumen

In the figure above, one can observe the black space curves of the REOB blends compared to the other unmodified bitumen. There is no drastic difference in behaviour to observe from this, however one can easily see that bit-K+10% overlaps the black space curve of the initial unmodified bit-K itself. This is the same for bit-P+10%.

This therefore indicates that regarding ageing, the bitumen is not “rheologically aged” when REOB is added to it. **The bitumen is softened and one can expect a REOB modified bitumen to take the same black space diagram shape, as the base bitumen used in the blending.**

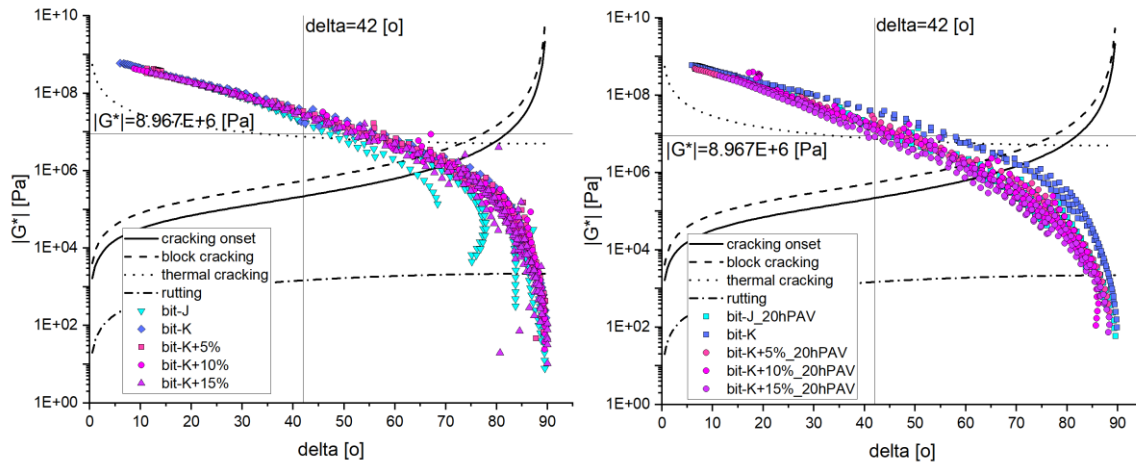


Figure 5.5: black space diagrams of (left) bit-J and bit-K blends and (right) bit-O and bit-P blends

One can see that the bit-K blends exactly overlap the unmodified bit-K black space curve, the same goes for bit-P blends overlapping the bit-P blends. The dosage does not matter and therefore it is clear that the REOB changes the time-temperature relation that the blend owns and not what its visco-elastic properties are. Based purely on rheology, the REOB does not age the bitumen in any way. The black space diagram of the used base bitumen is completely overlapped by the blends, regardless of the dosage used. Nonetheless, that does not say anything about an increased tendency to age, which will be evaluated later.

The feathering behaviour that was observed with bit-J (70/100) is not visible with the bit-K blends, further suggesting that the composition is clearly different. One can clearly see that the bit-O curve lies above the bit-P unmodified and blend black space curves. This shows it behaves as a less aged bitumen, than the bit-P or bit-P blends.

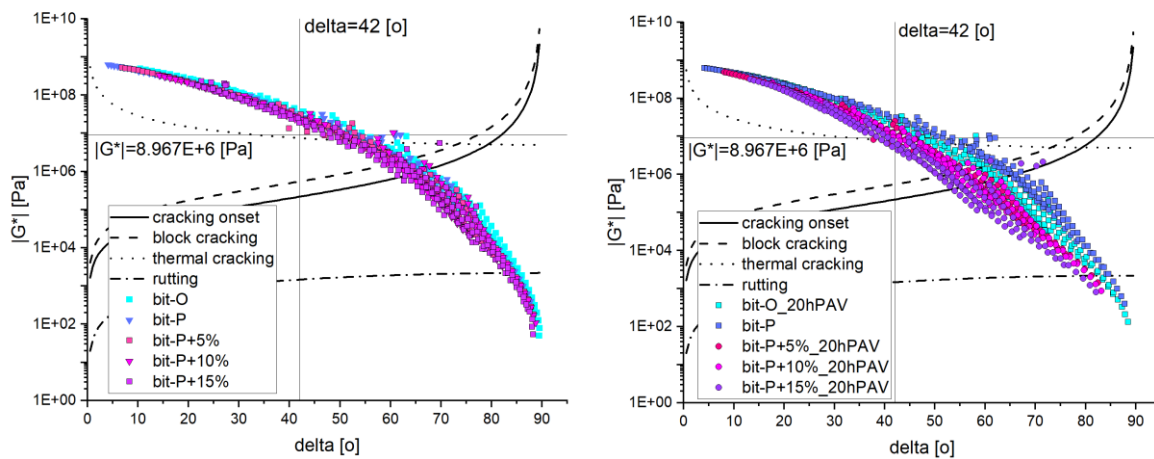


Figure 5.6: black space diagrams of (left) 20hPAV aged bit-J and bit-K blends and (right) 20hPAV aged bit-O and bit-P blends

The 20hPAV ageing makes the black space diagram change in different ways for both binders.

The bit-K blends seem to all keep overlapping, with only minimally the bit-K+15% at the bottom and bit-K+5% at the top (showing, though marginally small, that the more REOB the more the material ages). In the case of the bit-P blends however, the bit-P+15% has a distinctively more changed curve in the aged 20hPAV state as compared to the bit-P+5%, further proving that REOB changes the rheological behaviour more drastically at higher dosage.

Using the same REOB, one can clearly observe that the black space diagrams are different between both base bitumen (bit-K or bit-P), but one can also directly relate this to the ageing of the base bitumen itself. One can in fact see that the bit-K+10%_20hPAV and the bit-J_20hPAV directly overlap, showing that the black space diagram will take a shape that will always correlate to the base bitumen used. This is also observable for the bit-P blends, however one can see that the bit-O has aged less than the bit-P+5;10 and 15% blends.

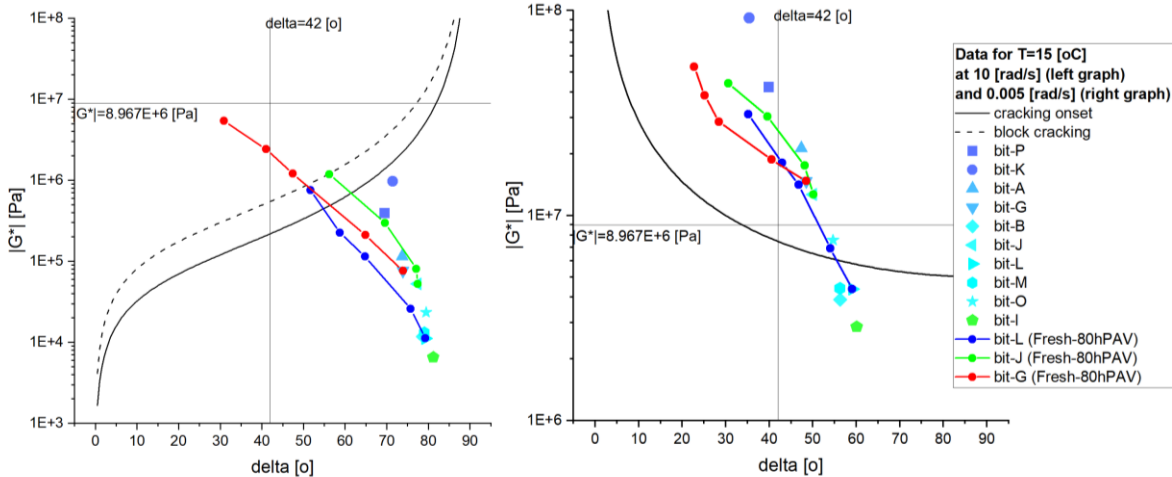


Figure 5.7: Glover-Rowe parameters plotted on black space diagram for unaged and aged bitumen for (left) cracking onset and block cracking and (right) risk to thermal cracking

The Glover-Rowe parameter plotted on the black space diagram shows the different starting points of the unaged bitumen and then their changes with ageing. In the case of block cracking, it is clear that the PEN grade does not have an influence anywhere on where the starting position will be of these points. The slope of the ageing behaviour seems to be quite similar for all three binders, although the ageing distance is different. When looking at the thermal cracking susceptibility, the PEN grade gives a good rough estimation where the binders would end up (bit-K lying very high and bit-I very low), but there is clearly a lot of variance between the 70/100 PEN grade bitumen.

Regarding block cracking, one can see that bit-J again outperforms both bit-L and bit-G. bit-J has the shortest distance with ageing and as its points lie higher than the others, it also has a higher phase shift angle at similar stiffnesses. Nonetheless, both bit-J and bit-L end up at the cracking border when they are 80hPAV aged, but bit-G has already passed this border when it was 40hPAV aged.

Looking at the thermal cracking limit, a different behaviour between the three binders can be found. In this case bit-L has the best performance, starting below the limit that is set, but with TFOT ageing all three aged binders can be seen as very susceptible to thermal cracking. This shows that all binders are too stiff at lower temperatures, allowing them to be so susceptible to thermal cracking.

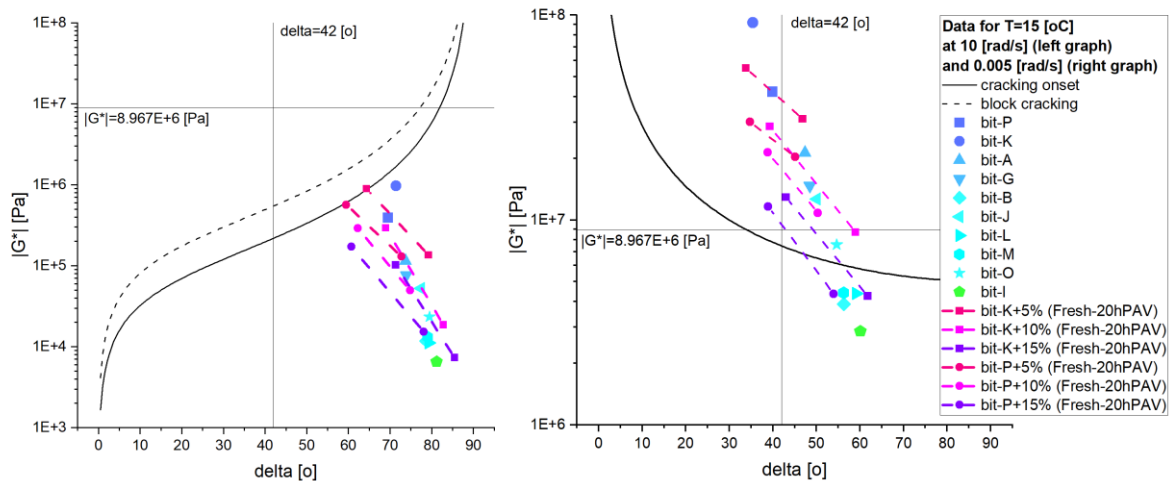


Figure 5.8: Glover-Rowe parameters plotted on black space diagram for unaged and (aged) REOB modified bitumen for (left) cracking onset and block cracking and (right) risk to thermal cracking

In the figure above, the effect of REOB on the bitumen regarding its susceptibility to cracking is shown. Both the unaged and the aged 5; 10 and 15% REOB blends are shown as compared to the unmodified bitumen.

For the cracking onset and block cracking, one can observe that both bit-K+5% and bit-P+5% will instantly reach the cracking onset after only 20hPAV ageing. Their unaged G-R parameter positions also lie close to bit-A and bit-G, corresponding to (30/50) and (40/60) grades bitumen. The bit-K+15% and bit-P+15% lie however significantly lower, more close to bit-M, bit-O and bit-I. This is in fact a good sign, as the binder shows to be very soft and far away from the cracking limit, where it not that the 20hPAV ageing changes significantly more for the 15% blends as opposed to the previous 5% blends. Here the severity of the ageing susceptibility to be increased by REOB dosage, is made very clear.

Regarding the thermal cracking limit, only the 15% blends seem to initially be low enough. But all bitumen have passed the limit after 20hPAV ageing. Also here the difference between using 5% and 15% shows to have increased the ageing susceptibility effectively. Although interestingly bit-K+10% specifically seems to have a similar change with ageing as the bit-K+15%, possibly this has to do with estimation inaccuracies of the datapoints.

5.2.3. Master curves of $|G^*|$ and δ

To review the changes in stiffness and the phase shift angle separately, one has need of using the time-temperatures superposition principle (TTSP). This principle explains the fact that frequency and temperature have a correlation between each other, allowing one to shift data according to this principle. This means that otherwise not reachable frequencies (very high and very low), will be able to be correlated to (very low testing temperatures and very high respectively). Using a single reference temperature, in this thesis set at the most common temperature measured for the asphalt in the Netherlands 20 [°C], all other data is shifted to fit a single curve for this temperature.

To be able to shift the data, one needs to assume a shape that the curve will take. One of the most recent developed and proven to be effective models, is the Christensen-Anderson-Marasteanu (CAM) model (Bayane et al., 2017; Chen et al., 2022; Christensen et al., 2017). The CAM model is used for the master curve of the complex shear modulus $|G^*|$ in the following way:

$$|G^*| = G_g \cdot \left[1 + \left(\frac{\omega_c}{\omega} \right)^v \right]^{-\frac{w}{v}} \quad (5.5)$$

Where the rheological index R is included as:

$$v = \log \left(\frac{2}{R} \right) \quad (5.6)$$

Where the phase shift angle δ has a corresponding curve following this formula:

$$\delta = \frac{90 \cdot w}{\left[1 + \left(\frac{\omega_c}{\omega} \right)^v \right]} \quad (5.7)$$

To effectively shift the test data from different temperatures, the most common practice is to use the William-Landel-Ferry (WLF) shift formula. Although a variant on this formula, the so-called Kaelble equation, has proven to be also quite favourable with fitting methods (Morian et al., 2015). This last formula is formulated in the following way:

$$\log(a_T) = \frac{-C_1(T - T_d)}{C_2 + |T - T_d|} - \frac{-C_1(T_{ref} - T_d)}{C_2 + (T_{ref} - T_d)} \quad (5.8)$$

Where both C_1 and C_2 are regression parameters, T is the measured temperature, T_{ref} is the reference temperature and therefore for most plots 20 [°C] and lastly T_d is a shift parameter to allow the curve to shift to a slightly different temperature for a better curve (this will reduce inaccuracy of the measurements at all temperatures together). The frequency measured at a specific temperature is shifted in the following way:

$$\log(f_{shifted}) = \log(f_{measured}) + \log(a_T) \quad (5.9)$$

Now that all these formulas are given, the most important factor in determining if the shifted curve is not altering the vertical data too much, is by calculating the accuracy. This is done by calculating the sum of the squared errors (SSE) and the root mean squared error (RMSE):

$$SSE = \sum \frac{(|y_{measured}| - |y_{predicted}|)^2}{|y_{measured}|^2} \quad \& \quad RMSE = \sqrt{\frac{SSE}{n}} \quad (5.10)$$

By minimising the RMSE, trying to approach a value of 1.0 (meaning perfect fitting), the master curves can be obtained.

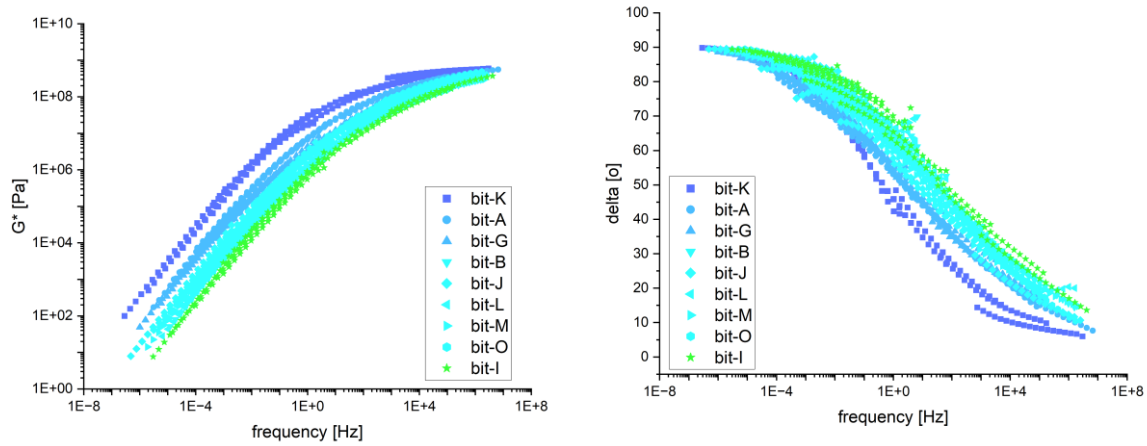


Figure 5.9: Master curve of the (left) complex shear modulus and (right) the phase shift angle of unaged bitumen

The first master curves are given for the unaged bitumen in the figure above. The PEN grades of these bitumen correspond very well to expected stiffnesses. Harder grades clearly lead to higher measured complex shear moduli, bit-K and bit-P clearly are stiffer than the 70/100 grade bitumen and bit-I clearly has the lowest shear stiffness. The phase shift angle curves show much more overlap however and harder grades are close to curves of 70/100 grades; although bit-K specifically lies significantly lower. Bit-I, which is a 160/220 grade, shows to be significantly more viscous than then other bitumen. The PEN grade shows to be much less reliable to show viscous properties.

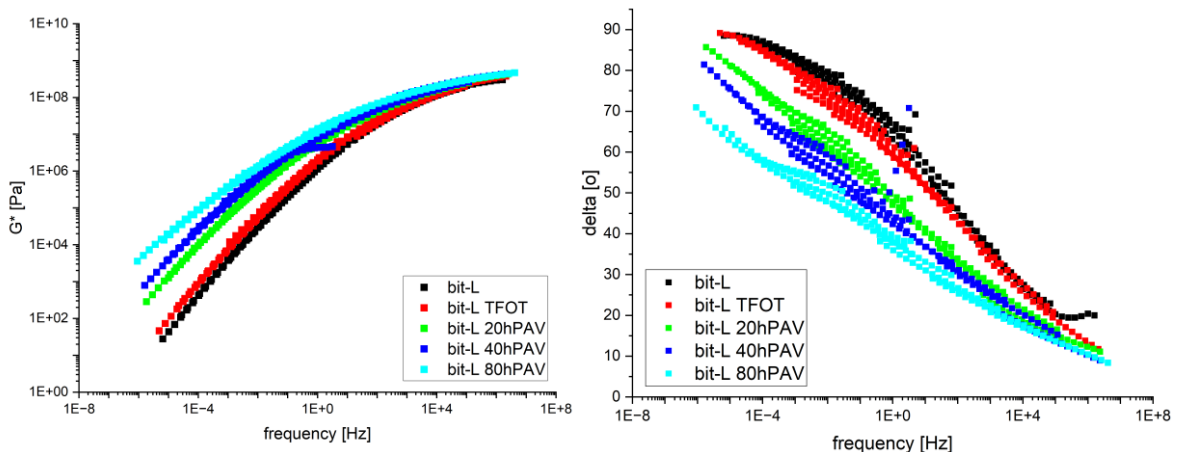


Figure 5.10: Master curves of the ageing levels of bit-L (70/100) of (left) the complex shear modulus and (right) phase shift angle

In Figure 5.10 one can observe the changes in both stiffness and phase shift angle for the bit-L (70/100) with ageing. One can see the stiffness curves have significantly increased stiffness at the lower frequencies, whereas the phase shift angle seems to have dropped a lot overall the frequencies. One can observe that a more horizontal curve is approached for the stiffness curve and the phase shift angle curve seems to lower its curve vertically.

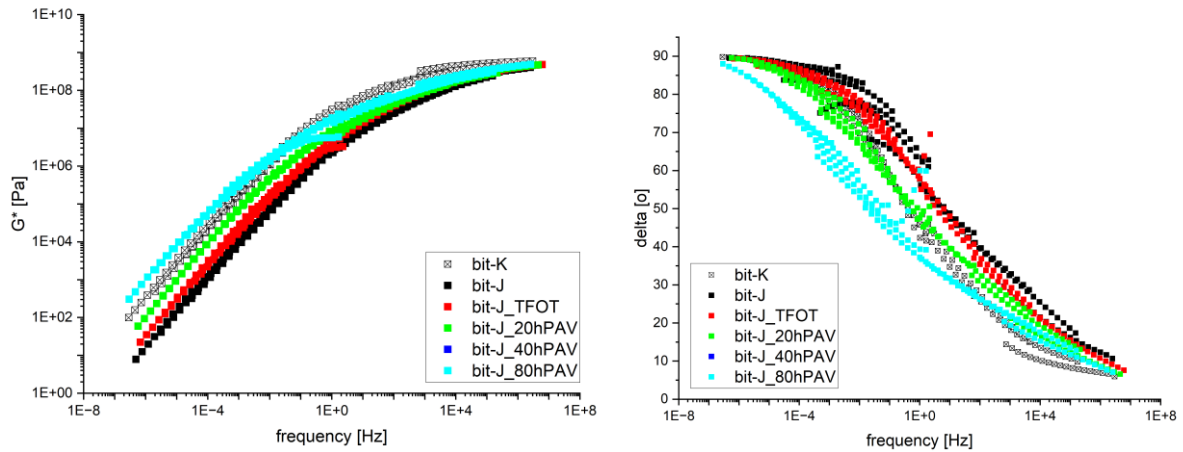


Figure 5.11: Master curves of the ageing levels of bit-J (70/100) of (left) the complex shear modulus and (right) phase shift angle

Opposed to the ageing behaviour of bit-L, bit-J shows to change its curves less drastically. One can see that the stiffness curve also tends to go towards a flatter curve and increases vertically (although at way smaller increments with ageing). The phase shift angle curves show something drastically different. Instead of having a vertical drop in this viscous property, it is clear that the bitumen only undergoes a horizontal shift. This shows that there is a fundamental difference in the loss of viscous property between this and the other binders.

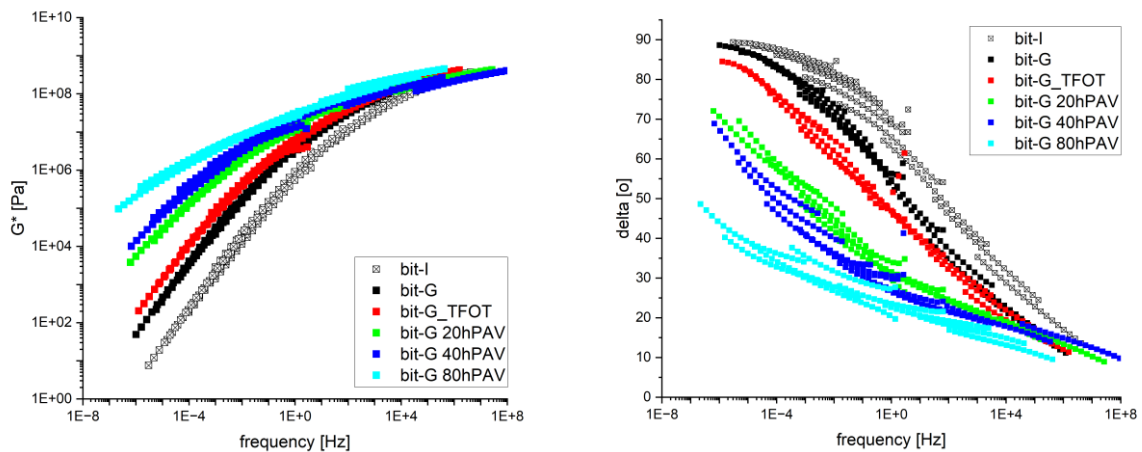


Figure 5.12: Master curves of the ageing levels of bit-G (40/60) of (left) the complex shear modulus and (right) phase shift angle

Comparing the bit-G results to the two other aged bitumens, one can see drastic differences. Changes in the slope/shape of the curves, comparing bit-G and bit-L, are very similar though. However the big difference is that the increment of these changes much higher for bit-G than bit-L. One can see that this binder undergoes heavy changes with ageing and therefore is clearly the most susceptible to it. The phase shift angle undergoes so much changes, that the 80hPAV variant almost reaches a flat curve, meaning it has almost completely lost its viscous property.

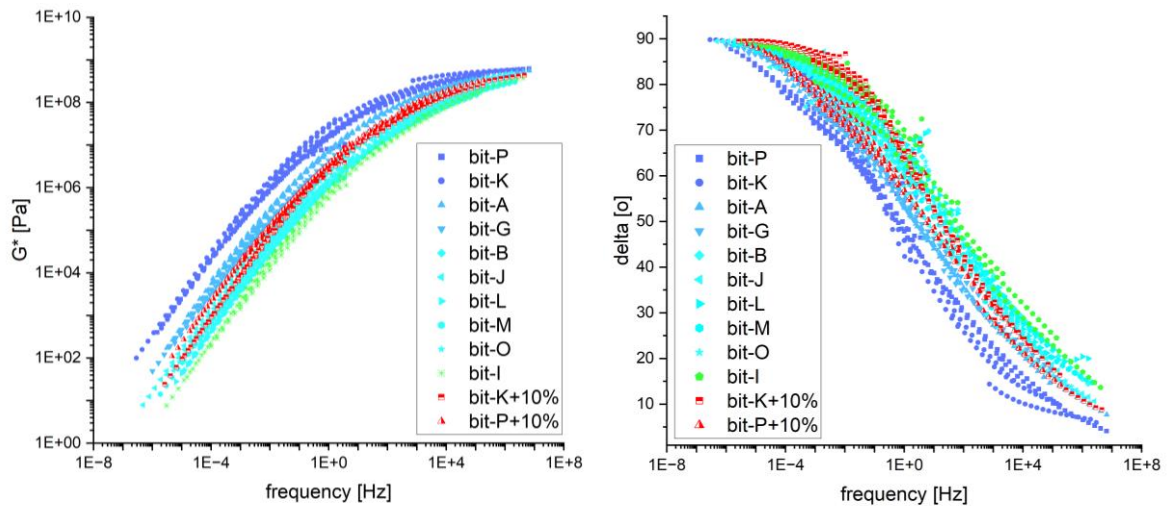


Figure 5.13: Master curves of the ageing levels of unmodified bitumen and REOB modified bitumen of (left) the complex shear modulus and (right) phase shift angle

Regarding the REOB modified bitumen, the bit-K+10% and bit-P+10% both have stiffnesses that align pretty well with all the other 70/100 grades bitumen. Bit-P+10% ends up a bit closer to the (40/60) grades though and bit-K+10% is actually closer to the (160/220) grade. The phase shift angle of bit-K+10% shows to have the highest viscous response at the low frequencies, but a relatively low angle at the higher frequencies. One can see that the curve of bit-K has not changed in shape and shifted to the right to create a softer binder this way. BitP+10% has a lower phase shift angle overall, which aligns as well with the shape of bit-P, but having its curve simply shifted to the right.

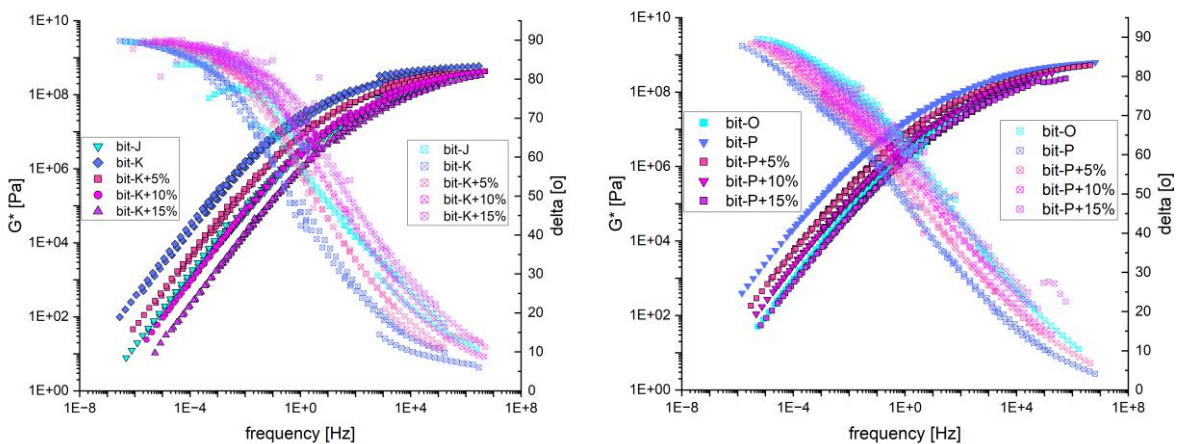


Figure 5.14: Master curves of the complex shear modulus and phase shift angle of (left) bit-J and bit-K blends and (right) bit-O and bit-P blends

Above are the master curves plotted for the reference bitumen and the REOB modified bitumen. The softening effect seems quite effective for both used binders, although softening changes the most for bit-K; both in stiffness as well as with phase shift angles. This was already visible with the different PEN grades that were measured for the REOB modified bitumen, as bit-K blends tended to reach higher PEN values with lower dosages than bit-P. The change in overall stiffness seems to be linearly correlated with dosage level for both bit-K and bit-P base bitumen.

It was expected that in both cases 10wt% REOB added would change the bitumen to a performance of a 70/100 grade bitumen. In fact ~9% seems to be enough to make a (70/100) grade out of the bit-K (20/30) and ~12% in the case of using bit-P (15) purely looking at the complex shear stiffness curve.

On the contrary, looking at the phase shift angle values, one needs to use ~6% to reach the same properties at low frequencies/high temperatures but ~12% at the high frequency/low temperature tail of the curve in the case of base bitumen bit-K. In the case of bit-P, one needs >15% to reach the same properties at the low frequencies and around 15% at the high frequency tail.

It is clear to see that both the stiffness and the phase shift angle curves are shifted to the right, creating lower stiffness/higher phase shift angle at previously the same temperature/frequency tested. This correlates well with the observation that the black space diagram has overlapped exactly, as in that case the time-temperature correlation seems to have changed only.

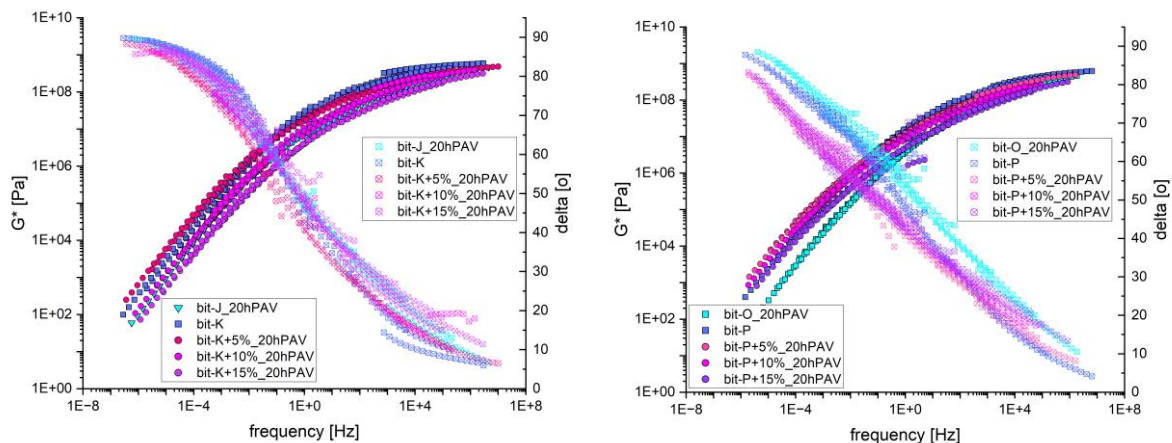


Figure 5.15: Master curves of the complex shear modulus and phase shift angle of (left) bit-J and bit-K blends and (right) bit-O and bit-P blends

N.B. the graphs do not show an aged version of bit-K and bit-P, as these were deemed unreasonably hard and stiff at 20hPAV ageing to be able to be tested in the DSR

Ageing has caused the stiffness to rise of the blends. Looking at bit-K, one can say that the most changes occurred to bit-K+15%, but parameters taken from the curves will show this more clearly. Compared to bit-P blends one can see that the REOB blends lie quite close to each other, although before there was more difference present between them. This indicates that bit-P+15% has changed relatively more than bit-P+5%. The phase shift angle seems to have changed with the same increment/step size as what happened to the curves of the stiffness. Interestingly, the bit-P binders have lost the most phase shift angle at the low frequencies/high temperatures.

One can easily observe that the REOB does not alter the rheological behaviour with ageing, it merely increases the ageing distance. What one could say, is that the components that are added by the REOB to soften the base binder, or their effect, are simply lost with ageing. This would therefore mean that a bit-P_20hPAV will overlap well with bit-P+5; 10 or 15%_20hPAV blends. **This will therefore always mean that the more REOB added, the bigger the distance of change will be with ageing.**

5.2.4. Cole-Cole & complex viscosity diagrams

Instead of evaluating the complete master curve and losing overview, one can also zoom in into the behaviour of the binders at specifically the low and high temperatures. The relationship between changing loss/storage shear modulus but also the loss/storage viscosity can show aging behaviour very clearly. These make it possible to see both how stiff a binder acts, but also what its viscous property is. Evaluating the changes in these parameters has been applied in several papers (Kaya et al., 2019; Porot, 2019), which have shown similar observations as are found here.

These loss shear modulus G'' and loss viscosity η'' can be calculated with the use of the complex shear modulus G^* , angular frequency ω and the phase shift angle δ :

$$|\eta^*| = \sqrt{(\eta')^2 + (\eta'')^2} \quad \eta' = \frac{G''}{\omega} \quad \eta'' = \frac{G'}{\omega} \quad (5.11)$$

$$|G^*| = \sqrt{(G')^2 + (G'')^2} \quad \frac{G''}{G'} = \tan(\delta) \quad (5.12)$$

These basis forming formulas lead to the following:

$$\frac{G''}{G'} = \frac{\sqrt{G^{*2} - G'^2}}{G'} = \tan(\delta) \quad G^{*2} - G'^2 = G'^2 \tan^2(\delta) \quad (1 + \tan^2(\delta))G'^2 = G^{*2}$$

$$G' = \sqrt{\frac{G^{*2}}{1 + \tan^2(\delta)}} \quad (5.13)$$

$$\frac{G''}{\sqrt{G^{*2} - G''^2}} = \tan(\delta) \quad G''^2 = \tan^2(\delta) * (G^{*2} - G''^2) \quad \left(1 + \frac{1}{\tan^2(\delta)}\right) G''^2 = G^{*2}$$

$$G'' = \sqrt{\frac{G^{*2}}{\left(1 + \frac{1}{\tan^2(\delta)}\right)}} \quad (5.14)$$

With these parameters all obtained, the Cole-Cole diagrams and dynamic loss viscosity diagrams can be plotted. The Cole-Cole diagrams will zoom into the low temperature/high frequency behaviour of binders. Therefore these will effectively show relaxation properties of the binders and the tendency to change in viscoelastic behaviour when coming close to a bitumen its glass transition temperature (Porot, 2019). The dynamic loss viscosity evaluates the high temperature/low frequency behaviour of a binder. Here one can see how stiff the binder will be still at high temperatures and this correlates well to conditions at which mixing of the binder happens. Both these type of diagrams will therefore give insights in these limits of the bitumen.

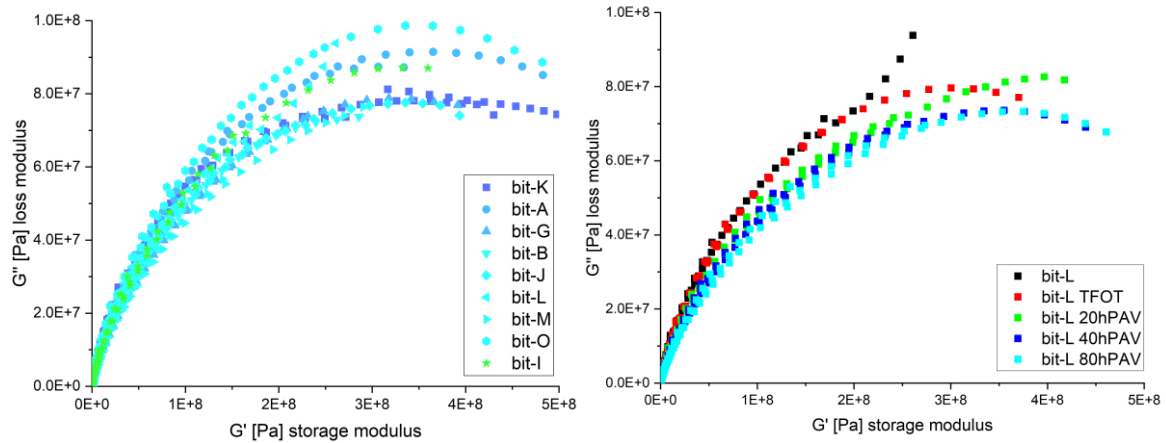


Figure 5.16: Cole-Cole diagrams; plotting the loss and storage moduli for (left) unaged bitumen and (right) aged variants of bit-L (70/100)

The fresh bitumen all show distinctively different behaviour at the low temperatures/high frequencies, which is not correlated to their different PEN grades. Bit-O, bit-A and bit-I all show to have the most favourable performance, as they have the highest loss modulus over storage modulus, indicating that they retain their viscous characteristic for longer at these extreme values. Specifically bit-K, bit-J, bit-B and bit-M show to have all quite low curves and therefore do not reach high loss modulus values. This indicates that these binders are more inclined to have an elastic response than a viscous-elastic response at low temperatures.

bit-L seems to follow the same trend, but looking at the top right graph, one can see that the measurements deviate from the assumed parabolic/ellipsoidal shape and therefore one can assume that these datapoints are actually inaccurately measured and deviate from the rest of the trend. Ageing generally tends to lower the loss modulus a little and increase the storage modulus more heavily (representing the stiffening and loss in viscous property of an aged bitumen).

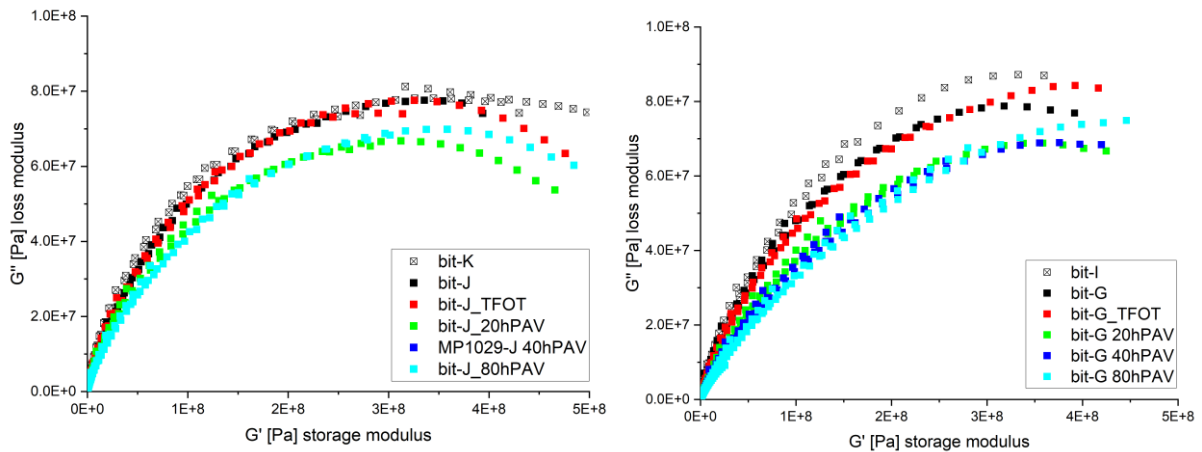


Figure 5.17: Cole-Cole diagrams; plotting the loss and storage moduli for (left) aged variants of bit-J (70/100) and (right) aged variants of bit-G (40/60)

All three aged binders show different ageing mechanisms at these low temperatures/high frequencies. bit-J clearly shows it has the lowest loss modulus values and also reaches its maximum the earliest out of the three. Ageing makes this actually worse for this binder. bit-L and bit-G both show to have a better performance and with ageing their change in maximum loss modulus seems to be relatively small.

Interesting to see, is the fact that bit-J reaches its maximum at the lowest storage modulus and with ageing this also worsens. But comparing this to bit-L and bit-G one can see that they actually reach their maximum loss modulus at higher storage moduli.

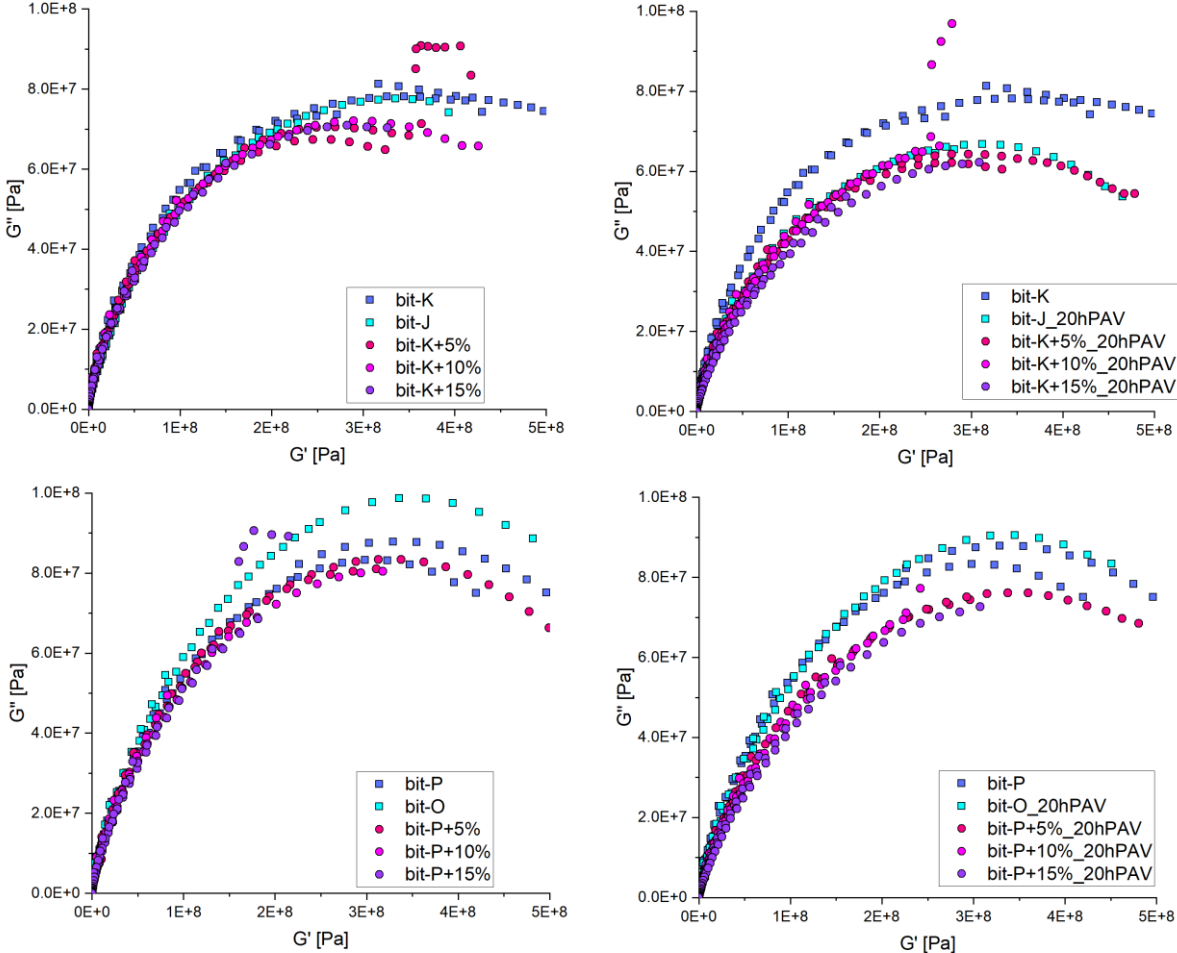


Figure 5.18: Cole-Cole diagrams; plotting the loss and storage moduli for (top-left) bit-J and bit-K blends, (top-right) aged versions, (bottom-left) bit-O and bit-P blends and (bottom-right) its aged versions

Bit-K and bit-J reach quite high storage moduli values but their loss modulus does not reach a high loss modulus as compared to their bit-P and bit-O counterparts. The REOB blends all show to create a decrease in loss modulus and therefore relaxation at low temperatures. Ageing causes bit-J to drop its curve significantly, performing similar to the aged blends of bit-K+5; 10 & 15%. This is not the case for bit-O, which slightly outperforms even the unaged bit-P at its 20hPAV aged version. Comparing the bit-K blends with bit-P, they seem to have a similar behaviour with their unmodified base binder at unaged stage. Increasing the REOB dosage will not increase the loss modulus. At ageing, both series seem to have a similar rate of change.

To effectively show this decline in viscoelastic property at low temperatures, the measured loss and storage moduli are noted for both 1 [rad/s] and 1 [Hz] measurements.

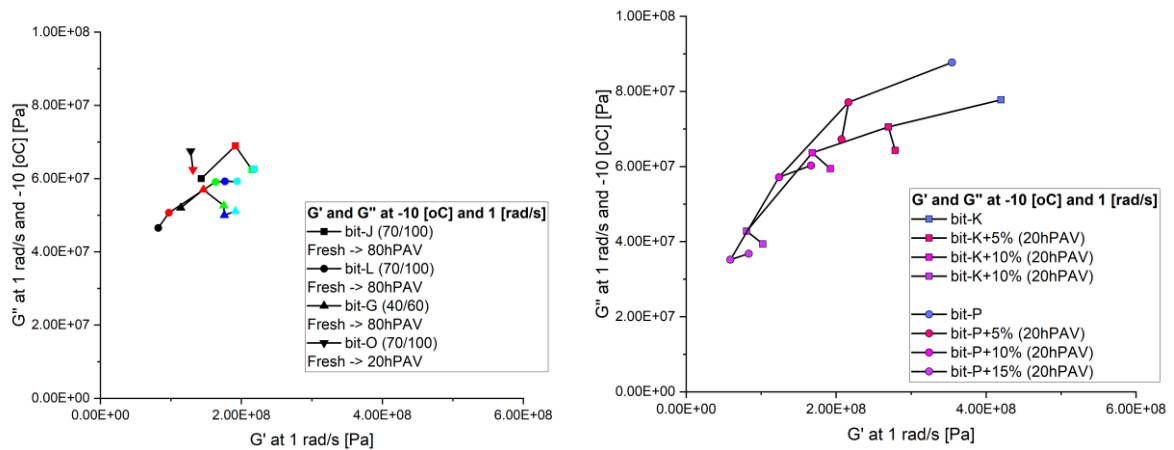


Figure 5.19: Loss and storage moduli values at -10 [°C] and 1 [rad/s] for both (left) the unmodified bitumen with ageing and the (right) blending of bit-K and bit-P with REOB and their ageing

At low temperatures (-10 [°C]) but also a low frequency (1 [rad/s]) one can observe that most data points lie very close to each other for the unmodified bitumen. With ageing one can observe a small shift towards lower loss moduli values with PAV ageing but higher loss moduli values with TFOT ageing. The storage modulus will increase for all of the binders, and as expected it lies lower for the higher PEN grade bitumen and lies higher for the higher PEN grade binders.

Modification with REOB effectively lowers the datapoints significantly. Incrementally one can clearly expect what the loss and storage moduli will be with a modification of either 5; 10 or 15%. Ageing of the blends does do something that is expected, as one can observe a lowering of the loss modulus and an increase in storage modulus. One can though observe that the decrease in loss modulus is higher for the 5% than the 15% blend, but the increase in storage modulus is higher for the 15% than the 5% blends.

This should be compared to a more extreme situation, namely one with a higher frequency. This results in the behaviour as observed in the figure below:

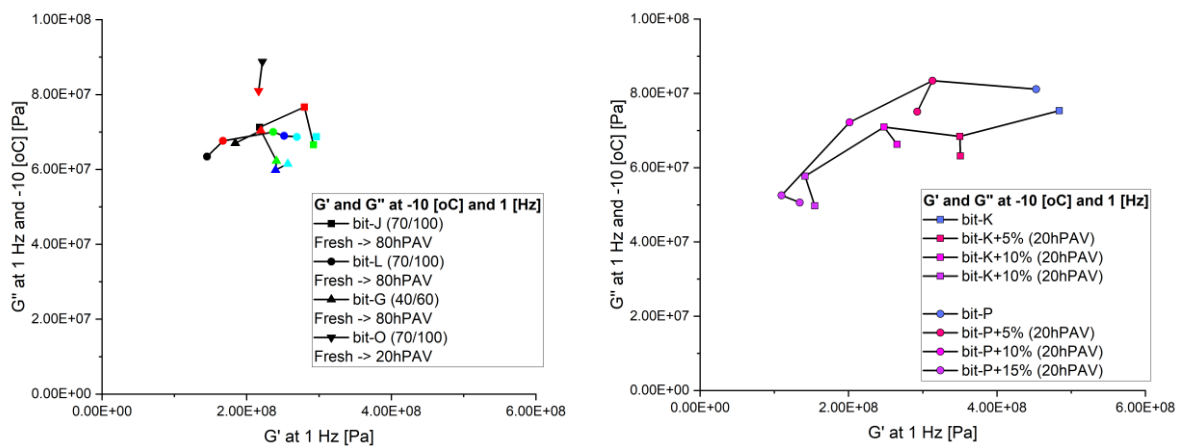


Figure 5.20: Loss and storage moduli values at -10 [°C] and 1 [Hz] for both (left) the unmodified bitumen with ageing and the (right) blending of bit-K and bit-P with REOB and their ageing

Here it becomes very clear that bit-O outperforms all other bitumen. The decrease in loss modulus is significant, but its starting position is so much higher that this does not matter, as it will still remain higher than all other bitumen. Again TFOT ageing shows no decrease in low temperature loss of viscous property, although a significant increase in storage modulus.

Adding to this, one can also observe that now the loss modulus decreases much more severely for all REOB blended bitumen, than it did with the lower frequency. Here one can see the limitation of the use of REOB clearly. The REOB will not improve any low temperature relaxation properties of the bitumen, it will merely decrease viscosity. One can observe that a worse capability will be obtained at very low temperatures or very high frequencies for REOB blended bitumen. If bit-P or bit-K would have had a much higher loss modulus, the buffer for this change in property with REOB modification would have been better. Purely based on a choice to be made between bit-P and bit-K, one can see that the viscous property of bit-P is significantly better and therefore one should prefer to use bit-P over bit-K in the case of low temperature susceptibility.

These observations come close to what was found before, where there was a good correlation found with the behaviour of bitumen below its glass transition temperature and the measurements performed there (D. Wang et al., 2020). Further suggesting that the behaviour of bitumen will become critically different at lower temperatures once coming close to or even passing a glass transition temperature of that bitumen. This suggests that REOB will have a significant impact on phase/glass transitions, especially resulting in changes in behaviour at low temperatures.

The low temperature behaviour was now evaluated with Cole-Cole diagrams, but the high temperature region is affected by REOB modification as well. This will be handled by plotting and evaluating the dynamic loss modulus of these bitumen, presented in the following diagrams.

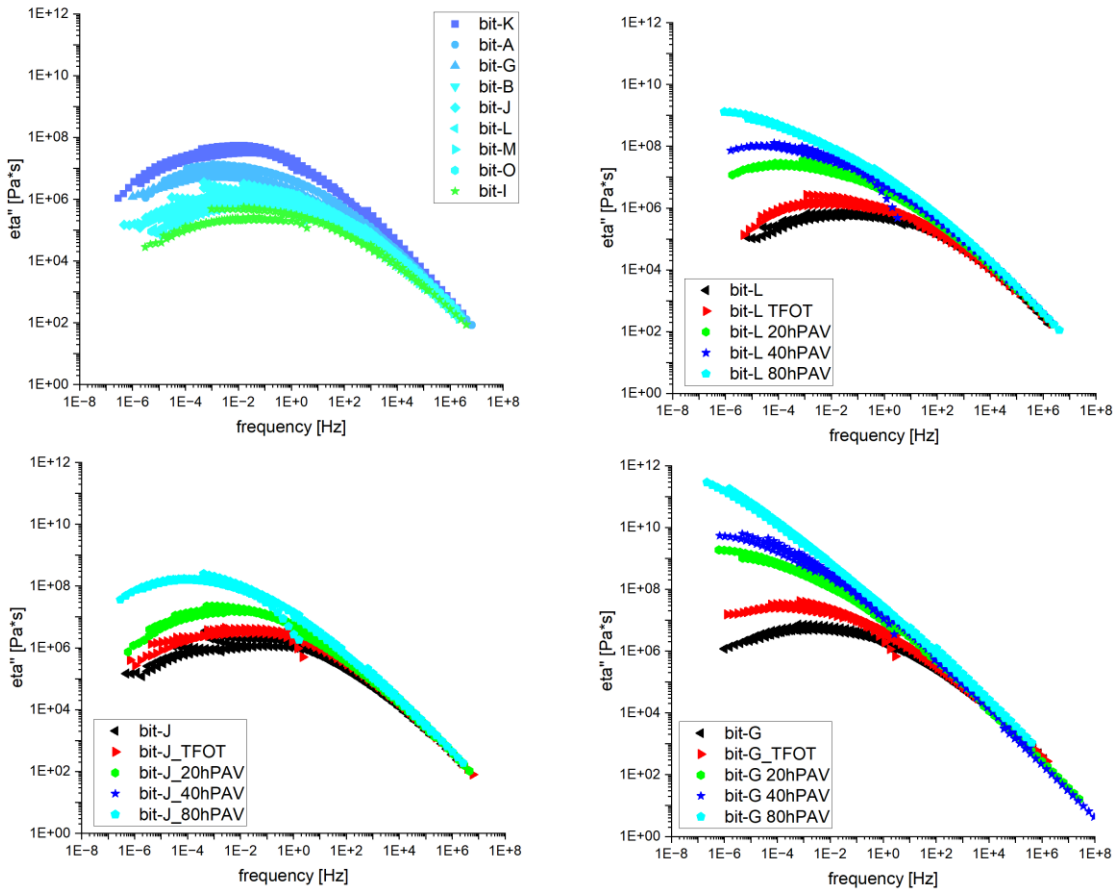


Figure 5.21: Dynamic loss viscosity diagrams; plotting the loss and storage moduli for (top-left) unaged bitumen, (top-right) aged variants of bit-L, (bottom-left) aged variants of bit-J and (bottom-right) aged variants of bit-G

The presented curves are approximated curves, being both horizontally and vertically shifted to allow for a complete master curve of the dynamic loss viscosity over frequency. Clearly all the fresh binders have dynamic loss viscosity levels that correspond to their PEN grades, higher viscosities hold true for the stiff binder such as bit-K and lower ones for the bit-I, with the 70/100 in between.

Dynamic loss viscosities, or in general dynamic viscosities, are more often used for polymers. Where one can see distinctive different behaviour when one changes the molecular weight distribution of the polymers. Higher molecular weights generally have a higher dynamic viscosity, whereas lower molecular weights (or more dispersed) will tend to have lower viscosities and thus lower curves. This corresponds to the ageing behaviour of bitumen, as it will gain in higher molecular weights with ageing and thus its viscosity should increase too.

Ageing causes for different behaviours to occur for all three binders tested. bit-J remains to have a curvature at the high temperature/low frequency tail, whereas both bit-L and bit-G lose these with ageing. The absolute changes that the curves undergo, are significantly the highest for bit-G. bit-L seems to change mediocre and bit-J seems to change again the least.

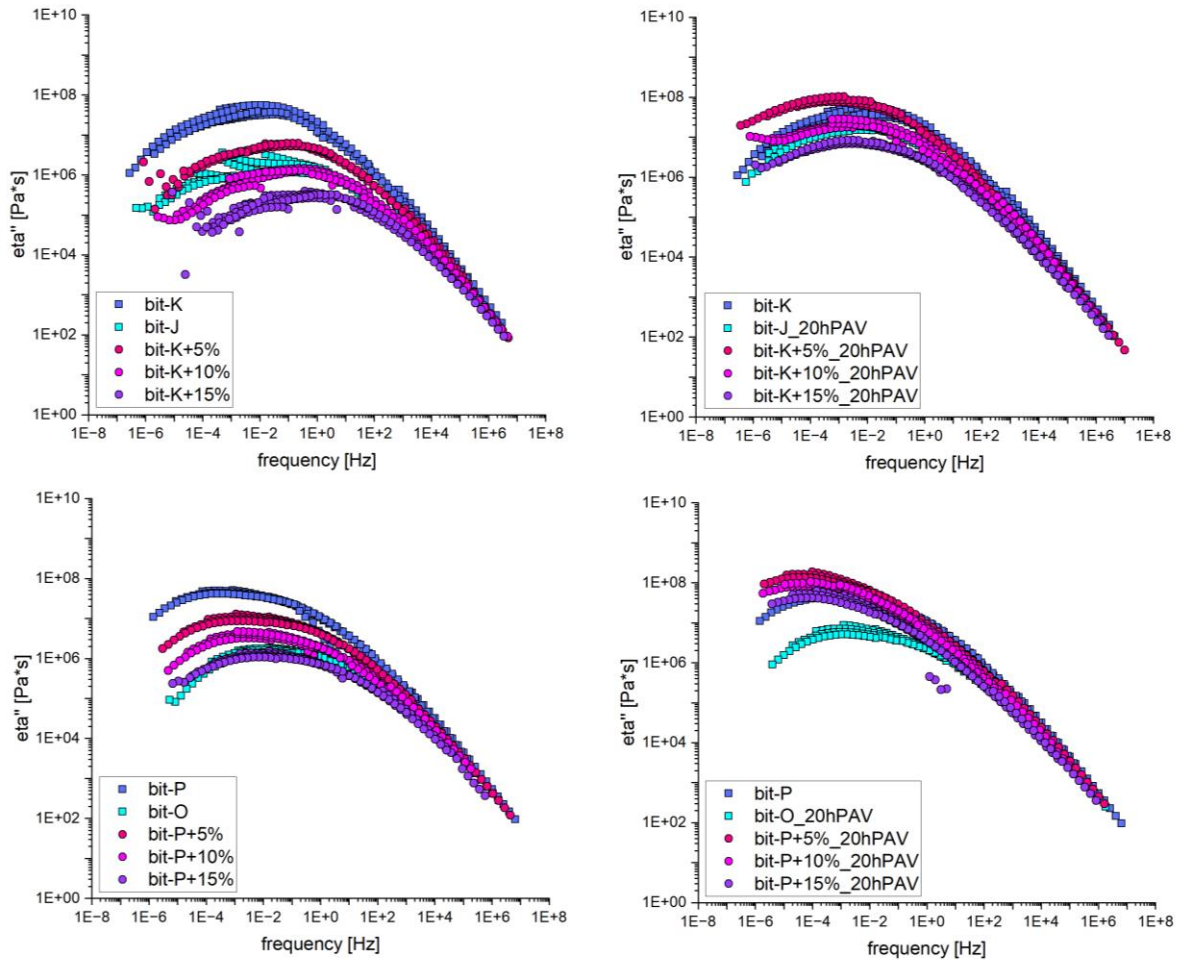


Figure 5.22: Dynamic loss viscosity diagrams; plotting the loss and storage moduli for (top-left) bit-J and bit-K blends, (top-right) aged versions, (bottom-left) bit-O and bit-P blends and (bottom-right) its aged versions

The feathering effect observed before, for bit-J, can be seen very clearly in this dynamic loss viscosity curve at the lower frequency range. Again one can see that this is not something present for the bit-K and its blends, or any other bitumen evaluated here.

The softening effect of the REOB is clear for both bitumen series and the rate of change seems to be a bit higher for bit-K than for bit-P. One can see that between 5-10% REOB added to bit-K gives a similar behaviour as bit-J. The 15% REOB added to bit-P shows a similar behaviour as bit-O. Ageing is a different story. Bit-K blends seem to age with similar increments between added percentages, leading to 5% being the stiffest of the three. Bit-K+10% at 20hPAV ageing shows a similar behaviour as the bit-K unaged. Comparing this with the bit-P blends, one can see that all three dosages end up with curve very close to each other. The bit-P+15% curve at 20hPAV ageing has already a similar behaviour as the unaged bit-P.

5.2.5. Parameters retrieved from DSR tests

To complement the qualitative analysis of the viscoelastic behaviour of the binders, as evaluated in the previous paragraphs, this paragraph will handle specific points in the behaviour of the tested bitumen. Several parameters can be retrieved from the DSR data, already mentioned in Chapter 5.2.2:

- | | |
|---|---|
| High temperature range: | |
| 1. The rutting limit | $G^* / \sin(\delta)$ |
| Intermediate temperature range: | |
| 2. The cross over modulus | G_c |
| 3. The cross over frequency | f_c |
| 4. The cracking limit; Glover-Rowe parameter | $G^* \cdot \cos^2(\delta) / \sin(\delta)$ |
| Low temperature range: | |
| 5. The thermal cracking limit | $G^* \cdot \sin(\delta)$ |
| 6. Kriz et al. modulus limit; $\delta = 42$ [°] | G_{PK} |
| 7. Kriz et al. phase angle limit $G = 8\,967$ [kPa] | δ_{PK} |

The cross over modulus and frequency are both parameters measured when the phase angle $\delta = 45^\circ$. A high modulus means that at low temperatures or high frequencies, such a bitumen still has a phase shift angle. A strongly aged material would not reach a phase shift angle above 45 [°], therefore showing a limitation in viscous property. Similarly the cross over frequency shows its correlation to the phase shift angle, although it is directly related to time-temperature shifts. A high cross over frequency lets one know that one can exert loads at higher frequencies or at lower temperatures, but still reach a high enough viscous response. A strongly aged bitumen would have strongly decreased cross over frequency. The thermal cracking limit is a parameter calculated at 20 [°C] and 10 [rad/s], indicating how susceptible the bitumen is to cracking at a limit around 5000 [kPa]. A very high value shows that a bitumen will become critically stiff with no room for a viscous/damping response, seriously risking thermal cracking of an asphalt pavement. The cracking limit is a parameter calculated at 15 [°C] and 0.005 [rad/s], indicating how susceptible a bitumen is to reach the cracking limit between 180 and 450 [kPa]. Like with the thermal cracking, here a too high value will show a risk in too stiff and no viscous response of the bitumen, leaving no room to heal cracks.

These all give their own indications of change of a binder and make them quantified to compare to other results. The goal is to discern which parts of rheological behaviour are actually affected by REOB modification, and which effectively change upon ageing of the bitumen blend.

This should hopefully indicate which are the most critical parts of rheological behaviour of a bitumen and thus which parameters show the most critical limitations to use of REOB in the pavement industry.

1. The rutting limit; $G^*/\sin(\delta)$ at 20 [°C] and 10 [rad/s]

To begin with the rutting parameter, one can notice that the PEN grade seems to fit well to the unmodified and unaged bitumen. Bit-K and bit-P will have a high value whereas the higher PEN grades will have lower values. REOB modification will drastically lower the parameter, showing that the 15% blends approach low levels. Interestingly the bit-P started at a lower value than bit-K, although with increasing the dosage one can notice a much more drastic decrease in this value for the bit-K blends than the bit-P blends. This shows that the bit-K blends are much more susceptible to rutting than the bit-P blends are.

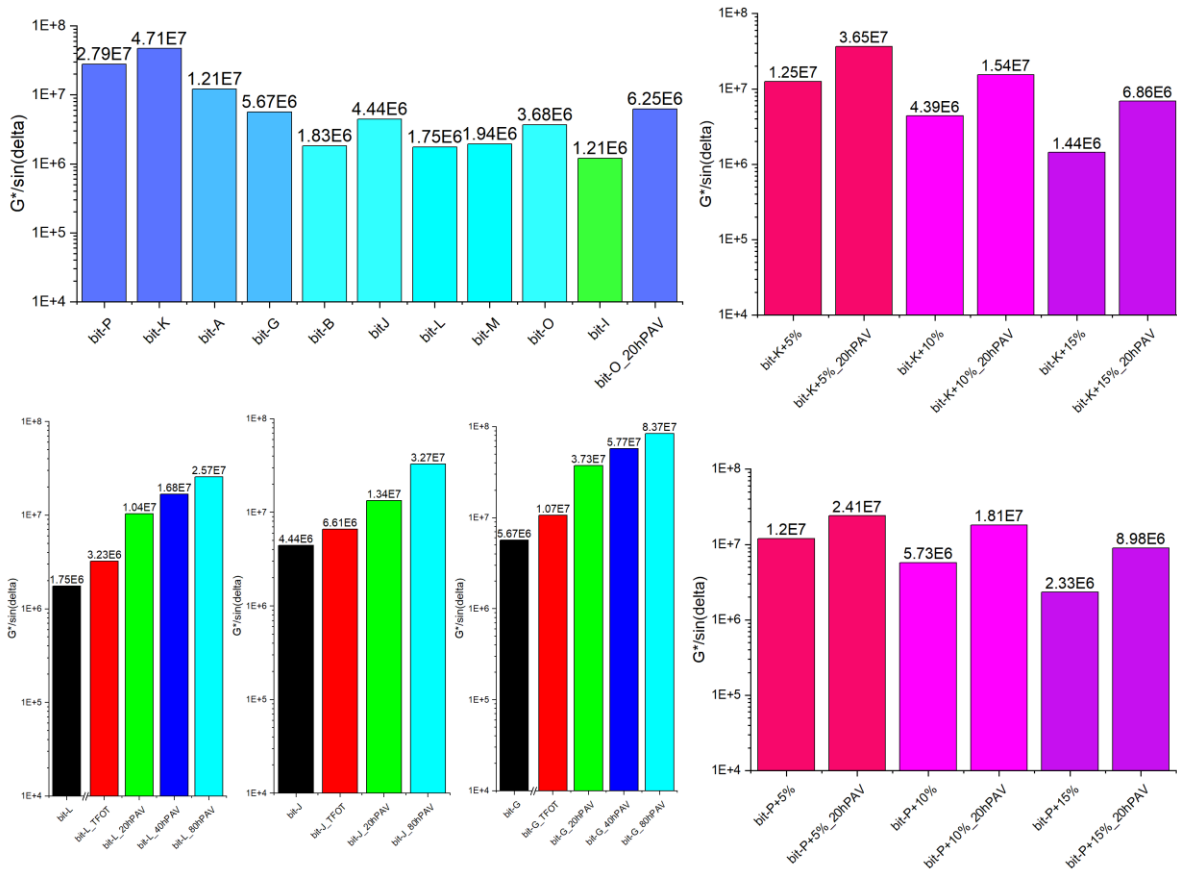


Figure 5.23: The rutting modulus $G^*/\sin(\delta)$ for unmodified bitumen, aged bitumen and aged REOB modified bitumen

This fact compared with the bit-L, bit-G and bit-J binders, one can see that bit-J and bit-G keep enough stiffness at the high temperatures and bit-L is most susceptible. However with ageing all bitumen will become less susceptible to rutting, where the least drastic changes are mainly seen for bit-J; whereas bit-L and bit-G change much more drastically. Ageing of the REOB modified bitumen seems to be more significant for the higher dosages, where the bit-P blends of course show to be more significantly stiff than the bit-K blends. This should therefore also be compared to the ageing indices of this parameter, which is done in the next figure. As was already noticed, the bit-L changes the most significantly but apparently bit-G does so equally. At the same time a higher REOB dosage shows to also steadily have more impact on the rutting susceptibility/stiffness at the high temperature range.

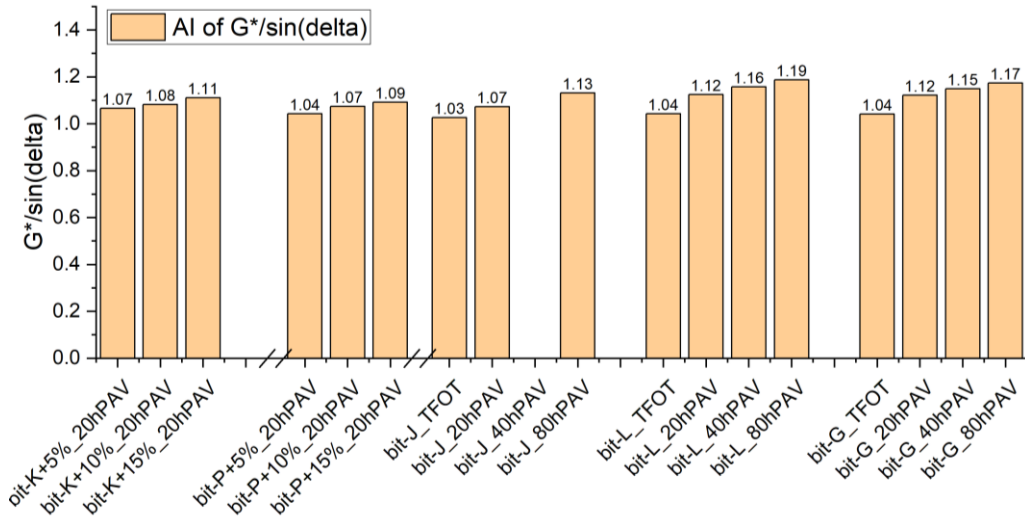


Figure 5.24: Ageing index of $G^*/\sin(\delta)$ for aged unmodified and REOB modified bitumen

2. Cross over modulus; G_c

One can observe that the cross over modulus differs much between binders and does not depend directly on PEN grade. Ageing of a binder causes this cross over modulus to drop, indicating that the stiffness at which a binder its phase shift angle is 45° , shows to decline. An unaged binder will have a very high stiffness at the moment that it has a 45° phase shift angle. Interestingly the decrease in G_c seems to be very high for bit-G, mediocre for bit-L and very low for bit-J. This shows which binders have a higher tendency to lose their viscous component and become brittle.

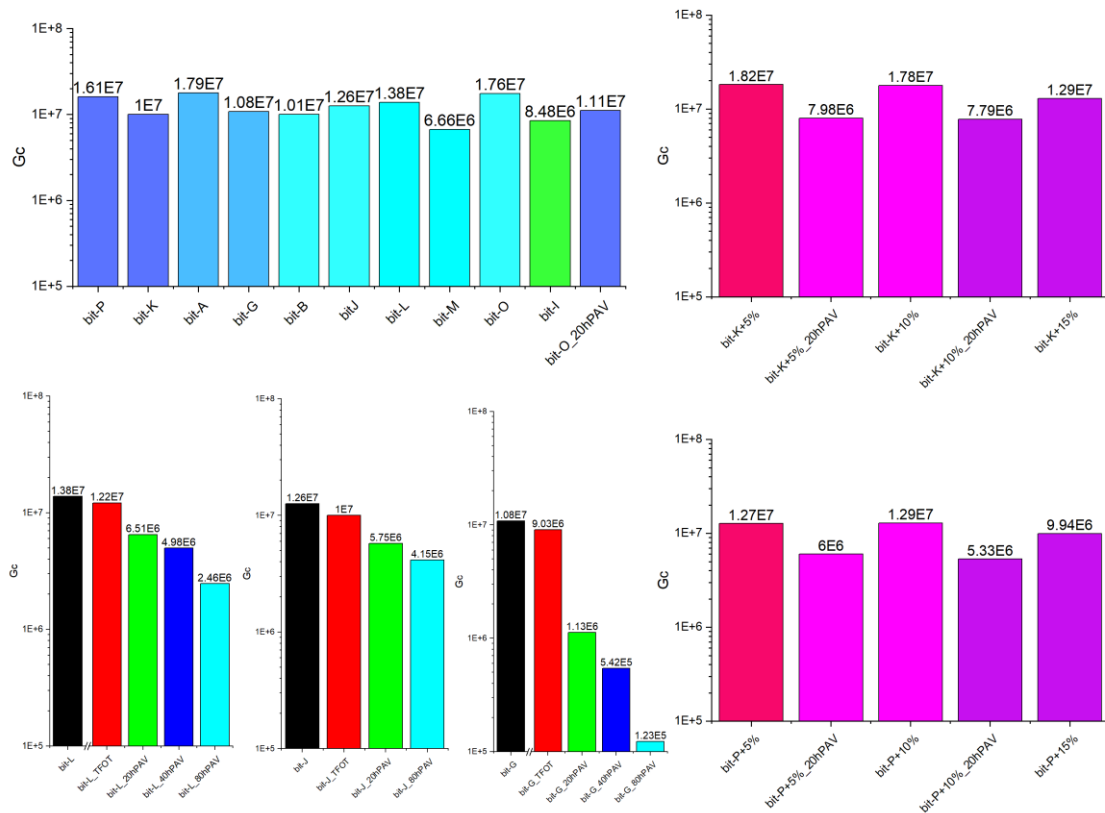


Figure 5.25: The cross over modulus G_c for unmodified bitumen, aged bitumen and aged REOB modified bitumen

Looking at the bit-K and bit-P blends with REOB, one can observe that the drop in G_c with 20hPAV seems to be significantly higher for the 15% blends than for the 5% blends. One can also see that the initial binder loses a little bit of G_c , but this is not too significant. By calculating the ageing index of this parameter, this can be zoomed into and is depicted below:

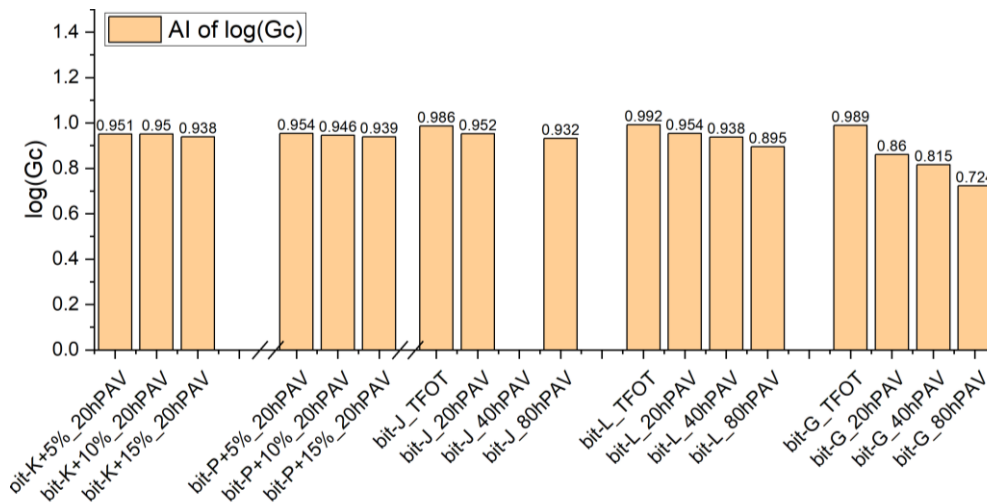


Figure 5.26: Ageing index of G_c for aged unmodified and REOB modified bitumen

This directly shows that the decrease of 15% dosage is almost equal to the ageing index of 40hPAV ageing of bit-L and bit-J. Higher REOB dosage thus does have a significant effect on rheological ageing behaviour.

3. Cross over frequency; f_c

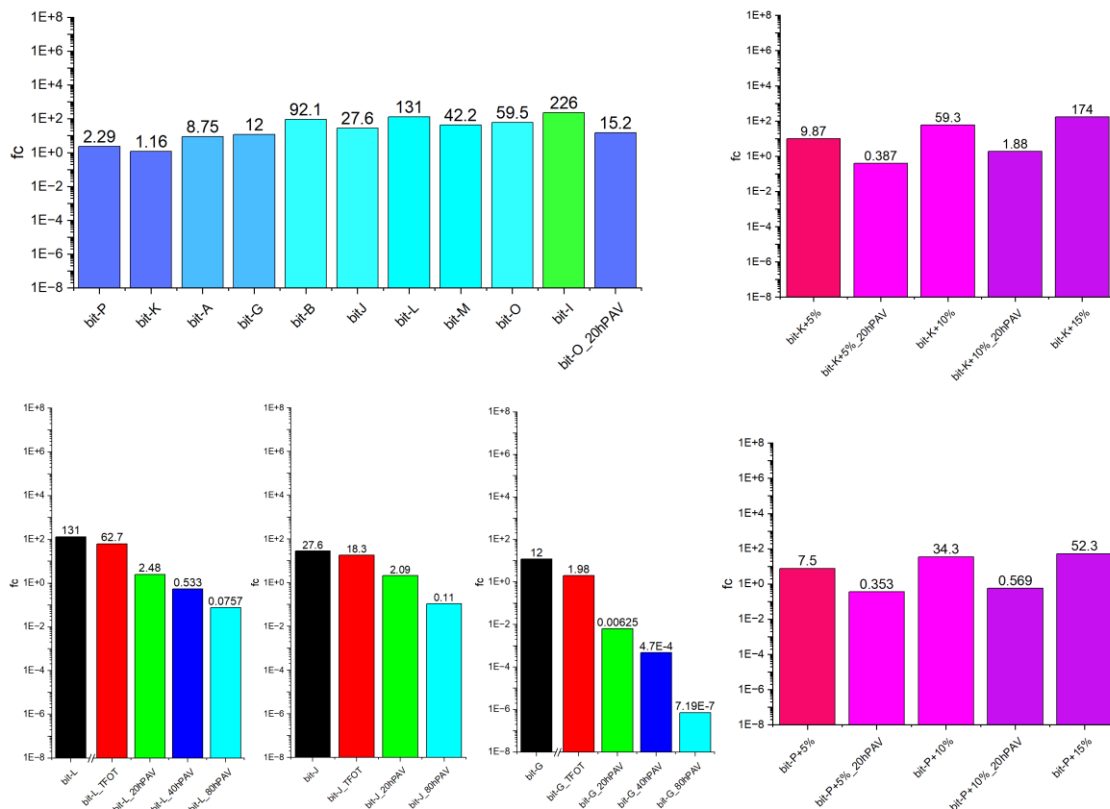


Figure 5.27: The cross over frequency f_c for unmodified bitumen, aged bitumen and aged REOB modified bitumen

As compared to the cross over modulus, the cross over frequency does clearly change according to PEN grade. Therefore not the stiffness, but the time-temperature relation of binders is what is connected the most to the PEN grade. The ageing of binders seems to have a very similar effect, as again bit-G changes the most, bit-L mediocre and bit-J does not change a lot in its f_c . Although overall changes seem less severe, than with the stiffness.

The REOB blends however show something different from before. One can see that addition of REOB causes an increase in f_c , which is reasonable, but what can also be seen is that ageing does not differ between low or high dosage of REOB. The ageing does not seem to have an effect on the time-temperature relation of a binder.

4. The cracking limit; $G^* \cdot \cos^2(\delta)/\sin(\delta)$

Alternatively to the cross over parameters, one can also evaluate the Glover-Rowe parameter, which is formulated in the following way:

$$G^* \frac{\cos^2(\delta)}{\sin(\delta)} \text{ at } 15 [^\circ\text{C}] \text{ and } 0.005 [\text{rad/s}]$$

This parameter is used to show how close a binder comes to its cracking limit in a full in-service pavement. A higher value means it was becoming more brittle, whereas a lower value means it has sufficient buffer before reaching the limit of cracking.

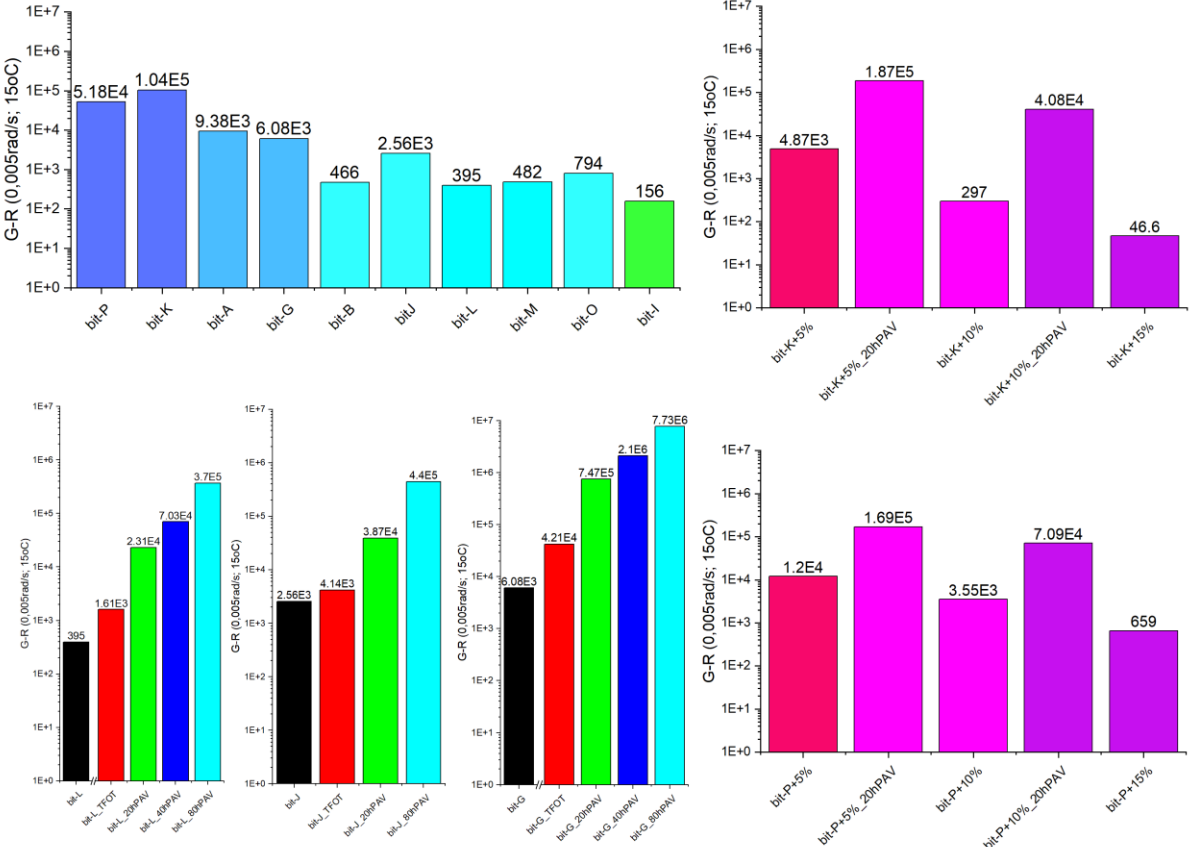


Figure 5.28: The cracking limit/Glover-Rowe parameter for unmodified bitumen, aged bitumen and aged REOB modified bitumen

For all binders one can easily observe that the PEN grade relates to the cracking limit, where the stiff binders are close to the cracking limit and the softer binders are not. Ageing of the bit-L, bit-G and bit-

J series has shown that bit-L and bit-G change similarly, although bit-G lies at significantly higher levels. bit-J shows the least increase, although one can observe a kind of exponential increase, whereas bit-L and bit-G seem to linearly increase their G-R parameter.

REOB modified bitumen shows to have a bigger decrease in G-R parameter for the bit-K series as compared to the bit-P, which corresponds to the PEN grade measurements mentioned before in paragraph 3.3. The increase in the parameter upon ageing shows a distinctively bigger increase for the higher dosages than the lower dosages, for both bit-K and bit-P series.

5. The thermal cracking limit; $G^* \sin(\delta)$

The thermal cracking parameter $G^* \sin(\delta)$ at 10 [rad/s] and 20 [°C] gives an indication on how stiff a binder will be at low temperatures. One can clearly see that the PEN grade seems to relate well to this parameter, being high for the stiff binders and low for the soft binders.

Ageing of the bitumen does not show large differences, although one can surprisingly see that bit-L is now the bitumen that alters the most, bit-G mediocre and bit-J least. bit-L does start however at lower stiffness and although the bigger increase with ageing, it also ends up at a lower stiffness than bit-J and bit-G after 80hPAV ageing.

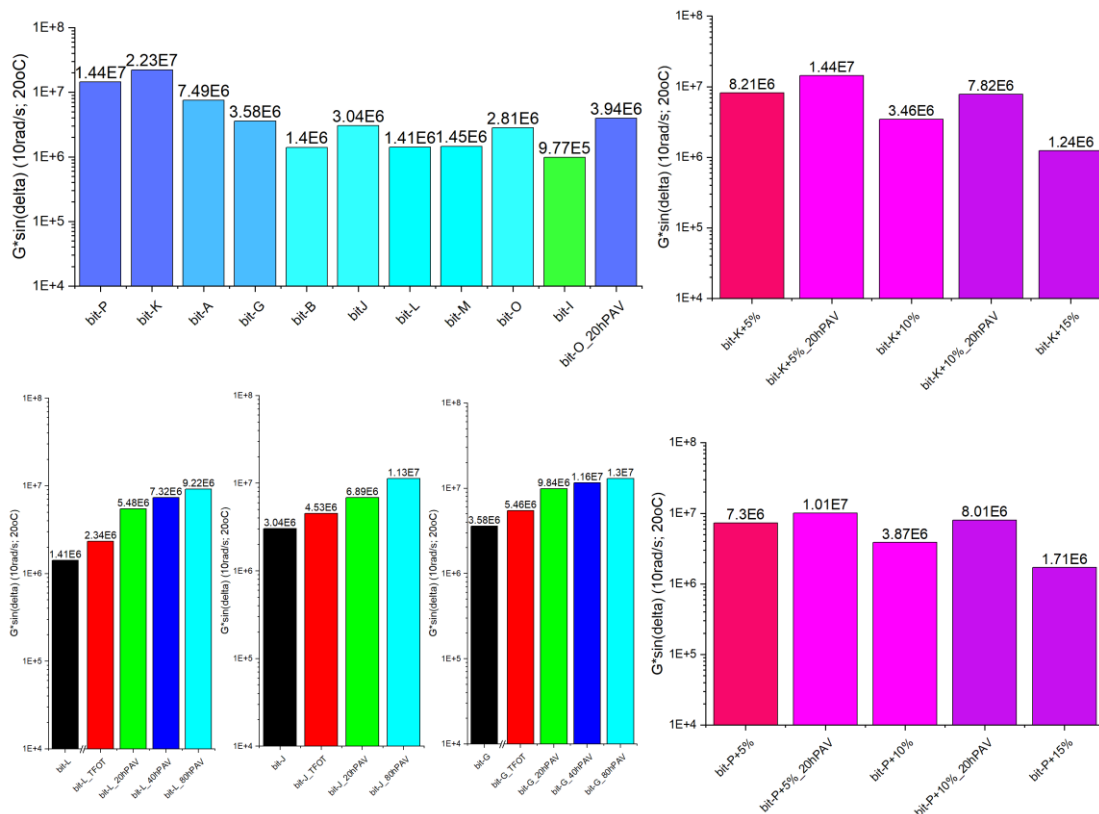


Figure 5.29: The thermal cracking limit $G^* \sin(\delta)$ for unmodified bitumen, aged bitumen and aged REOB modified bitumen

This can finally also be compared to the REOB blended bitumen, where one can see that the thermal cracking limit decreases linearly with increase in dosage. This is reasonable as the REOB makes a softer binder out of the bitumen and therefore will decrease its stiffness at higher temperatures as well, making rutting more of a problem. Ageing of the REOB modified bitumen shows to have more of an effect on the bitumen with higher dosage of REOB present, as for both the bit-K and bit-P 15% REOB modified bitumen the increase is very substantial.

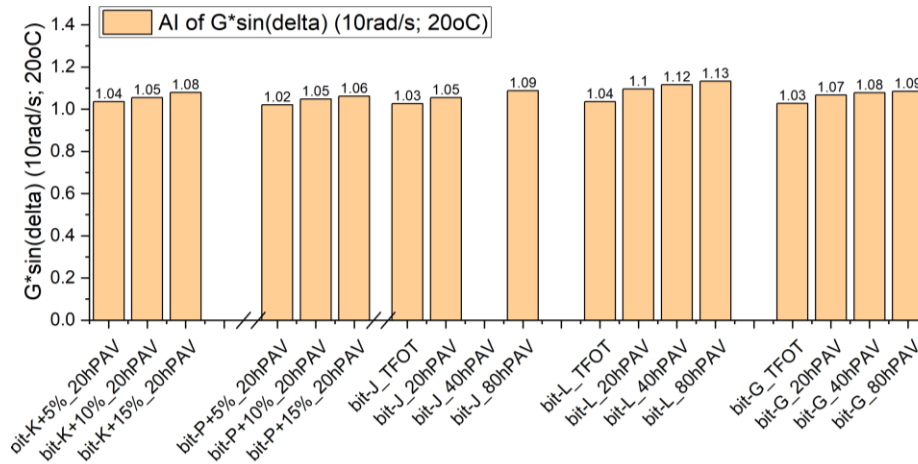


Figure 5.30: Ageing index of $G^* \sin(\delta)$ for unmodified bitumen, aged bitumen and aged REOB modified bitumen

The thermal cracking parameter, much closer to describing low temperature and high frequency behaviour of a bitumen, shows clear difference between the bitumen. Here high dosage REOB modification shows again to be more severe in stiffening the bitumen with ageing than lower dosage ones. Interestingly the bit-L seems to be more severe than bit-J and bit-G with respect to the thermal cracking limit, but one needs to keep in mind that bit-L was initially already substantially lower.

6. Kriz et al. modulus limit G_{PK} at $\delta = 42 [^\circ]$

Finding the complex shear modulus when $42 [^\circ]$ gives a good indication if a bitumen has aged significantly or not: a bitumen that has a very high complex shear modulus when $42 [^\circ]$ means that the bitumen has a very good viscous property although the temperature is very low/the frequency is very high.

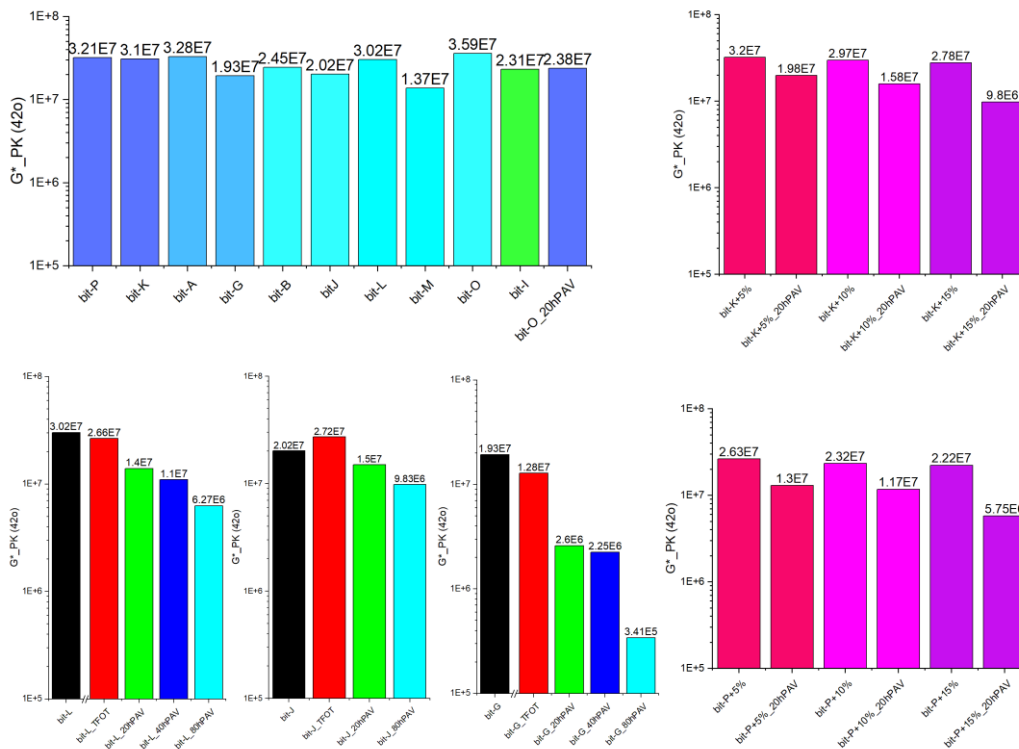


Figure 5.31: Measured complex shear modulus when $\delta = 42 [^\circ]$ with DSR test

With this in mind, one can easily observe that REOB modification has a much more significant effect on the stiffness (or actually the time-temperature relation) than on the viscous property (denoted by the phase shift angle). One can observe that the initial stiffness of $3.21e7$ [Pa] for bit-P has lowered significantly towards $2.63e7$ [Pa] with only 5% added, which lowers even more to $2.22e7$ [Pa] after adding 15%. Comparing this to the bit-K, which starts at a similar $3.1e7$ [Pa], adding a mere 5% seems to actually increase the stiffness to $3.2e7$ [Pa] and at 15% one obtains a stiffness of $2.78e7$ [Pa]. This then compared to the unmodified bitumen, shows that bit-L drops from $3.02e7$ [Pa] to $1.4e7$ [Pa]; bit-J drops from $2.02e7$ [Pa] to $1.5e7$ [Pa]; bit-G drops significantly from $1.93e7$ [Pa] to $2.6e6$ [Pa] and lastly bit-O from $3.59e7$ [Pa] to $2.38e7$ [Pa].

This shows that, out of all bitumen, the bitumen bit-O has the highest initial stiffness but drops significantly. BitK blends with 5%, 10% and 15% all have the smallest decrease in stiffness and bit-G the most decrease of all. One can thus say that the time-temperature relation is the most stable for the bit-K and bit-J bitumen and that the REOB merely accelerates the rate at which this changes. The bit-O will have the biggest buffer towards change, but does not clearly have a slower ageing rate which holds true for bit-P as well. This is why the rate of change in stiffness is significantly higher for the bit-P REOB modified bitumen, than for the bit-K blends.

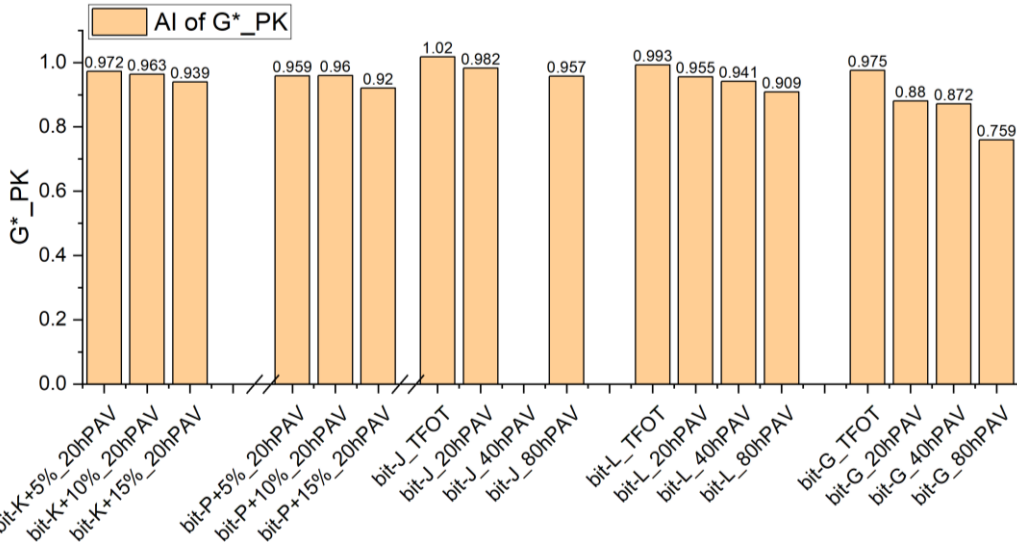


Figure 5.32: Ageing index of measured complex shear modulus when $\delta = 42$ [°] with DSR test

The ageing index of this parameter is able to show the more drastic decrease of bit-G in this low temperature region. Next to that again a higher REOB dosage clearly has more impact on the ageing degree.

7. Kriz et al. phase angle limit δ_{PK} at $G = 8967$ [kPa]

Mere REOB modification shows to have a significant effect in the case of using bit-P as the base bitumen, as starting from 58 [°] there is a measurable drop to 50 [°], although the used dosage does not seem to have a measurable effect. However the bit-K as base binder started at 55 [°] and the REOB modified bitumen shows to have roughly the same, although some more variance is measurable.

However ageing shows that a significant loss is possible after 20hPAV and this loss will increase further if the used REOB dosage is higher. One can see that the bit-P+5% has a decrease in phase shift angle from 50 [°] towards 45 [°], whereas bit-K+5% drops from 55 [°] to 47.5 [°].

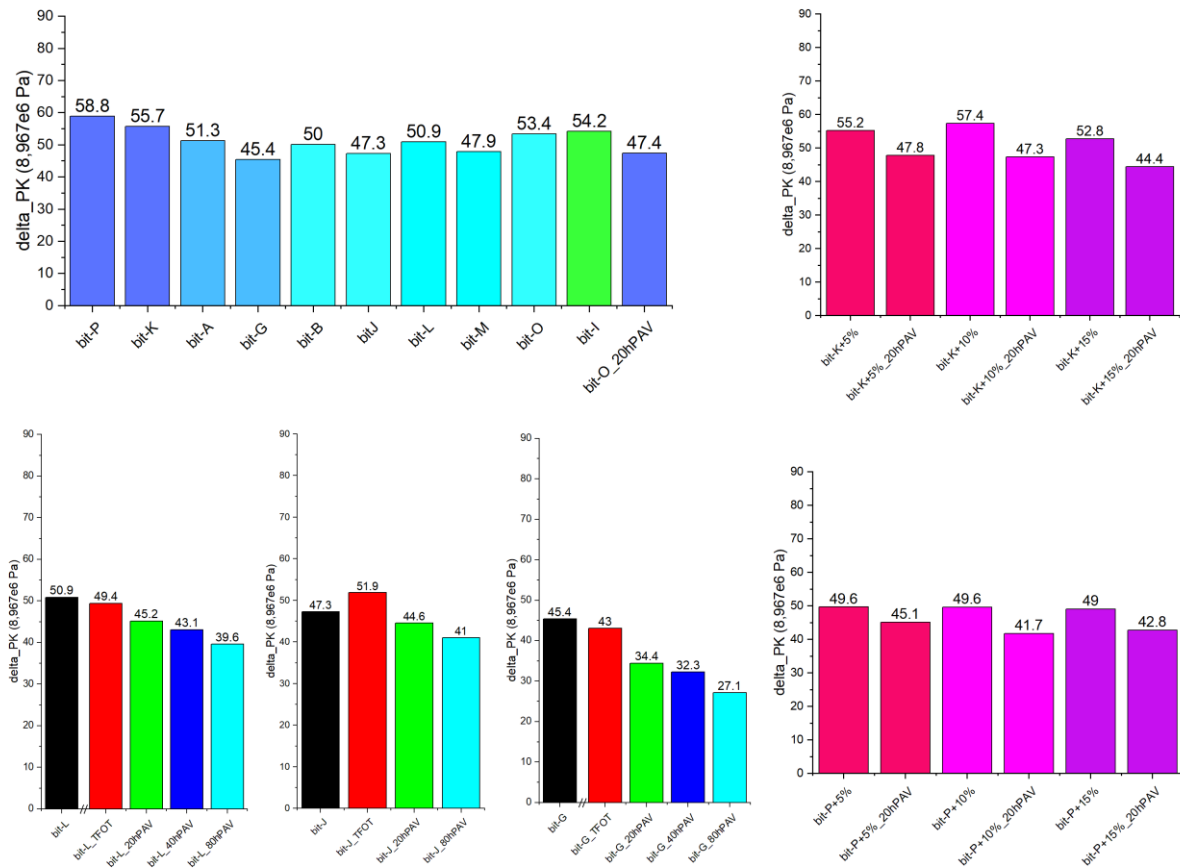


Figure 5.33: Measured phase shift angle when $|G^*| = 8.967e6 [Pa]$ with DSR test

The decrease of bit-L and bit-O after 20hPAV ageing seems quite comparable to the decrease of bit-P+15% in its loss in phase shift angle. bit-J shows that it will increase its phase shift angle after TFOT and then lose it again with PAV ageing, this binder shows the least decrease in phase shift angle of all bitumen. One can thus say that mainly bit-G and the bit-K+15% (high REOB dosage) have the most significant loss in viscous property of all bitumen.

Conclusion on DSR parameter variations

These parameters have therefore shown the expected changes for unmodified and REOB modified bitumen clearly. One can see how there can be big differences between bitumen of similar PEN grade, although these can be possibly related to the chemical composition of those bitumen. What is clear however, is the fact that REOB modification mainly alters the time-temperature relation of a bitumen, making it lose viscosity (which was its goal), but that it also with ageing excessively increases the stiffness or make it lose its phase shift angle of a binder, which is increased even more if a higher dosage of REOB is used.

- An explanation could be that the REOB modified bitumen wants to approach its base bitumen behaviour when it changes with ageing. At the end of this path it will reach the aged state of the base bitumen, therefore fully negating the initial REOB modification of the bitumen. This would therefore always mean that REOB would have accelerated ageing when higher dosages of REOB are used, as this softening compound is in a certain way lost during ageing.

5.2.6. Observations on general viscoelastic rheological behaviour

With the DSR frequency sweep measurements performed and the complex shear modulus and phase shift angle data analysed, one can draw conclusions about the differences in unmodified bitumen, ageing of bitumen and the REOB modification of bitumen.

The following main conclusions on the rheological viscoelastic behaviour of the binders can be stated:

- (1) Black space diagrams, combining both complex shear modulus and phase shift angle and not applying any shifting to the data, were effective in indicating ageing behaviours of bitumen. A significant difference can be found in bitumen to lose either more in phase shift angle or to change in time-temperature relation (gaining in stiffness with ageing). Bit-J for example mainly drops its black space diagram, having only a very small loss in phase shift angle. Whereas bit-G has a significantly higher gain in complex shear modulus than it loses in phase shift angle. bit-L seems to fall quite in between both bitumen.
- (2) Master curves have been able to show frequency dependent behaviour of bitumen their complex shear modulus and phase shift angles. Here it became clear that PEN grades have a good relation with the position of the master curve of the complex shear modulus does over frequency. Much more variance can be seen with the phase shift angles however. Next to that the master curves have shown that complex shear modulus over frequency will mainly increase in stiffness with ageing, between bitumen there only seems to be a difference in the step size that it increases in stiffness. The phase shift angle however shows that a completely different shape of curve will be approached with ageing, in the case of bit-G and bit-L. bit-J however shows only a horizontal shift taking place with the same amount of ageing.
- (3) REOB modification has shown in the black space diagrams, that it will initially perfectly overlap the curve of the base bitumen. This suggests no initial ageing will take place rheologically, however with further ageing one can clearly notice how higher dosage will increase the change in black space curve, lowering it more substantially for higher dosages. The shape of the black space diagram suggests that REOB does not change the way that a bitumen/blend ages, but merely accelerates the characteristic changes that the bitumen would go through. This is partly a new observation than what was found before (Mensching et al., 2017).
- (4) Master curves were able to show for the REOB modified bitumen that good overlap was possible with the complex shear modulus curves of reference bitumen using the 10% blends. Although to approach similar phase shift angle curves, one generally will have a better overlap when increasing the dosage to roughly 15%. This however shows a clear misalignment with the PEN grade measurements, shown in Figure 3.6. Here the PEN grade will change exponentially with REOB dosage, whereas the DSR frequency sweep measurements have shown that the stiffness and phase shift angle curves change linearly. This correlates well to what was found in other research (Mensching et al., 2017; Mogawer et al., 2017).
- (5) Cole-Cole diagrams have shown the rheological behaviour of bitumen when passing or coming close to their glass transitions (Porot, 2019; D. Wang et al., 2020). One can notice a maximum in loss modulus, describing viscous property of a bitumen, will be reached at the DSR measurements between 0 [°C] and -10 [°C]. In the case of some bitumen one can say they have a substantially high maximum value of loss modulus and lose this only little with ageing; i.e. only bit-O and bit-L do this. Interestingly the ageing of bitumen shows that TFOT will not change the Cole-Cole diagram at all and the 20hPAV, 40hPAV and 80hPAV show a significant drop. However all REOB modified bitumen have shown to lose this viscous property significantly after initial blending and further with ageing, suggesting these bitumen will have a poorer low temperature performance by approaching a different microstructural state and becoming brittle earlier.

5.3. Low temperature stiffness and relaxation properties (BBR)

5.3.1. Test preparation, method and calculation procedure with the BBR

The Cole-Cole diagrams obtained from the DSR tests at the low temperature have shown before that they indicate distinctively different behaviours between binders, and the low temperature behaviour of the REOB modified binders is important to be evaluated.

The dedicated machine for the SuperPave program in the USA, but also one used more often in Europe, is the Bending Beam Rheometer (BBR). This machine is able to cool small bitumen bars to temperatures as low as -40 [°C]. One uses an ethanol bath that is lowered to this temperature and small bitumen samples are made and placed in this bath conditioned for one hour.

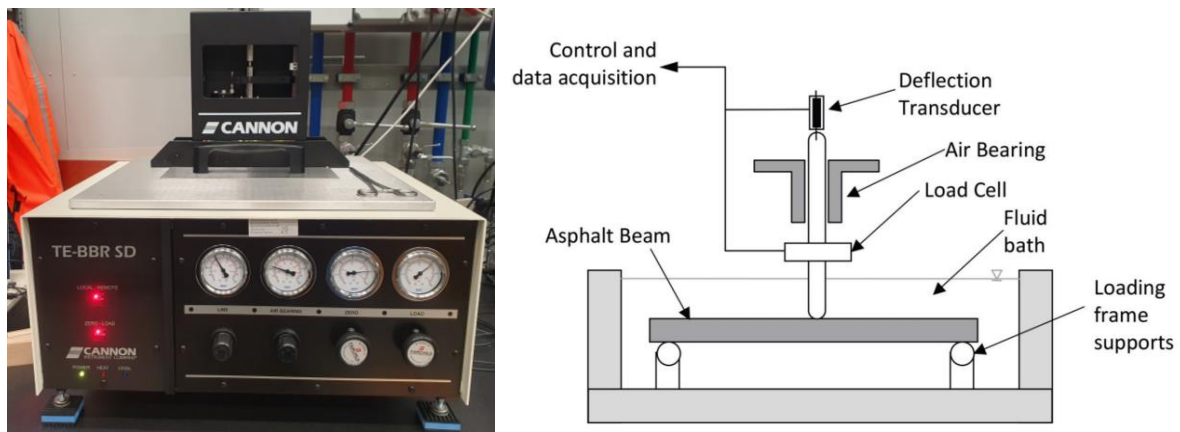


Figure 5.34: (left) the BBR setup and (right) the principle of a three-point bending test

These bitumen bars are made and tested in the following way, according to the NEN-EN 14771 Norm:

1. Place the respective bitumen in the oven at 163 [°C] for 1.5 hours (in the case of 70/100 grade bitumen) or 2 hours (in the case of 20/30 grade bitumen) and make it soft for pouring
2. In the meantime preparing the moulds, with standard geometries. The moulds their inside ends are coated with vacuum grease and small plastic strips are stuck on that surface. The small ends are coated with a little bit of glycerol + talcum powder (weight ratio 1:2)
3. The BBR is calibrated and set first to a temperature that is high enough to have a stiffness below $S=300$ [MPa] and a relaxation slope above $m=0.3$ [-]. In the case of a 70/100 grade binder one would use therefore the following testing temperatures: -10 | -16 | -22 [°C]. For a hard grade bitumen around 20/30 one should use a temperature range like: -4 | -10 | -16 [°C].
4. After performing tests at this temperature, the next batch of samples is tested at a temperature which causes the binder to have a stiffness above $S=300$ [MPa] and relaxation slope below $m=0.3$ [-]. Two samples are tested at each of the temperatures, performing a three point bending test according to the following stiffness model for the bitumen beam:

$$S_m(t) = \frac{PL^3}{4bh^3\delta(t)}$$

(5.15)

5. A test is then carried out applying ~980 [N] for 240 [sec] and the deflection is measured.

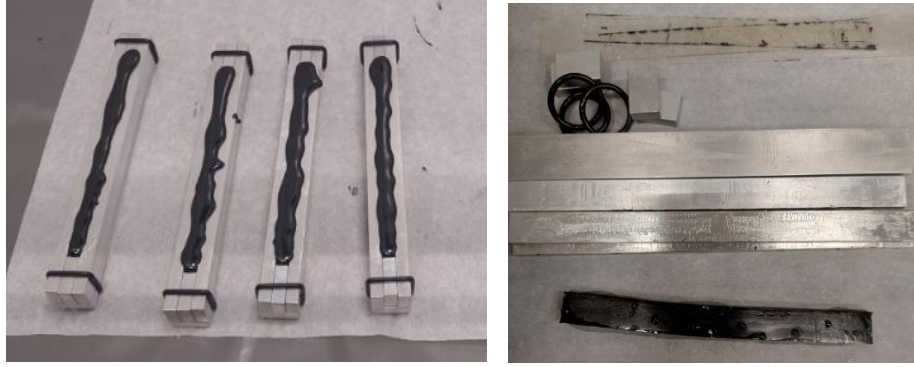


Figure 5.35: (left) several BBR bitumen samples just before cutting the top layer and (right) demoulded elements and a tested bitumen sample

Now that the deflection is measured overtime, and the dimensions of the bitumen beam are perfectly known, a stiffness (overtime) for the beam is obtained. This makes it possible to calculate the stiffness at 60 seconds, including the slope of the stiffness diagram, which correlates to the relaxation capabilities of the bitumen.

A second-degree polynomial is fitted to the stiffness data to obtain a realistic measurement and exclude deviations in the measurements:

$$\log[S_c(t)] = A + B \cdot \log(t) + C \cdot [\log(t)]^2 \quad (5.16)$$

Next to that this can be altered to calculate the slope at 60 seconds too:

$$m(t) = \left| \frac{d \log[S(t)]}{d \log(t)} \right| = |B + 2 \cdot C \cdot \log(t)| \quad (5.17)$$

To relate the creep stiffness and the relaxation slope to values that compares bitumen more easily to each other, one can also calculate the critical temperatures of the respective binders. These show the critical temperatures at which a higher stiffness or a lower relaxation slope is reached for a binder and therefore correlate well to specific ageing behaviour of that binder. They are calculated in the following way:

$$T_c(S) = T(S_{>300 [MPa]}) + \frac{T(S_{>300 [MPa]}) - T(S_{<300 [MPa]}) \cdot (\log(300) - \log(S_{<300 [MPa]}))}{(\log(S_{>300 [MPa]}) - \log(S_{<300 [MPa]}))} - 10$$

$$T_c(m) = T(m_{<0.3}) + \frac{T(m_{<0.3}) - T(m_{>0.3}) \cdot (0.3 - (m_{>0.3}))}{(m_{<0.3}) - (m_{>0.3})} - 10 \quad (5.18)$$

The calculation of the difference between $T_c(S)$ and $T_c(m)$, the so-called ΔT_c or deltaTc, gives an indication of how brittle a binder is. This is thus a very good indicator of how the low temperature sensitivity is of this bitumen, but also indicates how much a bitumen has aged. A strongly negative value of ΔT_c , relates to a strongly brittle or strongly aged bitumen (but in the case of polymer modified bitumen this can also drastically change, although the sensitivity has not per se decreased). One calculates ΔT_c in the following way:

$$\Delta T_c = T_c(S) - T_c(m) = T_c(S = 300 [MPa]) - T_c(m = 0.3 [-]) \quad (5.19)$$

With these tests and procedures, one can evaluate the BBR measurements effectively. BBR measurements have been carried out for REOB modified bitumen before though. It was found that the REOB alters the bitumen its behaviour in such a way that the ΔT_c will increase more with higher dosage but also with longer ageing times, as compared to unmodified bitumen (Arnold & Shastry, 2015; Bennert et al., 2016; Karki & Zhou, 2019; Mensching et al., 2017; Xin-jun et al., 2016).

It is therefore expected to be found as well with the REOB modified bitumen here, although the true difference between both base bitumen will be evaluated too, to see which bitumen (with its own known composition) will receive the REOB better. Most of the research papers only focussed on the ΔT_c parameter, although it is believed that the $T_c(S)$ and $T_c(m)$ on their own will give more insight in the direct properties of the bitumen, these cannot simply be reduced to the ΔT_c .

5.3.2. S- and m-values, critical temperatures $T_c(S)$, $T_c(m)$ and ΔT_c values

After performing the BBR measurements on a selection of different bitumen, the stiffness and slope of the force/displacement curve have been measured. The table below shows all the measured m- and S-values for the bitumen at their respective test temperatures:

Table 5.1: Obtained m&S-values of unmodified and REOB modified bitumen at different temperatures with the BBR

Bitumen/blend	PEN grade	Lower range temp.	m-value	S-value	Higher range temp.	m-value	S-value
bit-P	(15)	-10	0.306	430.9	-4	0.409	170.0
bit-K	(20/30)	-10	0.270	533.9	-4	0.368	242.4
bit-G	(40/60)	-18	0.319	322.1	-12	0.394	131.3
bit-L	(70/100)	-20	0.361	290.2	-12	0.508	63.4
bit-J	(70/100)	-24	0.234	704.5	-14	0.372	207.9
bit-O	(85)	-28	0.207	1001.3	-16	0.461	161.3
<hr/>							
bit-K+5%REOB		-16	0.242	605.8	-10	0.325	316.1
bit-K+10%REOB		-28	0.163	1052.6	-16	0.317	317.3
bit-K+15%REOB		-22	0.299	368.4	-16	0.383	157.5
bit-P+5%REOB		-16	0.293	450.3	-10	0.380	193.2
bit-P+10%REOB		-28	0.189	955.5	-16	0.362	255.3
bit-P+15%REOB		-22	0.336	282.0	-16	0.424	107.0
<hr/>							
Bitumen/blend		Lowest temp.	m-value	S-value	Highest temp.	m-value	S-value
bit-J 20hPAV		-22	0.22	631.1	-10	0.327	168
bit-O 20hPAV		-22	0.276	599.6	-10	0.435	105.4
<hr/>							
bit-K+5%REOB 20hPAV		-10	0.262	382.2	-4	0.331	191.5
bit-K+10%REOB 20hPAV		-22	0.207	663.9	-10	0.326	202.7
bit-K+15%REOB 20hPAV		-16	0.293	234.3	-10	0.356	108
bit-P+5%REOB 20hPAV		-10	0.316	225.9	-4	0.393	98.1
bit-P+10%REOB 20hPAV		-22	0.229	614.2	-10	0.347	143.6
bit-P+15%REOB 20hPAV		-22	0.275	337.6	-16	0.322	162.8

The testing temperatures were selected according to the found PEN grades, which gave good boundaries to be able to estimate the $T_c(S)$ and $T_c(m)$ with linear interpolation. The aim was to always have temperatures above and below the 0.3 for the m-value to use interpolation and extrapolation was sometimes accepted when values were very close.

Adding 5% of REOB, one can see that the m-value is changed roughly (in this case at -10 [°C] and an average of both bit-K and bit-P blends). A comparison between bit-K or bit-P and the +5% blend gives in that case for the m-value and S-value:

$$\Delta m_{value} = \frac{\frac{0.325 - 0.270}{0.270} + \frac{0.380 - 0.306}{0.306}}{2} * 100\% = +22.3\%$$

$$\Delta S_{value} = \frac{\frac{316.1 - 533.9}{533.9} + \frac{193.2 - 430.9}{430.9}}{2} * 100\% = -47.98\%$$

(5.20)

This concludes that REOB has more effect on the stiffness, than on the relaxation capabilities of a bitumen. When adding even more REOB, the difference between 5% and 15% can be seen in the m-value and S-value as (at -16 [°C] measurement):

$$\Delta m_{value} = \frac{\frac{0.383 - 0.242}{0.242} + \frac{0.424 - 0.293}{0.293}}{2} * 100\% = +51.5\%$$

$$\Delta S_{value} = \frac{\frac{157.5 - 605.8}{605.8} + \frac{107.0 - 450.3}{450.3}}{2} * 100\% = -75.1\%$$

(5.21)

Ageing the binders shows different behaviours as well. Clearly bit-J loses more m-value than bit-O does. Overall the blends of bit-P with REOB show to outperform the bit-K blends, as the m-values are higher and the S-values lower. To zoom in on these specific changes to the low temperature behaviour of the modified bitumen and also the aged variants, the previously mentioned critical temperatures are calculated. These are noted in the table below.

Table 5.2: Calculated critical temperatures $T_c(S)$, $T_c(m)$ and ΔT_c for unmodified and REOB modified bitumen

Bitumen/blend	Grade	Unaged			20hPAV aged		
		$T_c(S)$	$T_c(m)$	ΔT_c	$T_c(S)$	$T_c(m)$	ΔT_c
bit-P	(B15)	-17.7	-20.4	2.7			
bit-K	(20/30)	-15.6	-18.2	2.5			
bit-G	(40/60)	-27.5	-29.5	2.0			
bit-L	(70/100)	-30.2	-33.3	3.1			
bit-J	(70/100)	-27.0	-29.2	2.2	-25.3	-23.0	-2.2
bit-O	(B85)	-30.1	-33.6	3.5	-27.2	-30.2	3.0
<hr/>							
bit-K+5%REOB		-19.5	-21.8	2.3	-17.9	-16.7	-1.2
bit-K+10%REOB	~(70/100)	-25.4	-27.3	1.9	-24.0	-22.6	-1.4
bit-K+15%REOB		-30.5	-31.9	1.3	-27.9	-25.3	-2.6
bit-P+5%REOB		-23.1	-25.5	2.4	-22.0	-21.2	-0.8
bit-P+10%REOB	~(70/100)	-27.5	-30.3	2.8	-26.1	-24.8	-1.3
bit-P+15%REOB		-32.4	-34.5	2.1	-31.0	-28.8	-2.3

The calculated critical temperatures show distinctive differences between the binders. The binders that have low PEN, bit-K and bit-P, have low critical temperatures. This shows that they will turn brittle and lose viscous properties earlier with ageing, than binders with lower critical temperatures. Both bit-L and bit-O show to have the lowest critical temperatures, with $T_c(S)$ reaching the -30 [°C] and $T_c(m)$ the -33 [°C]. Next to that they also have the biggest, positive!, difference between these critical

temperatures, which is shown by their ΔT_c which are higher than $+3.0$ [°C]. Bit-J and bit-G already show to have quite low critical temperatures for a 70/100 grade bit and their ΔT_c is lower in a similar way, as compared to bit-L and bit-O.

Ageing the binders show very clear different behaviours. bit-J has lost its $T_c(m)$ very significantly and therefore obtains a negative ΔT_c already with only 20hPAV ageing. This is not the case for bit-O, which even remains to keep a positive ΔT_c after the same 20hPAV ageing period.

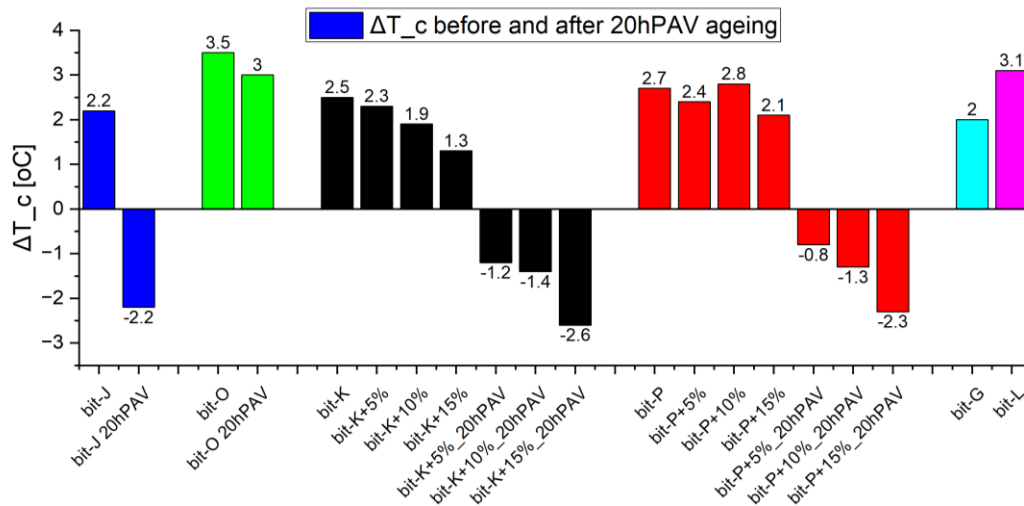


Figure 5.36: ΔT_c values of unmodified and REOB modified bitumen, as well as aged versions

The bit-P blend series shows to have a better ability to keep a low enough $T_c(m)$, but higher dosages of REOB seem to increase the change in properties as well with ageing.

Bit-P+5% drops ΔT_c with 3.2 [°C]

Bit-P+10% drops ΔT_c with 4.1 [°C]

Bit-P+15% drops ΔT_c with 4.4 [°C]

This compared to the bit-K blend series, one can see the bit-K blends underperform slightly:

Bit-K+5% drops in ΔT_c with 3.5 [°C]

Bit-K+10% drops ΔT_c with 4.1 [°C]

Bit-K+15% drops ΔT_c with 4.7 [°C]

Although at marginally small levels, the bit-P blends seem better receptive to the REOB modification, although both binders show that with increased dosage and ageing the change of the binder properties will increase exponentially.

In Figure 5.37 one can see that the effect of the REOB does exactly the same thing for both binders, the only difference is the base bitumen its starting point. As bit-P had already lower (more negative) critical temperatures (thus becomes brittle at a later stage as compared to bit-K), the REOB will decrease the critical temperatures with the same increments as with bit-K.

Comparing ageing of bit-K blends to bit-P blends, one can see that bit-K deviates a little more from the $\Delta T_c=0$ [°C] line, and therefore ends up with lower/more negative ΔT_c values than bit-P blends. The slope of ageing between bit-P+15% and bit-P+15%_20hPAV or bit-K+15% and bit-K+15%_20hPAV are visibly similar. There is a higher decrease in $T_c(m)$ than there is in $T_c(S)$. This is unfavourable, as this means the binder loses double as much in its relaxation properties as it gains in stiffness properties. This shows REOB blends and bit-J become more brittle, as opposed to how bit-O ages.

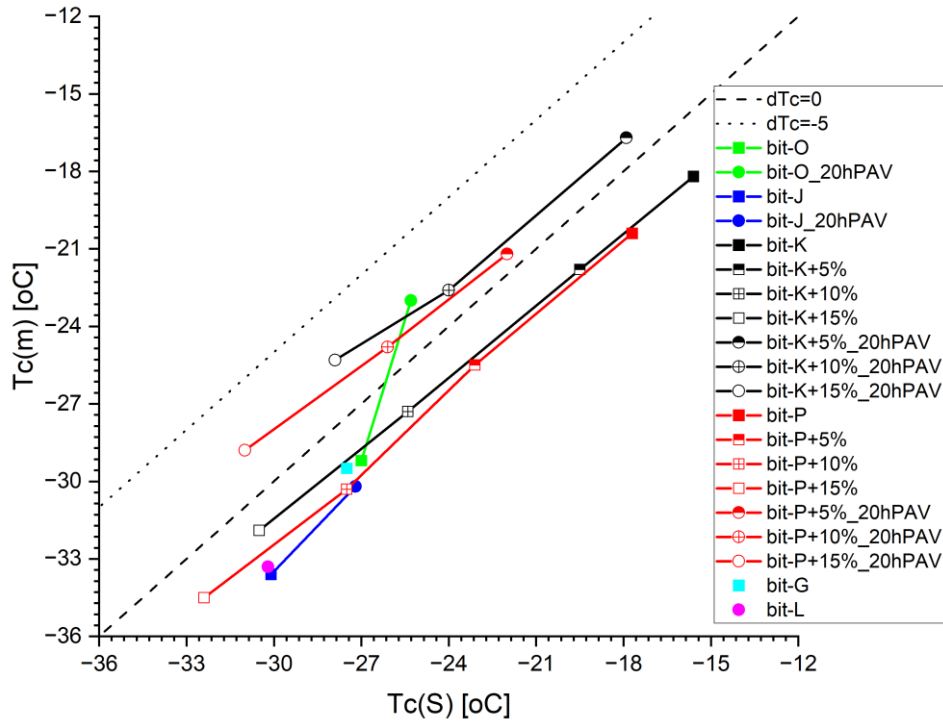


Figure 5.37: Critical stiffness and relaxation temperatures for unmodified, REOB modified and aged bitumen

5.3.3. Observations on low temperature rheological behaviour

With the BBR experiments and analysis performed, several conclusions can be drawn about the low-temperature performance of unmodified, aged and REOB modified bitumen.

- (1) The BBR has been effective in showing the $T_c(S)$ and $T_c(m)$ of different binders, where specifically the $T_c(S)$ is well correlated to PEN grades of unmodified bitumen. BitO and bit-L start initially at around similar low levels of $T_c(S)$ and $T_c(m)$ around -30 and -33 [°C], but bit-J and bit-G show to start at around -27 and -30 [°C]. The very stiff base bitumen bit-K and bit-P show to have the highest critical temperatures, ranging between -20 and -15 [°C]. This therefore shows that only bit-O and bit-L have the softest performance at low temperatures and bit-P and bit-K are of a very stiff nature.

Both bitumen bit-O and bit-J have shown to age differently, where bit-O shows to gain in stiffness equally as much as it loses in relaxation property and bit-J to decrease double as much in relaxation than it gains in stiffness. One can see the $T_c(S)$ goes from -30 [°C] to -27 [°C] and the $T_c(m)$ from -34 [°C] to -30 [°C]. Which can be compared to bit-J where the $T_c(S)$ goes from -27 [°C] to -25 [°C] and the $T_c(m)$ from -29 [°C] to -23 [°C].

- (2) REOB modification of the base bitumen bit-K and bit-P, shows to be very similar using the REOB-X. One can see in Figure 5.37 that consistent incremental steps of changes in dosage are followed, and the $T_c(S)$ and $T_c(m)$ can be lowered to a better level for the bitumen to act softer at low temperatures. Only bit-K+15% and bit-P+15% approach the bit-O and bit-L their performance at low temperatures. This correlates well to observations done before (Mensching et al., 2017; Xin-jun et al., 2016).

The ageing of REOB modified bitumen has shown that the higher the dosage, the bigger the change in measured ΔT_c . One can notice that base bitumen bit-K, already starting at a lower ΔT_c , shows to relatively drop more in ΔT_c with ageing at higher REOB dosages, than bit-P blends do. This shows that REOB modified bitumen are initially effective in bringing a bitumen to a good low stiffness and still high relaxation, but at the risk of losing this quickly after 20hPAV and more.

Chapter 6. Rheological and chemical property correlations of unmodified and REOB modified bitumen

In this Chapter a more in-depth look is given on the found differences between the unmodified and REOB modified bitumen and an interlink is sought between those chemical properties and the difference in viscoelastic behaviour described with rheology. Firstly, the differences in inherent properties that the bitumen have on chemical and rheological aspects are mapped. Then this is continued by describing the correlations between molecular weights and structures, the ageing susceptibility and lastly the low temperature sensitivity of a bitumen.

6.1. Intrinsic chemical and rheological properties of bitumen and REOB blends

To describe general behaviour, and not repeat the observations done in the Chapters before, a principal component analysis (PCA) will be carried out on parameters retrieved from several experimental results. The first of which will be on the found indices with the ATR-FTIR spectrograms. The found ICO, ISO, ARO, ALI, LCI, BAL and CAI indices will all be mapped in a component plot, to bring to light certain clusters that the bitumen will form.

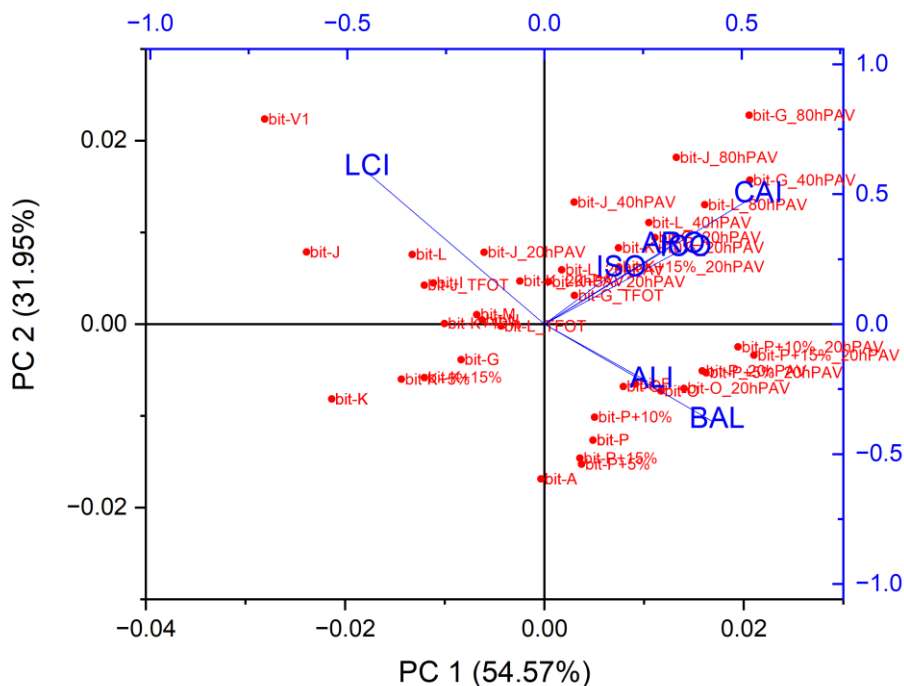


Figure 6.1: PCA analysis of FTIR retrieved parameters for unmodified, aged and REOB modified bitumen

From the figure above, one can notice that LCI will be directly negatively correlated to both ALI and BAL index measurements. This means that bitumen will either have a higher long chain index or a higher degree of (branched) aliphatic compounds present in the bitumen. Typically one can cluster the bitumen of bit-K, bit-J and bit-V1 at the higher end of LCI whereas the bitumen bit-P, bit-O, bitQ and bit-A will cluster more at the higher ALI/BAL end.

The second spread in difference between bitumen can be noticed for the ICO, ISO and ARO indices. Here one can see that they are either low or high for bitumen. Unaged bitumen generally lies lower and with ageing tends to go to the higher index values of these, with clearly the 80hPAV aged bitumen at the highest ends.

It is very clear that clustering of bitumen, differentiating between different suppliers/batches, will be possible very much using LCI, ALI and BAL indices. With the small selection of bitumen it is clear that one can get an indication of which that certain batches that come from the same supplier will truly have similar amounts of functional groups present. REOB modification does not show to initially change indices much, thus making it possible to relate it to where the base bitumen would come from, but it shows too that with ageing it will take much more drastic steps in the increase of ICO, ISO and ARO indices if higher dosages are used (this is shown by the 15% blends at 20hPAV ageing to be visible further than unmodified bitumen at 20hPAV ageing).

To complement this observation of functional group correlations, one can do something similar for the CHNOS elemental analysis results, of which the PCA is plotted below:

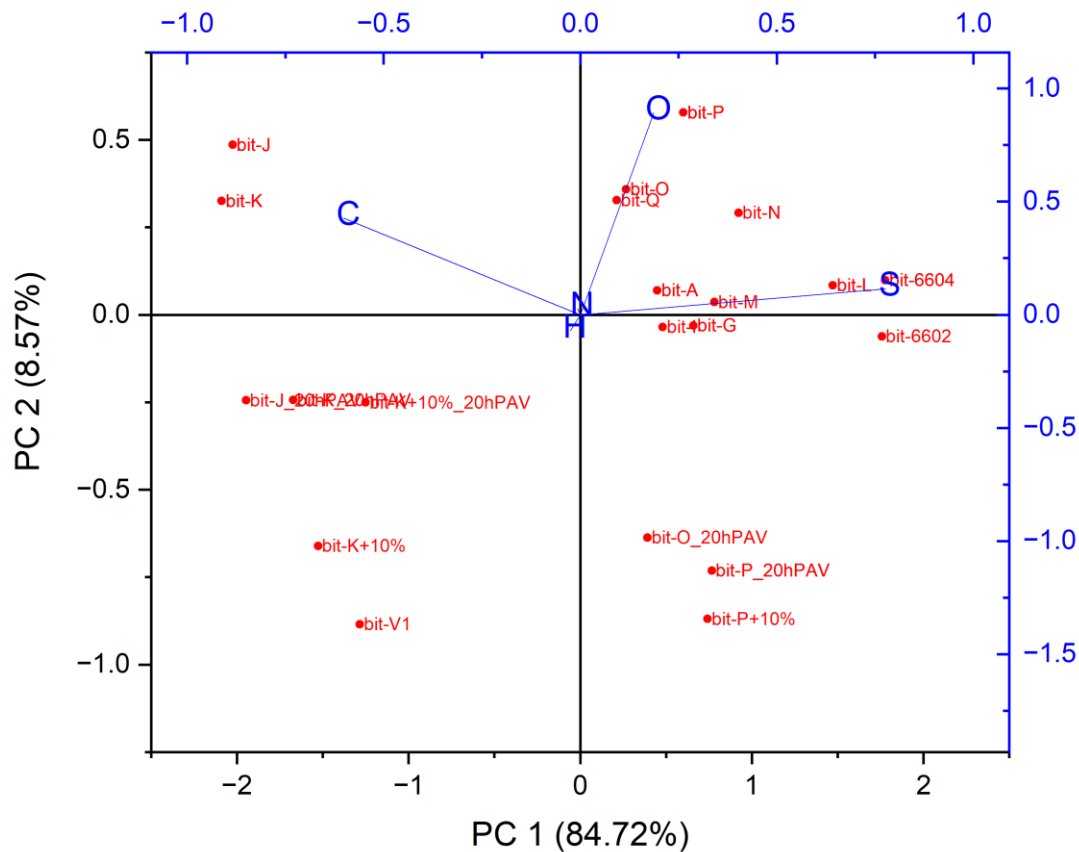


Figure 6.2: PCA analysis of CHNOS elemental results for unmodified, aged and REOB modified bitumen

Plotting the correlation of the weight fractions of these elements directly in PCA, one can obtain a clustering of bitumen again according to which suppliers have provided them. bit-J, bit-K and also bit-K+10% and bit-V1 show to have higher presence of carbon and low sulphur, although a bit lower oxygen in the case of the REOB modified bit-K+10% and the bit-V1. In stark contrast the bit-O, bit-Q, bit-A and bit-P show to initially have a medium amount of carbon and quite high amounts of both oxygen and sulphur. Ageing and REOB modification have actually shown to decrease both the oxygen and carbon ratios and increased the sulphur count more.

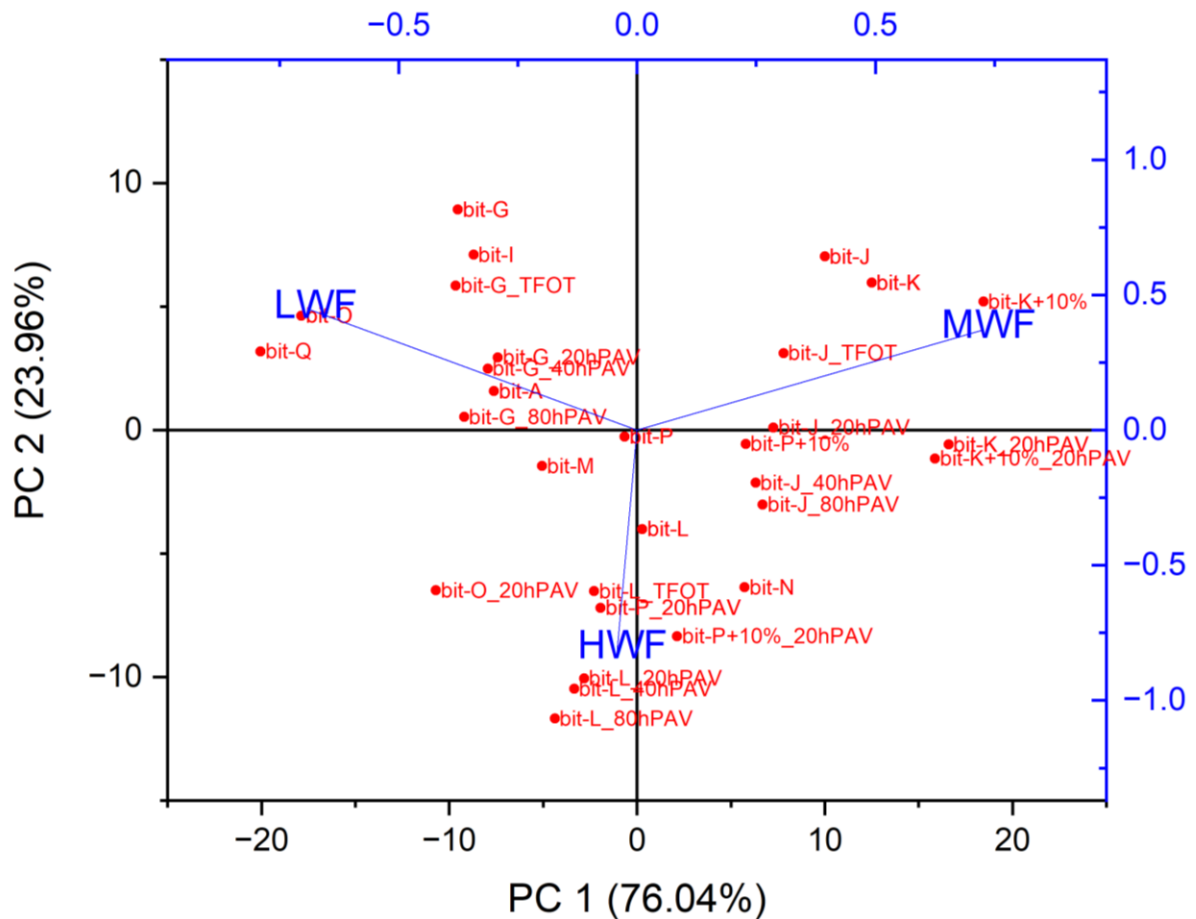


Figure 6.4: PCA analysis of weight fraction results from GPC for unmodified, aged and REOB modified bitumen

The LWF, MWF and HWF fractions that were obtained with the GPC weight distributions show in the PCA analysis some clear differences between bitumen. BitO, bitQ, bit-G, bitI and bit-A all show to have some of the highest LWF fractions. On the contrary the bit-J and bit-K show to have some of the highest MWF fractions. Other unmodified bitumen and unaged bitumen will be somewhere in between. However ageing and REOB modification shows a clear shift of these bitumen to first a higher MWF and especially after ageing a bigger HWF.

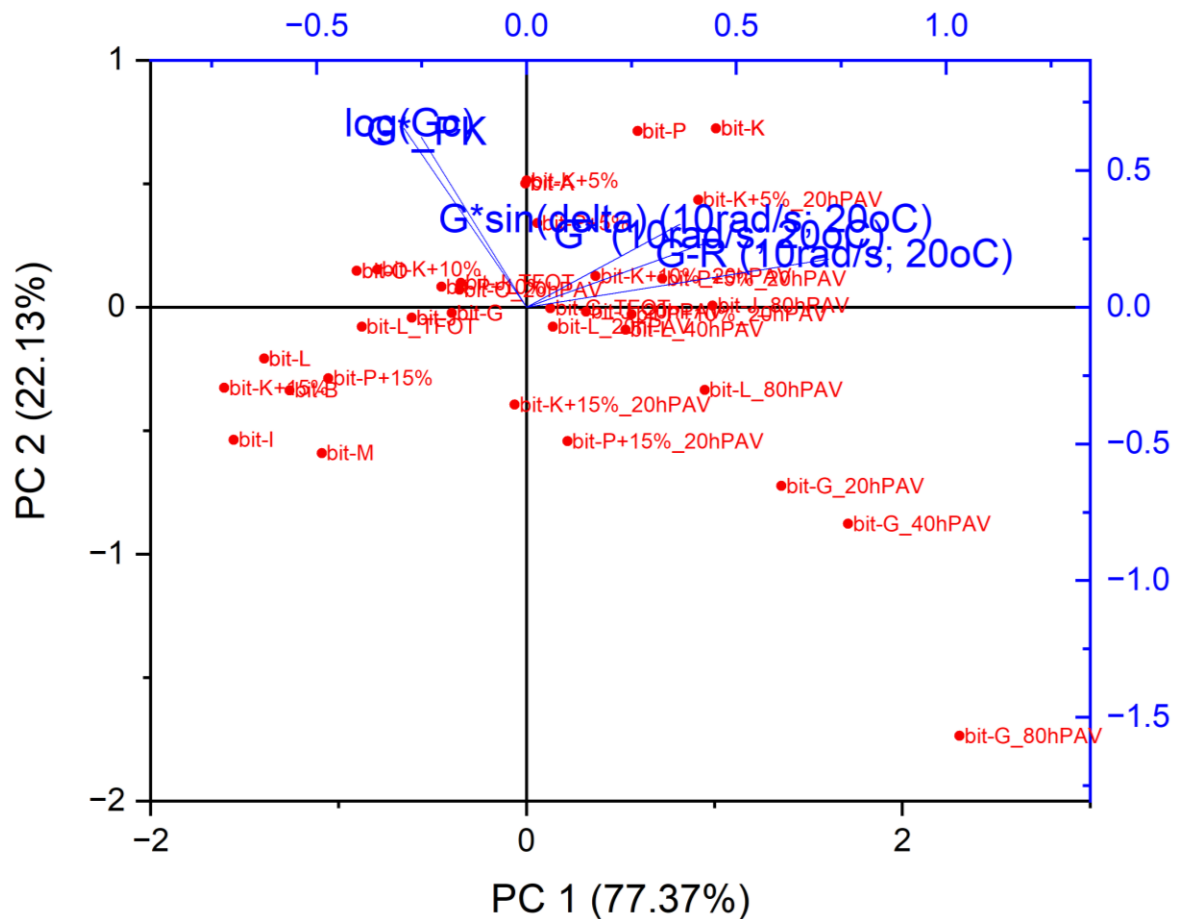


Figure 6.5: PCA analysis of complex modulus parameters from DSR for unmodified, aged and REOB modified bitumen

Cross-over modulus, the complex shear modulus at 42 [°], rutting parameter $G^* \sin(\delta)$, complex shear modulus at 20 [°C] and 10 [rad/s] and lastly the G-R parameter all show to be somehow correlated to each other. However there seems a clear shift between these values, as the cross over modulus and G_{PK} are clearly different. These are the parameters that are more so connected to lower temperature/higher frequency behaviour, higher values mean that a bitumen can still have a very viscous response (indicated by a phase shift angle being higher than 42 or 45 [°]) although it is stiff at that point. The other parameters mainly describe intermediate and higher temperature behaviour.

A spread is then noticeable in the different bitumen, where bit-G after ageing and the 15% dosage REOB modified bitumen show to have some of the lowest cross over modulus and G_{PK} values. This is generally not so good, as this means those bitumen have lost significantly in viscous response and thus indicate significant ageing.

Regarding the intermediate temperature behaviour bit-L, bit-M, bit-I, bit-B and bit-K+15% and bit-P+15% show to have some of the lowest stiffnesses. This can actually be a good thing, as it means that they are of relatively low stiffness in the cracking region, a very stiff and not sufficiently viscous material would be more susceptible to cracking.

6.2. Ageing susceptibility due to chemical composition and correlation with rheological change (FTIR-SARA-GPC-DSR)

One of the main problems for the use of bitumen, is the fact that the material can change significantly over time. The process bitumen undergoes with ageing is not fully understood and therefore there exists a wish to better understand the mechanism of ageing that it undergoes and what decides for a material to change fast or slow with ageing. This paragraph aims to bring all found results from the different tests together and find any correlations that could bring light to the most important aspects of the mechanism of ageing that a bitumen undergoes. One of the most effective ways to show ageing susceptibility, is by using ageing indices calculated in following way (Jing et al., 2021):

$$AI_{parameter} = \frac{parameter\ at\ aged\ state}{parameter\ at\ fresh\ state}$$

A high ageing index, > 1.0, means a bitumen has increased in this parameter substantially, and vice versa. An increase in stiffness with ageing would for example show in an increase in the Ageing Index. In this Chapter these ageing indices are calculated and evaluated of the parameters retrieved from FTIR, SARA, GPC and DSR tests. These indices will show how the 20hPAV ageing states for unmodified and REOB modified bitumen change, but also for the TFOT, 20hPAV, 40hPAV and 80hPAV ageing states for bit-J, bit-L and bit-G.

(FTIR)

One of the main components of ageing, is the effect of oxidation. This oxidation happens during storage, mixing and in the field and will be mainly resembled by the formation of carbonyl and sulfoxide functional groups in the bitumen. Measurements by FTIR have shown that carbonyl forms clearly linearly, but depending on the bitumen the slope of its increase with ageing degree will be different. Clearly bit-O has almost no formation and bit-L mediocre. bit-J and bit-G have quite similar increase, which is in fact quite substantial. The addition of REOB will increase the initial level of the carbonyl, but also increase its slope (thus leading to increased formation of carbonyls).

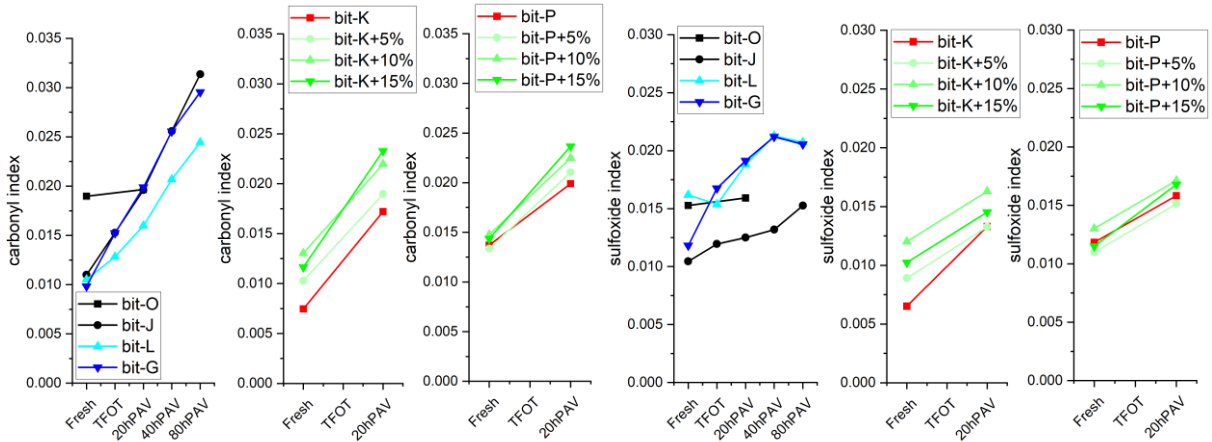


Figure 6.7: FTIR indices for the carbonyl and sulfoxide presence in aged bitumen, including REOB modified bitumen

Clearly different is the formation of sulfoxides. One can easily notice that bit-J has a very low index, which also does not increase that much upon ageing. In this case bit-L and bit-G are actually quite similar but again bit-O has a low increase in the formation of this group. REOB modification has shown that it will be able to initially increase the index substantially, especially if the index was low (in the case of bit-K). The slope of change is however decreased with ageing. The REOB surprisingly does not seem to have that much of an effect on an increased oxidation rate in the formation of sulfoxide.

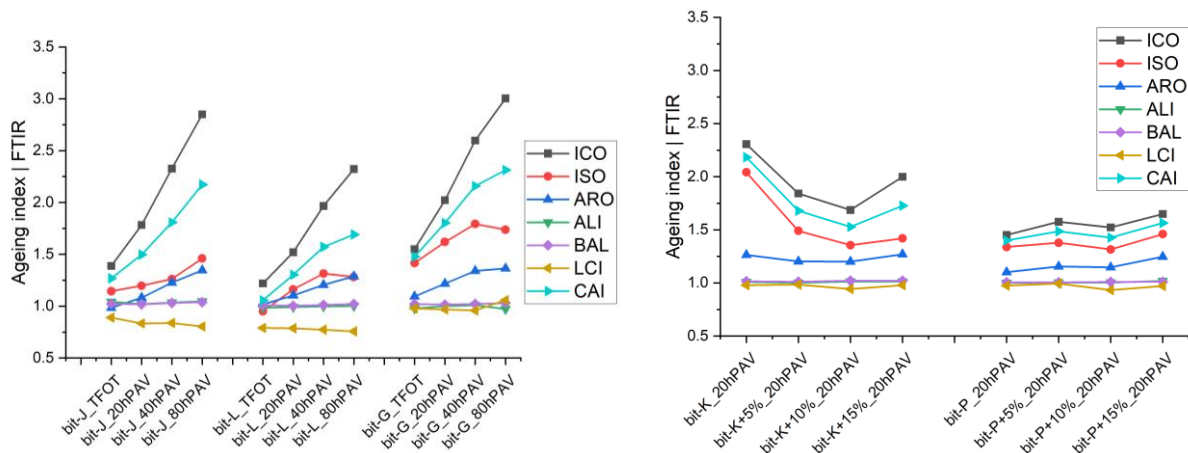


Figure 6.8: FTIR ageing indices for all the indices of unmodified aged bitumen (left) and aged REOB modified bitumen (right)

Ageing indices show that carbonyl formation is indeed affected substantially more after the REOB modification, in the case of bit-K much more than bit-P as base bitumen. The formation of sulfoxides however seems to be halted or not increased substantially with more REOB, this is completely different from the unmodified bitumen bit-J, bit-L and bit-G.

Simply put: this would mean that the effect of **general oxidation is not increased by REOB addition**, but the **formation of carbonyls specifically is**. Adding the REOB has a direct influence on carbonyl formation, which is not surprising, as the spectrograms of REOB itself already show a significant presence of carbonyl groups. The sulfoxides do not have a clear presence in REOB. Mainly two reasons are then possible:

1. The REOB adds molecules that already have high presence of carbonyls (increasing the initial level) and/or molecules that have a high susceptibility to forming more carbonyls (increasing the general rate)
2. The REOB contains other particles/atoms, like trace metals, which promote the formation of carbonyls and/or the presence of free oxygen is high, meaning that it is ready to be bound to accepting molecules.

(SARA)

Next to the drastic oxidative changes that these bitumen undergo according to the FTIR measurements, general changes in polarity occur too. The shifts happening in the SARA fractions are evaluated now. In Figure 6.9 one can see the changes of the five different indices that were evaluated before in Chapter 4.4. Colloidal instability index shows to increase always upon ageing. The rate at which this happens is different per bitumen however, showing a higher initial position but lower increase for the bit-P and bit-O binders than for the bit-K and bit-J bitumen, which start lower but have a bigger relative increase. REOB modification shows to have a significant effect on this index, suggesting there will be a mismatch after ageing in the ratio between micelle structures and the phase to disperse them based purely on SARA fractions (Lesueur, 2009).

A very clear different behaviour is observed for bit-K+10% upon ageing, clearly the formation of resins for this blend is much more substantial than the unmodified bitumen, and therefore suggests a big problem in ageing susceptibility. If there is such a drastic increase in resins, than there is an increase in asphaltenes, this will mean that with a little more ageing there shall also be a very drastic increase in asphaltenes for such binders (following the reasoning that aromatics turn towards resins and resins will turn into asphaltenes). Interestingly this problem is not at all present for the bit-P+10% binder.

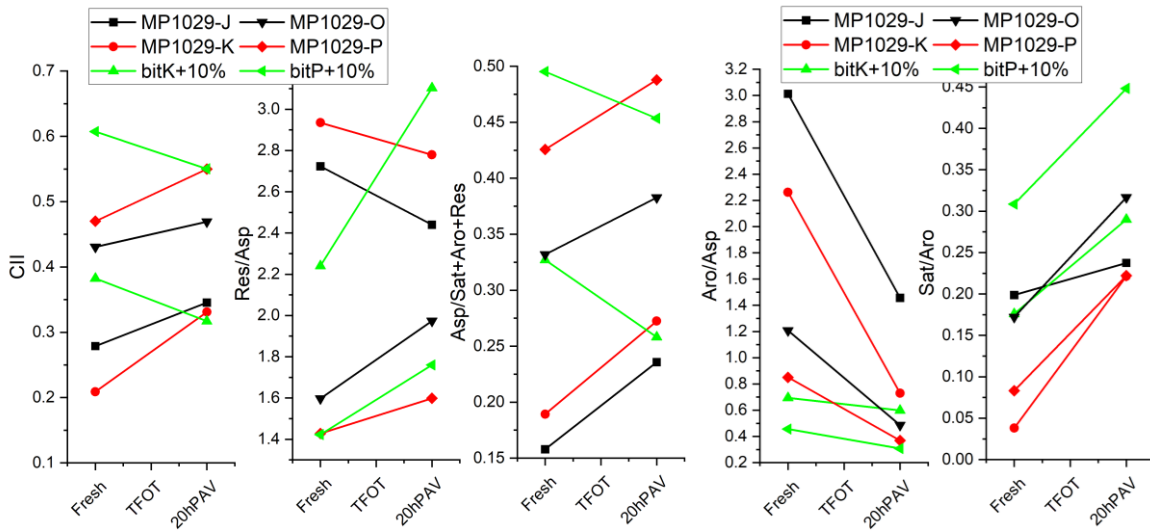


Figure 6.9: Indices retrieved from SARA fractions for aged and REOB modified bitumen

The decrease in aromatics is much more substantial for the bit-K and bit-J bitumen, and does not change after REOB modification. There is no improvement in this molecular group. There is also not a noticeable change for the bit-P and bit-O bitumen either, compared with the bit-P+10% REOB modified bitumen.

The loss of saturates fraction that has been found for the REOB and for the REOB modified bitumen, is also visible in the Sat/Aro ratio. One can see that the REOB modified bitumen are some of the highest in the initial ratio and in the increase of it with ageing. Although apparently again the bit-P+10% shows a better acceptance to the REOB modification, as its increase is actually very similar to bit-O.

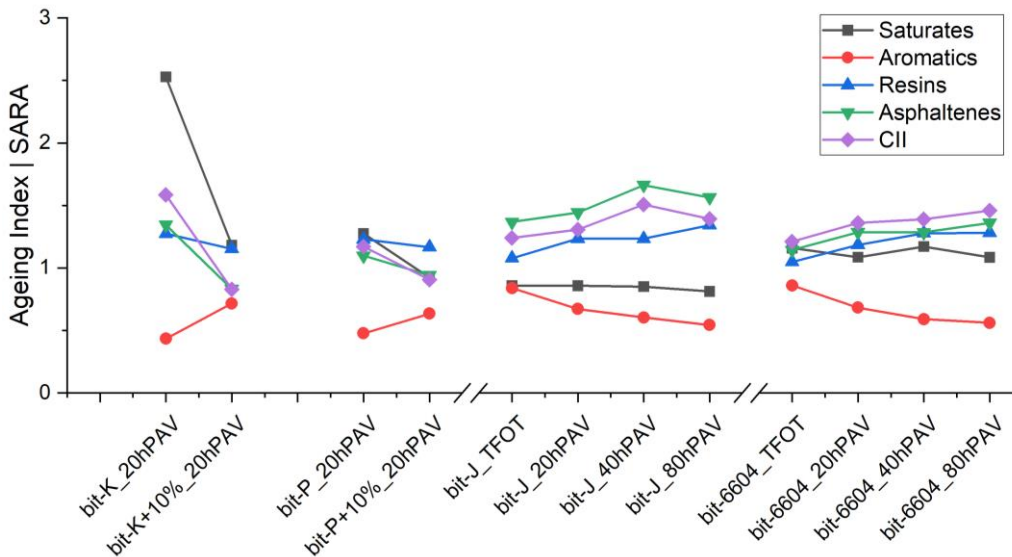


Figure 6.10: Ageing indices of the SARA weight fractions and the CII for unmodified and REOB modified bitumen

The ageing indices are able to zoom in more on the gravity of the change. Here it becomes very clear that the change in saturates was already substantial for base bitumen bit-K and bit-P and the addition of REOB made this less substantial, although this has more to do with the fact that the base bitumen already had a very low saturate content anyways. A change with ageing is therefore much more substantial. One can see something interesting however, in the case of bit-J one can see that the asphaltenes fraction undergoes the most change and for bit-6604 this is both the CII, asphaltenes and the resins. However in

the case of REOB modified bitumen one can see that the asphaltenes fraction is actually lower than that of the base bitumen and the resins fraction shows the highest change.

From this one can conclude the following:

1. The rate of the change in polarity does not seem to be accelerated; there seems to not be an increased rate of change in SARA fractions due to REOB addition
2. The saturates and aromatics fractions however are heavily impacted initially by REOB modification; the molecular composition of REOB modified bitumen is significantly different than unmodified bitumen.
3. The colloidal instability index shows to be decreasing with ageing, as both the saturates and asphaltenes fraction become smaller; this suggests that the bitumen is approaching a sol-type molecular phase structure, where thus less of an internal structure can be formed between asphaltenes and saturates; which is especially critical at lower temperatures.

(GPC)

To continue this ageing susceptibility analysis, changes in molecular weights measured with GPC are evaluated as well. Now one can easily notice how bit-L has some of the highest M_n and M_w values, and bit-G the lowest. Ageing however shows the most drastic changes happening for the bit-G, rising much more in its average molecular weights, than bit-L does, although bit-L lies initially higher. REOB modification shows to initially change the M_n and M_w averages only, where ageing shows to be of a similar order as the unmodified bitumen. However a big difference is present between two binder types where; bit-K+10% shows a significant change more close to the lower molecular weight M_n , and bit-P+10% changes more at higher molecular weights.

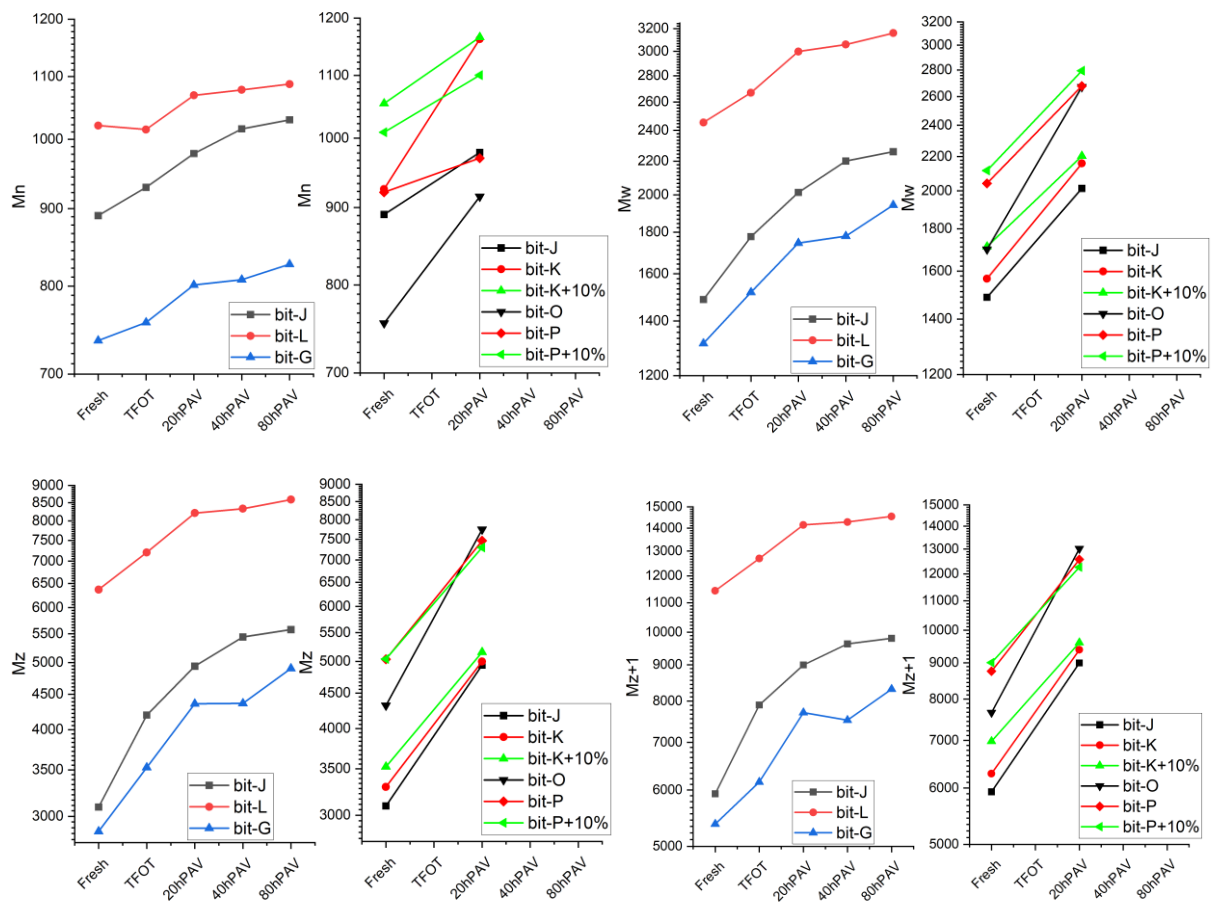


Figure 6.11: GPC molecular weight averages M_n , M_w , M_z and M_{z+1} for aged and REOB modified bitumen

This means that the base bitumen matters a lot in how the ageing behaviour will take place, although the rate at which it will, does not seem to differ too much. Interestingly the rate of change for the REOB modified bitumen seems to have lowered as compared to the base bitumen.

Comparing this with ageing indices of those previously shown weight averages shows that bit-J and bit-G change proportionally much more than bit-L. REOB modification shows that the HWF and LWF are affected a lot with ageing, as well as the M_n and M_w values.

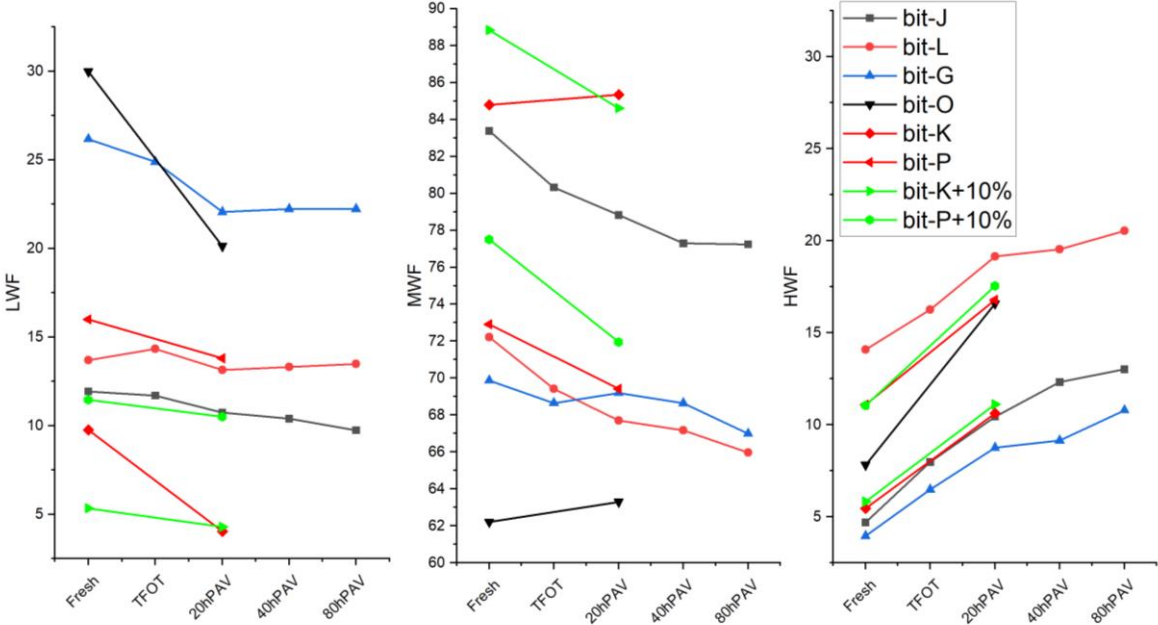


Figure 6.12: LWF and HWF ratios in [%] for aged and REOB modified bitumen

Comparing the changes in specific molecular weights (like M_n , M_w etc) to the change in the fractions within the molecular weight distribution (like LWF etc), different ageing behaviours come to light. Specifically bit-O and bit-G show to initially have a significant high portion of low molecular weights, interestingly bit-O loses this fraction substantially with ageing, as well as gaining in the high weight fraction. This seems counterintuitive, as with the FTIR and CHNO+S it was observed that this bitumen was one of the most stable and showed the least oxidation. Bit-G shows to surprisingly have the lowest change in its fractions of all bitumen, this also completely the opposite of what was observed before, as this bitumen was one of the few that had the biggest oxidation rate and underwent the most changes.

The REOB modified bitumen shows here clearly its effect on the LWF, as there is a significant initial decrease which lowers to even lower values with ageing. Especially the gain in HWF with ageing is clearly substantial too. Although the MWF shows most clearly the big decrease that the REOB modified bitumen go through. Here the effect of the REOB is initially to increase this MWF substantially as compared to the base bitumen, although after ageing it will reach easily towards the same level of the aged version of the base bitumen itself. Meaning that bit-K+10%_20hPAV comes close to bit-K_20hPAV and that bit-P+10%_20hPAV comes close to bit-P_20hPAV.

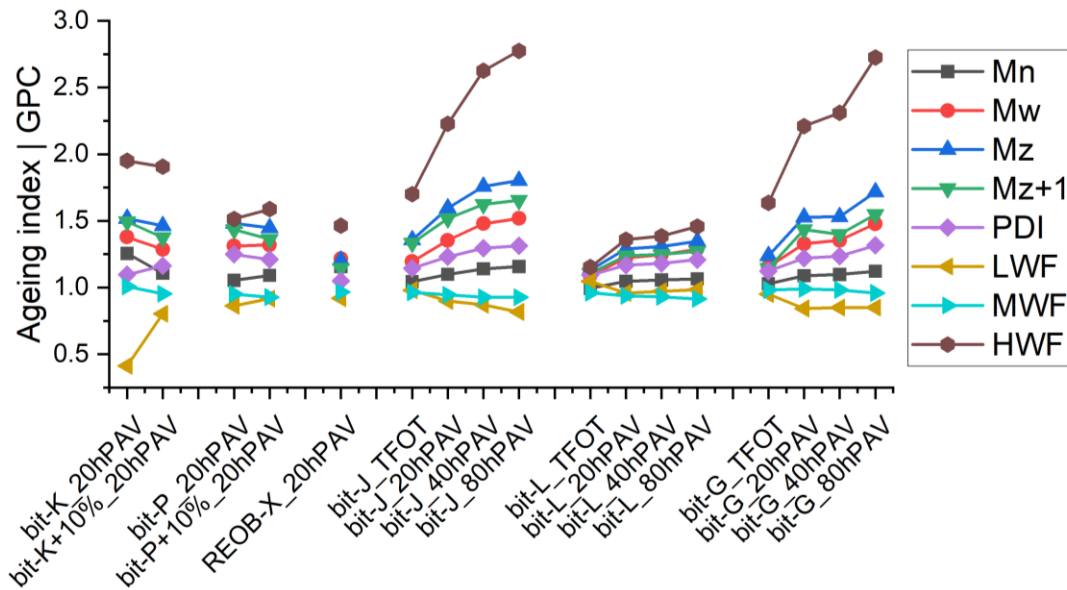


Figure 6.13: GPC molecular weight averages M_n , M_w , M_z and M_{z+1} for aged and REOB modified bitumen

The ageing indices of these same parameters confirm the same behaviours, specifically bit-L does not change much with ageing, which therefore correlates well to the oxidation rate that was found with FTIR. The base bitumen at aged state can also be compared to the REOB modified version, here one can see that apparently the LWF, or M_n and M_w actually have been slightly improved due to the REOB. Compared to the reference bitumen one can see that this improvement still does not come close to their behaviour. One can therefore conclude the following:

1. Regarding ageing susceptibility, one can notice that bitumen that already has a generally higher molecular weight (like bit-L) shows to have a slower further increase than bitumen that have an overall lower molecular weight (bit-G)
2. REOB modification has shown to not accelerate the blends molecular weight fractions in general, however the changes it undergoes in the decrease in LWF and in the increase of HWF, M_n and M_w are a bit more drastic than one can observe for unmodified bitumen.

(DSR)

Regarding rheological behaviour, the black space diagram can best depict the ageing degree of a bitumen. This has been already done in Paragraph 5.2.2 made visible in Figure 5.2, Figure 5.3, Figure 5.5 and Figure 5.6. Next to that the specific parameters that can be retrieved from these curves are already analysed in paragraph 5.2.5, therefore will not be repeated here.

Comparing the different black space diagrams of the bitumen of different sources and the REOB modified bitumen, including evaluation of parameters, one can notice the following deviations:

1. REOB modification changes all parameters linearly with increasing dosage; where the stiffness parameters are all lowered and the frequency and phase shift angle parameters are increased. Most influence of REOB modification is found for the intermediate and high temperature region.
2. Ageing of REOB modified bitumen shows an accelerated change in the parameters, when high dosages are used; this is noticeable for all three regions, where it becomes clear that the low temperature region becomes the most critical (as it has not been changed much initially)
3. bit-G has shown to overall lose the most in phase shift angle and increase in stiffness parameters, this therefore correlates well to the found chemical changes that it undergoes. bit-J has shown to increase in stiffness with marginally the smallest step size, and not lose

much in phase shift angle values. However general stiffness levels lie higher than most other bitumen for 70/100 grade. Lastly, bit-L has shown to have initially one of the lowest stiffnesses but increases with ageing significantly more than bit-J.

These observations have therefore shown a possible overlap with the chemical composition that was evaluated earlier. This will be evaluated in the following conclusion.

Conclusion on ageing susceptibility

Regarding the ageing susceptibility of bitumen from different sources one can therefore conclude the following:

1. Carbonyl growth is mainly linear, where bit-J and bit-G have a similar slope, bit-L clearly lower and bit-O almost no growth although a higher initial level. **REOB modification** does not increase the initial level significantly, although it **does increase the slope of the growth of carbonyl**. This is also much more significant in the case of bit-K than for bit-P blends. Sulfoxide growth is different, where bit-J and bit-O have almost no growth and bit-L and bit-G are quite similar and seem to reach a certain threshold. **REOB modification** seems to increase the initial number of sulfoxides, but **does not seem to influence the slope of the growth of sulfoxides**.
 - a. This could then be correlated to the difference in rheological changes between those bitumen stating that this effect of oxidation has most effect on the transition between aromatics, resins and asphaltenes. Recalling that bit-G and bit-J both have some of the lowest HWF fractions and/or lowest asphaltene fractions, it is logical that such bitumen will undergo very drastic changes after oxidation occurs on this fraction. Asphaltenes are seen as one of the most important molecular groups that contribute to the viscosity of a bitumen, therefore this would suggest that either **a very low HWF, low asphaltene fraction or both** will be **detrimental to ageing susceptibility**.
 - b. This would in fact mean there is a small buffer towards ageing and the effect of oxidation will therefore be substantial, much more than when a bitumen already has a high HWF and asphaltene fraction.
2. **REOB modification** has shown to **impact the saturates and asphaltene fraction** both, where asphaltene fraction of a REOB itself seems to be of lower molecular weight/size. Addition of such a compound will therefore **affect the asphaltene structure** that a bitumen can have, where the REOB does actually not improve the strength of it. It seems to dilute and bring the bitumen to **a sol-type bitumen**. The exceptional increase in resins fraction also would contribute to surge in the formation of small molecular weight asphaltenes with ageing, further promoting the already measured drastic changes with ageing.

To better understand what how these changes in SARA fractions and molecular weights are truly contributing to the rheological behaviour of a bitumen, the following paragraph will delve into deconvolution techniques to link the two theories together.

6.3. Ageing related to molecular weight distributions and molecular structures (GPC-SARA-DSC-DSR)

To combine the knowledge of both the SARA fractions and the GPC weight distributions, one can use the deconvolution tool to split the weight distributions in separate Gaussian curves, like the tool used for the iatrosan chromatograms used in Paragraph 4.4. The Gaussian curves are deemed to approach the weight distributions of the separate SARA fractions well, as they are shaped very similarly to the distributions found in other research (Guo et al., 2021; Lu et al., 2021).

One should already expect the SARA fractions to each have molecular weight averages around 566 [g/mol] for Saturates, 630 [Daltons] for Aromatics, 888 [Daltons] for Resins and 1937 [Daltons] for Asphaltenes (Guo et al., 2021). Which shows to be reasonably the same as what is obtained for bit-O shown in Figure 6.14, which were each: 310 [Daltons], 409 [Daltons], 900 [Daltons] and lastly the Asphaltenes at both 2244 and 15900 [Daltons].

The benefit of deconvolution of the weight distribution, means that one can have a better in-depth look into the weight distributions of the separate SARA fractions. These can, this way, never be the exact true distributions, although the deconvolution does give an rough indication for changes in specific parts of the distribution. If big differences can be noticed due to the REOB modification or ageing of the bitumen one can make a rough indication to what type of changes actually happen to the SARA fractions.

Fitting of the mentioned Gaussian curves happens under the following boundary conditions:

1. The following formula is used for the Gaussian function:

$$y = y_0 + \frac{A}{w \sqrt{\frac{\pi}{2}}} * e^{-2 * \left(\frac{x-x_c}{w}\right)^2} \quad (6.1)$$

Where one should see A as the distribution area, w as its width, x as the horizontal position on the curve and x_c as the horizontal position of the curve its centre.

2. The weight fractions that were obtained from the chromatograms measured with the iatrosan are used to represent the total areas underneath each Gaussian curve. So where the Saturates fraction was measured at 5%, one would use an “A” factor of 0.05 [-] in the Gaussian fitting tool.
3. The start of the Gaussian fitting is set for all bitumen at the following positions until a low enough R-square factor is reached:
 - Fit peak 1: representing the saturates fraction and positioned at
 $M = 566 \text{ [Daltons]} \rightarrow \log(M) = 2.752$
 - Fit peak 2: representing the aromatics fraction
 $M = 630 \text{ [Daltons]} \rightarrow \log(M) = 2.7993$
 - Fit peak 3: representing the resins fraction
 $M = 888 \text{ [Daltons]} \rightarrow \log(M) = 2.948$
 - Fit peak 4(&5): representing the (dual) peak asphaltene fraction
 $M = 1937 \text{ [Daltons]} \rightarrow \log(M) = 3.287$
 $M = 3,162.27 \text{ [Daltons]} \rightarrow \log(M) = 3.500$
4. The program is after this free in shifting the centre of the Gaussian, x_c , and changing the width of the curve, w .

Using the obtained SARA fractions, one can almost exactly obtain the weight distribution found with the GPC chromatograms using the deconvolution method and 4-5 separate gaussian curves. Bit-J and

bit-K bitumen seems to be sufficiently approached with just the four SARA fractions, but one can notice in Figure 6.14 that in the case of bit-O one needs an extra gaussian curve for the asphaltene fraction to approach a better fit.

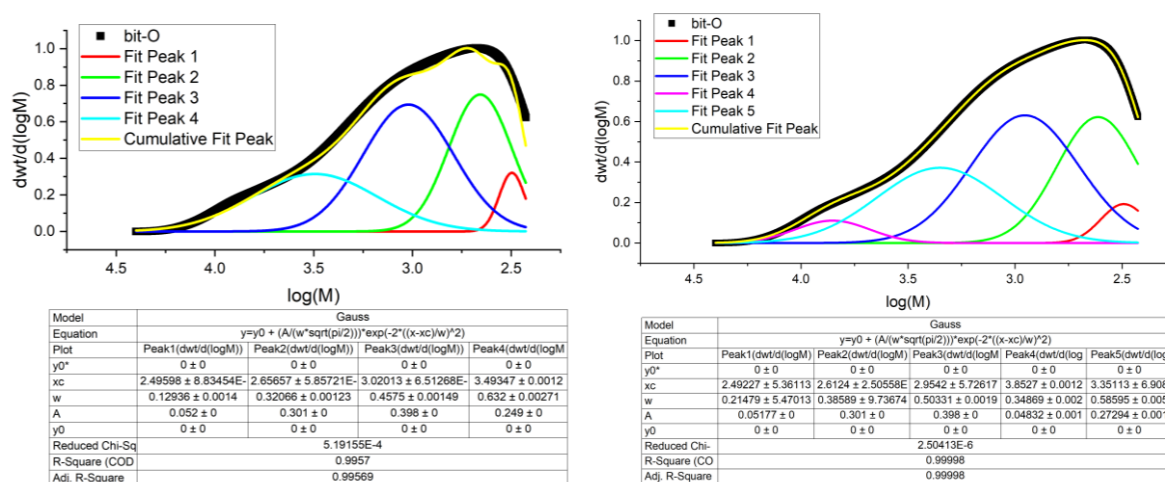


Figure 6.14: Deconvolution technique applying the SARA fractions in the GPC weight distributions; although using an extra Gaussian is necessary for the asphaltenes fraction for some bitumen

Applying this method to the other bitumen too will show the deviations and changes that occur within the SARA fractions themselves. This way the effect of REOB modification or ageing will be better explained and the hope is that more clear differences can be brought to light.

Using the found SARA fractions from the obtained iatroskan chromatograms, one can deconvolute bit-J, bit-K and the REOB modified bit-K+10% easily into four distinctive groups. With the saturates fraction always at the low molecular weight end and of small weight fraction, this red gaussian curve seems to be fitted properly. The asphaltenes fraction, becoming significantly increased with ageing, one can notice will shift in width and in area. Where the centre of the gaussian clearly starts at below $10^{3.5} \approx 3162$ [Daltons], but with ageing will lie significantly higher.

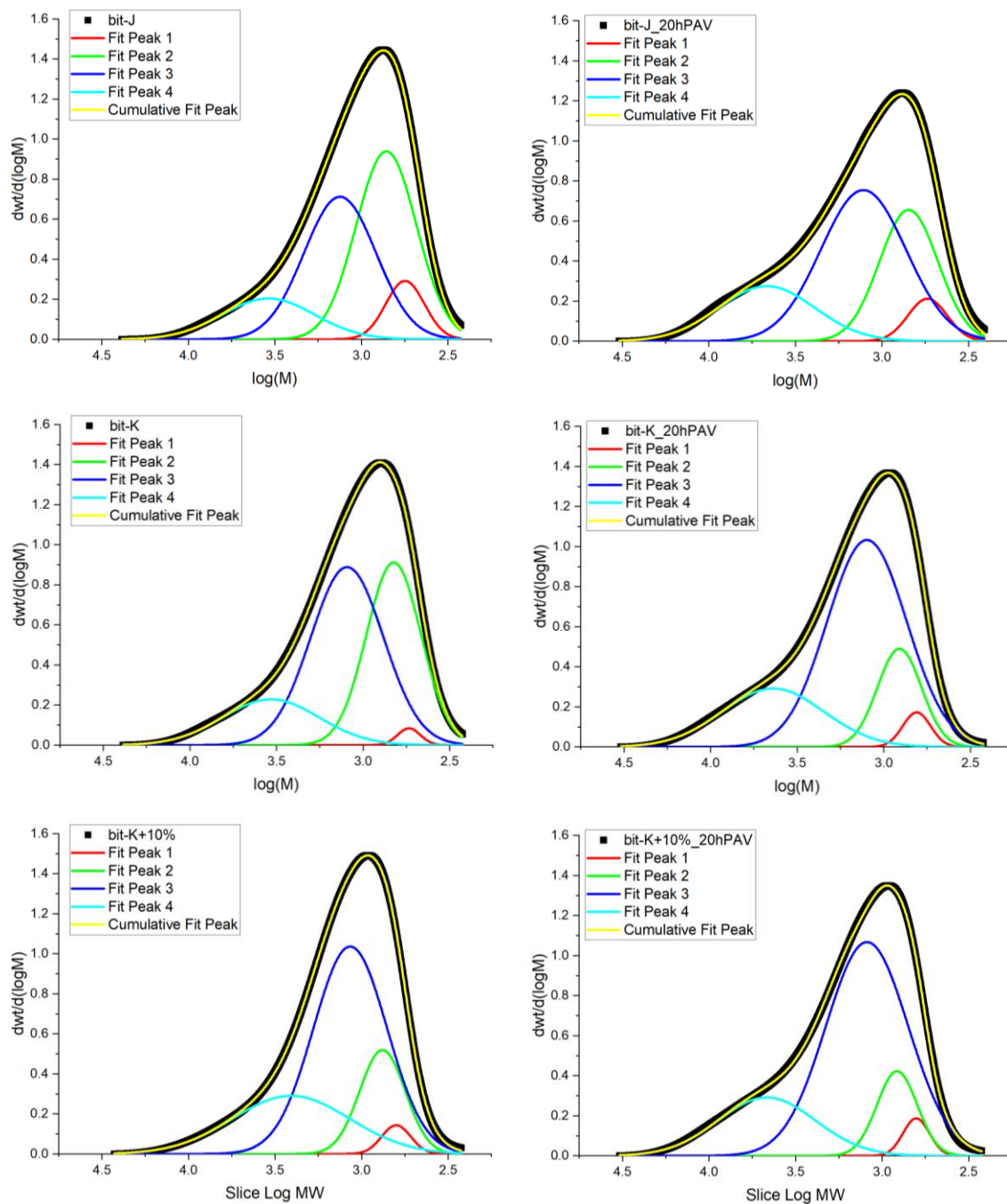


Figure 6.15: Deconvolution of SARA fractions in the GPC weight distributions of bit-J, bit-K and bit-K+10% including the 20hPAV aged variant

REOB modification very clearly increases both the resins and asphaltenes fraction. However the deconvolution brings to light that the resins fraction mainly increases in height, where the asphaltenes fraction increases in width (even to the lower molecular weights direction).

Ageing of the bitumen shows that the peak of the resins and the aromatics drastically drop. One can also notice that the width of those peaks increase slightly too. This shows both the effect of the oxidation that increases the general molecular weight of these fractions themselves, but the lowering of the peak also shows that there is a change in polarity (and thus in SARA fraction).

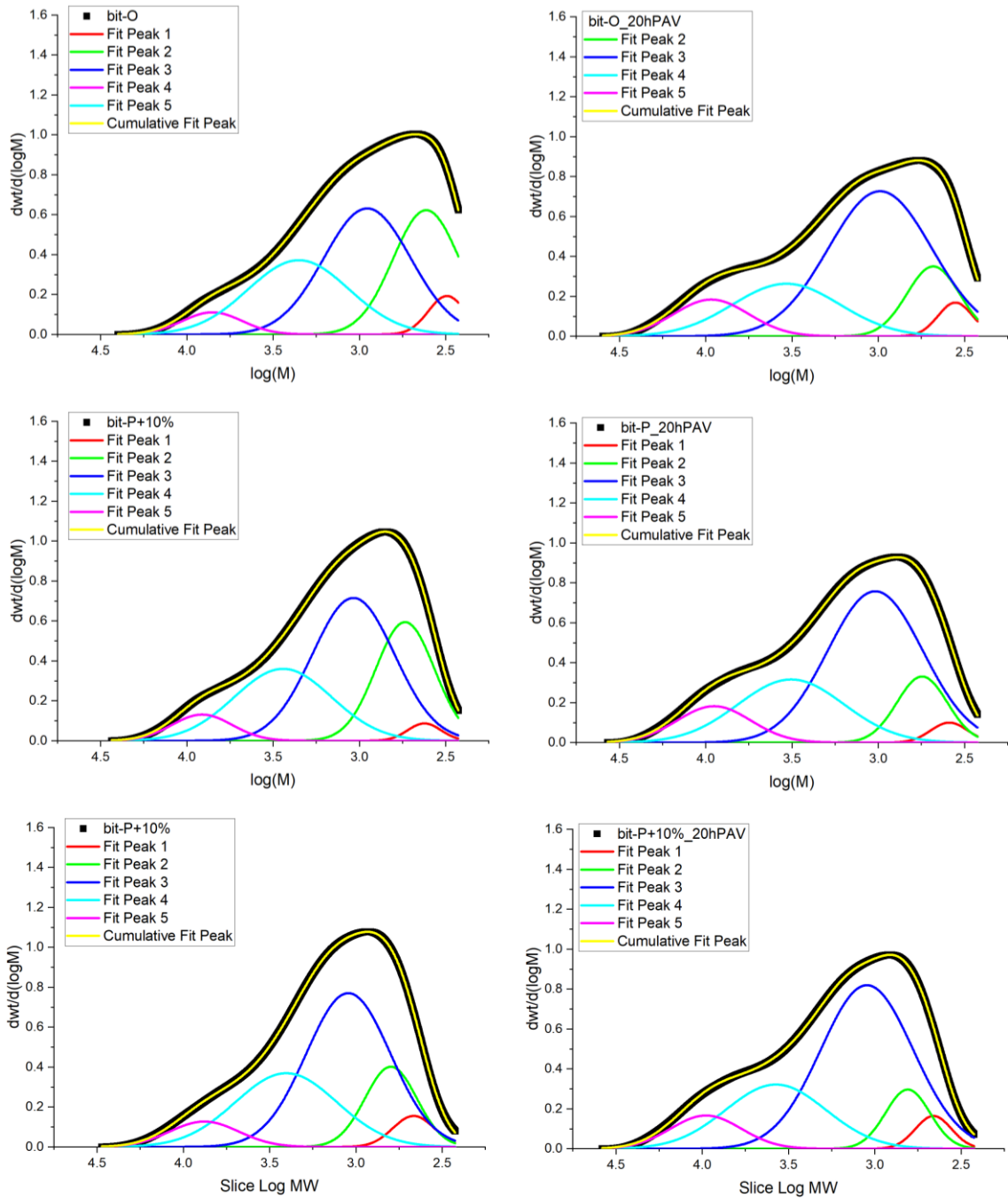


Figure 6.16: Deconvolution of SARA fractions in the GPC weight distributions of bit-J, bit-K and bit-K+10% including the 20hPAV aged variant

Firstly, before more conclusions are drawn, another bitumen will be analysed as well. The bit-O, bit-P and bit-P+10% are therefore deconvoluted as well. One can easily notice, like was shown in Figure 6.14, that the asphaltenes fraction has a significant shoulder towards the high molecular weights. This is really necessary to be included in the deconvolution fitting, to reach a fit that approaches the found weight distribution the best way possible.

Similar effects are noticed for this base bitumen, as with the bit-J, bit-K and bit-K+10% series. One can see again that REOB modification increases the asphaltene fraction, but not increasing it in height but mainly in width towards the lower molecular weights. Upon ageing these REOB modified binders again lose that extra portion in lower molecular weights, either them becoming like resins or increasing in molecular weight within the fraction.

Ageing generally means that the aromatics fraction will decrease significantly and both resins and asphaltene fractions should increase too, which is noticed for these binders as well. Generally speaking the saturates fraction should not alter much upon ageing, but can differ between binders. With all unmodified bitumen this is indeed the case. For the REOB modified bitumen one can easily notice that there is a change in the gaussian approached for the saturates fraction. The width of this fraction decreases and the peak height becomes higher. This means that different kind of saturates are present in the REOB modified bitumen, which definitely do change or possibly leave the bitumen, which alters the weight distribution significantly.

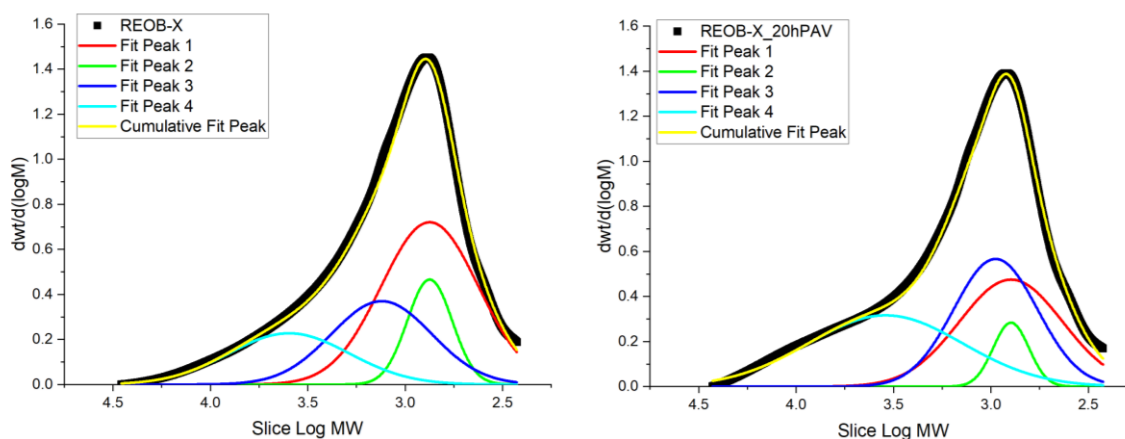


Figure 6.17: Deconvolution of SARA fractions in the GPC weight distributions of REOB-X including the 20hPAV aged variant

To further zoom in on the changes that REOB can bring to the bitumen composition, understanding the changes that it goes through itself will be valuable as well. By deconvoluting the REOB-X into the four SARA fractions, one can indeed conclude very interesting things.

First of all, the deconvolution seems to shift the fitted fractions more heavily as compared to what it does to distributions of bitumen. This brings to light how much more different the composition of REOB truly is. The fact that one can discern REOB into the SARA fractions shows here how much more different these SARA fractions truly are for the REOB than what they are for bitumen.

Upon ageing, the apparent asphaltene fraction rises. This does it by both an increase in peak height, but one can clearly notice an increase in width too. The position of the centre of the gaussian, which does not seem to move much, further suggests that no extreme changes other than oxidation and the transition of molecules from resins to asphaltenes is the case. However the saturate fraction changes very significantly different. As noticed before, it was known that this fraction decreases significantly upon ageing. The deconvolution shows however that mainly the peak decreases in height. The centre of the gaussian remains quite constant. What is clear however, is that this centre has a position very differently from the saturates present in the bitumen. One can see here that it is roughly around $10^{2.8} \approx 630$ [Daltons], whereas in bitumen it lies closer to somewhere around $10^{2.5} \approx 316$ [Daltons] for bit-O and in the case of bit-J around $10^{2.6} \approx 398$ [Daltons]. This would explain why the width increases of the saturates weight distribution, when REOB is added to the bitumen, but also why it is significantly lost after ageing. The saturates fraction decreases by a peak that decreases in height, but one can also see that the resins and aromatics fractions lie very close to this saturate fraction. Actually this makes it possible to say that there is less of a distinctive difference between the four SARA fractions in REOB, than there is for bitumen. The heavy decrease that is visible in the saturate fraction, but also the heavy decrease in aromatics, seem to be explained by the significant increase in resins fraction. The resins fraction of the REOB increases significantly in height, but it loses in its width toward the higher molecular weights. This can be explained by the transition of resins into asphaltenes, which explains the increase in width for the asphaltenes towards the lower molecular weights.

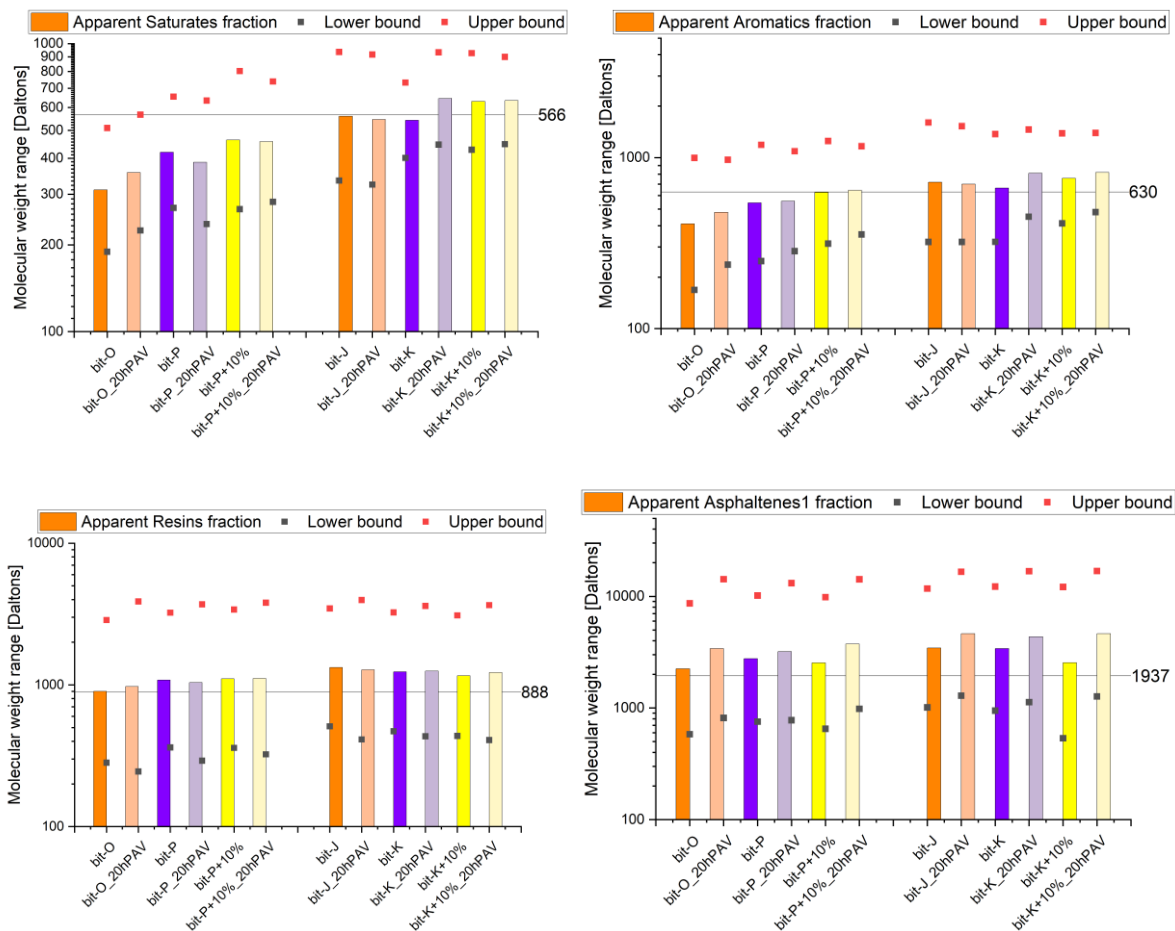


Figure 6.18: The apparent SARA fractions of the analysed bitumen showing the changes in molecular weight centres of the fitted Gaussian curves

The figure above shows the distinctive changes between the different bitumen, using the previously described deconvolution method. The apparent saturates fraction shows very drastic differences between bitumen groups bit-O & bit-P and bit-J & bit-K, while in general the bit-O & bit-P have a much lower molecular weight centre than the bit-J & bit-K bitumen. REOB modification shows to drastically increase the centre as well, as was already noted with the LWF and M_n and M_w values.

The apparent aromatics fraction shows actually a similar trend, although one can see that now with 20hPAV ageing the weight centres also shift towards higher values. Very clearly bigger shifts occur for the REOB modified bitumen, further suggesting the increased oxidation rate of such modified bitumen.

The apparent resins fraction tells a different story, when comparing bit-K and bit-P bitumen. Compared to the reference bitumen bit-O and bit-J, the stiffer bitumen bit-P and bit-K seem to have different centres. BitO has generally a lower weight centre than bit-P, although bit-J shows a higher weight centre than bit-K. REOB modification seems to have little to no effect on the weight centres as compared to the base bitumen.

Lastly, the apparent asphaltene fraction shows to be very stable around the 1937 [Daltons] weight centre. Upon ageing, all fractions show to shift to a higher molecular weight average. What is important to notice, is the fact that REOB modification initially seems to shift the molecular weight centre of this fraction downwards, but after only 20hPAV ageing one can notice that it ends up actually at a higher molecular weight than the base bitumen has at 20hPAV ageing. Here the accelerated oxidation/ageing seems to be very well represented.

6.4. Low-temperature susceptibility and behaviour (SARA-GPC-DSC-BBR-DSR)

Following from the rheological analysis, the DSR and BBR have been able to conclude which bitumen perform better and which perform worse at lower temperatures. Lower temperatures have been seen as the critical boundary for cracking susceptibility as well as a risk for ravelling of porous asphalt. A typical poor performance of a bitumen at cold temperatures, will be mainly determined by having a poor viscous property; i.e. having bad relaxation capabilities and creating more risk of brittle fracture.

The nature of low temperature susceptibility, or in other words brittle failure and cracking susceptibility, can be attributed to several factors:

1. High sensitivity to temperature changes; i.e. changes in phase structure
2. High oxidation rate; loss of initial flexibility
3. Loss of volatile components; lighter components that initially contribute to the flexibility
4. Chemical composition & molecular structure
5. Interactions with the aggregate, i.e. stress concentrations (in the case of mixture failure)
6. Asphalt mixture undergoing thermal cycles; i.e. repeated cycles of expansion, contraction and thus the formation of many microcracks

With the currently carried out and analysed tests, mainly points 1 and 4 are deemed to have an effect on the obtained results of DSR and BBR, and will be combined in the following analysis on **high sensitivity to temperature changes; i.e. changes in phase structure because of chemical composition and molecular structure.**

This problem can be reduced to the principle of bitumen acting in a sol- or a gel-phase manner, which can result from different chemical compositions in the bitumen. Hereafter the measurements done by DSR, DSC, GPC, SARA and BBR are evaluated to explain microstructural level changes in the bitumen and look if specifically the phase structure is leading in the poorer performance at lower temperatures. The rheological measurements performed with DSR have concluded, using the Cole-Cole diagrams to zoom in on low temperature performance, that some bitumen perform drastically better than others. The figure below depicts this difference clearly:

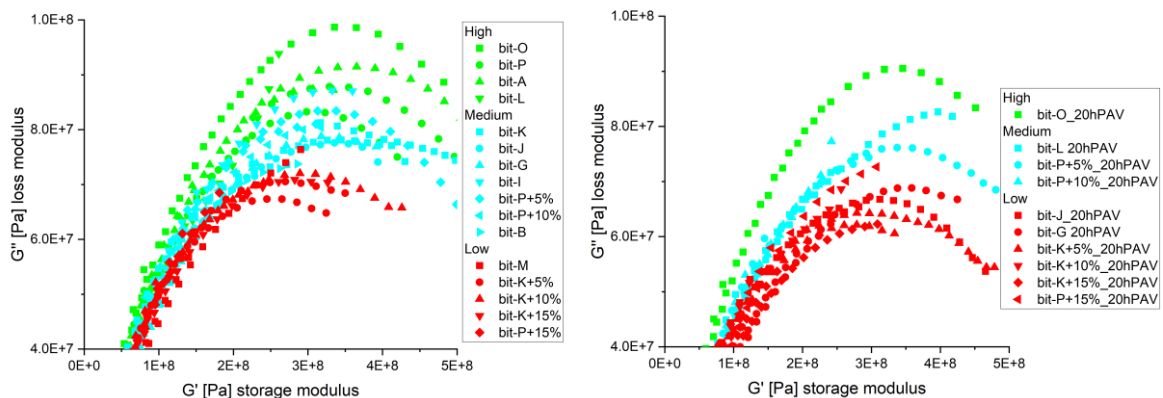


Figure 6.19: Cole-Cole diagrams showing low temperature susceptibility for unaged bitumen (left) and 20hPAV aged bitumen (right)

One can see that the glass phase for REOB modified bitumen is more easily reached, as well as this phase representing a much less flexible state of the microstructure of the bitumen, made visible by the lower loss modulus which is reached at a lower storage modulus. This significant limitation in loss modulus means that those bitumen have a much lower relaxation capability than for example bit-O.

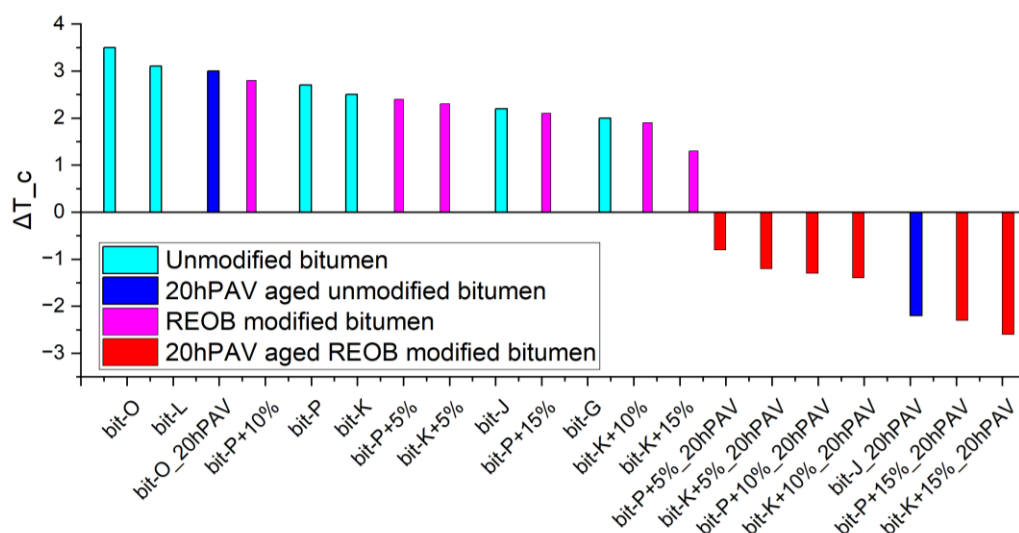


Figure 6.20: ΔT_c values of unaged, aged and REOB modified bitumen showing the low temperature susceptibility

An ordering of the low temperature performance in the BBR can be retrieved from that test and is shown by the ΔT_c in Figure 6.20. It is clear that the ΔT_c values are sufficiently high enough for all unaged bitumen, including the REOB modified bitumen, although the 20hPAV ageing shows that REOB modified bitumen and bit-J are very susceptible and change significantly in their relaxation capabilities at low temperatures. Bit-K+10% bitumen blend shows to be more susceptible to this than the bit-P+10% after 20hPAV ageing.

To find if any chemical parameters could have contributed to this totally different behaviour, one should find which chemical indices are higher for bit-O and bit-L (which perform exceptionally well on low temperatures) and which chemical indices are lower for REOB modified bitumen, bit-J and bit-G.

In Figure 4.12 one can notice that bit-L and bit-O have some of the highest aliphatic indices, these are somewhat a bit lower for all other bitumen and specifically bit-G shows a decrease of this index upon ageing. Typically the aliphatic index indicates the contribution of the “aliphatic solvent” matrix, in which non- and aromatic molecules can be solved (X. Yu et al., 2019).

The colloidal structure could therefore be compromised, indicating a risk for a gel-phase instead of a sol-phase of the bitumen, or vice versa (Karki & Zhou, 2019; Lesueur, 2009). Generally a bitumen in sol-phase is much more favourable at low temperatures, and the colloidal instability index obtained in Chapter 4.4 shows actually for these bitumen that bit-J is very low, bit-G is a bit higher but bit-O is actually one of the highest. Upon ageing one can notice that bit-J increases significantly in this index and bit-O does so less, but this does not explain the exceptionally better behaviour of bit-O. Next to that, for the REOB modified bitumen the CII does not seem to be increased initially much and does lower drastically upon ageing. Which is not deemed very logical, as it was shown previously that REOB and WEO modified bitumen do become a gel-type bitumen and therefore risk low temperature cracking failure (Freeston et al., 2015; Johnson & Hesp, 2014).

The DSC measurements have shown that bit-O, bit-P and bit-P+10% were bitumen with only a pair of glass transitions, also showing very small shifts of these transitions upon ageing. Bit-M, bit-N, bit-J, bit-K and bit-K+10% however have all shown much more glass transitions. This could thus be related to much more complexity in chemical composition and therefore the reached phase structure at the low temperature represents a totally different chemical composition than before. bit-L has also shown to reach a T_g3 , but it was of very small ΔC_p and there is no T_g4 . This clearly indicates that one can expect significantly different behaviours between the mentioned binders, shown already by the DSR results.

Typically one can say the following about bitumen changing its phases (Okhotnikova et al., 2020):

- At low temperatures (around -42°C to -14°C):
Low molecular weight saturated hydrocarbons form a weakly ordered phase in bitumen.
- In the middle temperature range (around -10°C to 70°C):
High molecular weight saturated hydrocarbons create an ordered phase within bitumen.
- At high temperatures (around 70°C to 90°C):
Asphaltenes form an amorphous phase in bitumen.

This shows specifically that, in the middle range temperature, the high molecular weight fraction matters the most for the phase transitions T_{g2} , T_{g3} and T_{g4} and the glass transition T_{g1} is more influenced by the lower molecular weights. One should thus remember that temperature has a huge effect on the phase of the microstructure, therefore a sol/gel phase structure at a certain temperature could be totally different at another temperature. DSC can directly point this out.

To make all these observations clearer, the following overview can be given of sol/gel phases, weight fractions, colloidal instability and phase transitions:

1. **Colloidal instability** is described by the ratio between saturates + asphaltenes and aromatics + resins and the following can be said about it (Lesueur, 2009):
 - a. A high value indicates a colloidal system where a big clustering of asphaltene like hard micelle structures are poorly distributed in the solvent matrix: i.e. **gel-type bitumen**
 - b. A medium value indicates a good micelle structure where the micelle structure is well distributed but can still form an internal molecular structure that can take on forces: i.e. **elasto-type bitumen**
 - c. A low value alternatively indicates a colloidal system where the solvent matrix is very big and the micelle structures are very diluted and distributed: i.e. **sol-type bitumen**
2. **Molecular weight distributions** give an indication on what typical molecular weights and sizes can be expected for each SARA fraction too, as seen in paragraph 6.3, which is describing (Weigel & Stephan, 2018):
 - a. Higher weight fractions correlate well to the asphaltene portion in a bitumen, therefore a high value of HWF will indicate that the asphaltenes are of high molecular weight/large molecular size and vice versa:
i.e. the present **micelle structure** heavily depends on **molecular size of asphaltenes**.
 - b. Lower weight fractions correlate well to the saturates and aromatics portion in a bitumen, meaning that LWF will give an indication of the low molecular weights/small molecular size of these type of molecules:
i.e. the **dispersion** of the **micelle structure** is correlated to the **molecular sizes** of the **saturates and aromatics** fraction.
3. **Phase transitions** show if a bitumen goes through a transition of microstructural change, with which it indicates it will have a different microstructural response to forces exerted on it at the temperatures above and below that certain transition temperature (Kriz et al., 2008):
 - a. A bitumen with a **many phase transitions** shows that its microstructural behaviour will be drastically changing and the different phases show how certain molecular groups will be more dominant than others i.e. having many phase transitions at medium temperatures show that the solvent matrix/**maltenes fraction is large and a complex combination of medium weight fraction** molecules.
 - b. A bitumen with **few phase transitions** shows to have more stable phases that are equally distributed: i.e. having few or no phase transitions at medium temperatures show that the solvent matrix/**maltenes fraction is small** and a **well compliant mix of medium weight fraction molecules**

Recalling the measurements of GPC, the following plot should show the deviations in molecular weights that would explain the found changes in glass transitions.

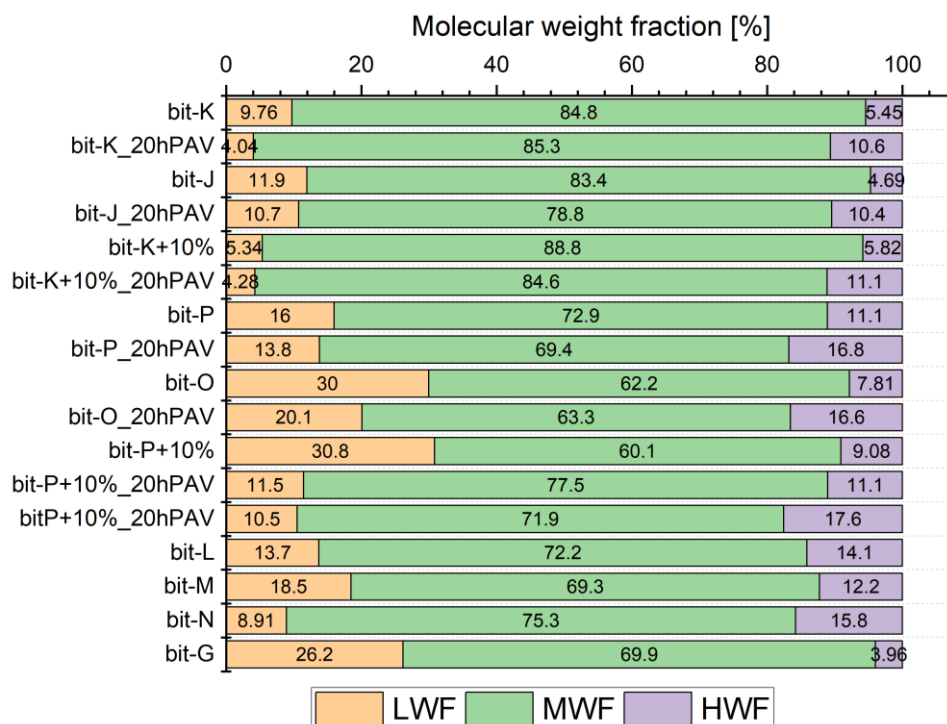


Figure 6.21: Molecular weight fractions for bitumen also tested with DSC with boundaries set 500 and 4500 [Daltons]

The obtained deviations in weight fractions should then be correlated to the distribution between different molecular structures, describing the changes in polarity, by SARA. Which brings to light the following:

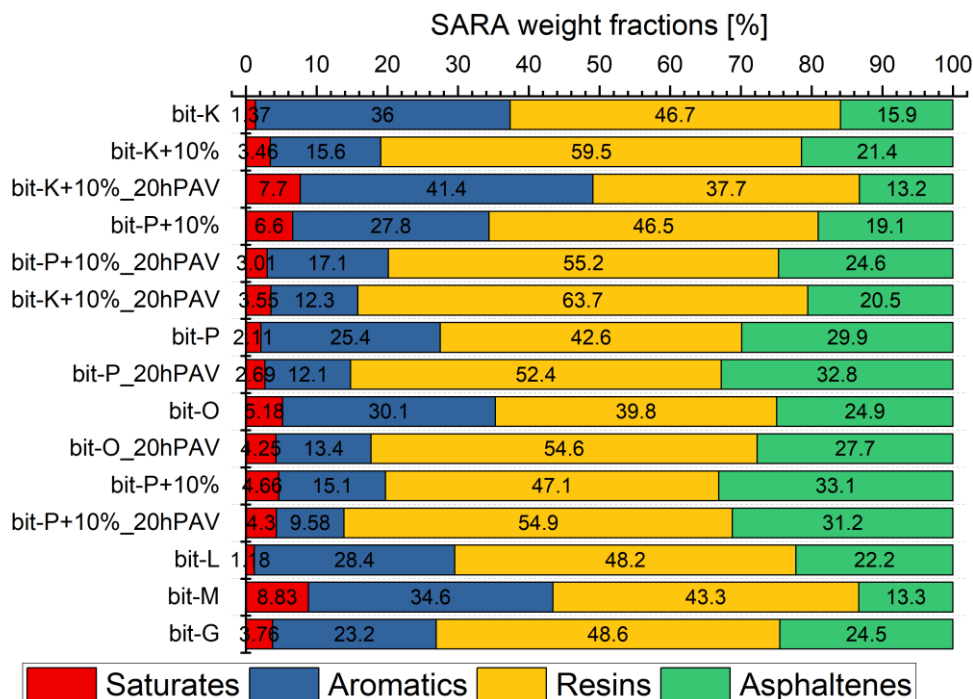


Figure 6.22: SARA fractions for bitumen also tested with DSC

To give an overview of the described behaviours and measurements for several specific bitumen, the following table is presented. The CII is used indicates the sol/elasto/gel phase structure; low index value indicating a sol-phase and vice versa. The HWF indicates the elastic strength of the micelle structure; bigger molecules allow for a stronger structure. Lastly the LWF indicates the solvent mobility at lower temperatures; a high amount of smaller sized molecules shows a good ability for the bitumen to remain mobile at lower temperatures.

Table 6.1: Overview of the determination of sol or gel type bitumen

Bitumen	PEN grade/aged state	CII	Phase structure: Sol/elasto/gel	HWF	Micelle structure strength	LWF	Solvent mobility
bit-K	(20/30)	0.2089	Sol	5.45	Low	9.76	Bad
bit-J	(70/100)	0.2644	Sol	4.69	Low	11.94	Bad
bit-K+10%	(40/60)	0.3824	Elasto	5.82	Low	5.34	Very bad
bit-K	20hPAV	0.3310	Sol	10.62	Medium	4.04	Very bad
bit-J	20hPAV	0.3454	Sol	10.45	Medium	10.74	Bad
bit-K+10%	20hPAV	0.3170	Sol	11.11	Medium	4.28	Very bad
bit-P	(15)	0.4699	Gel	11.08	Medium	16.00	Good
bit-O	(70/100)	0.4306	Elasto	7.81	Medium	29.98	Very good
bit-P+10%	(40/60)	0.6072	Gel	11.05	Medium	11.45	
bit-P	20hPAV	0.5498	Gel	16.78	High	13.80	Medium
bit-O	20hPAV	0.4692	Gel	16.58	High	20.12	Good
bit-P+10%	20hPAV	0.5503	Gel	17.55	High	10.50	
bit-L	(70/100)	0.3053	Sol	14.09	Medium	13.70	Medium
bit-G	(70/100)	0.3937	Elasto	3.96	Low	26.17	Very good
bit-M	(70/100)	0.2847	Sol	12.24	Medium	18.48	Good

The molecular weight fractions of bit-K, bit-J and bit-K+10% bitumen shows to be mainly governed by the MWF. This means that phase structures evaluated with DSC will grow more according to this fraction than according to the others. Effectively this means that the saturates and aromatics, because of the very low LWF fraction, and the asphaltenes, typically contributing the most to the HWF fraction, will have very little impact of the microstructural phases.

It was also observed that especially the saturates and asphaltenes fractions itself for these bitumen is exceptionally low. This has also been shown by the applied deconvolution method in Chapter 6.2, concluding for phase changes that these bitumen will tend to have phase transitions mainly determined by the solvent fraction, the aromatic & resin part of the bitumen.

Recalling the effect of REOB on both the weight distributions and the SARA fractions, this effect will be increased even more. As the REOB will further decrease LWF and actually add saturates of generally higher molecular weights, thus of a different nature than standardly present in bitumen. This would explain the shift for T_{g2} , T_{g3} and T_{g4} towards lower temperatures.

- This suggests that bit-J and bit-K are heavily inclined to act initially like sol-type bitumen. When REOB is added for bit-K+10% the present saturates and asphaltenes fractions actually are increased in the solvent matrix of aromatics and (mostly) resins. The asphaltenes in REOB are of different nature however and the structuring of this fraction will therefore actually be worse, indicating a weaker micelle structure. Ageing will actually worsen this problem even further, as the present asphaltenes will now oxidise and the REOB added saturates will leave/change in the bitumen, therefore the sol-type phase will be more governing and elasticity of the bitumen will be worse. This poor structuring of asphaltene micelles in the solvent matrix can actually lead to brittle fracture, as this type of bitumen cannot take on forces well and will deform poorly.

A completely different picture can be drawn for bit-O and bit-P, as these bitumen have much higher values of HWF and LWF. This means that the saturates and aromatics, well correlated to the LWF, are much more pronouncedly present in this bitumen. Meaning the glass transition and the intermediate phase changes will be of a different nature completely, which was indeed noticed in DSC scans. Asphaltenes are significantly more present, while being of higher HWF nature. A higher amount of asphaltenes could reduce the effect of phase structures appearing at intermediate temperatures and describe why the bit-P and bit-O have no T_g3 and T_g4 in the obtained DSC heat flow diagrams. The addition of the REOB does therefore have an expectable effect. The LWF of bit-P was sufficiently high to keep the saturates and aromatics fraction more present as compared to bit-K+10%. The HWF being already high, makes sure that the asphaltenes are enough present to prevent the maltenes to create more phase transitions next to the T_g1 and T_g2 .

- This mainly suggests that bit-O and bit-P, having a better representation of the saturates and asphaltenes (also shown by the higher CII), will be more of a gel-type nature. The higher saturates and asphaltenes fraction, also being of a higher molecular weight ratio, will be better dispersed and interconnected in the solvent medium which the aromatics and resins provide. This means these bitumen will be generally more stiff and have high viscosity at lower temperatures, suggesting a higher risk to brittle failure. Performance of bit-O suggests however that it has not reached such a limit and one can say that it actually remains perfectly in the middle of sol/gel behaviour. The LWF seems to be big enough to disperse this stronger micelle structure.

REOB modification disturbs this good dispersion though, increasing the amount of solvent with more resins but also making this solvent of higher molecular weights, increasing this effect on the microstructure, while giving lower molecular weights asphaltenes to the micelle structure. Lastly, the saturates and asphaltenes that are added with the REOB are of such a different nature that the micelle structure will be affected significantly.

The REOB initially makes the base bitumen bit-P from a gel-type into a stiffer gel-type bitumen, although with ageing the saturates are lost and therefore it decreases again to more sol-type behaviour.

bit-G and bit-M have shown to differ in low temperature susceptibility as well. These bitumen, being very sensitive to the lower temperatures according to the Cole-Cole diagrams, show to have a very high LWF but also a very low HWF. This shows that the saturates and aromatics fraction, are of low molecular weight nature, although the asphaltenes, being also of very low molecular weight nature, will have a different contribution as compared to other bitumen.

- The small saturates fraction and the large, but of low molecular weights, asphaltene fraction will therefore disperse well in the aromatics and resins solvent matrix. This means this bitumen will act more like a sol-type bitumen, while also having a very weak micelle structure of small molecular size asphaltenes. Relaxation capabilities will therefore be much more compromised.

Lastly the bit-L bitumen has shown quite similar low temperature behaviour to bit-O, both in DSR and BBR. Therefore one should expect this bitumen to be of sol-type. Looking at the molecular weight distribution it is known that the LWF and HWF fractions are both significantly present. While at the same time the saturates + aromatics fractions are combined significantly representing the LWF, while the asphaltenes fraction is also significantly high. This means there is an equal combination between weight fractions and SARA fractions.

- This means the CII but also the general weight distribution of bit-L both suggest that this bitumen acts like an intermediate sol/gel-type bitumen, although because of the generally higher molecular weights, is much more close to becoming too stiff as compared to bit-O its composition.

6.5. Conclusions on intrinsic properties, ageing susceptibility, colloidal structure related to molecular weights and low temperature susceptibility

The principal component analysis (PCA) has been effective in showing intrinsic chemical and rheological properties between different bitumen, where especially the FTIR and CHNO+S measurements were able to cluster bitumen which came from the same suppliers. The PCA plots on SARA fractions, GPC molecular weight fractions and rheological parameters have been able to show extremes between bitumen, where changes because of ageing or REOB modification become clear in what general effect they have.

Evaluating the ageing susceptibility of the different bitumen has shown that REOB modification mainly alters the oxidation rate for the formation of carbonyls and not sulfoxides. The accelerated ageing of REOB modified bitumen at high dosages, seems to be related to the significant impact on the saturates and asphaltenes fractions, as the saturates fraction decreases (less stable than unmodified bitumen) and the asphaltenes fraction seems to be of a significantly different order. It seems that, like with bit-J and bit-G, the molecular structure that the asphaltenes can form is heavily impacted when either the asphaltene fraction is low or the HWF is not high. REOB modification also has a direct impact on this as the asphaltene fraction is significantly different.

To evaluate this further, deconvolution has been applied on the weight distributions retrieved with GPC in combination with the SARA fractions measured. This therefore gives an indication of the molecular weight distributions of each separate fraction itself. Here it became clear that bit-O and bit-P had significantly lower molecular weights for their apparent Saturates and aromatics fractions. The apparent resins fraction was actually similar for most bitumen. However especially the apparent asphaltene fraction has shown significant changes after REOB modification, this therefore correlates well to the observation done before in the ageing susceptibility paragraph. A critical conclusion on this would therefore be:

- **The asphaltene fraction and its molecular weight** seem to be related to how it can form internal structures within a bitumen; this is **heavily impacted by REOB modification** and could explain why the bitumen **ages in an accelerated way**.

Next to ageing susceptibility, the increased loss in relaxation capabilities found with DSR and BBR for REOB modified bitumen is also a critical aspect in performance of a bitumen. This has been evaluated further, and like with the ageing susceptibility, this seems to be related to the SARA fractions and weight distributions.

Especially the colloidal stability index, combined with LWF and HWF, has been effective in showing why bit-J and bit-G are much more critical to brittle failure and a loss in relaxation capability. This has then also shown why REOB modified bitumen become so much more susceptible to lower temperatures as well. The main conclusion is that REOB modifies a bitumen into a gel-type bitumen and that the micelle structure is affected by the asphaltene portion added by the REOB. A critical conclusion on this would therefore be:

- The REOB causing initially a **transition of a sol-type towards a gel-type**, but also **negatively affecting the strength of the micelle structure** will be **detrimental to low temperature resistance**.
- **Ageing of REOB modified bitumen** suggests that another mechanism occurs in REOB modified bitumen, as saturates decrease significantly and asphaltenes are of a different kind, the **colloidal stability is very much compromised** and ageing will make a REOB modified bitumen **more prone to brittle failure** and **reduce relaxation capabilities**. This is heavily supported by previous research that went into detail on SARA and AFM measurements on REOB modified bitumen (Karki & Zhou, 2019).

Chapter 7. Mechanical characterization of REOB modified bitumen, mastic and asphalt mixtures

Next to the chemical and rheological analysis of bitumen, the goal is to relate this to ultimate performance in the field as asphalt mixtures. The bitumen, as key component in asphalt pavement mixtures, acts as the binder and is wished for to perform well on adhesive & cohesive strength but also on cracking, ravelling and moisture susceptibility.

To tackle adhesive and cohesive properties of a bitumen, the DMA (dynamic mechanical analyser) will be used to pull apart a bitumen film between two stones and to test mastic (bitumen mixed with filler). This will show low temperature and ravelling susceptibility and compatibility with fillers.

To tackle cracking ravelling and moisture susceptibility, asphalt mixtures will be made and tested with several tools. With a gyrator compactor the workability of a mixture (specifically the compactability of a mix) will be analysed, the IDT test will be carried out on dry and wet conditioned samples and lastly a few mixture slices will be tested with the Cantabro Abrasion test, to indicate impact resistance of the mixture and its resistance to freeze-thaw conditioning.

7.1. DMA adhesive & cohesive analysis

7.1.1. Adhesive/cohesive stone-bitumen-stone column DMA tensile pull test

The addition of lubrication oils to bitumen seems contradictory to improving adhesion properties of a binder. Adding a lubricant, which has the sole purpose to reduce wear and prevent friction between engine parts, one would not expect that its effect on the adhesive properties of a bitumen will be beneficial. No direct research has yet been produced zooming in on the adhesive (or cohesive) behaviour of REOB modified binders however. As REOB is a direct descendant of a lubricant, it is expected that parts of its consistency (or maybe its whole) will have a negative effect on the capabilities regarding adhesion between bitumen and aggregates. To evaluate if this assumption is correct, adhesive tests are performed with the Dynamic Mechanical Analyser (DMA).

This test will be performed by applying a tensile force on a thin bitumen film of 0.2 [mm]; adhered by rising the temperature and pressed between two small stones of 8 [mm] diameter (and each 15 [mm] high). According to experiments done by Mo et al. one should actually make sure only a film thickness between 15 – 25 [μm] exists between the stones (Mo et al., 2009). However a film thickness of this thin is near impossible to achieve with the current setup and available materials, especially when trying to prevent this bitumen film to break before testing. Therefore the stones that are used are polished heavily, to decrease the depth the bitumen can protrude into the stone surface and the bitumen thickness is increased to the mentioned 0.2 [mm] to allow the binder enough strain movements. This makes the measurement less comparable to true bestone aggregates (which have a roughness and porosity), but will allow the comparison of unmodified and REOB modified binders, while still saying something about adhesive discrepancies.

The table below shows the four bitumen that are evaluated in this paragraph:

Table 7.1: Selected unaged adhesive/cohesive stone-bitumen samples tested with DMA

Binder	Unaged/aged	PEN grade	Measured PEN
bit-J	Unaged	(70/100)	95
bit-K+10%	Unaged	(40/60)	53
bit-O	Unaged	(70/100)	88
bit-P+10%	Unaged	(30/50)	39

To make a reasonable evaluation of the effect of REOB, it is chosen to use the 10% blends, as these have the most similar rheological behaviour as to their (70/100) reference bitumen, made visible in Figure 7.1. The PEN grades, as shown before in Figure 3.5, increase exponentially when dosage is increased and are thus not deemed accurate to evaluate the low temperature susceptibility of the binders with the DMA. This way, one is purely focussing on seeing if adhesive/cohesive behaviour is different and not the general rheological behaviour. Bit-J (70/100) and bit-O (70/100) will both act as the reference bitumen, expecting bit-O to perform better because of its higher viscous capabilities.

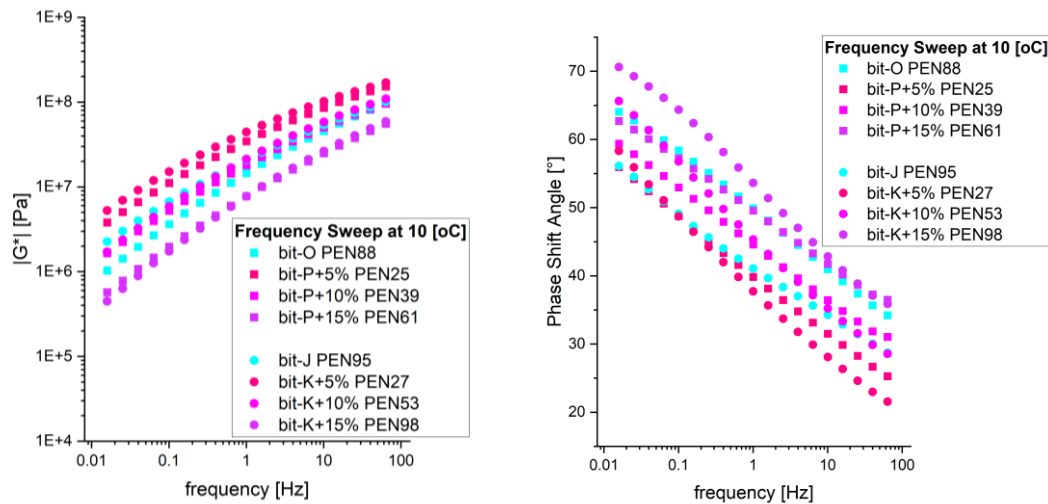


Figure 7.1: DSR frequency sweep results at 10 [°C], indicating how close the 10% blends come to the reference bitumen bit-J and bit-O

Bit-K+10% and bit-P+10% will each act as the REOB modified bitumen, expecting to see especially exactly similar behaviour between bit-J and bit-K+10% (indicating REOB does not have an influence on adhesion) or otherwise poor performance of bit-K+10% (showing REOB has a very clear negative impact on adhesion). Similar for the bit-P+10% blend, although the rheological behaviour already showed that the bit-P+10% blend will act stiffer than the bit-O.

As was found in Chapter 5.3, the Cole-Cole diagrams already indicated big differences in viscous property between binders in the range of 10, 0 and -10 [°C]. Therefore the Cole-Cole diagrams of the four tested bitumen are plotted on the right. One can therefore already expect that the, unaged, bitumen will have significant differences in relaxation properties. BitO should perform the softest and most ductile, bit-J and bit-P+10% are deemed similar and bit-K+10% should be the worst in tensile strength performance.

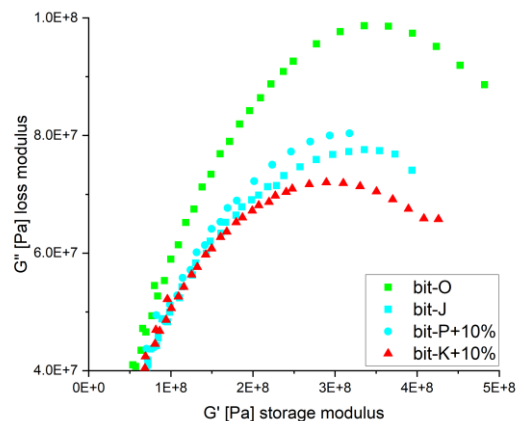


Figure 7.2: Cole-Cole diagram of four bitumen that will be tested with the DMA

All samples are prepared in a similar way. One needs to create a thin film of bitumen on silicon paper, so this can be easily cut into separate small pieces for samples in the DMA. A thermal scoop is used to scoop out a small bitumen sample from a storage can with the respective bitumen, and the heated bitumen is mixed sufficiently to create a homogeneous sample. These are then poured out on silicon paper and spread out into a thin film. Such a bitumen film is shown in Figure 7.3.



Figure 7.3: (left) thermal scoop, heat gun and metal rod and (right) a spread-out bitumen thin film on silicon paper

The bitumen is spread out using the small metal rod shown in Figure 7.3, be first heating it up with a heat-gun to make it hot and not stick to the bitumen instantly. Once the thin films are all prepared, they are all placed in the fridge (at ~5 [°C]) to keep them hard and easy to cut for the DMA preparations.



Figure 7.4: (left) smooth stone surfaces and (right) bad and too rough corners/sides which would influence test

Bestone polished stone columns are used, to represent the bestone aggregate used specifically for the ZOAB mixtures (porous asphalt) in the Netherlands. Preparation of the columns will be done at initially 0; 10 or 20 [°C] (at which the test will be performed), but the bitumen will be placed there once the machine is calibrated at this temperature. Then the temperature will be brought to 100 [°C] and now one waits for 4 [min] for the bitumen to lose its viscosity, after which the gap distance will be set to:

$$t_{gap;100 [oC]} = 0.225 + 0.2 = 0.425 [mm]$$

$$t_{gap;0 [oC]} = 0.250 + 0.2 = 0.45 [mm]$$

$$t_{gap;20 [oC]} = 0.2 + 0.2 = 0.40 [mm]$$

(7.1)

This ensures that the extension of the axles and clamps of the machine, because of the high temperature at 100 [°C], will be accounted for (this is only representable for this DMA specifically; the denoted 0.225) and next also the thickness meant for the bitumen film between the stone is accounted for (the 0.2 mm distance). For 4 [min] one waits for the bitumen to adhere well to both of the stone surfaces at this temperature of 100 [°C].

Finally, both the temperature and the gap will be reduced over a timespan of half an hour:

- From 100 [°C] towards 0; 10 or 20 [°C] with a rate of 0.005 [°C/s]
- Distance of the top axle downwards for a total of 0.250; 0.225 or 0.200 [mm] with a rate of 0.000125 [mm/s]

Once the testing temperature of 0; 10 or 20 [°C] is reached, and the final thickness of the bitumen is only 0.2 [mm], then the tensile test can be carried out.

N.B. One should always wait for an isothermal temperature to be reached, so once the sample is done with the 0.05 [°C/s] cooling, wait for at least 15 [min] at the testing temperature!

An overview of these different tests, four per bitumen sample, is given in the table below:

Table 7.2: DMA test conditions; temperatures and strain rates

Test	Temperature		
	0 [°C]	10 [°C]	20 [°C]
Strain rate			
0.002 [mm/s]	T0-S2	T10-S2	
0.004 [mm/s]		T10-S4	
0.006 [mm/s]		T10-S6	T10-S6

Using these five different conditions, the hope is that a clear picture can be drawn about the performance of these binders at different temperatures and strain rates. In Figure 7.5 the failure surface is shown of the four different bitumen failing at all five different conditions.

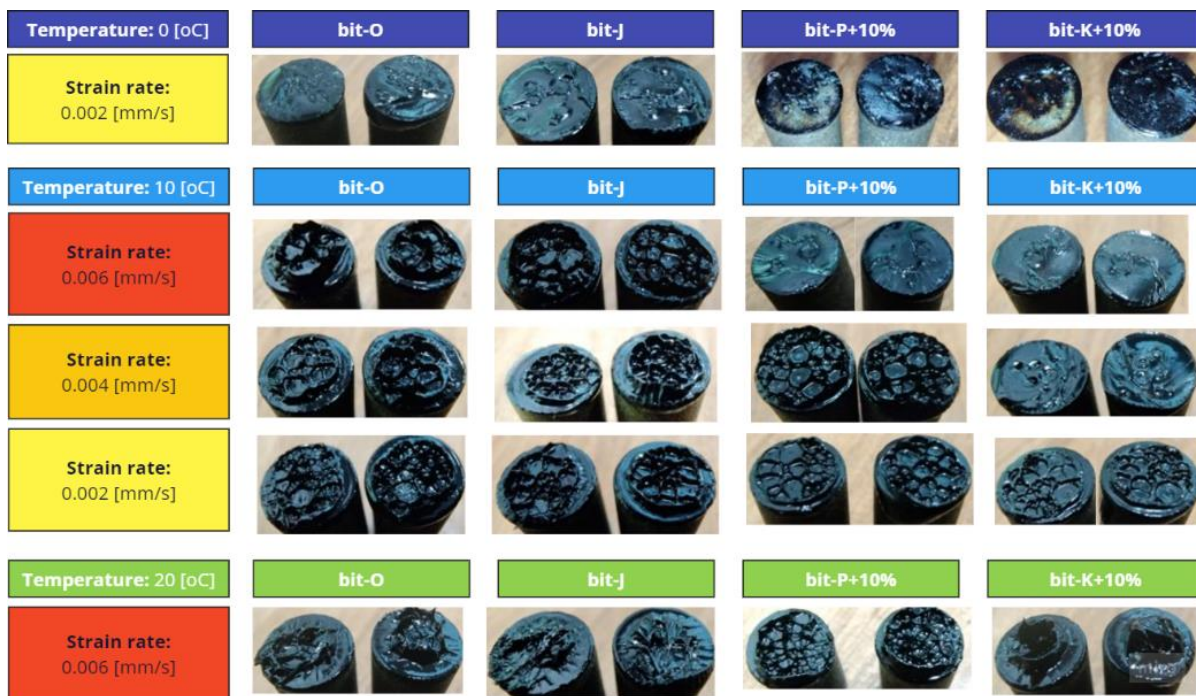


Figure 7.5: DMA failure surfaces for all three temperatures and the three different strain rates used

From the photographed failure surfaces, one can easily notice the generally brittle failure of bit-K+10% and bit-P+10%. For bit-K+10% one can still observe much brittle failure for the bitumen at 10 [°C], whereas this is not at all the case for the other binders. BitO is generally observed to fail in a very ductile nature. One can notice that failure generally is occurring because of the development of small and localised adhesive/cohesive failure. At specific points in the bitumen/the stone surface there is a loss of adhesion/cohesion which will slowly spread to cover a larger area of failure. In the case that stresses are very high (for relatively stiff binders), this will then develop in a sudden and brittle failure. Bitumen that is generally not too stiff, will allow for a more slow and ductile transition, where clear stretching of the bitumen can be observed.

A schematic diagram, of this described development of failure, is presented below for the REOB modified bitumen (bit-P+10%) in Figure 7.6 and unmodified bitumen (bit-O) in Figure 7.7. By pure observation of the failure surface, one can observe that clear different failure developments occur at the used conditions. Specific points in the bitumen itself or between the stone-bitumen will lose their cohesive/adhesive strength. From this point on, a small area of failure will spread. This area will continuously grow and, when given enough time (at lower strain rates), more points of failure will occur as well.

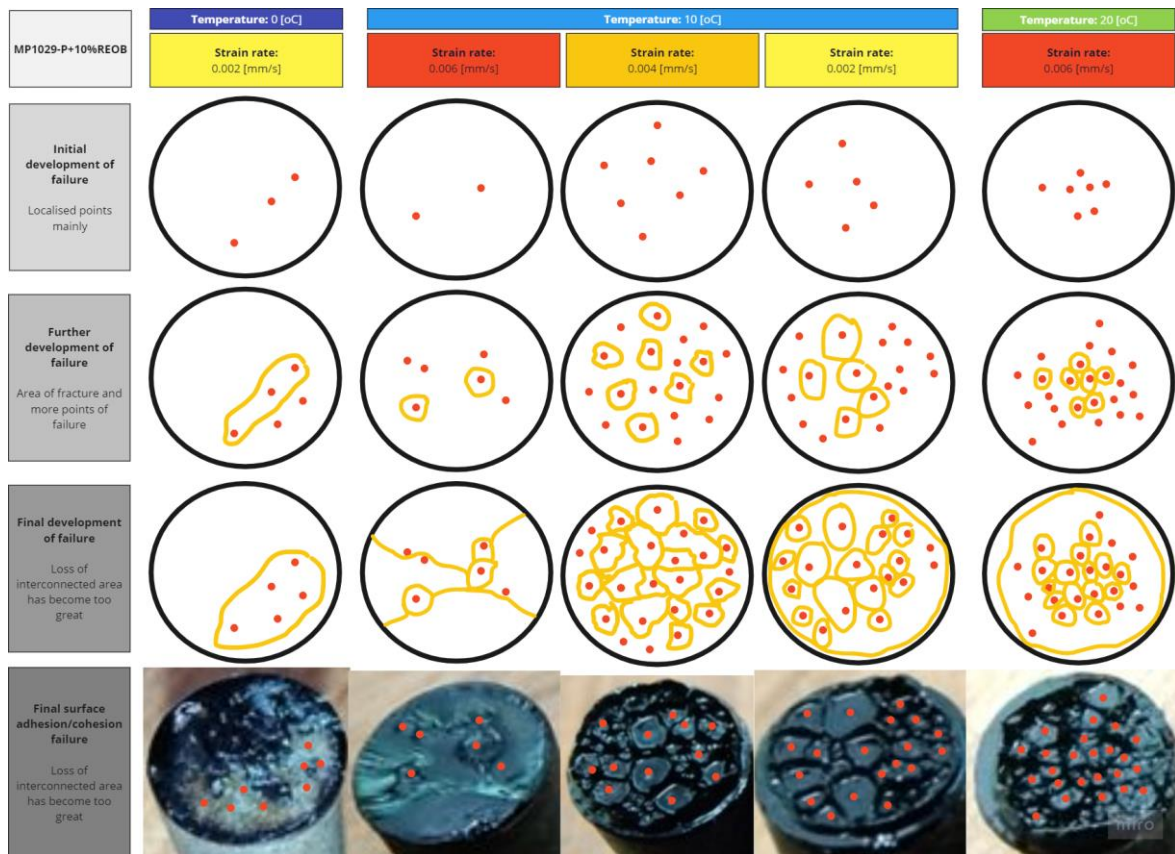


Figure 7.6: Visually analysed failure development and schematised for REOB modified bitumen (bit-P+10%) at five different conditions of deviating temperatures and strain rates

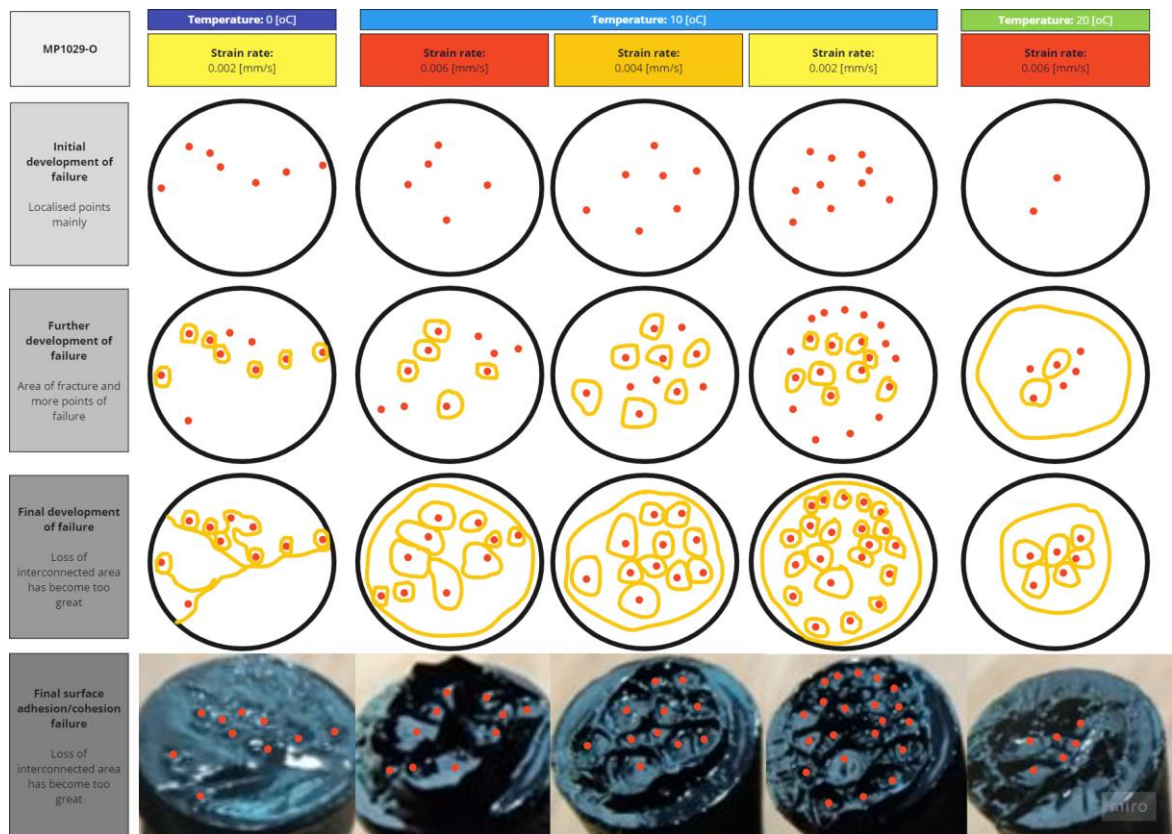


Figure 7.7: Visually analysed failure development and schematised for unmodified bitumen (bit-O) at five different conditions of deviating temperatures and strain rates

Extremely low temperatures like 0 [°C] seem to risk adhesive failure the most, which is seen only for the REOB modified bitumen at the current testing conditions. Here the low temperature has the most influence on the interconnection between the bitumen and stone. The low temperature will also increase the stiffness significantly, so lower strain rates like 0.002 [mm/s] strain will still be sufficient to make the stone-bitumen connection break in a brittle way. As one can notice from the failure surface in Figure 7.6. Here the failure points are clearly located very close to each other, leading to a significant loss in area to transfer the load/stress, resulting in a sudden failure of the connection.

A higher temperature like 10 [°C], or a lower strain rate, will allow a binder to have a slower development in loss of area of adhesion/cohesion, however more points of failure will start to appear. The fact that more and further spread between points of failure occur, means that the areas of failure around each localised point will be of smaller nature. This therefore suggests that a bitumen failing in this way would allow a better recovery, when the bitumen would be warmed up again and compressed (something that does occur in practice). This means a better fatigue resistance and should therefore be investigated further.

Increasing the temperature even more, for example 20 [°C], one can observe that the sides of the bitumen film will shrink. Here the ductile nature of the binder comes in play, and the general loss in area comes more from the stretching of the binder. This is thus the effect of the material being stretched out from its original horizontal alignment towards a vertical form (the volume/mass of the bitumen cannot be lost nor can it increase).

One can notice that there exist big differences between both bitumen, being REOB modified or not. REOB modified bitumen shows to be much more susceptible to a sudden and brittle fracture. There is much more growth in failure areas and multiple points of failure. Whereas the unmodified bitumen shows to develop much less points of failure, but more drastically decreases in width of the film. The general area is decreasing much more significantly and shows that the bitumen is much more ductile at the same test conditions. It is thus noticeable that the failure development of bit-P+10% at 10 [°C] and 0.002 [mm/s] is actually very similar to the failure of bit-O at 0.006 [mm/s]. Therefore one can conclude that bit-O is much less susceptible to tensile adhesive/cohesive failure than bit-P+10%. Although it was not possible to perform fatigue testing, bit-O suggests to be much more resistant to long fatigue damage and is able to heal cracks easier because of its ductile capabilities at lower temperatures. BitP+10% shows to be much more susceptible to irreversible damage and closer to brittle fracture.

To not only evaluate the failure modes of these bitumen qualitatively, the measured force and displacement of the top stone are converted to stresses and strains and plotted below. The forces and the displacements are translated into stresses and strains, for which the following formulas are used to convert the variables:

$$\sigma = \frac{F}{A} = \frac{F}{\frac{1}{4}\pi D^2} = \frac{F \text{ in } [N]}{\frac{1}{4}\pi(7.5)^2 \text{ in } [mm^2]} \text{ in } [N/mm^2]$$

$$\varepsilon = \frac{d_i - d_1}{d_{total}} * 100 = \frac{d_i - d_1 \text{ in } [mm]}{0.2 \text{ in } [mm]} * 100 \text{ in } [\%]$$

(7.2)

In Figure 7.8, one can immediately observe that both bit-K+10% and bit-P+10% REOB modified bitumen are much stiffer and especially bit-K+10% undergoes a lot of brittle failure. The general maximum stresses that are significantly higher for the REOB modified bitumen and the total energy needed until the material fails is significantly greater (higher stress and higher strains combined = the total area beneath the stress-strain diagram).

BitO specifically shows to have the lowest stresses of all bitumen and has only failed brittle once at 0 [°C], next to the stress/strain diagrams shown here, this is also made visible in Figure 7.9. This bitumen seems therefore the most resistant to low levels and tensile forces. Although cohesive loss would more easily occur, it would allow the most recovery from these tensile strains as compared to other binders. The maximum stresses at 10 [°C] seem to all lie quite close to each other, although changing the strain rate. Bit-J shows to be stiffer, although the maximum stresses reached are significantly lower as compared to the REOB modified binders. Again the maximum stresses at 10 [°C] lie pretty close to each other. Comparing this behaviour to the REOB modified bitumen one can see easily that the strain rate has a much higher effect. The time-temperature relation is therefore more heavily affected by the REOB in those binders, than they are for unmodified bitumen.

Instead of comparing the different conditions per each sample type, now the samples are compared within the specific test conditions at 10 [°C] and 0.006; 0.004 and 0.002 [mm/s] which are shown in Figure 7.8.

Within the 0.006 [mm/s] and 10 [°C] one can observe that bit-K+10% has only failed sudden and brittle and only one measurement out of three was not of brittle nature for the bit-P+10%. This can easily be compared to the bit-J and bit-O which generally are not susceptible to a brittle failure and show significantly lower maximum stresses reached.

The 0.004 [mm/s] at the same 10 [°C] shows a significant decrease in overall maximum stresses reached. BitK+10% has now once not reached a brittle failure and shown its full stress-strain curve. BitP+10% has still a brittle nature but the full stress-strain curve that was obtained has lowered significantly.

This can be compared to the unmodified bitumen bit-J and bit-O, which have had no brittle failures and show a much lowered diagram.

Lastly, the 0.002 [mm/s] at 10 [°C] condition can be evaluated. All bitumen, including the REOB modified binders, have not shown any brittle failure. One can observe that the maximum stresses reached for the bit-K+10% and bit-P+10% still lie higher than the unmodified bitumen, however surprisingly the bit-K+10% has reached a lower maximum stress than the bit-P+10%.

This suggests that the bit-K+10% changes its rheological properties at the low temperatures much more drastically with changing strain rate (or in other words a frequency) than all other bitumen evaluated.

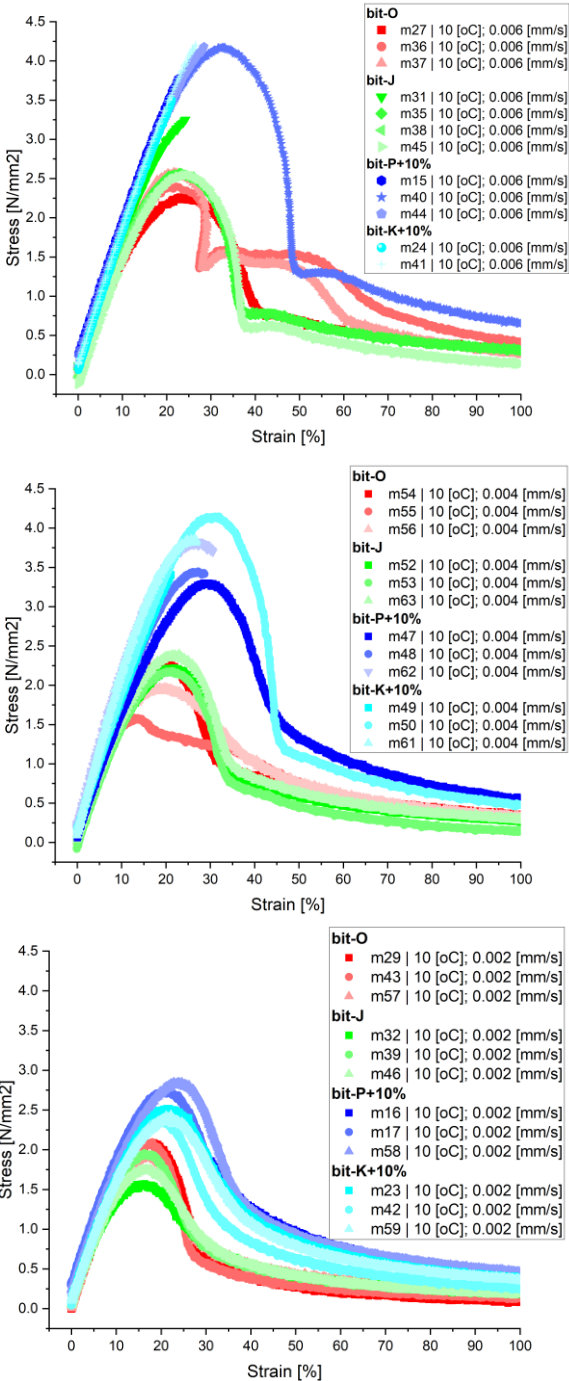


Figure 7.8: DMA test at 10 [°C] and 0.006 [mm/s] strain rate for all four bitumen (top); at 0.004 [mm/s] (middle) and lastly the 0.002 [mm/s] (bottom)

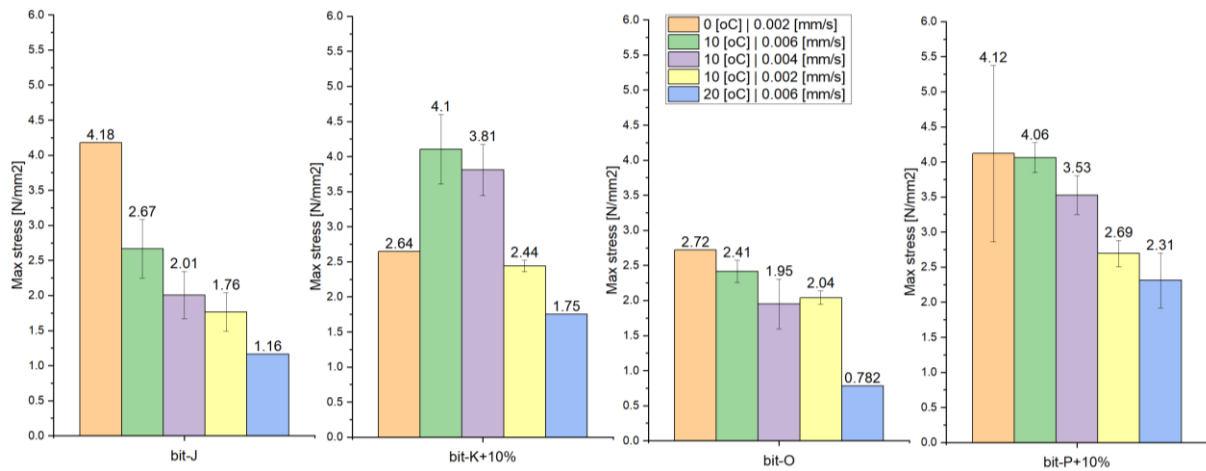


Figure 7.9: The maximum stress and its variances measured with DMA for all four different bitumen

Like observed from the stress-strain diagrams, here the maximum stresses show that the REOB modified binders have a much more drastic increase in maximum stresses with a decreasing temperature or an increasing strain rate, as compared to the unmodified bitumen. Next to that the overall maximum stresses reached are also significantly higher. At the 0 [°C] and 0.002 [mm/s] condition one can observe that again lower maximum stresses are obtained. This however is because the bitumen has failed substantially earlier in a brittle way. This is why it has not reached its maximum potential and lies lower.

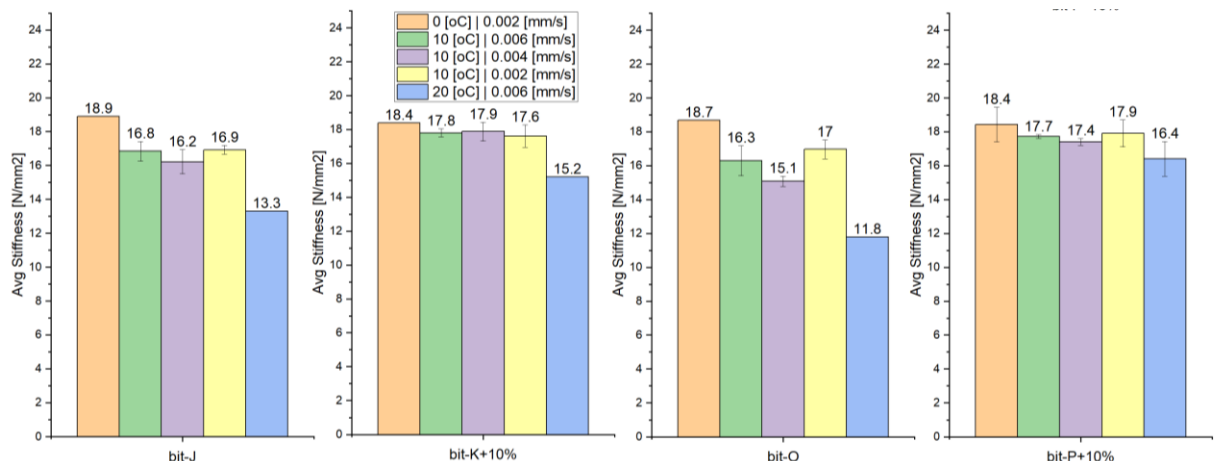


Figure 7.10: The average initial stiffness and its variances measured with DMA for all four different bitumen

When the average stiffness of the bitumen is calculated, obtained from the first few strains (between 0.5 and 2%) in the diagram, one can see that this changes differently as well. One can observe that the unmodified bit-J and bit-O have a more drastic decrease in stiffness with changing temperature and strain rate, as compared to the REOB modified binders.

The stiffnesses of all bitumen lie very close to each other at the 0 [°C] temperature. However already increasing the temperature to 10 [°C] one can notice that the REOB modified bitumen remain significantly stiffer as compared to the unmodified binders. At the 20 [°C] this difference is the most clear to observe. What is interesting to see, is the fact that bit-K+10% seems to drop its stiffness with a more exponential decline, whereas the bit-P+10% seems to more linearly decline. This is interesting to see, as the maximum stresses would suggest a different nature. BitK+10% was there of significantly higher maximum stress levels and broke much more brittle, however from the general stiffness one would expect it to actually be less susceptible with how easy it loses in stiffness with changing its temperature or strain rate.

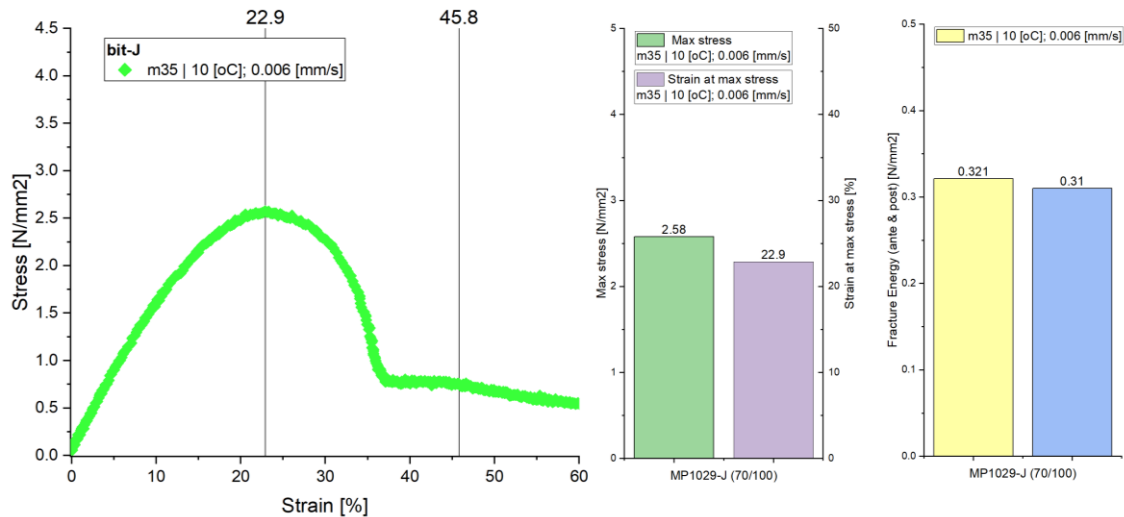


Figure 7.11: Schematic on stress/strain diagram of bit-J m35, to indicate where the pre-fracture energy and where the post-fracture energy is taken from

Next to maximum stresses reached or the stiffnesses of the bitumen, one can also look into the energy it takes to make the sample lose its cohesion or adhesion to the stone surface. This can be done by calculating the surface underneath the stress-strain diagram, until the maximum stress is reached. This is called the fracture energy. Next to that, the post fracture energy can also be calculated, which is taken as the area underneath the stress-strain diagram which takes the same strains to reach as the pre-fracture energy that was needed until fracture. Lastly, a ratio can be noted of the fracture energy compared to the post fracture energy:

$$Fracture\ Energy\ ratio = \frac{FE}{PE} * 100\ in\ [\%]$$

(7.3)

How those parameters are obtained is schematised in Figure 7.11.

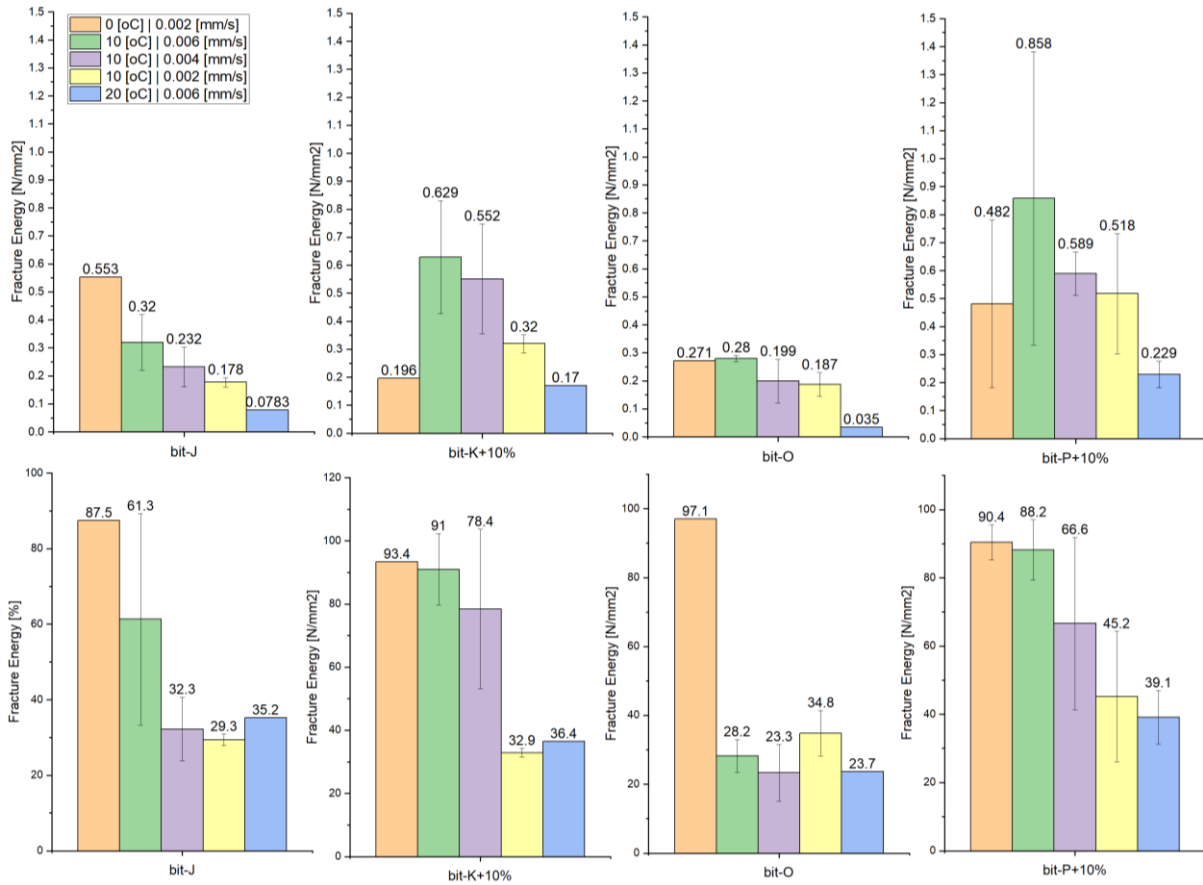


Figure 7.12: The fracture energy and fracture ratio measured with DMA for all four different bitumen at different conditions

This is then also carried out on all other sample results, and the calculated fracture energies and the fracture energy ratio are plotted in Figure 7.12. One can easily observe that the energy needed until fracture, is much greater in general for the REOB modified bitumen. Whenever the fracture energy is drastically low, one should look to the fracture energy ratio, as when this is very high (above 80%) one can say that a brittle fracture has occurred. This therefore translates to an early limit reached and a very sudden/quick/instant dissipation of energy, which is not a good failure for a binder.

It is easy to state therefore that these REOB modified bitumen, although they have similar rheological properties at the 10 [°C] as was observed with the DSR, they still perform significantly worse in low temperatures on their adhesive/cohesive strength. There apparently is a more drastic shift in failure modes to more critical and brittle fracture in the case of REOB modified bitumen as compared to the reference bitumen. REOB modified bitumen can therefore be seen as very susceptible to low temperature cracking and will, expectedly, not be a good application for bitumen that needs resistance to low temperatures or ravelling.

7.1.2. Cohesive mastic column DMA test tensile pull test

To say something about the adhesive properties of the binder with the filler, or the general cohesion of mastic (bitumen + filler), this should be researched separately. Mere adhesion of an aggregate stone surface alone, will not show the full picture of the performance of the REOB modified binders. The fact that fillers alone can differ heavily is also an interesting angle to evaluate. There is the suspicion that the REOB (or the lubricant additives still residing there), could have an impact on the these fillers or the mastic as a whole.

Only a small selection of papers have delved into mastic behaviour for different fillers, and not a single researched was published on the behaviours of mastics that include REOB. The effect of different fillers was evaluated before (Woldekidan & Gaarkeuken, 2013), one of the results concluding that filler using hydrated lime, Ca(OH)_2 , would increase stiffness of a bitumen substantially. This effect should therefore be found again.

To evaluate the performance of the REOB modified bitumen, in the case of using non-reactive and reactive fillers, a small number of samples is tensile tested in the DMA (similar as to the previously described adhesive test).

Table 7.3: Mastic samples of un-/REOB modified bitumen with non-reactive and reactive fillers for cohesion analysis

Binder	PEN grade	Measured PEN	Non-reactive filler		Reactive filler	
			Wigro	CaCO ₃	Wigro 60K	CaCO ₃ & Ca(OH) ₂
bit-J	(70/100)	95	bit-J-NR-1,2,3,4,5	bit-J-RF-1,2,3,4,5	bit-J-RF-1,2,3,4,5	bit-J-RF-1,2,3,4,5
bit-K+10%	(40/60)	53	bit-K+10%-NR-1,2,3,4,5	bit-K+10%-RF-1,2,3,4,5	bit-K+10%-RF-1,2,3,4,5	bit-K+10%-RF-1,2,3,4,5
bit-O	(70/100)	88	bit-O-NR-1,2,3,4,5	bit-O-RF-1,2,3,4,5	bit-O-RF-1,2,3,4,5	bit-O-RF-1,2,3,4,5
bit-P+10%	(30/50)	39	bit-P+10%-NR-1,2,3,4,5	bit-P+10%-RF-1,2,3,4,5	bit-P+10%-RF-1,2,3,4,5	bit-P+10%-RF-1,2,3,4,5

It is chosen to create an overlap with the adhesive/cohesive performance tests on the bitumen-stone interaction, by selecting the same four bitumen and now mixing them each with two different fillers at a 1:1 weight ratio of bitumen and filler. The mastics are prepared in the following way:

1. Place bitumen and filler both in oven at 163 [°C], for at least one hour
2. Pour the bitumen in a container at around a mass of ~30 [g] followed by pouring either filler Wigro or Wigro60K ~30 [g]
3. Place the container of bitumen+filler again in the oven for ~30 [min]
4. Take one container out, mixing it on a heating plate for around 20 [min] to ensure no clumps/agglomerations are present
N.B. some filler material will settle, but just before the mastic columns are poured one can mix the mastic again
5. Do this again for the other bitumen+filler combination

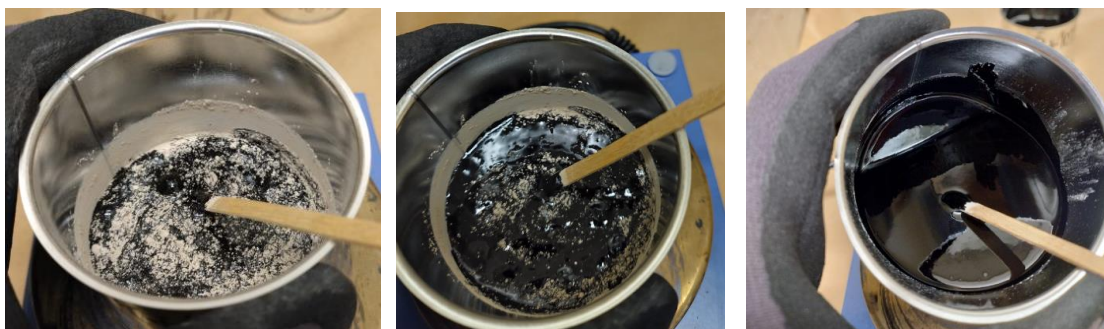


Figure 7.13: Visualised stages of mixing; (left) the beginning, (middle) after 1 minute of mixing and (right) after 20 [min] of mixing (some filler is more concentrated at the bottom)

This is done for all bitumen and filler combinations, after which the process of making the mastic columns can start. This is done in the following way:

4. Place the container with the mastic in the oven at 163 [°C], waiting for around 3/4 hour
5. Take the mastic out and mix it again properly to reduce the amount of settled filler and place it back in the oven for 15 [min]
6. Now the pouring can be done in the mould shown in Figure 7.14
7. When mastic columns have been poured, let them first settle and condition at room temperature for at least an hour, after which they can then be placed in a fridge ~10 [°C] to let them turn hard for testing



Figure 7.14: Mastic columns poured in mould with bit-J started at position 1 with Wigro filler, continuing counter-clockwise and starting with Wigro 60K at position 6 (left and middle pictures) and samples placed in another mould ready for testing (right picture)

To be able to compare the results from mastic tensile tests as for the adhesive/cohesive bitumen film testing, a similar testing condition will be imposed on the mastic. The testing condition easiest to reach, but also showing the best difference between bitumen, was deemed at 10 [°C] and had an initial strain of 3% after 1 second. As the mastic columns are around 12 [mm] in height, this means a strain rate of $\epsilon' = \frac{12}{100} * 3 = 0.36$ [mm/s] should be used.

Carrying out the cohesive mastic tensile pull test on the mentioned conditions, one will obtain a failure of the following nature, shown below in Figure 7.15.

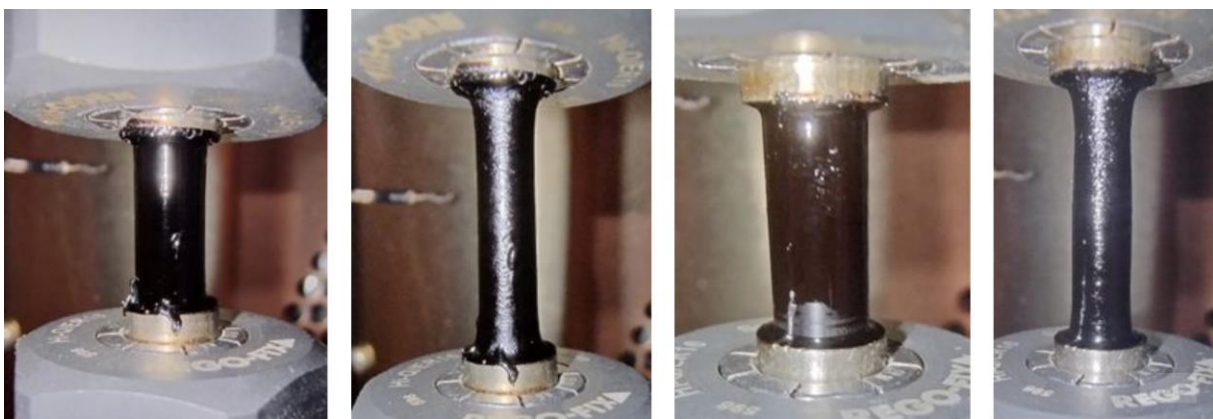


Figure 7.15: Cohesive mastic failure after tensile pull test at 0.36 [mm/s] strain rate at 10 [°C]; showing initial condition and then failed condition of (left) bit-O and (right) bit-P+10%

One can observe that initially no filler grains can be seen in the bitumen/mastic, they can be deemed smooth and completely black. After stretching out the mastic for around 60% initial height, one can see that the surface turns glossy and a matrix structure of the filler inside the mastic becomes clear to the

eye. Bit-O clearly stretches out along a straight line, not showing any part of the column to decrease in area more than another. Bit-P+10% shows that it will reduce in width significantly more at 1/3 of its height and 2/3 of its height, although at half its height it seems to have remained its initial thickness. One can therefore schematise the failure in the following way shown in Figure 7.16.

The heights of the samples is 12 [mm] and the diameter is around 7 [mm], which means that the stresses and strains should be calculated in the following way, recalculating the obtained forces and displacements:

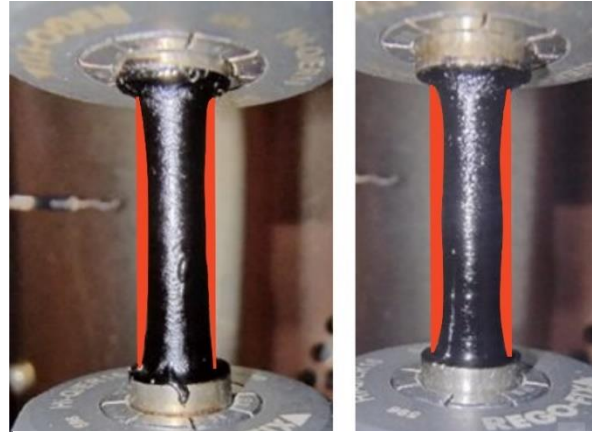


Figure 7.16: Schematised failure development in mastic showing the difference between unmodified bitO (left) and REOB modified bitP+10% (right) mastics

$$\sigma = \frac{F \text{ in } [N]}{\frac{1}{4} * \pi * 7^2 \text{ in } [mm^2]} \text{ in } [N/mm^2]$$

$$\varepsilon = \frac{d_i - d_0 \text{ in } [mm]}{12 \text{ in } [mm]} * 100 \text{ in } [\%]$$

(7.4)

Using those formulas the stress/strain diagrams are obtained for the mastic tensile failure tests and are shown in Figure 7.17.

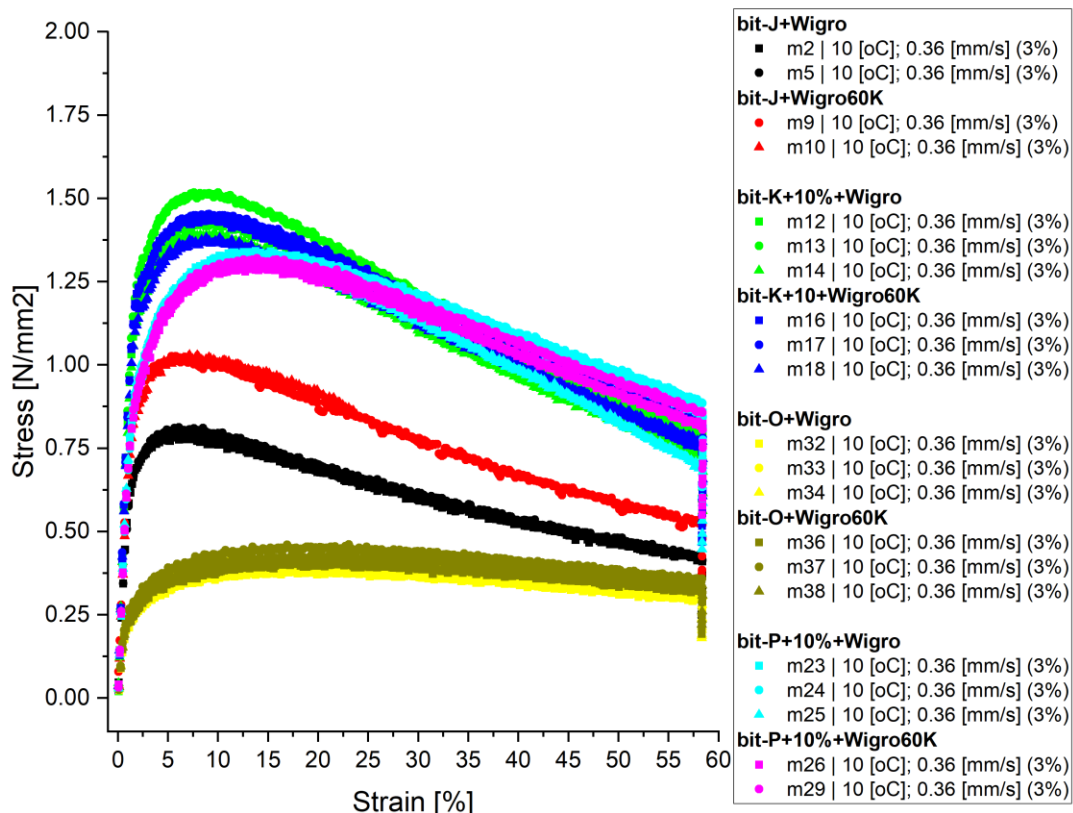


Figure 7.17: Mastic tensile failure stress/strain diagrams of mastics using different fillers and comparing unmodified and REOB modified bitumen

The stress/strain diagrams on the mastic columns have made visible that drastic differences are present between the four different bitumen, but also differences are possible between the filler types.

Like before with the adhesion/cohesion bitumen film testing in paragraph 7.1.1, the REOB modified bitumen show to be of stiffer and stronger nature (which is not a bad thing per se, but further proves the misalignment with frequency sweep measurements with the DSR). The REOB modified bitumen show to have maximum stresses reaching above 1.25 [MPa] at the tested condition of 0.36 [mm/s] and 10 [°C]. This is significantly higher than the reference bitumen of bit-O, which averages at only 0.4 [MPa] and bit-J at around 0.9 [MPa]. This is made more clearly visible in the plot below:

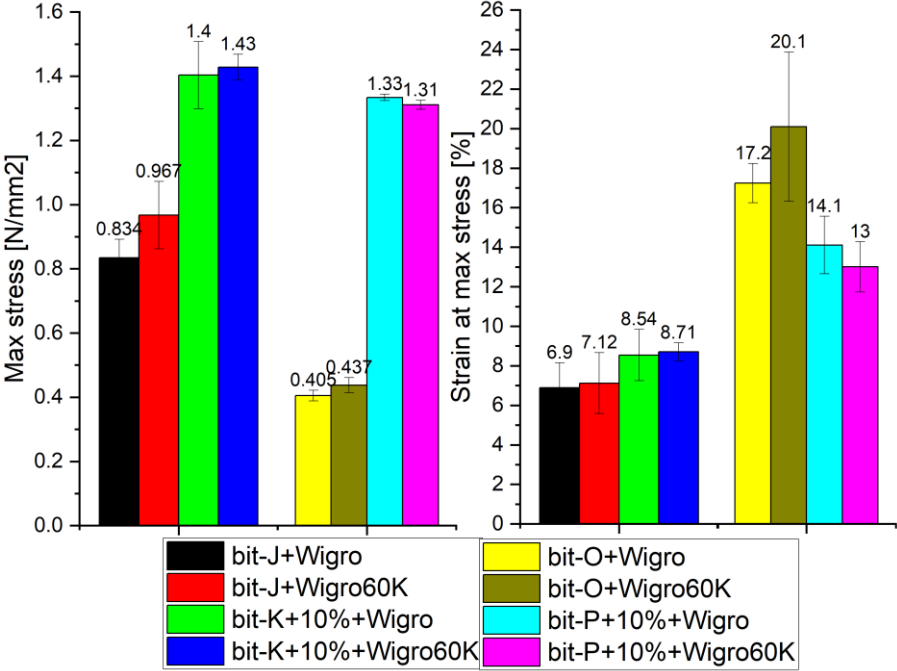


Figure 7.18: Maximum stress and the strain measured for all 8 different mastic types

The moment at which the maximum stress is reached is also different, but clearly has more to do with the base bitumen than the REOB modification. bit-J and bit-K+10% show to reach the maximum stress at a total strain of around 8%, whereas bit-O at around 18% and bit-P+10% at around 13.5%. This shows that the REOB has more impact on energy build-up for bitumen under tensile stress, like the brittle nature observed with the adhesive/cohesive testing. It does not like deforming and prefers to increase the stress on it, than to deform and give a viscous response.

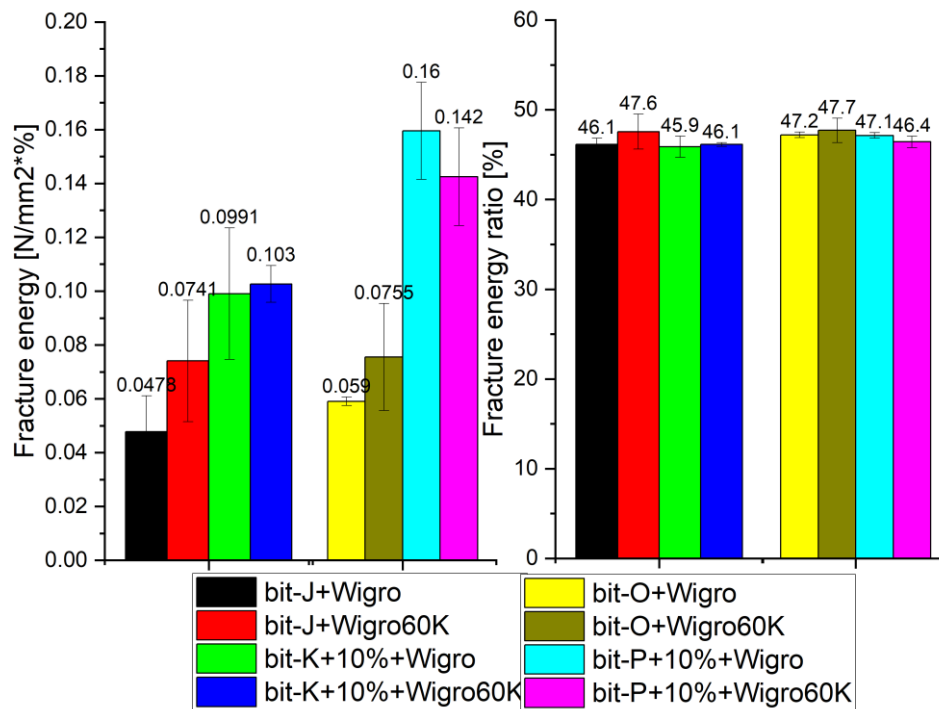


Figure 7.19: Fracture energy and ratio for all 8 different mastic types

Interesting to see is that specifically the reference bitumen differ a lot under the effect of using different fillers. bit-J shows a clear difference in maximum stresses reached between using Wigro or Wigro60K, but the strains at which these maxima are obtained are quite similar. On the contrary bit-O shows to have less variance in maximum stresses reached, although the strains at which they are reached are significantly different. REOB modified bitumen shows much less variance in this aspect, both maximum stresses and the strains at which they happen lie very close to each other regardless of using a filler with hydrated lime or not.

It is known that bitumen bit-O and bit-P are of higher acidity, and it is also known that higher acidity promotes a reaction with basic filler and aggregates (Airey et al., 2008; Mastoras et al., 2021; Valentin et al., 2021). By mere speculation this would mean that an increase in the adhesion between the filler and bitumen in the mastic, it should be visible in the tensile cohesion mastic tests that there is actually an increase in cohesive strength. The fact that the REOB modified bitumen are of significantly higher strength, this could very much be related to a chemical reaction that was promoted after the addition of the REOB. This could therefore mean that the REOB, possibly of significantly higher acidity than the base & reference bitumen, will promote an (excessive) chemical reaction with filler material, therefore creating a more elastic and less viscous mastic.

7.1.3. Observations on adhesive and cohesive performance

Now with the adhesive/cohesive bitumen film and the cohesive mastic tensile failure tests performed, some conclusions can be drawn about the difference in performance between unmodified and REOB modified bitumen.

- (1) From the five different conditions, varying in both temperature between 0; 10 and 20 [°C] and in strain rate varying between 0.002; 0.004 and 0.006 [mm/s], one can qualitatively observe that the REOB modified bitumen will generally break in a brittle way. BitK+10% continuously broke in a brittle way at both 0 [°C] and 10 [°C], where bit-P+10% had a more ductile behaviour at 10 [°C]. bit-J had even better resistance to brittle failure and bit-O had almost no brittle failure. It was possible to make a distinction between different failure developments at the mentioned five different conditions. This made it clear how failure could develop, being of the following nature:
 - a) Small localised points initialise the failure, developing a growing loss in connected area between bitumen itself (cohesion) or bitumen and stone (adhesion)
 - b) Low temperature determines if stress build-up will be higher, risking brittle/sudden fracture. There is an increased risk of adhesion failure as compared to cohesion, when temperatures go down (around 0 [°C]) and strain rates are sufficiently high.
 - c) Low strain rate enables the binder to have more localised points of failure, whereas high strain rate will enable faster loss of connected area.

These observations seem to align well with observations done before on adhesive/cohesive tensile failure of a stone-bitumen film surface (Mo et al., 2009; Mo et al., 2011).

- (2) Maximum stresses that are reached, are much higher for REOB modified bitumen. In general these REOB modified bitumen will increase in maximum stresses much more drastically, when the strain rate is increased, as compared to unmodified bitumen (comparing the different strain rates at 10 [°C]). In the case of bit-O one can almost observe a straight line in the maximum stresses reached at around an average of 2.1 [MPa], whereas bit-P+10% drops from 4 [MPa] to 2.6 [MPa].

The fracture energy needed is also greater for these REOB modified bitumen. Because brittle fracture is much more common for the REOB modified bitumen the fracture energy ratio can be much higher than expected from the ductile failure broken samples, at lower temperatures/high strain rates.

- (3) Mastic cohesive failure has shown that REOB modified bitumen has a general higher stiffness after the addition of filler, regardless of filler type (with or without hydrated lime). bit-J, an unmodified bitumen, shows however a significant difference in strength as compared to the modified bitumen. The Wigro (without hydrated lime) has shown to create less strong/more ductile mastic than the Wigro60K (including hydrated lime). It was found before that Wigro60K, as it contains $\text{Ca}(\text{OH})_2$, can have a stiffening effect on mastics and mortars as compared to fillers without it (Woldekidan & Gaarkeuken, 2013).

The effect of REOB seems to reduce difference between the two filler types, and speculatively speaking this could have to do with acidity of the bitumen. BitO and bit-P are known to be relatively high in acidity, which promotes a reaction with fillers/aggregate and specifically the CaCO_3 . The REOB is expected to be of a higher acidity and would therefore create a stronger reaction (than can be intended) with the present filler & aggregates.

7.2. Asphalt mixture workability and performance

7.2.1. Resistance to densification and the cohesion of asphalt mixtures with REOB; mixture preparation and gyrator compacting

The researched adhesive and cohesive behaviour of bitumen and REOB modified bitumen, is not the only aspect that will determine if a binder is good or bad. Only making an asphalt mixture will show the behaviour of such a binder clearly and is therefore necessary to perform, before conclusive statements can be drawn.

To limit the amount of samples to be made and still be able to draw reasonable conclusions, two mixture series of different bitumen will be made with a gyratory compactor. Four samples are made with bit-J (70/100) bitumen and four samples are made with a REOB modified bitumen: bit-K (20/30) + 15% REOB-X. This specific blend is chosen for mixture evaluation, as this blend has the closest PEN grade 98 possible to the reference bitumen, in this case bit-J PEN 93. This will therefore come close to practice results, as main mixture design and a contractor their delivery of an asphalt mixture depends on the PEN grade and not necessarily on rheological behaviour. The REOB modified mixture is therefore expected to be much more viscous and supple, considering rheological behaviour of bit-J. A lower stiffness is expected for the REOB mixture, but also lower strength, as it is expected that the binder will have worse cohesion when blended with the aggregates and filler.

The gyrator samples are sawed in separate slices, to make 3 slices per mould and thus in total 3x8=24 slices. Half of the samples are made with unmodified bitumen and the other half REOB modified. For each 12 samples per series, six will be tested with the Indirect Tensile Test (IDT) and six with the Cantabro Abrasion test (CB). To include moisture susceptibility, three of the six samples for IDT are put in a water bath and are tested in wet condition. To include ageing and more specifically, freeze-thaw susceptibility, three of the six CB samples undergo freeze-thaw cycles, according to the AASHTO 283 norm.

In Figure 7.20, one can see all eight gyrator samples cut into each three slices. Each slice is accounted its own code, but also the respective test it will be undergoing. The slices are chosen in such a way that each IDT test will have a top, middle and bottom part, but also each from a different column. The Cantabro test is deemed to be able to achieve enough accuracy with only one sample per condition, but higher accuracy is needed for the IDT test. This is why there are 5 samples per mixture and condition tested for the IDT and only one for the Cantabro abrasion test. The samples per test are chosen in such a way that the Cantabro Abrasion test takes up centre pieces of a mixture column and the IDT samples have void ratios in such a way that they have comparable void ratios between the two mixture types. These void ratios per test can be seen in Figure 7.23 .

bit-J (70/100) series ABCD				[mm]	bit-K+15% REOB-X (70/100) series EFGH			
A	B	C	D		E	F	G	H
Top				0	Top			
A-1	B-1	C-1	D-1	40	E-1	F-1	G-1	H-1
ITT-dry	ITT-wet	ITT-dry	ITT-wet		ITT-dry	ITT-wet	ITT-dry	ITT-wet
Gap 1				5	Gap 1			
A-2	B-2	C-2	D-2	40	E-2	F-2	G-2	H-2
ITT-wet	ITT-dry	CB-cond	CB-dry		ITT-wet	ITT-dry	CB-cond	CB-dry
Gap 2				5	Gap 2			
A-3	B-3	C-3	D-3	40	E-3	F-3	G-3	H-3
ITT-dry	ITT-wet	ITT-dry	ITT-wet		ITT-dry	ITT-wet	ITT-dry	ITT-wet
Bottom				0	Bottom			
Total				130	[mm]			

Figure 7.20: Overview of all 8 gyrator samples of un-/REOB modified mixtures split into separate slices, 24 in total; including their codes and respective tests that will be carried out on each slice

As a representative situation of the problems occurring in the field (in the Netherlands) is needed to be reproduced, the mixtures are designed using the recipe for Duurzaam ZOAB (or otherwise called ZOAB+). To be able to make these chosen mixtures, one needs to calculate the necessary amount of materials needed. The total volume per mould is calculated as:

$$V_{total} = \frac{1}{4}\pi D^2 h = \frac{\pi \cdot 100^2 \cdot 130}{4} = 1021017.612 [mm^3] \quad (7.5)$$

With the theoretical maximum density of the gyrator sample:

$$\rho_{max} = \frac{100}{\sum \frac{\%m/m_{fraction,i}}{\rho_{fraction,i}}} = \frac{100}{0.04054685} = 2466 [kg/m^3] \quad (7.6)$$

And the target density will be, accounting for 20% voids:

$$\rho_{target} = \left(1 - \frac{voids\%}{100}\right) \rho_{max} = \left(1 - \frac{20}{100}\right) \cdot 2466 = 1973 [kg/m^3] \quad (7.7)$$

Therefore the total mass per mould should thus be counted as:

$$m_{total} = V_{total} \cdot \rho_{target} = 1021017,612 \cdot 1973 = 2014 [g] \quad (7.8)$$

Table 7.4: Mixture design of 8 gyrator samples; according to ZOAB+

Sieved fraction	Type	% (m/m)	Density [kg/m ³]	Specific volume [m ³ /kg]	Amount per mould [g]	Total masses for bit-J samples (8x) [g]	Total masses for BitK+15% samples (8x) [g]	Total all moulds [g]
[mm]			[kg/m ³]	[m ³ /kg]	[g]	[g]	[g]	[g]
11/16	Bestone	28.1	2685.9	0.01046081	566.0	2264.0	2264.0	4528.0
8/11	Bestone	32.9	2678.1	0.01229274	663.2	2652.8	2652.8	5305.5
5/8	Bestone	14.2	2669.8	0.00531509	285.9	1143.4	1143.4	2286.9
2/5	Bestone	6.5	2672.9	0.00244210	131.5	526.0	526.0	1052.0
<2	Sand	8.1	2657.6	0.00306120	163.9	655.6	655.6	1311.1
Filler	Wigro 60K	4.7	2638.0	0.00179303	95.3	381.1	381.1	762.3
Additive	Fibres	0.2	1500	0.00013333	4.0	16.1	16.1	32.2
Bitumen or blend	bit-J or bit-K+15% (70/100)	5.2	1030	0.00504854	104.8	419.0	419.0	838.0
Bitumen	bit-J (70/100)	100.0			104.8	419.0		419.0
	bit-K (20/30)	85			89.0		356.2	356.2
REOB	REOB-X	15			15.7		62.9	62.9

With the mass, the densities and selected sieve fractions, the total amount of weights of materials that is necessary per sieve fraction can be calculated. Their fractions are all noted in Table 7.4.

With the mixture design ready, the mixtures can be made. In Figure 7.21 one can see the mixer, the spindle and the gyrator compactor that were all used in the mixture preparations. Now the mixtures are made with the presented method, one can measure the time that the gyrator takes to compact these mixtures. Problems with compacting and mixing a REOB modified ZOAB mixture have been observed in the field, therefore it is expected that the REOB modified mixture will take relatively longer to compact to the 130 [mm] height that is aimed for.



Figure 7.21: (Left) mixture blender with heated pan; (middle) spindle for the mixture which can also rotate its axis and (right) the gyrator mixture compactor

After demoulding and cutting, the samples of bit-K+15% had excessive oil on the outside, visible in Figure 7.22. As oil is used to coat the gyrator moulds for easy removal of the columns, it is unsure if an excess of this was used or if the bitumen has leaked oil itself. Although it was interesting to notice that it seemed to be worse in the case of the bit-K+15% than for the bit-J gyrator columns. In the case that oil indeed has exuded from the bitumen itself, this should be noticed in both the IDT and the Cantabro tests as these samples would become way more stiff than expected. Especially after conditioning of the samples in water or with freeze-thaw cycles.



Figure 7.22: (Left) One gyrator sample of ZOAB+ and (right) after making the samples and before storage at ~15 [°C], the samples were cut. The hand shows that an oil (or REOB) seems to still exudate from the binder, significantly more in the case of bit-K+15% than for bit-J.

From the retrieved gyrator measurements, shown in Figure 7.23, one can see that specifically mixtures A and B made with bit-J were of very soft nature. They were able to be compacted to the intended 130 [mm] height within alerting short time. The suspicion arises that these mixtures, as they were the very first two mixtures made, are made of too little material. Some of the intended mixture mass could have been stuck still in the pan, a much bigger portion than with the other mixtures.

Void ratios have been calculated from the measured dry mass per sample, the measured volume directly and the using the intended maximum density set at 2465 [kg/m³]. According to the evaluated air void ratios, the slices are selected for each test condition to make an effective estimation and good comparison between properties. This is made visible in the column plot, also shown in Figure 7.22.

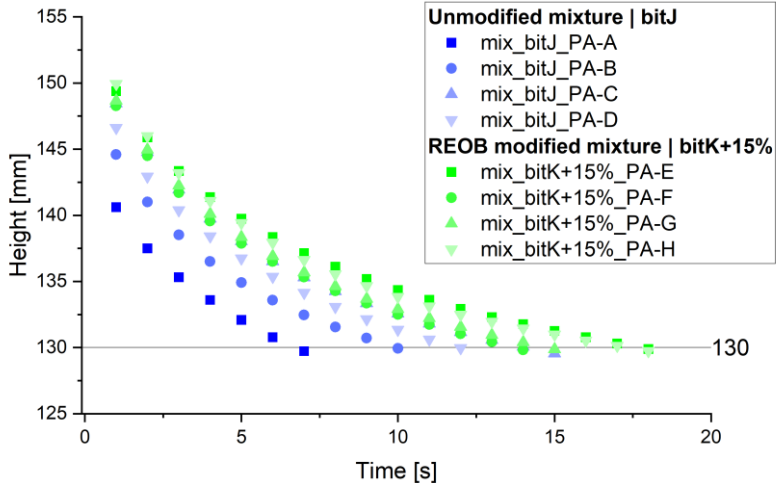


Figure 7.23: Gyrator compaction height from initial position towards the final 130 [mm]

To make all measured masses and calculated volumes visible to the reader, the measurements are noted in the following table. One can see that varying void ratios are obtained and thus careful selection and analysis of results should be done, such that assumptions and conclusions are taking into account these changes.

Table 7.5: Measured slice height, width and weight of the different mixtures; mixtures A, B, C and D are made with bit-J and mixtures E, F, G and H with bit-K+15%; the top slice is denoted with number 1 and the bottom slice with 3

	D1	D2	D3	t1	t2	t3	Davg	tavg	V	m	rho_target	voids	
							[mm]	[mm]	[mm ³]	[g]	[kg/m ³]	[%]	
A	1	99	99	99	41	41	40	99.0	40.7	3.13E+05	614.10	1961.73	20.45
	2	100	100	99	40	40	40	99.7	40.0	3.12E+05	591.20	1894.46	23.18
	3	100	100	100	40	40	39	100.0	39.7	3.12E+05	562.00	1803.93	26.85
B	1	100	100	100	40	40	40	100.0	40.0	3.14E+05	604.50	1924.18	21.97
	2	100	100	99	41	41	40	99.7	40.7	3.17E+05	642.90	2026.35	17.83
	3	100	100	99	39	41	40	99.7	40.0	3.12E+05	605.00	1938.68	21.38*
C	1	100	100	99	41	40	40	99.7	40.3	3.15E+05	644.80	2049.14	16.90
	2	99	99	99	41	40	40	99.0	40.3	3.10E+05	630.00	2029.16	17.71
	3	100	100	99	40	40	40	99.7	40.0	3.12E+05	616.70	1976.17	19.86
D	1	100	100	99	40	40	40	99.7	40.0	3.12E+05	632.20	2025.84	17.85
	2	100	100	99	40	40	40	99.7	40.0	3.12E+05	636.90	2040.90	17.24
	3	100	100	99	42	42	41	99.7	41.7	3.25E+05	633.70	1949.42	20.95*
E	1	99	99.5	99.5	40	40	41	99.3	40.3	3.13E+05	627.00	2005.97	18.66
	2	100	99.5	99.5	41	41.5	40	99.7	40.8	3.19E+05	641.30	2013.06	18.37
	3	100	99.5	99.5	41	40	40	99.7	40.3	3.15E+05	627.40	1993.84	19.15
F	1	100	99	99	41	40	41	99.3	40.7	3.15E+05	621.20	1971.12	20.07
	2	100	100	99.5	41	41.5	41	99.8	41.2	3.22E+05	642.80	1994.75	19.11
	3	100	100	99.5	41	40	41	99.8	40.7	3.18E+05	629.90	1978.75	19.76
G	1	100	100	100	40	40	39	100.0	39.7	3.12E+05	635.60	2040.18	17.27
	2	100	99	99	41	41	41.5	99.3	41.2	3.19E+05	613.80	1923.98	21.98*
	3	100	99.5	100	41	41	40.5	99.8	40.8	3.20E+05	618.20	1934.07	21.57*
H	1	100	100	100.5	41	41.5	40.5	100.2	41.0	3.23E+05	649.00	2008.74	18.54
	2	100	99.5	99.5	41	41.5	40	99.7	40.8	3.19E+05	640.30	2009.92	18.49
	3	100	99.5	100	41	41	40.5	99.8	40.8	3.20E+05	630.30	1971.93	20.04

* the asterisk means those slices were missing one or two small stones, which have reduces the measured mass heavily; this therefore means the calculated high void ratio is not a good representation

7.2.2. Dry & wet cracking resistance of asphalt mixtures; indirect tensile strength ratio test (ITSRT)

According to NEN-EN 12697-23 (2018), the Indirect Tensile Test (IDT) will be carried out on twelve asphalt mixture samples. The test is split into two parts: six samples will be tested in dry conditioning at 10 [°C] (as the binders are of grades 70/100), and additionally the other six samples will be tested in wet condition. This will lead to a strength ratio that describes susceptibility to moisture damage.

The **dry conditioning** of the samples is done by:

- Acclimatising the samples to the testing temperature of 10 [°C] for at least 2 hours (this was ultimately roughly around 24h)

The **wet conditioning** of the samples is done by:

- Vacuum saturating the samples using a pressure of around 6.73 [kPa]
First by slowly increasing to this pressure for 10 [min], then stabilising for at least 30 [min]
- Next placing the samples in a hot water bath of around 40 ± 3 [°C] for a total of 72 hours
- Then drying the samples for 30 [min], followed by measuring changes in volume
- Then acclimatising the samples for at least 4 hours at 10 [°C] (this was roughly around 24h)

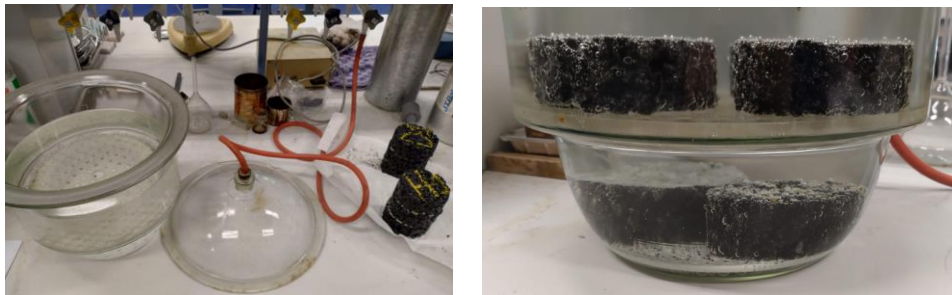


Figure 7.24: Saturation of the mixture slices in a vacuum; using ~6.73 [kPa] of pressure so the pores in the mixture (containing air) will be filled with water

The hope is that clear differences will be found with this small set of samples. If this is not the case, then it is deemed that the REOB will not make too much of a difference regarding moisture susceptibility. The Cantabro abrasion test will act as a second check to see if the stiffness of the REOB modified mixtures are more heavily affected after conditioning, than the unmodified mixtures.

The conditioning of these samples in these two different ways, will give a comparison between the moisture susceptibility of the mixtures. It is expected that the REOB modified bitumen will be more susceptible to the moisture and lose more of its cohesive strength as a mixture.

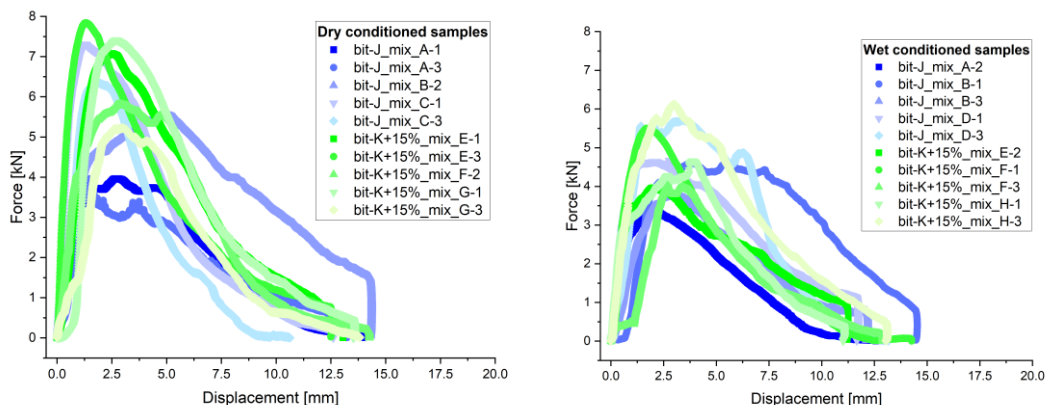


Figure 7.25: Dry and wet conditioned mixture slices, tested with IDT at 10 [°C]

The indirect tensile strength test are carried out by applying a constant speed of deformation of 50 ± 2 [mm/min]. This will give a measurement of the load over the displacements measured by the LVDTs, as seen in Figure 7.25.

The measured peak load can be used to calculate the Indirect Tensile Strength (ITS) and comparing the dry to the wet conditioning, named the Indirect Tensile Strength Ratio (ITSR), the following formulas are used:

$$ITS = \frac{2 \cdot P}{\pi \cdot D \cdot H} \cdot 1000 \approx \frac{2 \cdot P}{\pi \cdot 100 \cdot 40} \cdot 1000 \quad ITS_R = 100 \cdot \frac{ITS_w}{ITS_d} \quad (7.9)$$

The vertical induced force can be translated to the horizontal (thus indirect tensile) stress, which is calculated by:

$$\sigma_h = \frac{P}{D \cdot t} \text{ in } [N/mm^2] \quad (7.10)$$

And the compressive strains, which can be converted to tensile strains, using the Poisson's ratio $\nu \approx 0.35$ [–] for asphalt mixtures, are both shown as well:

$$\varepsilon_n = \frac{h_0 - h_n}{h_0} * 100 \text{ in } [\%] \quad \varepsilon_x = -\frac{\varepsilon_y}{\nu} \quad (7.11)$$

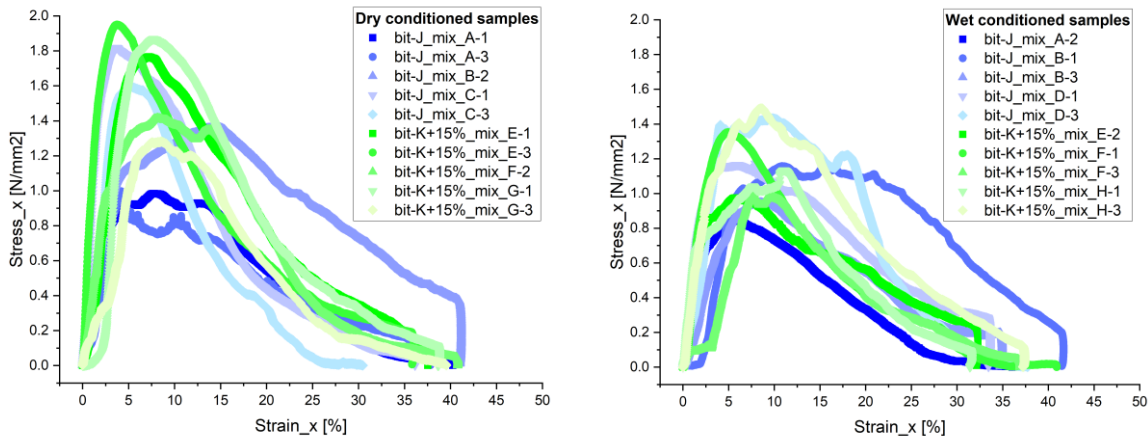


Figure 7.26: Stress and strain diagrams of the dry and wet conditioned IDT tested samples

N.B. one has to notice the fact that the bit-K+15% mixtures were made later than the bit-J mixtures; mixtures ABCD were made earlier than EFGH. This could therefore have an influence on how well the mixtures were made and clearly the variance is much higher for bit-J mixtures than bit-K+15% mixtures. This could thus mean that the first bit-J mixtures have much lower strength, as they are made less accurately, therefore resulting in lower initial (dry) stiffnesses and possibly higher susceptibility with moisture and/or ageing.

This is why the mixtures that performed clearly bad, should be removed from the analysis. Specifically mixture slices A-1, A-3 and B-2 seems to have a significantly lower stiffness and stones were observed to come loose more easily from mixture A (possibly indicating a bit too much binder was added, or not properly/not fast enough mixed). The results from the tests from these specific samples are deemed to be less reliable than the other tests, and thus removed for the selection shown in Figure 7.30.

To qualitatively analyse the difference in failure between the mixtures, their fracture surfaces are also photographed. A sideview of their fractured state is shown in the figure below:

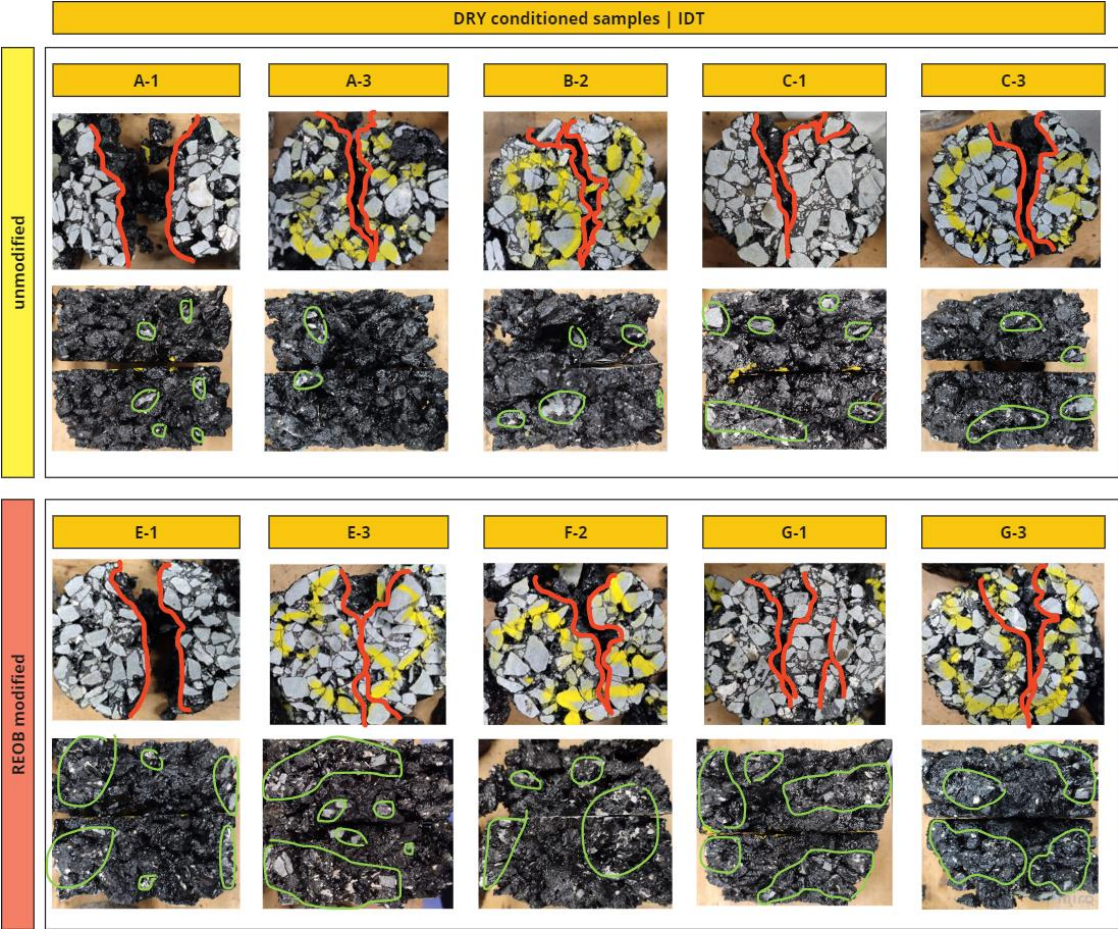


Figure 7.27: The fracture path and surface of all dry conditioned and at 10 [°C] tested IDT samples

From the visual analysis of the cracked surface of these dry IDT samples shown in Figure 7.27, one can easily notice that a lot of variance in the cracking path takes place. Mixtures made with bit-J, being mixtures A, B and C, clearly seem to fail along a very straight path. The failure surface follows a direct path downwards and mixtures A and B show clear extra loss of stones along that surface. Mixture C is clearly performing better. The mixtures with REOB modification show however a different nature. One could say that more like a half-moon path is followed. One side of broken slice being significantly bigger than the other. Only mix G shows some extra cracks to appear in some parts of the mixture.

The failure surface however shows something drastically different between the mixture types. A lot more adhesive failure or even stone failure is visible in the REOB modified mixture. The bit-J mixture shows to mainly fail in a cohesive nature, showing that mainly the bitumen is the limiting factor here.

Overall one would say according to this that the REOB modified mixture performs better, showing generally a stronger behaviour than bit-J, as the:

- Bitumen cohesion seems to be stronger than the stones themselves are
- The cracking path is more difficult to follow, not being a straight path throughout the slice

However this also shows that the mixture is more susceptible to a brittle fracture and also irreversible stone fracture. The mixture with bit-J would allow more healing of cracks that occur in the sample and is therefore not drastically worse.

This can also be compared to the fracture surfaces of the wet conditioned IDT samples, which is shown in Figure 7.28. One can see that generally all the fracture paths follow either a direct route, or failure happens at multiple paths.

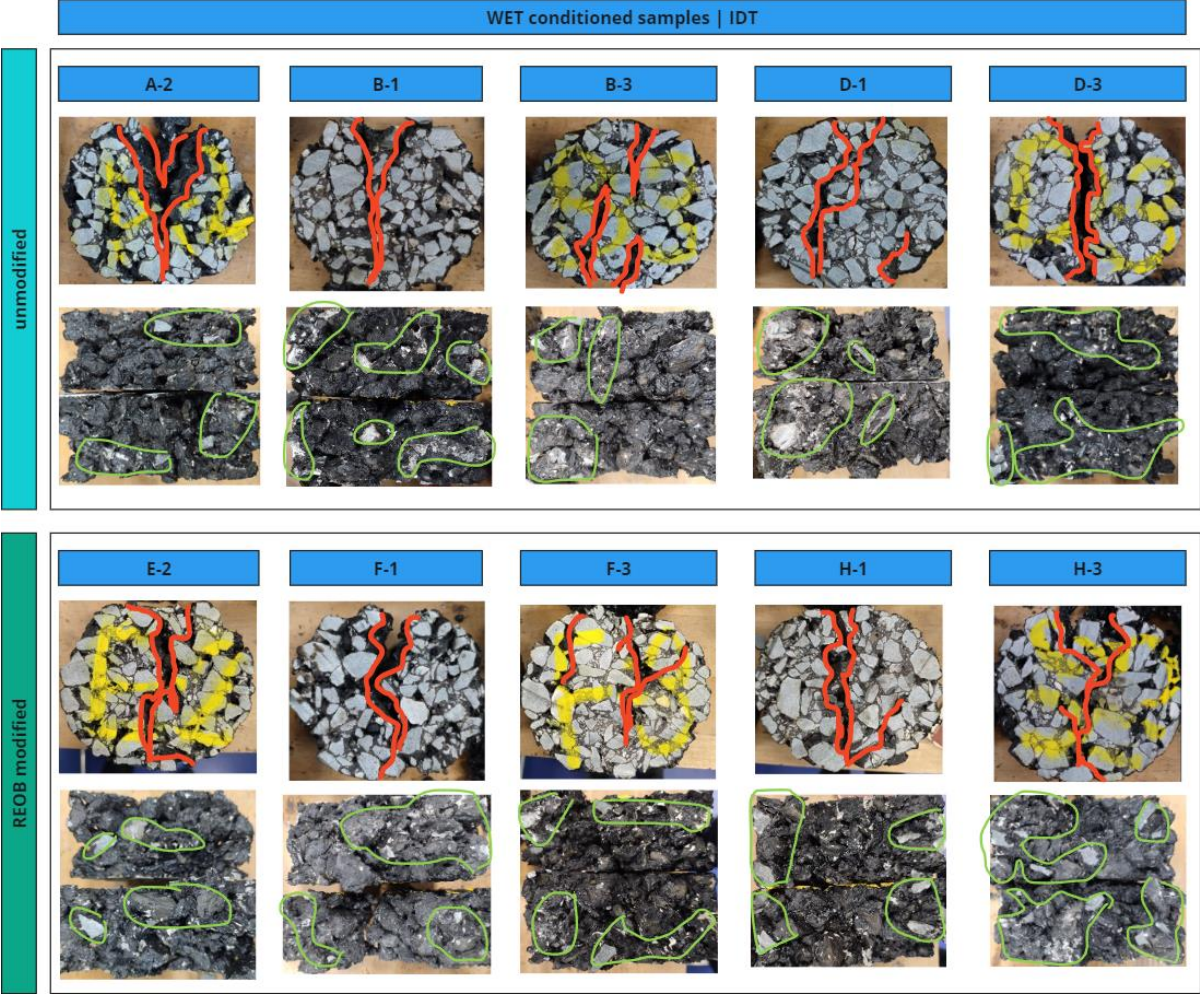


Figure 7.28: The fracture path and surface of all wet conditioned and at 10 [°C] tested IDT samples

The bitumen surface is also heavily different from the dry IDT broken slices, as one can see they look much more grey/brown. This clearly shows the effect that the moisture has had on the binder (and interconnection with stones). Next to that the overall surface area shows a lot more stones. One can thus say that the adhesion/cohesion of the stone-bitumen-stone contact has been significantly worsened for both mixture types.

The following bar plots in Figure 7.30 show the directly measured ITS and ITSR (moisture susceptibility ratio) on the left and the selective measurements on the right. All measurements together show that there is much variance in results, seemingly mainly contributed by the bad strength of mixture A & B of bit-J and mixture G of bit-K+15%. When one removes these measurements from the results, the selection presents a better approximation shown on the right. Variance has been reduced and visibly only a small difference can be noticed between the mixtures and a lot of variance is present between the measured strengths of the mixtures.

Removing some specific measurements from the analysis, namely mixture A, some from B and G, one receives a way better behaviour. The samples that had excessive strains (especially mixture B) or way too low strength (especially mixtures A and G) are removed and the measurements that are used are plotted in Figure 7.29.

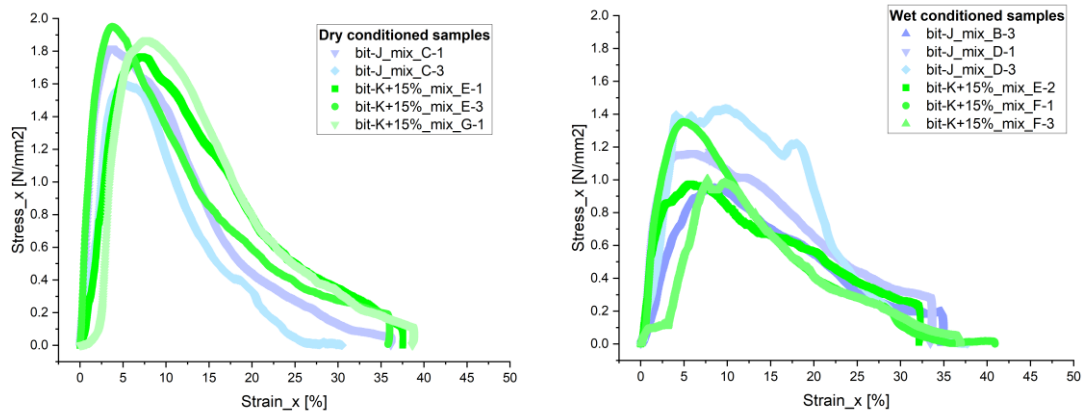


Figure 7.29: Stress and strain diagrams of a selection of the dry and wet conditioned IDT tested samples

From the measured ITS values and the ITSR, the differences between both bit-J and bit-K+15% remain not significantly large. Based solely on the results from this very small dataset, one can still observe that the REOB modified bitumen has higher susceptibility to moisture and cracks easier.

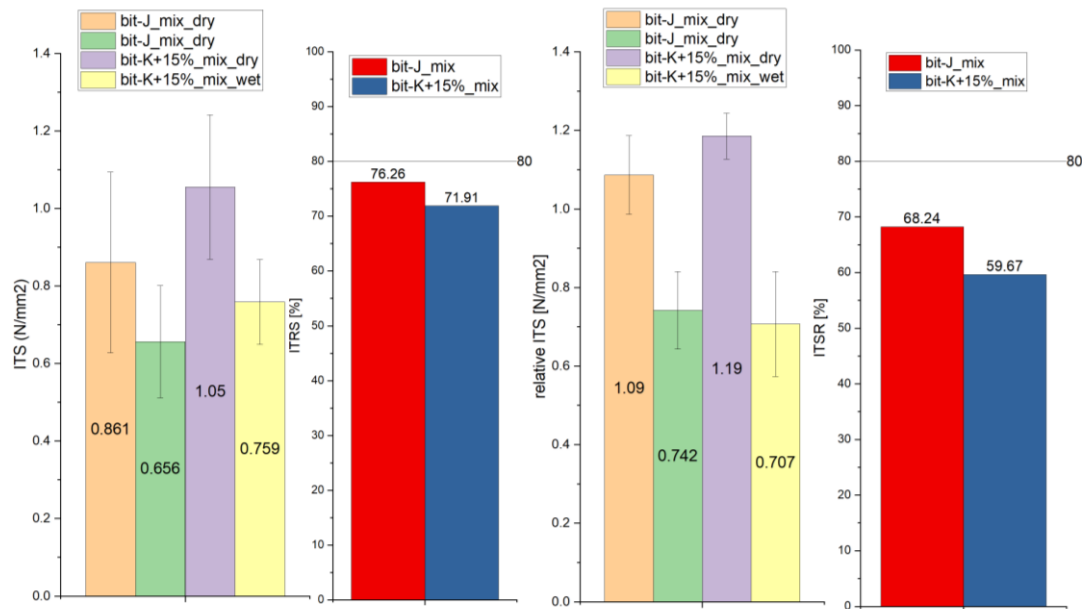


Figure 7.30: All IDT measurements their ITS values (on the left) and selection of best ITS measurements (right)

What is clear from these results however, is that both mixtures are very susceptible to moisture damage. A mixture (or bitumen) with good resistance to this condition will normally have an ITSR value that is at least above 80%. The other important effect to notice, is the fact that the selected REOB modified binder, which used a dosage of 15% of REOB, apparently is initially stronger/stiffer than the bit-J binder. Which is very counterintuitive, as the bit-K+15% has shown in the DSR complex shear modulus values to be softer than the bit-J and its PEN grade was higher too (PEN 98 as compared to PEN 93). This therefore suggests actually that workability and compactability of mixtures using REOB in its bitumen, do not follow an expected behaviour as with unmodified bitumen. Especially using more REOB in a binder is thus deemed to increase this problem even more.

7.2.3. Impact resistance of asphalt mixtures (Cantabro abrasion test)

In total 12 samples are tested with the Los Angeles/Cantabro abrasion test. Of these six will be tested unconditioned, the six other will be freeze-thaw conditioned to observe moisture sensitivity. Half of all samples are resulting from a ZOAB+ mix using bit-J (70/100) and the other half is bit-K+15% (70/100) REOB modified bitumen. The goal is to see if the modification with REOB imposes implications to the binders resistance to lose its stones and to see if moisture has a significant impact on performance. As discussed before, the test has been used to simulate the resistance to ravelling by several researches (Herrington et al., 2005; Mabui et al., 2020; Xu et al., 2018). Some other researches showed how fraction energy could be retrieved (Huang et al., 2022), how the use of recycled concrete aggregate would affect the resistance to ravelling (Elmagarhe et al., 2024) or how a different filler will impact this resistance (Zhang et al., 2018).

The Cantabro abrasion test uses a drum (and in the case of asphalt mixtures: no steel balls) to use the force of impact to create stone loss on aggregates or asphalt mixtures. The drum is turned between 30-33 revolutions per minute, for a total of 300 revolutions/10 minutes. Just before testing, the sample should be weighed accurately and conditioned at the testing temperature, chosen to be 20 [°C] (room temperature). After the test has been carried out, the broken sample is sieved on a sieve of 1.6 [mm] as well as 2, 4 and 5.6mm sieves. Then the masses on the sieves are weighed, showing how much small particles are lost with this test. This will give an indication as to how good the strength of the mixture is and give an indication if one should expect ravelling to be a significant issue or not.

Only two samples of bit-J and two samples of bit-K+15% will be tested, as no more material was available to produce more mixtures. For each sample type one will be tested unconditioned and one will be tested using freeze-thaw cycles, which is done in the following way:

Freeze-thaw cycles

The norm of AASHTO 283 will be applied. The samples are placed in plastic bags with first an extra 10 ± 0.5 [mL] of water, but this was deemed insufficient so enough water was extra added until a thin layer of water was standing on top the sample. Each cycle consists out of two parts:

Part 1: put in a freezer for 24h at -18 ± 3 [°C]

Part 2: followed by 24h in water bath at 60 ± 1 [°C]

This is done for a total of three cycles, as described in ASTM norm D7064/D7064M – 21; Open-Graded Friction Course (OGFC) Asphalt Mixture Design.

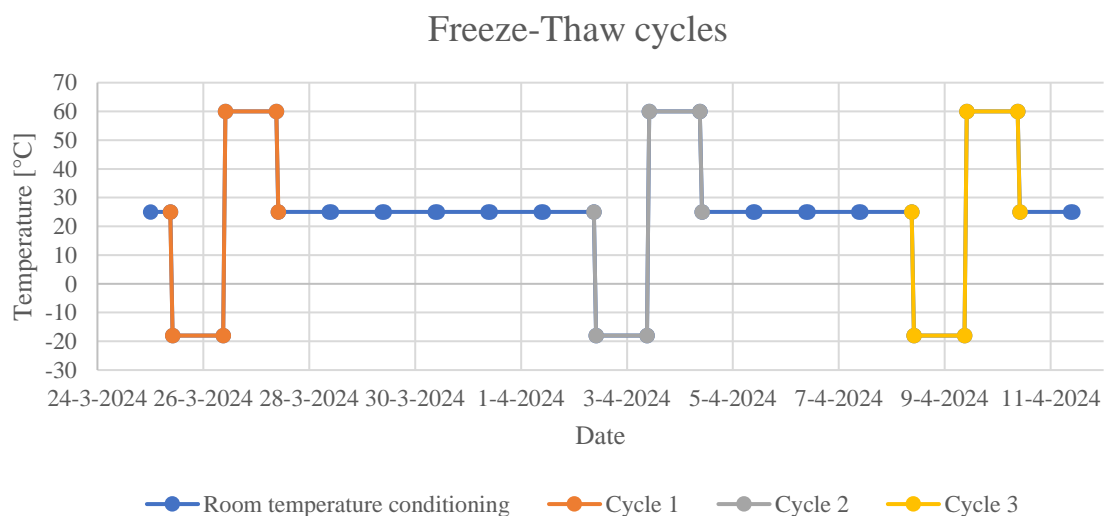


Figure 7.31: Three freeze-thaw cycles procedure; for a total of 12 days; ranging between -18; 25 and 60 [°C]

N.B. As it is impossible to make use of the lab in the weekends, an alternative is proposed, to be able to impose the freeze-thaw cycles on the samples, but also to bridge the weekend. The cycles shown in Figure 7.31 are therefore proposed.

Instead of the commonly used five freeze-thaw cycles, only three are selected. This is deemed sufficient to show freeze-thaw condition susceptibility for the binders in the straightforward Cantabro Abrasion test, as well as the problem of having only limited time available. The samples are sealed in plastic bags that are fit for a freezer and can be sealed to not lose the water added.

With the three freeze-thaw cycles performed, the Cantabro Abrasion tests can be carried out. In Figure 7.32 and Figure 7.33 the dry and the freeze-thaw conditioned states are shown of both mixture types tested with the Cantabro abrasion test.



Figure 7.32: “ravelled” asphalt mixtures with bit-J after dry (left) and Freeze-Thaw conditioning (right) Cantabro Abrasion test (more damage is visible after conditioning)

The mixture made with bit-J shows initially to have some loss of stones, but the freeze-thaw conditioning has shown more deterioration. This can then be compared to the bit-K+15% mixture shown in the following figure:



Figure 7.33: “ravelled” asphalt mixtures with bit-K+15% after dry (left) and Freeze-Thaw conditioning (right) Cantabro Abrasion test (significantly more damage is visible after conditioning)

The impact resistance that the mixture, made with bit-K+15%, has shown to initially have a bit better cohesion in dry state, but after the same freeze-thaw conditioning as bit-J one can notice that for the REOB modified mixture almost no parts remain that still have a cohesion to them. This shows that REOB modified mixtures are much more sensitive to freeze-thaw conditioning. To evaluate the loss of cohesion, the stones that were lost can be sieved and the fractions can be weighed. The 1.6 [mm] sieve is used like the ASTM norm D7064/D7064M – 21 describes, but as this is only one fraction also sieving is done with 2; 4 and 5.6 [mm] sieves.

The intact parts of the slices (still having some cohesive strength) are measured as the intact weight fraction. The remainder that stays on a sieves is noted as the weight fraction of that sieve and the last

portion is caught by the pan and obtains this fraction. The figures below show the respective measured weight fractions indicating the stone loss of each condition and mixture type:

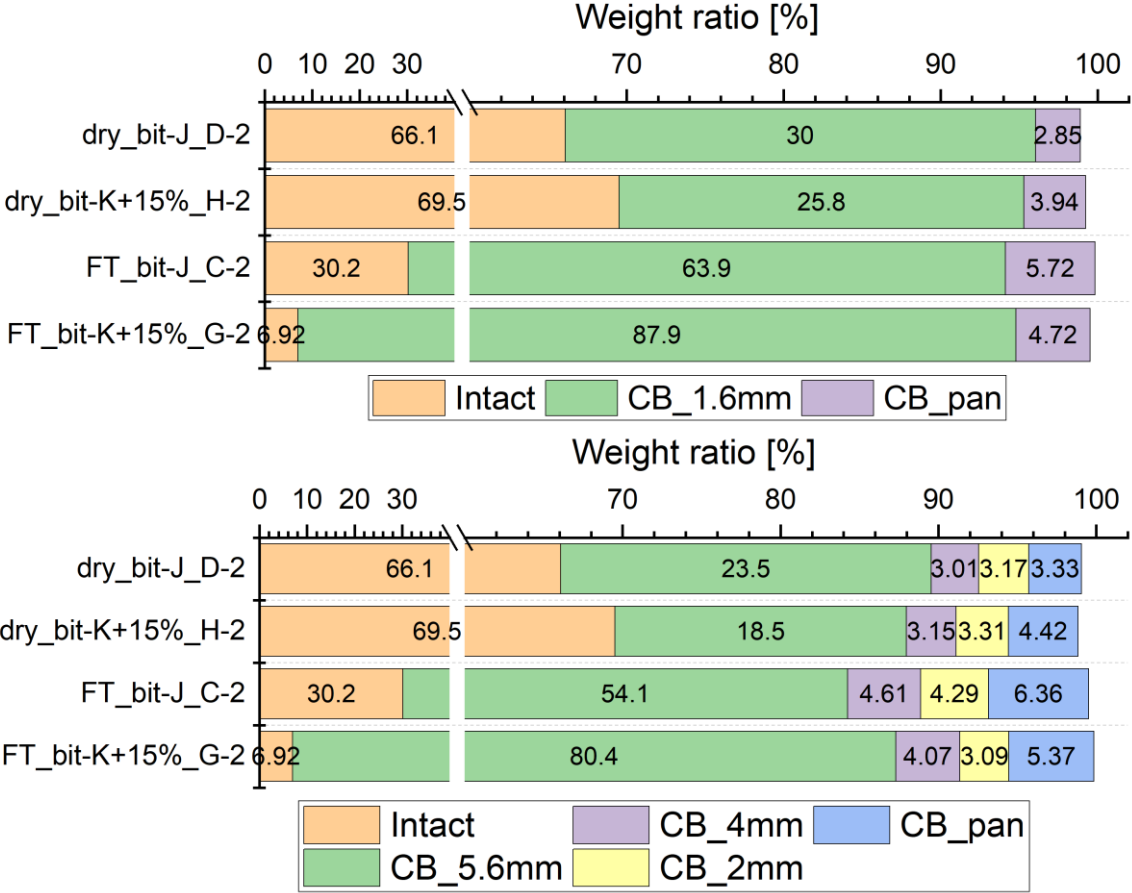


Figure 7.34 (top) the 1.6 [mm] sieve fraction according to the ASTM norm and (bottom) the 2; 4 and 5.6 [mm] sieve fractions

From the simple Cantabro Abrasion test one can thus conclude that initially REOB modified mixtures will have a slightly better cohesion and more resistance to impacts/“ravelling”, but after freeze-thaw conditioning the REOB modified mixtures are much more keen to lose cohesive strength.

7.2.4. Observations on mixture performance

With the analysis on the compactability, represented by the difficulty the gyrator compactor had to bring the sample to the intended height, but also the dry and wet conditioned IDT tests and lastly the Cantabro Abrasion test, one can give an indication on how well REOB modified mixtures perform as compared to unmodified bitumen from a similar source.

- (1) The resistance that mixtures had while compacting in the gyrator has shown that the REOB modified mixture was in general more difficult to compact. Although some of the early mixtures of the reference unmodified mixture, bit-J, were deemed insufficiently strong and seemed to have been made poorly (this was deemed the result of inexperience making the first mixtures: using slightly too much bitumen, working too slow and the mixture cooling down etc).
- (2) This was further proven by IDT tests on the dry conditioned samples, which have shown that the REOB modified bitumen mixtures result in initially significantly stiffer and stronger mixtures, which is very counterintuitive regarding the known significantly softer nature that bit-K+15% should have as compared to bit-J (recalling the DSR frequency sweep measurements in Chapter 5). Although PEN grade or PG grade indicates binders are within similar boundaries, other research has shown too that a lot of variance in expected strength is measured with REOB modified bitumen (Mensching et al., 2017; Mogawer et al., 2017; Xin-jun et al., 2016).
- (3) With IDT wet tests it is made clear that the REOB modified mixtures have an ITSR value of around 60%, signifying a very drastic loss in cohesive strength of the mixture after moisture conditioning the samples. When comparing this to the bit-J reference mixture, one finds an ITSR value of 70% which is still showing a loss in strength, although less significant. This loss in strength due to moisture damage was indeed found before (Xin-jun et al., 2016).
- (4) The Cantabro test, although using only a few samples, has further proven the same conclusion as the IDT presented. Initially a REOB modified mixture seems to be a bit stiffer and stronger, although after freeze-thaw conditioning it has shown substantially more susceptibility moisture damage.

This concludes that REOB mixtures are generally more stiff and moisture susceptible, than one would expect initially from rheological measurements; meaning REOB modified bitumen changes in expected properties significantly when mixed into an asphalt mixture.

Chapter 8. Discussion, conclusion and recommendations on REOB modified bitumen

8.1. Discussion of chemical, rheological and mechanical results

With the multi-scale analysis of REOB modified bitumen and asphalt mixtures performed on nano, molecular, micro and macro scale; the use of this re-refined oil for fluxing with bitumen are discussed and conclusions are drawn in this Chapter.

In Chapter 4.2.1 the identification of REOB in a bitumen has been successfully demonstrated with XRF and ICP, to detect the trace elements and metals, where bitumen from some sources can naturally contain distinct trace metals which are indicative of REOB or WEO. The FTIR measurements in Chapters 4.2.4 and 4.2.5 have shown however that one can effectively measure functional groups indicating the trace of lubricant additives, of which PIB specifically can be used to identify and quantify REOB in a bitumen. As REOB itself can have a varying intensity in PIB, however quantification of the dosage of REOB in a bitumen remains problematic. It was noticed however that when high PIB amounts are present then other lubricant additives will also be following the same trend apparent from the intensity of the peaks. An index for lubricant additives present in a bitumen is therefore suggested, instead of one for a REOB dosage.

Further elemental analysis has shown that REOB modified bitumen has a stronger degree of initial oxygen content and propensity for further oxidation, visible in Chapters 4.2.4 and 4.3. REOB modification primarily influences the increased formation of carbonyl groups but not for sulfoxide. SARA fractions have shown that the aromatics and saturates fractions have been affected the most, where saturates fractions show a decline already during storage of the REOB -although it remains ambiguous whether this is due to the loss of the specific fraction or its chemical transition into more polar fraction. Molecular weight distributions suggest that REOB modified bitumen tends to have a higher molecular weight compared to unmodified bitumen, with specific influence on M_n and M_w weight averages. Ageing of the REOB shows to follow a similar trend as bitumen does, although REOB modified bitumen show to have their maltene peak to be shifted towards higher molecular weights, suggesting an initial shift that brings the bitumen to a more aged state. Phase transitions through thermal events in REOB modified bitumen, measured by DSC, do not show distinct differences compared to unmodified bitumen.

Rheological behaviour evaluated in Chapter 5.2 has shown that initial modification with REOB achieves the intended comparable viscoelastic response properties, where showing an overlap in black space diagram curves. The PEN grades in Chapter 3.3 appear to be uncorrelated with the viscoelastic behaviour of REOB modified bitumen, where the 70/100 grade reference bitumen overlaps in rheology with the 40/60 grade REOB modified bitumen. Ageing studies has shown that REOB modified bitumen exhibits drastic change in rheological behaviour with higher dosages. Low temperature behaviour measured with DSR frequency sweep tests, were able to distinguish bitumen with good or bad properties using Cole-Cole diagrams. The BBR tests in Chapter 5.3 has suggested similar relaxation problems of those bitumen at low temperatures, by showing how the relaxation of the material decreases (shown by $T_c(m)$) much faster than the stiffness (shown by $T_c(S)$) increases for REOB modified bitumen after ageing. REOB modified bitumen approaches limitations in relaxation properties with increasing dosage, as indicated by the loss modulus from DSR and $T_c(m)$ from BBR. While Ageing of these bitumen shows effects more pronounced.

Correlations between bitumen has shown in Chapter 6.1 that chemical PCA analysis can effectively cluster bitumen according to the respective supplier and/or crude source. Next to that the ageing susceptibility of REOB modified bitumen appears to be primarily explained by an increased oxidation

in the form of carbonyl formation than sulfoxide, a significant impact on the colloidal instability of a bitumen, as seen in Chapter 6.2. Saturates and asphaltenes are particularly impacted initially, influencing the internal structure of the bitumen. The changes of these fractions due to ageing are reflected in the rheological behaviour with a more drastic rate compared to unmodified bitumen that have a high asphaltene and HWF already, which is shown by the correlated SARA and GPC results in Chapter 6.3. Next to that the colloidal instability evaluated in Chapter 6.4 shows how REOB modified bitumen are - susceptible to brittle failure due to its transition towards a gel-type structure, although with ageing one can see a change back towards a sol-phase microstructure. The microstructure of REOB modified bitumen seems to therefore be heavily compromised and which might be resulting from the distinct saturates and asphaltenes present in REOB.

The adhesive/cohesive stone-bitumen interaction behaviour evaluated in Chapter 7.1.1 indicate that REOB modified bitumen are more sensitive to change in strain rate while exhibits increased brittleness. There is more stress build-up and the cohesive strength of the bitumen shows to be limited in response to higher strain rate. Chapter 7.1.2 further confirms the limitation on cohesive strength from the mastic column testing for REOB modified bitumen. Next to that, the test results point out a difference in the effect of fillers. The REOB modified bitumen is deemed to be of higher acidity, promoting reaction between bitumen and filler and thus increasing in adhesive strength. The difference in response can be due to the difference in selective adsorption of REOB phase in these two types of fillers which are different in chemistry and believed to be different in microporosity.

The IDT tests and the Cantabro Abrasion test have shown in Chapter 7.2 that initially the REOB modified mixtures, although the bitumen is selected at the same PEN grade, will be of higher stiffness and strength. Although they were also way more susceptible to moisture and freeze-thaw cycles than the compared reference bitumen was. This shows therefore a good connection to the DMA measurements, which had also shown an increased strength and brittleness for REOB modified bitumen. Based purely on these statements, mixing of REOB modified bitumen with polymers, recovered bitumen or reclaimed asphalt in a mixture is deemed therefore to bring the mixture even closer to too brittle/stiff nature and cracking limits, than what one would expect from rheological measurements alone. This should however be evaluated further to prove this suspicion.

8.2. Conclusions on REOB modified bitumen

To recall the goal of this thesis, the following questions should be answered:

- A. Is there an effective way to **identify** and **quantify** REOB when added to bitumen?
- B. How does REOB modification, at **different dosages** and **ageing** levels, alter bitumen characteristics; *chemically, rheologically* and *mechanically*?
- C. How does REOB modified bitumen perform as **compared to original/unmodified bitumen**?
- D. What **correlations** exist between *rheological* and *chemical* characteristics of (non-) modified bitumen?

Regarding question A, about identification of REOB in bitumen, the following conclusion can be drawn:

- (1) REOB can be identified with FTIR technique and evaluating the derivative of the retrieved spectrogram. The polyisobutylene peak (PIB) at ~ 1230 [cm^{-1}] can be used to quantify REOB in a bitumen. Bitumen does not have this compound, but as REOB itself can differ in its content means that quantification remains problematic.

The retrieved PIB index can however indicate a large or low presence of lubricant additives that still reside in the REOB, as a high content of PIB shows to correlate to a high content of other additives (like Si-O-Si or P-O-C). Compared to measured variance in trace metals contents with XRF this works more effectively and does not depend on base bitumen consistency.

Regarding question B one can state the following:

- (2) It was noticed that PEN grade was ineffective in describing the rheological behaviour of REOB modified bitumen, where there was an viscoelastic overlap in complex shear modulus values between 70/100 reference bitumen and a 40/60 grade REOB modified bitumen. PEN grade changes exponentially with REOB dosage, whereas the softening temperature and other rheological parameters show a linear change when dosage is increased.
- (3) Mechanically REOB modified asphalt mixtures have shown in IDT, Cantabro abrasion and DMA mastic cohesion tests to become stiffer and stronger than expected, while also having a substantial susceptibility towards moisture and freeze-thaw damage. REOB modified bitumen, when mixed with filler and aggregate material, show to approach a stiffer and stronger state much more than can be expected from sole rheological experiments.

Question C seems to be answered by the whole multi-scale approach as:

- (4) The chemical composition of bit-P and bit-K compared has shown that bit-P has much higher resistance to oxidation and has larger LWF and aromatics fractions that can act as a buffer to ageing, as compared to bit-K. Regarding rheological behaviour the rheological behaviour of the base bitumen is reflected in the REOB modified bitumen and has shown that bit-P has much better properties at lower temperatures. Bit-K blends have shown however to have higher stiffnesses and phase shift angles at intermediate temperatures, suggesting a slightly better performance there. Changes with ageing however shows to be slightly bigger in the case of bit-K blends than the bit-P blends. This suggests that bitumen with broader weight distributions, substantial asphaltenes fractions and lower susceptibility to form carbonyls will receive REOB better.

N.B. Both bit-P and bit-K however had a substantially low saturates fraction which was thus heavily increased after REOB addition; it is thus unknown what REOB would do in a bitumen that has a high saturates fraction already.

Question D seems to be answered best by the correlation Chapter 6 and the mechanical performance in Chapter 7:

- (5) Ageing susceptibility of REOB modified bitumen has shown chemically that there is an increased initial oxygen content, increased carbonyl growth rate (although not sulfoxide), loss of saturates and loss of low weight fraction. There seems to be a mismatch between molecular SARA fractions of REOB modified bitumen, where the asphaltenes seem to be impacted the most, suggesting the relation with increased oxidation rate. This can thus be related to the accelerated increase in viscosity with ageing. Translating this to the rheological behaviour that shows the bitumen with higher REOB dosage gain in stiffness and loss in viscous property with ageing at a higher rate than lower dosages.
- (6) Low temperature behaviour of the REOB modified bitumen has shown in DSR, BBR and DMA that there is an increased loss in relaxation capabilities, suggesting that REOB modification initially makes a bitumen of a gel-type nature. After ageing however the loss in saturates and the change in asphaltenes suggest the colloidal stability is compromised and the strength of the micelle structure is lowered. This means such bitumen are much more susceptible to having brittle failure and relaxation problems at lower temperatures, but could also explain the mentioned initial mismatch between PEN grade and complex shear modulus measurements.

With these conclusions, now recommendations can be formed on both the suggestion on future research and suggestions for the industry on how best to handle REOB modified bitumen.

8.3. Recommendations on REOB modified bitumen

Finally, the following recommendations are drawn up concerning both the use of REOB in practice and the best way to approach future research on this subject. Regarding future research, the following subjects on REOB modified bitumen should be evaluated further:

1. Investigating the chemical differences between REOB sources; to map especially the variance in SARA fractions, molecular weight distributions and oxidation rates when blended with bitumen. GC-MS analysis on REOB should bring light to what type of molecules are present in it, evaluating especially the types of saturates and asphaltenes would be valuable in this case. Lastly, the (storage) stability of the REOB itself is not yet fully understood, where the variance in chemical composition REOB could play a big role when modifying bitumen.
2. A combined chemical and rheological study on ageing susceptibility of different REOB with the same base bitumen should be performed; to see what specifically in REOB actually promotes the increased ageing rate of the modified bitumen (in this research the difference in base bitumen was evaluated); suggestion would be to go more into detail on the formation of carbonyls and the change in molecular weights of asphaltenes in REOB and modified bitumen.
3. Evaluate the effect of trace metals and lubricant additives that reside in a REOB; do these trace metals promote the increased oxidation rate in the form of carbonyls? Do the lubricant additives pose a problem on adhesive properties of a bitumen and at how high can the limit on the trace metals and lubricant additives be set?
4. Low temperature performance should be evaluated further with 4-mm DSR and DMA adhesion tensile (fatigue) testing, combined with chemical profiling of SARA and GPC, to further evaluate what aspects of the REOB cause the increased brittle nature and better understand the sol/gel phase behaviour. This could be expanded by further evaluating the microstructure that REOB modified bitumen has, performing microscopy experiments on such blends.
5. Optimisation of mixture design; by altering aggregate sieve fractions or the filler to bitumen ratio with the goal to reach an allowable performance regarding workability, ageing susceptibility and moisture sensitivity to allow the use of REOB in asphalt mixtures.
6. Based on observations from DMA mastic cohesion tests, the effect of the acidity of REOB on a bitumen and its reaction with filler material and aggregates should be evaluated further. Here the benefit of using REOB could already occur at lower dosages <5% and REOB could possibly be used as an adhesion reaction promotor instead of a fluxing material.
7. The use of REOB to flux with straight-run hard grade bitumen seems to be heavily reflecting bad performance of the base bitumen itself in the resulting modified bitumen; one could therefore set up a completely controlled set of base bitumen of different hard grades, air-blown/oxidised and polymer modified bitumen to evaluate what base bitumen actually would be a fitting to flux with REOB.

Alternatively to recommendations for future research, a suggestion for the pavement industry can also be given on how one deals with REOB and modified bitumen. Therefore, on the following page a flow-chart is presented which describes a step-by-step plan one can follow to evaluate the effectiveness of using a REOB modified bitumen and its critical behaviours shown in Appendix part B. In Appendix part A one can find the approach on how to identify REOB in a bitumen.

Next to the flow chart, general recommendations on the usage of REOB for bitumen and mixture modification, can be summed up to the following points:

1. In the case of blending hard grade base bitumen with REOB:

- a. Choose a base bitumen which has a substantial fraction of asphaltenes (of relatively high molecular weights) and saturates fraction, to create a buffer for low temperature susceptibility
- b. Choose a REOB with low amounts of lubricant additives, which is stable during storage and has a molecular weight distribution which spreads to both HWF and LWF substantially
- c. Check different dosages to find the best match between PEN grade, low and high temperature rheological behaviour and if ageing susceptibility will still be small

2. In the case of receiving a REOB modified bitumen:

- a. Check PIB maximum derivative or trace metal count to see how high the dosage is
- b. Evaluate ageing behaviour for SARA fraction stability and rheological behaviour
- c. Be aware of PEN grade deviations from DSR rheological behaviour
- d. Watch out with blending of REOB modified bitumen with:
 - i. Polymers; these will further increase the already heavily influenced viscosity
 - ii. Recovered bitumen or recycled asphalt concrete as aged bitumen would be a different story than REOB modification of “fresh” straight run bitumen

3. In the case of handling a pavement that was REOB modified

- a. Recovering bitumen or reclaiming asphalt mixtures that have been modified with REOB does not promise good properties to be used in making a new asphalt mixture; this should be evaluated and optimised first.
- b. Applying rejuvenators on the road to extend service life do not per se have to work well with REOB modified bitumen; its consistency is totally different to unmodified bitumen.

References

- Airey, G., Collop, A., Zoorob, S., & Elliott, R. (2008). The influence of aggregate, filler and bitumen on asphalt mixture moisture damage. *Construction and Building Materials*, 22(9), 2015-2024.
- Airey, G. D. (2002). Use of black diagrams to identify inconsistencies in rheological data. *Road Materials and Pavement Design*, 3(4), 403-424.
- Airey, G. D., Rowe, G. M., Sias, J. E., Di Benedetto, H., Sauzeat, C., & Dave, E. V. (2021). Black Space Rheological Assessment of Asphalt Material Behavior. *Journal of Testing and Evaluation*, 50(2).
- Anderson, D. A., Christensen, D. W., Bahia, H. U., Dongre, R., Sharma, M., Antle, C. E., & Button, J. (1994). Binder characterization and evaluation, volume 3: Physical characterization. *Strategic Highway Research Program, National Research Council, Washington, DC*.
- Apostolidis, P., Elwardany, M., Porot, L., Vansteenkiste, S., & Chailleux, E. (2021). Glass transitions in bituminous binders. *Materials and Structures*, 54(3), 132.
- Arnold, T. S., & Shastry, A. (2015). *Analysis of asphalt binders for recycled engine oil bottoms by X-ray fluorescence spectroscopy*.
- AsphaltInstitute. (2016). *The use of REOB/VTAE in Asphalt* (Information Series 235; ISBN 978-1-934154-74-8, Issue).
- AsphaltInstitute. (2019). *USE OF THE DELTA Tc PARAMETER TO CHARACTERIZE ASPHALT BINDER BEHAVIOR* (Information Series 240; ISBN 978-1-934154-77-9, Issue).
- Barborak, R. C., Coward Jr, C. E., & Lee, R. E. (2016). Detection and estimation of re-refined engine oil bottoms in asphalt binders: Texas department of transportation's approach with wavelength dispersive X-ray fluorescence spectroscopy. *Transportation Research Record*, 2574(1), 48-56.
- Baumgardner, G., Hand, A. J., Hajj, E. Y., & Aschenbrener, T. B. (2023). Responsible Use of Re-Refined Engine Oil Bottoms (REOB).
- Bayane, B. M., Yang, E., & Yanjun, Q. (2017). Dynamic modulus master curve construction using Christensen-Anderson-Marasteanu (CAM) model. *Int. J. Eng. Res. Appl*, 7(1), 53-63.
- Bennert, T., Ericson, C., Pezeshki, D., & Corun, R. (2016). Fatigue performance of re-refined engine oil bottom-modified asphalt: laboratory study. *Transportation Research Record*, 2574(1), 1-16.
- Besamusca, J., Poeran, N., & Sluer, B. (2021). The unexpected addition of materials to bitumen in the Netherlands. 9th EATA Conference
- Boysen, R., & Schabron, J. (2015). Laboratory and field asphalt binder aging: Chemical changes and influence on asphalt binder embrittlement. *Technical White Papers of 17 WRI*, 18.
- Chailleux, E., Queffelec, C., Borghol, I., Farcas, F., Marceau, S., & Bujoli, B. (2021). Bitumen fractionation: Contribution of the individual fractions to the mechanical behavior of road binders. *Construction and Building Materials*, 271, 121528.
- Chen, H., Barbieri, D. M., Zhang, X., & Hoff, I. (2022). Reliability of Calculation of Dynamic Modulus for Asphalt Mixtures Using Different Master Curve Models and Shift Factor Equations. *Materials*, 15(12), 4325.
- Christensen, D. W., Anderson, D. A., & Rowe, G. M. (2017). Relaxation spectra of asphalt binders and the Christensen-Anderson rheological model. *Road Materials and Pavement Design*, 18(sup1), 382-403.
- Cooper Jr, S. B., Negulescu, I., Balamurugan, S. S., Mohammad, L., Daly, W. H., & Baumgardner, G. L. (2017). Asphalt mixtures containing RAS and/or RAP: Relationships amongst binder composition analysis and mixture intermediate temperature cracking performance. *Road Materials and Pavement Design*, 18(sup1), 209-234.
- D'ANGELO, J. A., Grzybowski, K., Lewis, S., & Walker, R. (2013). Evaluation of the performance properties of asphalt mixes produced with re-refined heavy vacuum distillate bottoms. PROCEEDINGS OF THE FIFTY-EIGHTH ANNUAL CONFERENCE OF THE CANADIAN TECHNICAL ASPHALT ASSOCIATION (CTAA): ST. JOHN'S, NEWFOUNDLAND AND LABRADOR, NOVEMBER 2013,
- Daly, W. H., Negulescu, I. I., & Balamurugan, S. S. (2019). *Chemical characterization of asphalts related to their performance*.

- Eleyedath, A., & Swamy, A. K. (2020). Use of waste engine oil in materials containing asphaltic components. In *Eco-Efficient Pavement Construction Materials* (pp. 33-50). Elsevier.
- Elmagarhe, A., Lu, Q., Alamri, M., Alharthai, M., & Elnihum, A. (2024). Laboratory performance evaluation of porous asphalt mixture containing recycled concrete aggregate and fly ash. *Case Studies in Construction Materials*, 20, e02849.
- Elwardany, M., Planche, J.-P., & King, G. (2020). Universal and practical approach to evaluate asphalt binder resistance to thermally-induced surface damage. *Construction and Building Materials*, 255, 119331.
- Fernandes, S. R., Silva, H. M., & Oliveira, J. R. (2018). Developing enhanced modified bitumens with waste engine oil products combined with polymers. *Construction and Building Materials*, 160, 714-724.
- Frąckowiak, E., Płatek-Mielczarek, A., Piwek, J., & Fic, K. (2022). Advanced characterization techniques for electrochemical capacitors. In *Advances in Inorganic Chemistry* (Vol. 79, pp. 151-207). Elsevier.
- Freeston, J.-L., Gillespie, G., Hesp, S. A., Paliukaite, M., & Taylor, R. (2015). Physical hardening in asphalt. Proceedings of the Sixtieth Annual Conference of the Canadian Technical Asphalt Association (CTAA): Winnipeg, Manitoba,
- Golalipour, A. (2013). *Investigation of the effect of oil modification on critical characteristics of asphalt binders* [The University of Wisconsin-Madison].
- Guo, M., Liang, M., Fu, Y., Sreeram, A., & Bhasin, A. (2021). Average molecular structure models of unaged asphalt binder fractions. *Materials and Structures*, 54(4), 173.
- Hagos, E. T. (2008). The effect of aging on binder properties of porous asphalt concrete.
- Herrington, P. (1992). Use of re-refined oil distillation bottoms as extenders for roading bitumens. *Journal of materials science*, 27, 6615-6626.
- Herrington, P., Dravitzki, V., Wood, C., & Patrick, J. (1993). Waste oil distillation bottoms as bitumen extenders. *Road and transport research*, 2(4).
- Herrington, P., & Hamilton, P. (1998). *Recycling of waste oil distillation bottoms in asphalt*.
- Herrington, P., Reilly, S., & Cook, S. (2005). *Porous asphalt durability test*. Transfund New Zealand Lower Hutt.
- Hesp, S., Genin, S., Scafe, D., Shurvell, H., & Subramani, S. (2009). Five Year Performance Review of a Northern Ontario Pavement Trial: Validation of Ontario's Double-Edge-Notched Tension (DENT) and Extended Bending Beam Rheometer (BBR) Test Methods.
- Hesp, S. A., & Shurvell, H. F. (2010). X-ray fluorescence detection of waste engine oil residue in asphalt and its effect on cracking in service. *International Journal of Pavement Engineering*, 11(6), 541-553.
- Hofko, B., Alavi, M. Z., Grothe, H., Jones, D., & Harvey, J. (2017). Repeatability and sensitivity of FTIR ATR spectral analysis methods for bituminous binders. *Materials and Structures*, 50, 1-15.
- Huang, W., Yu, H., Lin, Y., Zheng, Y., Ding, Q., Tong, B., & Wang, T. (2022). Energy analysis for evaluating durability of porous asphalt mixture. *Construction and Building Materials*, 326, 126819.
- Jing, R., Varveri, A., Liu, X., Scarpas, A., & Erkens, S. (2021). Ageing effect on chemo-mechanics of bitumen. *Road Materials and Pavement Design*, 22(5), 1044-1059.
- Johnson, K.-A. N., & Hesp, S. A. (2014). Effect of waste engine oil residue on quality and durability of SHRP materials reference library binders. *Transportation Research Record*, 2444(1), 102-109.
- Karki, P., Meng, L., Im, S., Estakhri, C. K., & Zhou, F. (2019). *Re-refined Engine Oil Bottom: Detection and Upper Limits in Asphalt Binders and Seal Coat Binders*.
- Karki, P., & Zhou, F. (2019). Impact of re-refined engine oil bottoms on asphalt binder properties. *Journal of Transportation Engineering, Part B: Pavements*, 145(4), 04019033.
- Kaskow, J., van Poppelen, S., & Hesp, S. A. (2018). Methods for the quantification of recycled engine oil bottoms in performance-graded asphalt cement. *Journal of Materials in Civil Engineering*, 30(2), 04017269.

- Kaya, D., Topal, A., & McNally, T. (2019). Relationship between processing parameters and aging with the rheological behaviour of SBS modified bitumen. *Construction and Building Materials*, 221, 345-350.
- Kim, K. W., & Burati Jr, J. L. (1993). Use of GPC chromatograms to characterize aged asphalt cements. *Journal of Materials in Civil Engineering*, 5(1), 41-52.
- King, G., Anderson, M., Hanson, D., & Blankenship, P. (2012). Using black space diagrams to predict age-induced cracking. 7th RILEM International Conference on Cracking in Pavements: Mechanisms, Modeling, Testing, Detection and Prevention Case Histories,
- Kleizienė, R., Panasenkienė, M., & Vaitkus, A. (2019). Effect of aging on chemical composition and rheological properties of neat and modified bitumen. *Materials*, 12(24), 4066.
- Kontou, A., Taylor, R., & Spikes, H. (2021). Effects of dispersant and ZDDP additives on fretting wear. *Tribology Letters*, 69(1), 6.
- Kriz, P., Campbell, C. M., Kucharek, A. S., & Varamini, S. (2020). A simple binder specification tweak to promote best performers. *Proc., Can. Tech. Asphalt Assoc.*
- Kriz, P., Stastna, J., & Zanzotto, L. (2008). Glass transition and phase stability in asphalt binders. *Road Materials and Pavement Design*, 9(sup1), 37-65.
- Lee, S.-J., Amirkhanian, S. N., Shatanawi, K., & Kim, K. W. (2008). Short-term aging characterization of asphalt binders using gel permeation chromatography and selected Superpave binder tests. *Construction and Building Materials*, 22(11), 2220-2227.
- Lesueur, D. (2009). The colloidal structure of bitumen: Consequences on the rheology and on the mechanisms of bitumen modification. *Advances in colloid and interface science*, 145(1-2), 42-82.
- Lesueur, D., Elwardany, M. D., Planche, J.-P., Christensen, D., & King, G. N. (2021). Impact of the asphalt binder rheological behavior on the value of the ΔT_c parameter. *Construction and Building Materials*, 293, 123464.
- Li, X., Guo, D., Xu, M., Guo, C., & Wang, D. (2023). REOB/SBS Composite-Modified Bitumen Preparation and Modification Mechanism Analysis. *Buildings*, 13(7), 1601.
- Liu, S., Peng, A., Wu, J., & Zhou, S. B. (2018). Waste engine oil influences on chemical and rheological properties of different asphalt binders. *Construction and Building Materials*, 191, 1210-1220.
- Lu, X., Soenen, H., Sjövall, P., & Pipintakos, G. (2021). Analysis of asphaltenes and maltenes before and after long-term aging of bitumen. *Fuel*, 304, 121426.
- Lushinga, N., Cao, L., & Dong, Z. (2019). Effect of silicone oil on dispersion and low-temperature fracture performance of crumb rubber asphalt. *Advances in Materials Science and Engineering*, 2019, 1-12.
- Ma, J., Sun, G., Sun, D., Yu, F., Hu, M., & Lu, T. (2021). Application of gel permeation chromatography technology in asphalt materials: A review. *Construction and Building Materials*, 278, 122386.
- Ma, L., Varveri, A., Jing, R., & Erkens, S. (2023). Chemical characterisation of bitumen type and ageing state based on FTIR spectroscopy and discriminant analysis integrated with variable selection methods. *Road Materials and Pavement Design*, 24(sup1), 506-520.
- Mabui, D., Tjaronge, M., Adisasmita, S., & Pasra, M. (2020). Resistance to cohesion loss in cantabro test on specimens of porous asphalt containing modified asbuton. IOP Conference Series: Earth and Environmental Science,
- Marateanu, M., & Anderson, D. (1996). Time-temperature dependency of asphalt binders--An improved model (with discussion). *Journal of the Association of Asphalt Paving Technologists*, 65.
- Mastoras, F., Varveri, A., van Tooren, M., & Erkens, S. (2021). Effect of mineral fillers on ageing of bituminous mastics. *Construction and Building Materials*, 276, 122215.
- Mensching, D. J., Andriescu, A., DeCarlo, C., Li, X., & Youtcheff, J. S. (2017). Effect of extended aging on asphalt materials containing re-refined engine oil bottoms. *Transportation Research Record*, 2632(1), 60-69.
- Minami, I. (2017). Molecular science of lubricant additives. *Applied sciences*, 7(5), 445.

- Mirwald, J., Werkovits, S., Camargo, I., Maschauer, D., Hofko, B., & Grothe, H. (2020). Investigating bitumen long-term-ageing in the laboratory by spectroscopic analysis of the SARA fractions. *Construction and Building Materials*, 258, 119577.
- Mo, L., Huurman, M., Wu, S., & Molenaar, A. (2009). Ravelling investigation of porous asphalt concrete based on fatigue characteristics of bitumen–stone adhesion and mortar. *Materials & Design*, 30(1), 170-179.
- Mo, L., Huurman, M., Wu, S., & Molenaar, A. A. (2011). Bitumen–stone adhesive zone damage model for the meso-mechanical mixture design of ravelling resistant porous asphalt concrete. *International Journal of Fatigue*, 33(11), 1490-1503.
- Mogawer, W. S., Austerman, A., Al-Qadi, I. L., Buttlar, W., Ozer, H., & Hill, B. (2017). Using binder and mixture space diagrams to evaluate the effect of re-refined engine oil bottoms on binders and mixtures after ageing. *Road Materials and Pavement Design*, 18(sup1), 154-182.
- Morian, N., Zhu, C., & Hajj, E. Y. (2015). Rheological indexes: Phenomenological aspects of asphalt binder aging evaluations. *Transportation Research Record*, 2505(1), 32-40.
- Mousavi, M., Kabir, S. F., & Fini, E. H. (2022). Effects of sulfur phase transition on moisture-induced damages in bitumen colloidal structure. *Journal of Industrial and Engineering Chemistry*, 107, 109-117.
- Nahar, S., Schmets, A., & Scarpas, A. (2016). Probing Trace-elements in Bitumen by Neutron Activation Analysis. CROW InfraDagen 2016,
- Nahar, S., Teugels, W., van der Wall, A., Poeran, N., & van Vilsteren, I. (2020). Grip on Bitumen: Mapping the Changes in Bitumen Market and it's impact on performance. 7th E&E Congress, Eurasphalt & Eurobitume, 16-18 June 2021.,
- Nunn, S., & Nishikida, K. (2003). Advanced ATR correction algorithm. *Thermo Electron Corporation Application, Note AN, 1153*.
- O'Brien, J. (1983). Lubricating oil additives. *CRC Handbook of Lubrication*, 2, 301-315.
- Okhotnikova, E., Ganeeva, Y. M., Frolov, I., Ziganshin, M., Firsin, A., Timirgalieva, A., & Yusupova, T. (2020). Thermal and structural characterization of bitumen by modulated differential scanning calorimetry. *Journal of thermal analysis and calorimetry*, 142, 211-216.
- Paliukaite, M., Assuras, M., & Hesp, S. A. (2016). Effect of recycled engine oil bottoms on the ductile failure properties of straight and polymer-modified asphalt cements. *Construction and Building Materials*, 126, 190-196.
- Porot, L. (2019). Rheology and Bituminous binder, a review of different analyses. RILEM 252-CMB Symposium: Chemo-Mechanical Characterization of Bituminous Materials,
- Ratiu, S., Tirian, G., Mihon, N., & Armioni, M. (2022). Overview on globally applied used engine oil recycling technologies. IOP Conference Series: Materials Science and Engineering,
- Read, J., & Whiteoak, D. (2003). *The shell bitumen handbook*. Thomas Telford.
- Ren, S., Liu, X., Lin, P., Jing, R., & Erkens, S. (2023). Toward the long-term aging influence and novel reaction kinetics models of bitumen. *International Journal of Pavement Engineering*, 24(2), 2024188.
- Rowe, G. (2016). ΔT_c -Some thoughts on the historical development. *Presentation from*, 16, 25-28.
- Rubab, S., Burke, K., Wright, L., Hesp, S. A., Marks, P., & Raymond, C. (2011). Effects of engine oil residues on asphalt cement quality. CTAA annual conference proceedings-Canadian Technical Asphalt Association,
- Sandrasagra, J., Ma, J., & Hesp, S. A. (2023). Understanding the field performance of asphalt binders in continental climates through modulated differential scanning calorimetry. *Construction and Building Materials*, 391, 131857.
- Sarkar, S., Datta, D., Deepak, K., Mondal, B. K., & Das, B. (2023). Comprehensive investigation of various re-refining technologies of used lubricating oil: a review. *Journal of Material Cycles and Waste Management*, 1-31.
- Soenen, H., Besamusca, J., Fischer, H. R., Poulikakos, L. D., Planche, J.-P., Das, P. K., Kringos, N., Grenfell, J. R., Lu, X., & Chailleux, E. (2014). Laboratory investigation of bitumen based on round robin DSC and AFM tests. *Materials and Structures*, 47, 1205-1220.
- Soleimani, A. (2009). Use of dynamic phase angle and complex modulus for the low temperature performance grading of asphalt cements. *Kingston, ON: Queen's Univ.*
- Speight, J. G., & Exall, D. I. (2014). *Refining used lubricating oils* (Vol. 99). CRC Press Boca Raton.

- Tang, N., Lv, Q., Huang, W., Lin, P., & Yan, C. (2019). Chemical and rheological evaluation of aging characteristics of terminal blend rubberized asphalt binder. *Construction and Building Materials*, 205, 87-96.
- Torres-Lapasió, J., Baeza-Baeza, J., & Garcia-Alvarez-Coque, M. (1997). A model for the description, simulation, and deconvolution of skewed chromatographic peaks. *Analytical Chemistry*, 69(18), 3822-3831.
- Valentin, J., Trejbal, J., Nežerka, V., Valentová, T., Vacková, P., & Tichá, P. (2021). A comprehensive study on adhesion between modified bituminous binders and mineral aggregates. *Construction and Building Materials*, 305, 124686.
- Van den Bergh, W. (2011). The effect of ageing on the fatigue and healing properties of bituminous mortars.
- Van Lent, D. Q. (2014). Interfacial interactions and mass transfer at the interfacial region of bituminous hydrocarbon mixtures.
- Villanueva, A., Ho, S., & Zanzotto, L. (2008). Asphalt modification with used lubricating oil. *Canadian Journal of Civil Engineering*, 35(2), 148-157.
- Wang, C., Castorena, C., Zhang, J., & Richard Kim, Y. (2015). Unified failure criterion for asphalt binder under cyclic fatigue loading. *Road Materials and Pavement Design*, 16(sup2), 125-148.
- Wang, D., Falchetto, A. C., Riccardi, C., & Wistuba, M. P. (2020). Investigation on the low temperature properties of asphalt binder: glass transition temperature and modulus shift factor. *Construction and Building Materials*, 245, 118351.
- Wang, H., Liu, X., Apostolidis, P., van de Ven, M., Erkens, S., & Skarpas, A. (2020). Effect of laboratory aging on chemistry and rheology of crumb rubber modified bitumen. *Materials and Structures*, 53, 1-15.
- Wang, X., Ren, J., Gu, X., Li, N., Tian, Z., & Chen, H. (2021). Investigation of the adhesive and cohesive properties of asphalt, mastic, and mortar in porous asphalt mixtures. *Construction and Building Materials*, 276, 122255.
- Weigel, S., & Stephan, D. (2018). Relationships between the chemistry and the physical properties of bitumen. *Road Materials and Pavement Design*, 19(7), 1636-1650.
- Werkovits, S., Bacher, M., Mirwald, J., Theiner, J., Rosenau, T., Hofko, B., & Grothe, H. (2023). The impact of field ageing on molecular structure and chemistry of bitumen. *Fuel*, 343, 127904.
- Wielinski, J., Kriech, A., Huber, G., Horton, A., & Osborn, L. (2015). Analysis of vacuum tower asphalt extender and effect on bitumen and asphalt properties. *Road Materials and Pavement Design*, 16(sup1), 90-110.
- Woldekidan, M., & Gaarkeuken, B. (2013). Investigation into the Effects of Filler on the Mechanical Behavior of Bituminous Mortar. Proceedings of the international conferences on the bearing capacity of roads, railways and airfields,
- Wong, V. W., & Tung, S. C. (2016). Overview of automotive engine friction and reduction trends—Effects of surface, material, and lubricant-additive technologies. *Friction*, 4, 1-28.
- Wright, L., Kanabar, A., Moul, E., Rubab, S., & Hesp, S. (2011). Oxidative Aging of Asphalt Cements from an Ontario Pavement Trial. *International Journal of Pavement Research & Technology*, 4(5).
- Xin-jun, L., GIBSON, X., & ANDRIESCU, A. (2016). Performance evaluation of REOB-modified asphalt binders and mixtures. Association of Asphalt Paving Technologists,
- Xu, B., Li, M., Liu, S., Fang, J., Ding, R., & Cao, D. (2018). Performance analysis of different type preventive maintenance materials for porous asphalt based on high viscosity modified asphalt. *Construction and Building Materials*, 191, 320-329.
- Xu, J., Pei, J., Cai, J., Liu, T., & Wen, Y. (2021). Performance improvement and aging property of oil/SBS modified asphalt. *Construction and Building Materials*, 300, 123735.
- Yadykova, A. Y., Gorbacheva, S. N., & Ilyin, S. O. (2023). The deasphalting of heavy crude oil by silicone oil is a green method of removing heavy compounds and producing bitumen. *Geoenergy Science and Engineering*, 227, 211940.
- Yan, C., Huang, W., Xu, J., Yang, H., Zhang, Y., & Bahia, H. U. (2022). Quantification of re-refined engine oil bottoms (REOB) in asphalt binder using ATR-FTIR spectroscopy associated with partial least squares (PLS) regression. *Road Materials and Pavement Design*, 23(4), 958-972.

- Yang, X., Mills-Beale, J., & You, Z. (2017). Chemical characterization and oxidative aging of bio-asphalt and its compatibility with petroleum asphalt. *Journal of Cleaner Production*, 142, 1837-1847.
- You, T., Shi, Y., Mohammad, L. N., & Cooper III, S. B. (2018). Laboratory performance of asphalt mixtures containing re-refined engine oil bottoms modified asphalt binders. *Transportation Research Record*, 2672(28), 88-95.
- Yu, M., Li, J., Cui, X., Guo, D., & Li, X. (2019). Antiageing performance evaluation of recycled engine oil bottom used in asphalt rejuvenation. *Advances in Materials Science and Engineering*, 2019, 1-8.
- Yu, X., Burnham, N. A., Granados-Focil, S., & Tao, M. (2019). Bitumen's microstructures are correlated with its bulk thermal and rheological properties. *Fuel*, 254, 115509.
- Yut, I., & Zofka, A. (2011). Attenuated total reflection (ATR) Fourier transform infrared (FT-IR) spectroscopy of oxidized polymer-modified bitumens. *Applied spectroscopy*, 65(7), 765-770.
- Zhang, H., Li, H., Zhang, Y., Wang, D., Harvey, J., & Wang, H. (2018). Performance enhancement of porous asphalt pavement using red mud as alternative filler. *Construction and Building Materials*, 160, 707-713.
- Zhang, J., Ma, J., & Hesp, S. (2023). Development of an oil exudation test for asphalt binder. Available at SSRN 4588846.
- Zhao, W., Li, X., & Feng, Z. (2022). Infrared Spectrum Analysis of Aged Asphalt Regenerated by Recycled Engine Oil Bottom. *Mathematical Problems in Engineering*, 2022.

Appendix

On the following pages several tables and graphs are plotted, which did not fit in the report itself due to their size or the analysis they performed was partly outside of the scope of the thesis itself.

A small overview of these additions are:

- A. **Flow diagram for identification of REOB in bitumen**
- B. **Flow diagram for evaluation of REOB modified bitumen**
- C. **Identification of REOB in bitumen from “GOA” and “Leerruimte” data**
- D. **Comparison of frequency sweep (DSR) data to field performance of bitumen**
- E. **X-ray CT scanning of small REOB modified bitumen films on aggregates**

A. Flow diagram for identification of REOB in bitumen

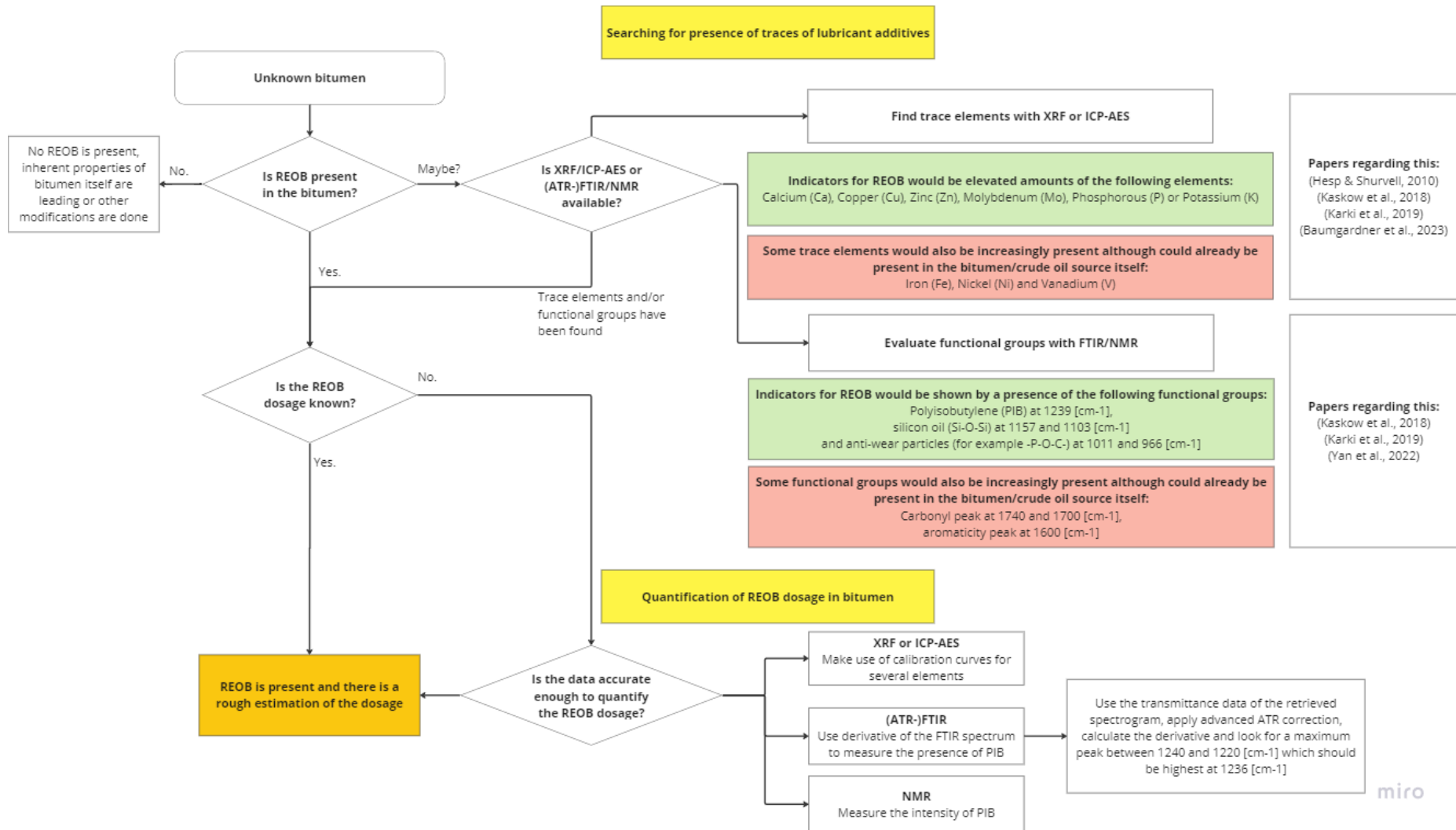
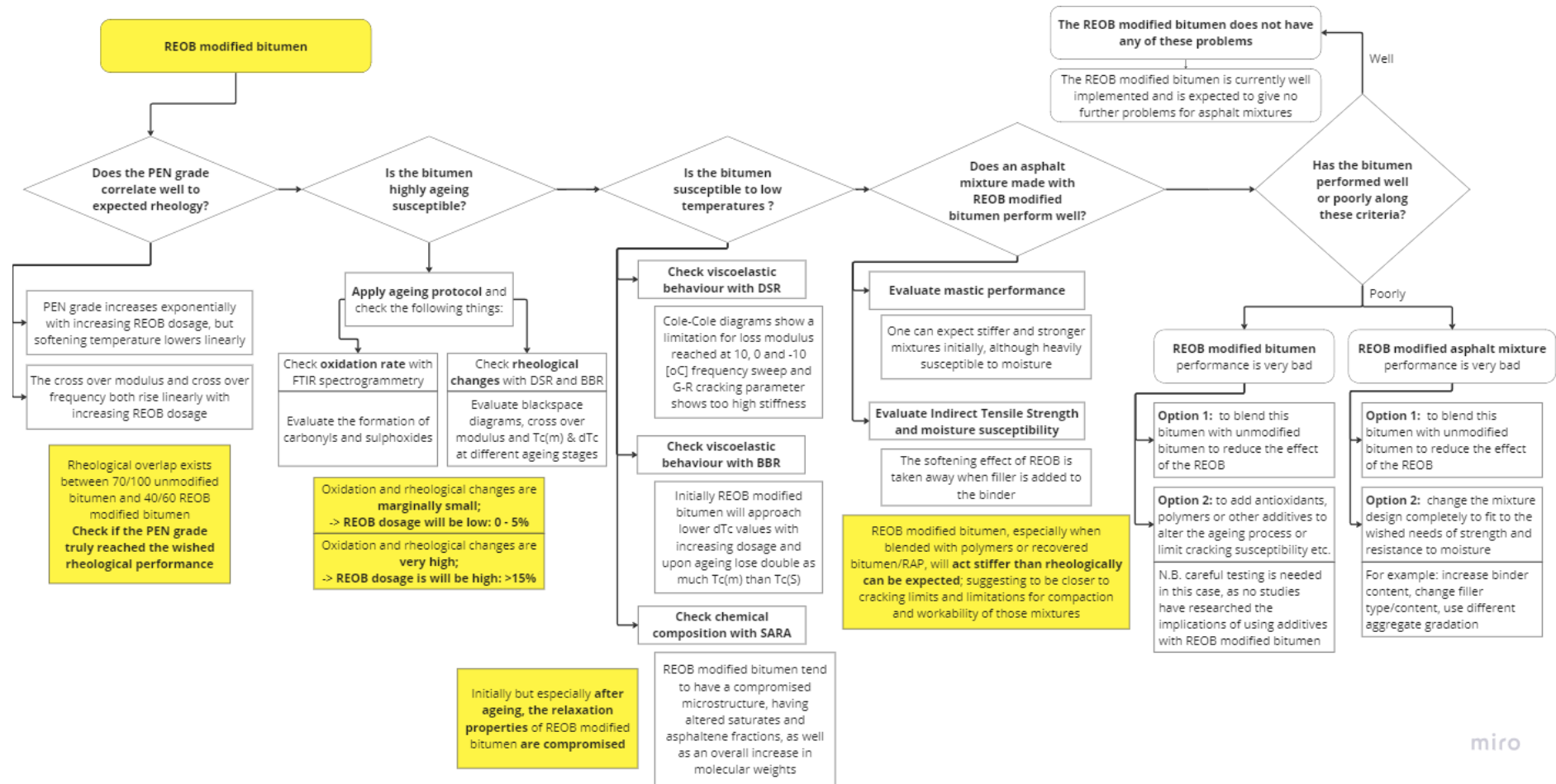


Figure A.1: Flow chart to be used for identification of REOB in bitumen

B. Flow diagram for evaluation of REOB modified bitumen



miro

Figure B.1: Flow chart to be used for evaluation of the performance of REOB in bitumen and asphalt

C. Identification of REOB in bitumen from “GOA” and “Leerruimte” data

To provide a check of the proposed method to identify and quantify REOB in a bitumen, a separate list of bitumen will be evaluated and compared to measurements from XRF. These bitumen are evaluated and used in the project between RWS and industry in the “Grip op asfalt” (GOA) program and the “Leerruimte” program from the industry, where the quality of bitumen is evaluated.

If the overlap of XRF measurements and the used FTIR measurements show an overlap in determining if REOB has been fluxed with the bitumen, then this would prove that both methods can basically do the same thing. A standardised check if REOB is present in bitumen will therefore be easily performed with either XRF or FTIR and thus contractors and refineries will have an easy job determining if received bitumen was modified with REOB. The following table presents the XRF measurements carried out on the GOA project samples.

N.B. that the sample codes are not the same as were used throughout the thesis, this is a set of 16 different bitumen than handled before.

Table C.1: XRF measurements of the PEN grade bitumen and PmBs in the “Leerruimte” project

Sample	PEN grade or PmB	XRF					ICP	REOB Y/N
		Calcium mg/kg	Nickel mg/kg	Phosphorous mg/kg	Vanadium mg/kg	Zinc mg/kg		
K	70/100	8	83	6	309	0	8.8	
N	160/200	1	50	10	138	0	4.28	
M	160/200	2	37	3	183	0	4.21	
I	40/60	1	64.4	19	224	0	6.9	
J	40/60	3	44	2	156	0	5.5	
F	PmB	2	33	3	120	0	4.58	
E	PmB	10	38	13	215	3	5.3	
D	PmB	11	49	9	216	10	4.77	
A	PmB	129	19.1	30	208	5.8	3.93	Y
C	PmB	8	16	13	257	0.3	5.6	
B	PmB	11	21	9	203	0	4.04	
O	PmB	367	22.2	140	243	26.6	5	Y
P	70/100	1270	28.9	840	386	470	6.8	Y
L	70/100	2	29.5	5	383	8.8	4.89	
G	10/20	486	43	17	61	5	2.03	Y?
H	10/20	5	61	3	295	0	9.3	

To see if the FTIR scan results conclude the same statement if REOB would be present or not, Figure C.1 shows the evaluation of FTIR data between regions 1300 [cm⁻¹] and 1100 [cm⁻¹].

It can be concluded that mainly PEN grade bitumen bit-P and bit-G seem to indeed contain REOB, bitP at a much higher and clearer content too. The PMBs of bit-A and bit-O are much harder to discern the REOB in there; especially EVA being present in the bit-A seems to mask the PIB, as the EVA is measured at 1243 and 1740 [cm⁻¹].

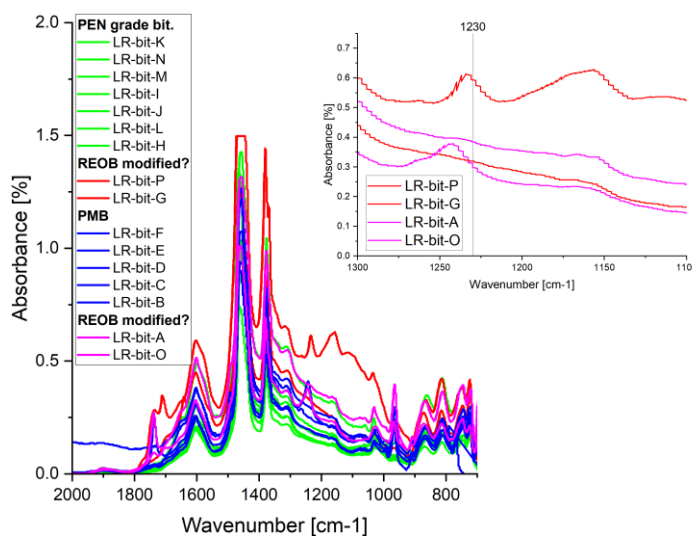


Figure C.1: FTIR measurements of the PEN grade bitumen and PmBs in the “Leerruimte” project

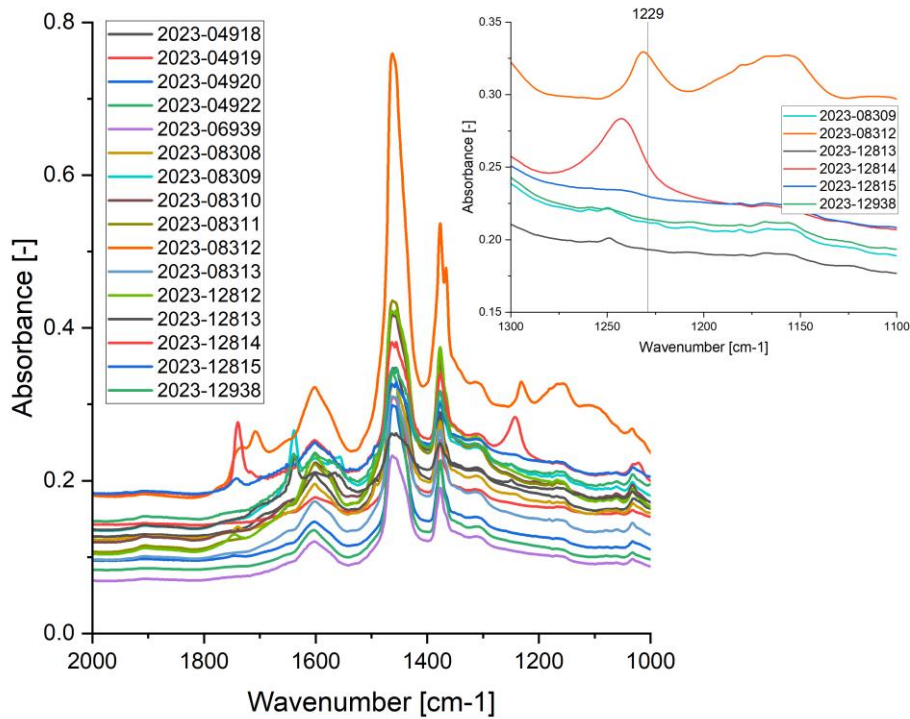


Figure C.2: FTIR measurements of GOA bitumen samples

Only sample 2023-08312 has the clearest presence of REOB. However, samples 2023-08309; 2023-12813; 2023-12815; 2023-12938 seem to have both increases in carbonyl peaks and suggest a very small peak in PIB. The peak measurable for 2023-12814 is again for EVA, but no hill can be measured from the side therefore does not suggest that there is REOB modification. This can be clarified by using the derivative of these bitumen as shown in the following figure:

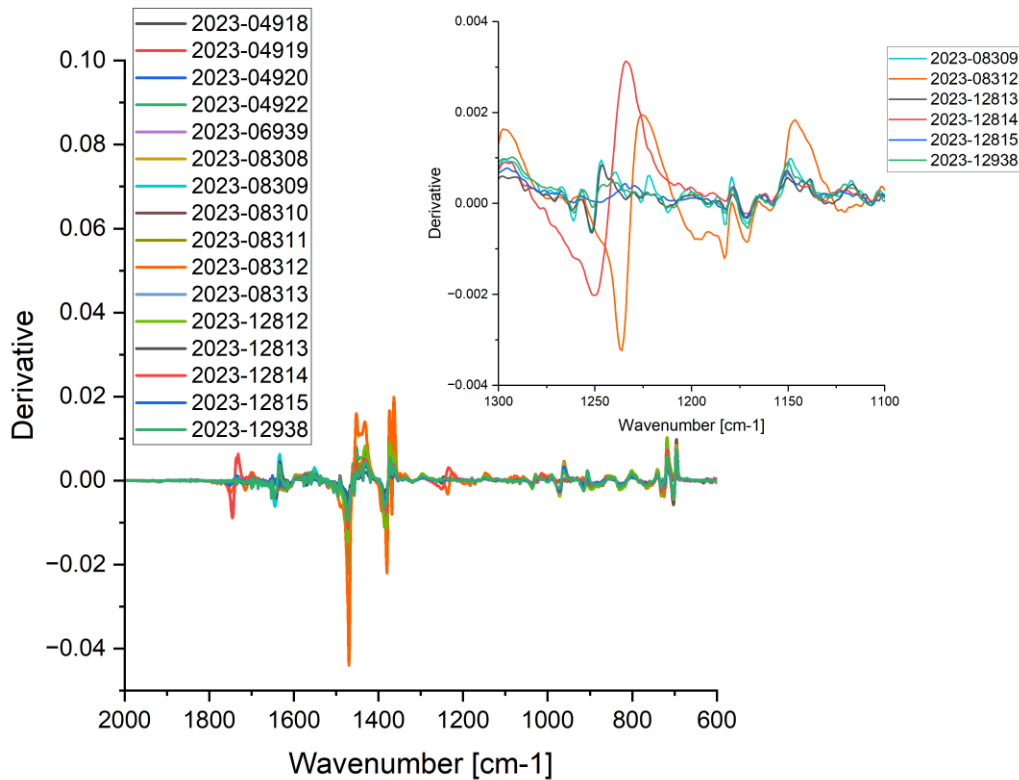


Figure C.3: Derivative of the FTIR measurements of GOA bitumen samples

D. Comparison of frequency sweep (DSR) data to field performance of bitumen

The obtained DSR frequency sweep data can be compared to the TNO blackspace diagram database, which gives an indication on how the aged bitumen compares to in-field ageing of bitumen in an asphalt mixture.

Table D.1: DSR frequency sweep data on all bitumen used in this thesis

Sample	G* at 10 [rad/s] and 20 [°C] [Pa]	δ at 10 [rad/s] and 20 [°C] [°]
Unaged and unmodified bitumen		
bit-P	2.0048E7	46
bit-K	3.2415E7	43.45
bit-A	9530800	51.76
bit-G	4505100	52.66
bit-B	1599900	61.14
bit-J	3675400	55.86
bit-L	1571300	63.89
bit-M	1676300	59.98
bit-O	3218000	60.93
bit-I	1086100	64.14
Aged bitumen		
bit-L	1571300	63.89
bit-L_TFOT	2745700	58.3
bit-L_20hPAV	7550400	46.49
bit-L_40hPAV	1.1109E7	41.25
bit-L_80hPAV	1.5382E7	36.84
bit-J	3675400	55.86
bit-J_TFOT	5472900	55.9
bit-J_20hPAV	9606300	45.84
bit-J_80hPAV	1.9253E7	36.05
bit-G	4505100	52.66
bit-G_TFOT	7640700	45.64
bit-G_20hPAV	1.916E7	30.89
bit-G_40hPAV	2.5901E7	26.69
bit-G_80hPAV	3.2945E7	23.19
bit-O	3218000	60.93
bit-O_20hPAV	4962300	52.61
REOB modified & aged bitumen		
bit-K+5%REOB	1.0146E7	54
bit-K+5%REOB_20hPAV	2.2943E7	38.94
bit-K+10%REOB	3895300	62.63
bit-K+10%REOB_20hPAV	1.0979E7	45.44
bit-K+15%REOB	1336600	68.56
bit-K+15%REOB_20hPAV	5100600	48.06
bit-P+5%REOB	9361600	51.28
bit-P+5%REOB_20hPAV	1.5586E7	40.38
bit-P+10%REOB	4708800	55.22
bit-P+10%REOB_20hPAV	1.2034E7	41.7
bit-P+15%REOB	1997800	58.9
bit-P+15%REOB_20hPAV	6077600	42.6

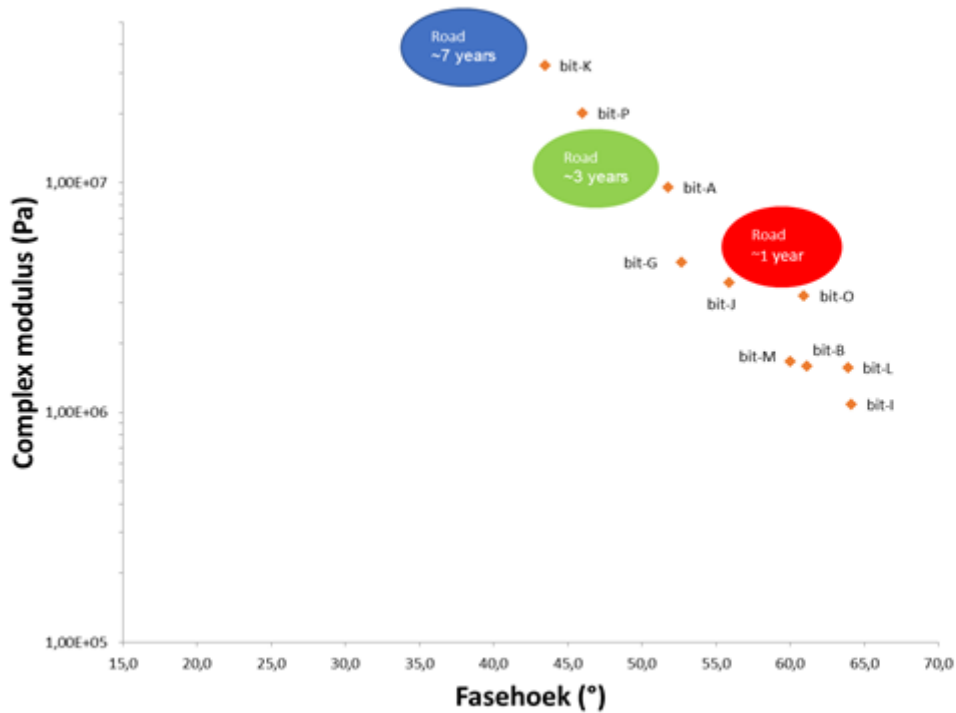


Figure D.1: Unaged and unmodified bitumen plotted around the field ageing behaviours



Figure D.2: Aged but unmodified bitumen plotted around the field ageing behaviours

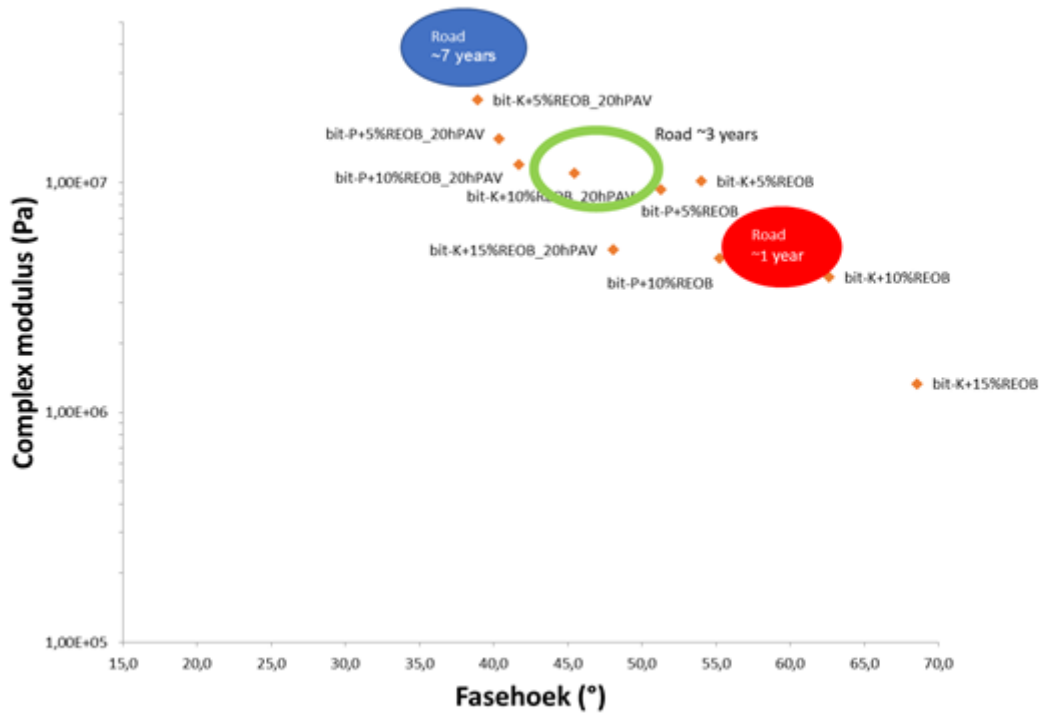


Figure D.3: Aged and REOB modified bitumen plotted around the field ageing behaviours

From this alone, one can easily see how heavily REOB modified bitumen (around 15% dosage) will initially have a very good soft nature and high phase shift angle. Although after 20hPAV, which normally seems to relate to ~3 years of in-field ageing, this softer nature will be lost just as easily as for lower dosages.

This shows how a higher REOB dosage will only initially make a bitumen softer, but will not at all grant a good buffer towards the ageing of the bitumen. Only a base bitumen which is already close to the wished performance and then modified with not more than 5% REOB, seems to keep this increased tendency towards getting stiffer in check.

E. X-ray CT scanning of small REOB modified bitumen films on aggregates

As was stated in Chapter 4.2.1, the trace metals found in REOB modified bitumen and in REOB itself, can be linked to lubricant additives of the initial WEO. Although the REOB seems to blend and spread itself well inside the bitumen, it has been found that some microstructural inefficiencies occurred for these REOB modified bitumen in Chapter 6. The spread of the REOB compounds throughout the bitumen could actually be poor, especially after mixing with fillers and aggregates as was found in Chapter 7.

To effectively see changes in consistency, one could apply X-ray CT-scanning techniques to effectively evaluate density differences throughout the bitumen on microscale. This technique can scan small bitumen (+stone) samples to see the spread in densities and notice localised points of higher density; for example indicating heavy metals (as found in REOB) or filler material (CaCO_3) etc.

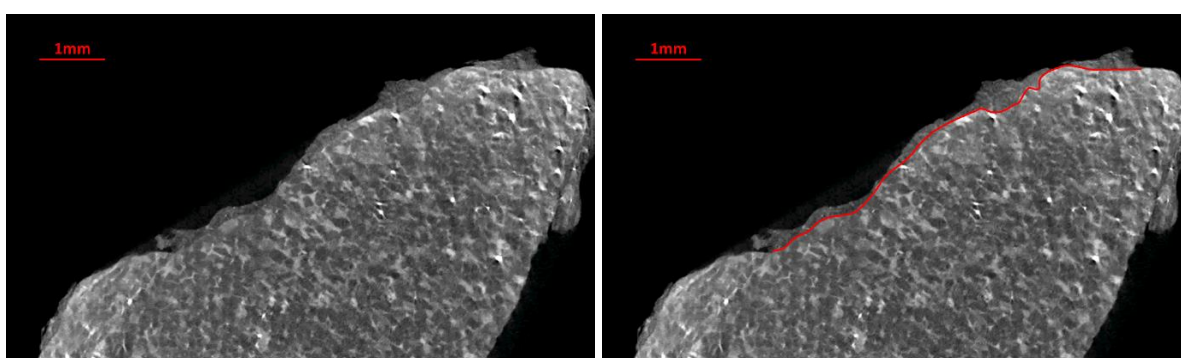


Figure E.1: X-ray CT scans of a single cross-section (left) and the bitumen-film indicated by the red line (right)

The figures above and below show a 2D view of a cross-section of a very small part of stone partly covered with bitumen. The bitumen present on the stone can be singled out and one can indeed distinguish different parts in it, see the right figure in Figure E.2.

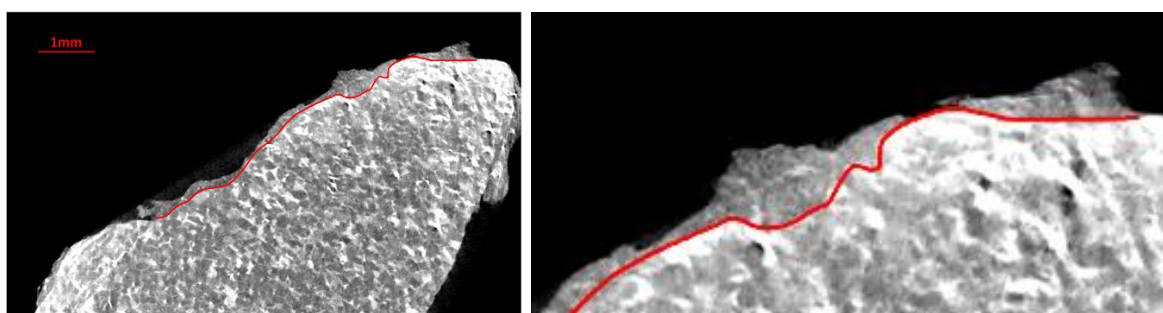


Figure E.2: Increased contrast of the X-ray CT scans (left) and a zoomed in part of the bitumen-film (right)

Clearly one can discern a few separate phases in the bitumen and (although not shown here) the 3D imaging has shown clear white spots in the bitumen. This could indicate the presence of either the heavy metals from REOB or the present filler material.

Recommended is therefore to further zoom in and measure even smaller samples (instead of a stone of 1.5 [cm] measuring one at around 0.5 [cm]). This will allow a higher resolution of the image and the effect of REOB on the filler or how filler spreads throughout the mastic in a mixture can then be evaluated. Alternatively one could also make very small bitumen/mastic samples in PMMA cylinders, and see how the filler or REOB distributes throughout the binder with this technique.